Unesco reports
in marine science 64

Mud volcanism in the Mediterranean and Black Seas and shallow structure of the Eratosthenes Seamount

Initial results of the geological and geophysical investigations during the Third UNESCO-ESF "Training-through-Research" Cruise of RV *Gelendzhik* (June-July 1993)

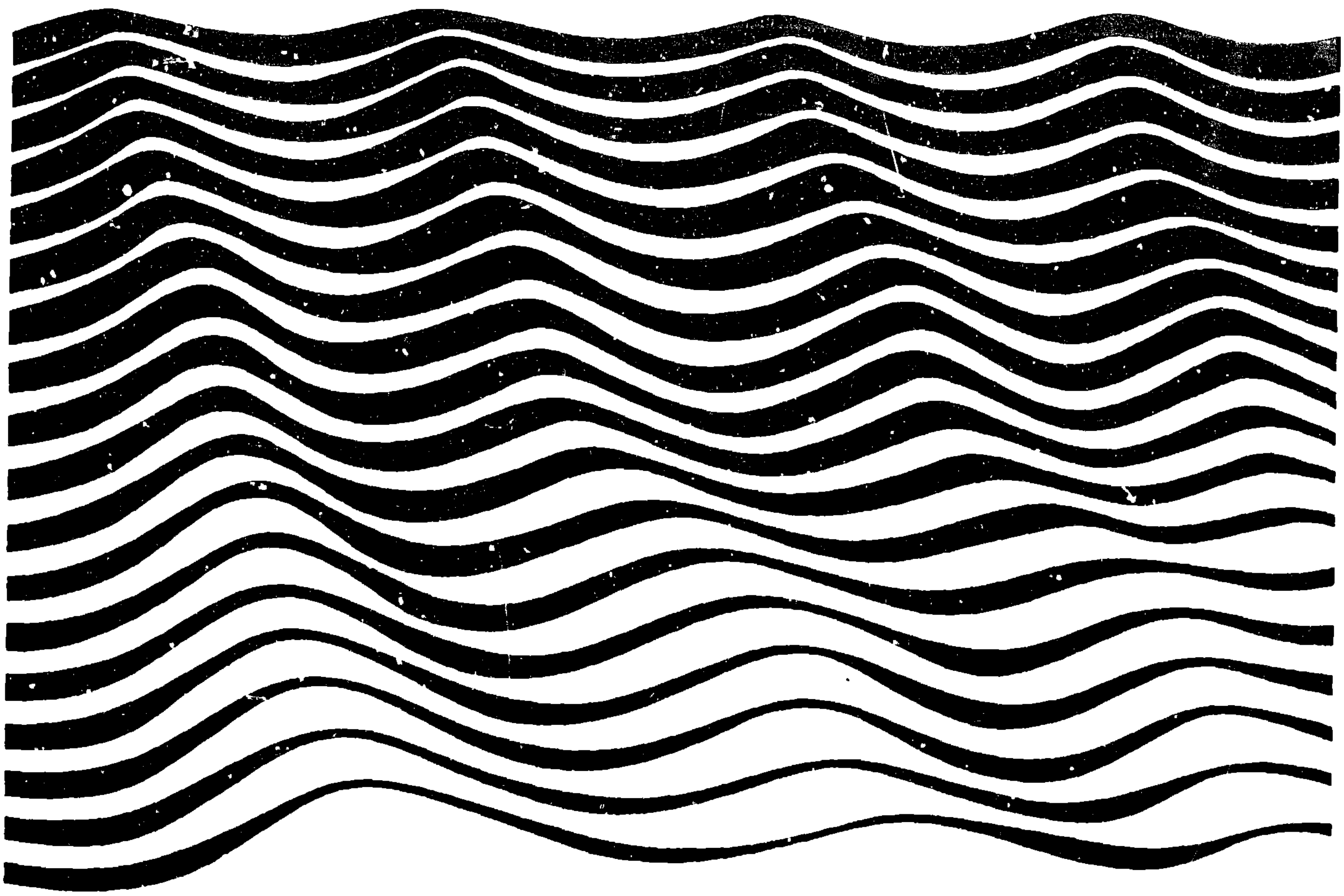

UNESCO 1994

UNESCO REPORTS IN MARINE SCIENCE

For availability in microfiche form please write to:
UNESCO (DIT/AM), 7, place de Fontenoy, 75352 Paris 07 SP, France.
Out of stock titles are listed on the back cover.

No.		Year
4	Syllabus for training marine technicians. Report of an IOC/UNESCO workshop held in Miami, Florida, 22-26 May 1978. Available in English, French, Russian and Spanish	1979
5	Marine science syllabus for secondary schools. Report of an IOC workshop held at United World College of the Atlantic, United Kingdom, 5-9 June 1978. Available in Arabic, English, French, Russian and Spanish	1979
6	Organization of marine biological reference collections in the Mediterranean Arab countries. Expert meeting held in Tunis, 20-23 September 1978. Available in Arabic, English and French	1979
8	The mangrove ecosystem: Human uses and management implications. Report of a UNESCO regional seminar held in Dacca, Bangladesh, December 1978. English only	1979
9	The mangrove ecosystem: scientific aspects and human impact. Report of the seminar organized by UNESCO at Cali, Colombia, 27 November-1 December 1978. Available in English and Spanish	1979
10	Development of marine science and technology in Africa. Working Group of Experts sponsored by ECA and UNESCO, Addis Ababa, 5-9 May 1980. Available in English and French	1980
14	Marine science and technology in Africa: present state and future development. Synthesis of UNESCO/ECA survey missions to African coastal states, 1980. Available in English and French	1981
15	Fishery science teaching at the university level. Report of a UNESCO/FAO workshop on university curricula in fishery science, Paris, May 1980. Available in Arabic, English, French, Russian and Spanish	1981
20	Quantitative analysis and simulation of Mediterranean coastal ecosystems: The Gulf of Naples, a case study. Report of a workshop on ecosystem modelling, Ischia, Naples, Italy, 28 March to 10 April 1981. Organized by the United Nations, Educational, Scientific and Cultural Organization (UNESCO) and the Stazione Zoologica, Naples. English only	1983
21	Comparing coral reef survey methods. A regional UNESCO/UNEP workshop, Phuket Marine Biological Centre, Thailand, December 1982. English only	1983
22	Guidelines for marine biological reference collections. Prepared in response to a recommendation by a meeting of experts from the Mediterranean Arab countries. Available in English, French and Arabic	1983
23	Coral reefs, seagrass beds and mangroves: their interaction in the coastal zones of the Caribbean. Report of a workshop held at West Indies Laboratory, St Croix, U. S. Virgin Islands, May 1982. English only	1983
24	Coastal ecosystems of Latin America and the Caribbean. The objectives, priorities and activities of UNESCO's COMAR project for the Latin America and Caribbean region, Caracas, Venezuela, 15-19 November 1982. Available in English and Spanish	1983
25	Ocean engineering teaching at the university level. Recommended guidelines from the UNESCO/IOC/ECOR workshop on advanced university curricula in ocean engineering and related fields, Paris, October 1982. Available in English, French, Spanish, Russian, Arabic and Chinese	1983
26	Global survey and analysis of post-graduate curricula in ocean engineering. English only	1984
28	Oceanographic modelling of the Kuwait Action Plan (KAP) Region. Report of symposium/workshop, University of Petroleum and Minerals, Dhahran, Kingdom of Saudi Arabia, 15-18 October 1983. English only	1984
29	Eutrophication in coastal marine areas and lagoons: a case study of 'Lac de Tunis'. Report prepared by Dr M. Kelly and Dr M. Naguib. English only	1984
30	Physical oceanography of the Eastern Mediterranean: an overview and research plan. Report of a workshop held in Lerici, La Spezia (Italy), September 1983. English only	1984
31	MABAHISS/John Murray 50th anniversary: Marine science of the North West Indian Ocean and adjacent waters. Report of a symposium on the occasion of the 50th anniversary of the MABAHISS/John Murray Expedition (1933/34), University of Alexandria, Egypt, 3 to 7 September 1983. English only	1985
32	L'estuaire et la mangrove du Sine Saloum. Résultats d'un Atelier régional UNESCO-COMAR tenu à Dakar (Sénégal) du 28 février au 5 mars 1983. French only	1985
33	Coral taxonomy. Results and recommendations of a regional UNESCO (COMAR)/UNEP workshop with advanced training Phuket Marine Biological Centre, Thailand, 10-26 February 1984. English only	1985
34	Bibliography on coastal lagoons and salt marshes along the Southern Mediterranean coast (Algeria, Egypt, Libya, Morocco, Tunisia). Available in Arabic, English and French	1985
37	Principles of Geological Mapping of Marine Sediments (with special reference to the African continental margin). Available in English and Russian	1986
39	Development of marine sciences in Arab Universities. Meeting of experts held at the Marine Science Station Aqaba, Jordan, 1-5 December 1985. Available in Arabic, English, French	1986
40	Human induced damage to coral reefs. Results of a regional UNESCO (COMAR) workshop with advanced training, Diponegoro University, Jepara and National Institute of Oceanology, Jakarta, Indonesia, May 1985. English only	1986
41	Caribbean coastal marine productivity. Results of a Planning Workshop at Discovery Bay Marine Laboratory, University of the West Indies, Jamaica, November 1985. English only	1986
42	The application of digital remote sensing techniques in coral reef, oceanographic and estuarine studies. Report on a regional UNESCO/COMAR/GBRMPA Workshop, Townsville, Australia, August 1985. English only	1986
43	Quaternary coastal geology of West Africa and South America. Papers prepared for the INQUA-ASEQUA Symposium in Dakar, April 1986. Available in English only	1987
44	Physical oceanography of the Eastern Mediterranean (POEM): Initial Results UNESCO/IOC First POEM Scientific Workshop, Erdemli, Turkey, 16-20 June 1986. English only	1987
45	Marine science teaching and training at first degree (undergraduate) level. Recommended guidelines from a UNESCO workshop on university curricula, Paris, November 1986. Available in Arabic, Chinese, English, French, Russian, Spanish	1987
46	Comparison between Atlantic and Pacific tropical marine coastal ecosystems: community structure, ecological processes, and productivity. Results and scientific papers of a UNESCO/COMAR workshop, University of the South Pacific, Suva, Fiji, 24-29 March 1986. English only	1987
47	Temperate coastal systems of Latin America. Report on meeting on COSALC Pilot Project No. VII, November 1986. Spanish only	1987
48	Coastal marine ecosystems of Africa. Objectives and strategy of the COMARAF Regional Project English only	1988

Cont'd on inside of back cover

UNESCO reports
in marine science 64

Mud volcanism in the Mediterranean and Black Seas and shallow structure of the Eratosthenes Seamount

Initial results of the geological and geophysical investigations during the Third UNESCO-ESF "Training-through-Research" Cruise of RV *Gelendzhik* (June-July 1993)

Editors: A.F. Limonov
J.M. Woodside
M.K. Ivanov

UNESCO 1994

ISSN 0253-0112

Published in 1994
by the United Nations Educational,
Scientific and Cultural Organization,
7, place de Fontenoy, 75352 Paris 07 SP
Printed in UNESCO's workshops.

PREFACE

UNESCO Reports in Marine Science are designed to serve specific programme needs and to report on developments in projects conducted in the context of UNESCO's marine science-related activities.

Designed to serve as a complement to the *UNESCO Technical Papers in Marine Science*, the systematic distribution of *Reports* is restricted to libraries of oceanographic institutions and governmental authorities, and documentation centres. Individual requests from specialists will, however, be examined by the Marine Information Centre and dealt with on a selective basis.

Requests for specific titles or additions to the mailing list should be addressed to:

Marine Information Centre
UNESCO
1 rue Miollis
75732 Paris Cedex 15
France

The designations employed and the presentation of the material in this document do not imply the expression of any opinion whatsoever on the part of the UNESCO Secretariat concerning the legal status of any country, territory, city, or area or of its authorities, or concerning the delimitation of its frontiers or boundaries. The ideas and opinions expressed are those of the authors and do not necessarily represent the views of UNESCO.

ABSTRACT

The 3rd Training through Research cruise of the R/V *Gelendzhik* (June-July 1993) was focused on the investigations of the mud volcanism in the deepest part of the Black Sea and on the Mediterranean Ridge accretionary complex, as well as study of the shallow structure of the Eratosthenes Seamount in the easternmost Mediterranean. The cruise was sponsored by UNESCO, European Science Foundation and national founding organizations of the Netherlands, United Kingdom, Italy, Spain and Russia.

In the Black Sea, some mud volcanoes, including the TREDMAR mud volcano discovered during the 1st Training through Research Cruise (1991), were studied in detail with the use of the MAK-1 deep-tow acoustic system, underwater TV and gravity corer. It was found that sliding of the bottom sediments is widespread in the area of the mud volcanoes. Enigmatic criss-cross lines were discovered in the vicinity of the MSU and Yuzhmorgeologiya mud volcanoes. Gas hydrate crystals were sampled from the TREDMAR mud volcano.

About twenty new mud domes were discovered on the Mediterranean Ridge, in the area of the Olimpi mud diapir field, and nine of them were checked by coring. Most of them are not mud diapirs but mud volcanoes with extensive mud flows on their slopes. The Olimpi and Prometheus 2 mud diapir fields were proven to be the single area that presumably extends further east- and westwards. Extensive gas and fluid seepages were recorded by the underwater TV on the Napoli Dome. The Cretaceous rock was found in the mud breccia from the Toronto Dome.

Interpretation of the newly obtained seismic data from the Eratosthenes Seamount gave the indication that this structural high is very active tectonically. Its northern slope underthrusts beneath the Cyprus margin while the southern slope is overthrust by the Levantine plate. The upper crustal level of the seamount is under tectonic extension and is cut by normal fault. The thickness of the Plio-Quaternary sediments on the seamount averages about 130 m. Circular holes interpreted to be pockmarks were found on the top of the seamount.

RESUME

La troisième campagne de formation par la recherche effectuée (en juin-juillet 1993) à bord du N/O *Gelendzhik* était axée sur l'exploration du volcanisme de boue de la zone la plus profonde de la mer Noire et du complexe d'accrétion de la dorsale méditerranéenne, ainsi que sur l'étude de la structure superficielle du mont sous-marin Eratosthène à l'extrême est de la Méditerranée. Cette campagne était parrainée par l'UNESCO, la Fondation européenne de la science et des organismes nationaux de financement des Pays-Bas, du Royaume-Uni, d'Italie, d'Espagne et de Russie.

En mer Noire, quelques volcans de boue, dont le volcan TREDMAR découvert lors de la première campagne de formation par la recherche (1991), ont fait l'objet d'une étude détaillée au moyen du système d'exploration acoustique remorqué en profondeur MAK-1, d'une caméra de télévision sous-marine et d'un carottier à gravité. On a constaté que le glissement des sédiments du fond était un phénomène très courant dans la région des volcans de boue. D'énigmatiques lignes entrecroisées ont été découvertes dans le voisinage des volcans MSU et Yuzhmorgeologiya. Des échantillons d'hydrates de gaz cristallisés ont été prélevés sur le volcan TREDMAR.

Une vingtaine de nouveaux dômes de boue ont été découverts sur la dorsale méditerranéenne, dans la région du champ de diapirs Olimpi ; neuf ont été examinés par carottage. La plupart ne sont pas des diapirs mais des volcans de boue dont les pentes sont recouvertes de vastes coulées de boue. Il a été prouvé que les deux champs de diapirs de boue Olimpi et Prometheus appartenaient à une zone unique se prolongeant vraisemblablement vers l'est et vers l'ouest. D'importants suintements gazeux et fluides ont été filmés sur le dôme Napoli grâce à la caméra de télévision sous-marine. Des roches crétacées ont été trouvées dans les brèches de boue provenant du dôme Toronto.

L'interprétation des nouvelles données sismiques recueillies sur le mont Eratosthène indique que cette élévation est le site d'une intense activité tectonique. Sa pente septentrionale exerce une poussée sous la marge de Chypre tandis que sa pente méridionale est chevauchée par la plaque levantine. La zone crustale supérieure de ce mont sous-marin subit une distension tectonique et est coupée par une faille normale. Les sédiments plio-quaternaires qui le recouvrent ont une épaisseur moyenne d'environ 130 mètres. On pense que les trous circulaires découverts au sommet ont été creusés par le dégagement de gaz ou de fluides.

RESUMEN

El tercer crucero de formación por medio de la investigación del buque de estudio *Gelendzhik* (junio-julio de 1993), se centró en las investigaciones del volcanismo del lodo en la parte más profunda del Mar Negro y en el complejo acrecionario de la cordillera mediterránea, así como en un estudio de la estructura superficial del monte submarino Eratóstenes en la región más oriental del Mediterráneo. Financiaron el crucero la UNESCO, la European Science Foundation (Fundación Europea para la Ciencia) y organizaciones nacionales de financiación de los Países Bajos, el Reino Unido, Italia, España y Rusia.

Algunos volcanes de lodo del Mar Negro, entre ellos el volcán TREDMAR, descubierto en el primer crucero de formación por medio de la investigación (1991), fueron estudiados detenidamente con el sistema acústico de remolque profundo MAK-1, televisión submarina y sacatestigos por gravedad. Se descubrió que el corrimiento de los sedimentos del fondo es muy frecuente en la zona de los volcanes de lodo. Se descubrieron unas enigmáticas líneas entrecruzadas en las proximidades de los volcanes de lodo MSU y Yuzhmorgeologiya. Se tomaron muestras de cristales de hidrato de gas del volcán TREDMAR.

En la cordillera mediterránea se descubrieron unos 20 domos nuevos de lodo, concretamente en la zona del terreno de diapiros de lodo Olimpi, y se tomaron muestras de nueve de ellos. La mayoría no son diapiros de lodo sino volcanes, con extensas corrientes de lodo en sus laderas. Se comprobó que los terrenos de diapiros de lodo Olimpi y Prometheus 2 constituyen una sola zona que probablemente se extiende más hacia el este y hacia el oeste. La televisión submarina permitió grabar abundantes infiltraciones de gas y de líquido en el domo Napoli. En la brecha de lodo del domo Toronto se encontró roca cretácea.

La interpretación de los nuevos datos sísmicos obtenidos del monte submarino Eratóstenes puso de relieve que esta altura estructural es muy activa tectónicamente. Su ladera septentrional se desliza bajo el margen de Chipre, en tanto que la ladera meridional se desliza bajo la placa levantina. El nivel superior de la corteza del monte submarino está sometido a extensión tectónica y está cortado por una falla normal. El espesor de los sedimentos pliocuaternarios del monte submarino es de 130 m por término medio. En su cumbre se descubrieron agujeros circulares que se identificaron como posibles alvéolos.

РЕЗЮМЕ

Третий рейс НИС "Геленджик" ЮНЕСКО/ТРЕДМАР (июнь–июль 1993 г.) по программе "Обучение через исследования" имел целью изучение грязевого вулканизма в наиболее глубокой части Черного моря и на аккреционном комплексе Средиземноморского вала, а также выяснение поверхностной структуры подводной горы Эратосфена на самом востоке Средиземного моря. Рейс финансировался за счет средств ЮНЕСКО, Европейского научного фонда и национальных фондов Нидерландов, Великобритании, Италии, Испании и России.

В Черном море несколько грязевых вулканов, в том числе вулкан Тредмар, открытый во время 1-го рейса по программе "Обучения через исследования" (1991 г.), были детально изучены при помощи глубоководной буксируемой акустической системы МАК–1, подводного телевидения и пробоотбором ударными трубками. Обнаружено, что в районе грязевого вулканизма широко развит процесс оползания донных осадков. Загадочные перекрещивающиеся линии на дне моря были найдены поблизости от вулканов МГУ и Южморгеология. На грязевом вулкане Тредмар отобраны кристаллы газогидратов.

Около двадцати новых грязевых куполов было открыто на Средиземноморском валу вокруг района глиняного диапиризма Олимпи; девять из них были опробованы пробоотбором. Большинство из них оказались не глиняными диапирами, а грязевыми вулканами с обширными грязевыми потоками на их склонах. Было доказано, что районы Олимпи и Прометей–2 составляют единую зону, которая, вероятно, протягивается дальше на восток и запад. Обширные выходы газов и флюидов зафиксированы подводным телевидением на куполе Наполи. Обломки пород мелового возраста обнаружены в грязевой брекчии купола Торонто.

Интерпретация полученных новых данных по подводной горе Эратосфена показала, что эта структурная возвышенность очень активна в тектоническом плане. Ее северный склон пододвигается под кипрскую окраину, в то время как на ее южный склон надвигается Левантийская плита. Верхние горизонты земной горы подводной горы испытывают тектоническое растяжение и рассечены сбросами. Мощность плиоцен-четвертичных осадков на горе в среднем составляет 130 м. На своде горы обнаружили округлые впадины, интерпретированные как следы выходов газов или флюидов.

مستخلص

لقد ركزت الرحلة البحرية الثالثة للتدريب من خلال البحث على متن سفينة البحوث غيلنزيك (Gelendzhik) (يونيو/حزيران - يوليو/تموز ١٩٩٣) على استقصاء البراكين الطينية في أعمق مواقع البحر الأسود وعلى ارتفاع تراكمات الحاجز الجبلي في البحر المتوسط وعلى دراسة البنى القليلة العمق من التل البحري الواقع في أقصى شرق البحر المتوسط. وتولت اليونسكو ومؤسسة العلوم الأوروبية والمنظمات الوطنية الممولة من هولندا والمملكة المتحدة وايطاليا واسبانيا وروسيا رعاية هذه الرحلة البحرية.

وفي البحر الأسود، درست بعض البراكين الطينية بالتفصيل بما فيها البركان الطيني "تردمار" الذي اكتشف أثناء الرحلة البحرية الأولى للتدريب من خلال البحث (عام ١٩٩١) وذلك عن طريق استخدام جهاز ماك - ١ (MAK - 1) الصوتي المتطور على القاع، وكذلك كاميرا تلفزيونية تعمل في الماء، وثاقب للقاع بالجاذبية الأرضية. وتبين أن انزلاق الرواسب في القاع ظاهرة منتشرة في منطقة البراكين الطينية. واكتشفت خطوط متقاطعة المنشأ وذلك بالقرب من البركانين الطينيين المعروفين باسم "جامعة موسكو للدولة" و"يوشمورجيولوجيا" (Yuzhmorgeologiya). وأخذت عينات من بلورات هيدرات غازية من البركان الطيني "تردمار".

واكتشف نحو عشرين قبة طينية جديدة على الحاجز الجبلي في البحر المتوسط، في منطقة "أوليمبي" للطبقات الطينية المطوية، وفحصت تسع منها بأخذ العينات من القاع. ومعظم هذه القبب ليست طبقات طينية مطوية وانما براكين طينية ذات تدفقات طينية كثيرة على منحدراتها. وتبين أن حقلي "أوليمبي" و"بروميتوس ٢" للطبقات الطينية المطوية عبارة عن منطقة واحدة يفترض أنها تمتد الى مناطق أخرى شرقا وغربا. وسجلت الكاميرا التلفزيونية في الماء تسرب كميات كبيرة من الغاز والسوائل على قبة "نابولي". وتم العثور على صخر كريتاسي في بريشيا طينية من قبة "تورنتو".

ويستنبط من تفسير بيانات الزلازل التي تم الحصول عليها منذ فترة قريبة من التل البحري الواقع في شرق البحر المتوسط أن هذا التل ذو نشاط تكتوني كبير. فيمارس منحدره الشمالي ضغطا سفليا على حافة قبرص بينما تنطوي لوحة منطقة شرق البحر المتوسط على منحدره الجنوبي. والقشرة الأرضية العليا من هذا التل البحري معرضة لشد تكتوني وتتسم بانكسار عادي. ويتراوح سمك الرواسب الموجودة على التل البحري، والتي يرجع تاريخها الى نهاية العصر الثالث والعصر الرابع ١٣٠ مترا تقريبا. كما تم العثور على حفر دائرية على قمة التل، وتفسر على أنها بثرات ناجمة عن تدفق السوائل والغازات.

摘　要

由俄罗斯调查船“Gelendzhik”号进行的第三次调查培训航行主要是对黑海最深层部分以及地中海海脊堆积杂岩的泥火山活动进行调查，并对地中海最东部的埃拉拖色尼海山的浅层结构进行研究。这次调查航行是由教科文组织、欧洲科学基金会以及荷兰、英国、意大利、西班牙和俄罗斯各国的发起组织主办的。

在黑海，利用 MAK-1深水拖曳声学系统、水下电视和重力岩芯提取器对某些泥火山，包括第一次调查培训航行（海洋科学培训与教育计划(TREDMAR)）（1991年）发现的泥火山，进行了详尽的研究，研究发现泥火山区底部沉积物的滑动是很普遍的现象。在MSU与 Yuzhmorgeologiya 泥火山附近发现了奇异的交叉线。从TREDMAR 泥火山中提取的气体水合物晶体的样本。

在地中海 Olimpi 泥底辟区范围内的海脊上发现了大约二十处新的泥丘，利用岩芯取样法对其中九处进行了检测。大部分泥丘不是泥底辟，而是泥火山，坡上有大量泥流。Olimpi和 Premetheus 两个泥底辟区被证明是可能继续向东、西方向推进的唯一地区。拿波利泥丘上的水下电视记录下了大量的气体和液体渗出现象。从多伦多泥丘的尼角砾岩中发现了白垩纪岩石。

对于新近从埃拉拖色尼海山获得的地震数据的解释说明，这一高结构区的构造运动十分活跃，其北坡一直延伸到塞浦路斯境内下层，而其南坡上部则被黎凡特板块冲断。该海山的外壳上层处于构造延伸区，被正常断层切断。海山的上新第四纪沉积物平均厚达130 米。海山顶部发现了被说成是麻点的圆洞。

Acknowledgements

The editors of the report and the cruise participants wish to express their appreciation to UNESCO and European Science Foundation for the valuable financial contribution through the Training and Education in Marine Science programme (TREDMAR) of UNESCO and the Network on Advanced Field Study Workshops on Mediterranean Marine Geosciences of ESF. We would like to thank personally the representatives of these organizations Alexei Suzyumov, Dirk Troost and Peter Colyer for constant encouragement and help.

V.A. Dvurechenskiy and I.F. Glumov from the Committee for Geology of Russian Federation and B.G. Saltykov, the Minister of Science and Technical Policy of Russian Federation are gratefully thanked particularly for providing the well equipped R/V Gelendzhik and financial support.

Financial management, advice and support were provided to the programme by the Netherlands Marine Research Foundation (SOZ); and we wish to thank especially E. Bringmann and J. Stel (Director, SOZ) for their personal efforts and support.

The authorities of Turkey lent support to the cruise by granting free port calls and free entry to the ship in their waterways. The U.K., the Netherlands, Italy and Spain provided financial and organizational contribution to the cruise.

For their help during preparation and execution of the cruise and carrying out the field excursion and midcruise meeting we also thank to Dr. M. Ergün and Prof. Dr. M.K. Düzbastilar (Dokuz Eylul University, Izmir, Turkey).

CONTENTS

1. INTRODUCTION

R. Kidd and A. Limonov

The Third UNESCO-ESF Training Through Research (TTR-3) Cruise aboard the R/V *Gelendzhik* took place between the 5th of June and the 19th of July 1993 in the Black Sea and the Eastern Mediterranean Sea. The principal topic of the cruise was the investigation of the mud diapirism process in deep-sea environment and the elucidation of the tectonic features of the Eratcsthenes Seamount in the easternmost Mediterranean Levantine Basin. Traditionally, the Cruise had both the scientific and educational tasks, and specialists and students were gathered aboard the ship from Russia, the Netherlands, England, Ireland, Spain, Italy, Turkey, and Tunisia (Table I). The participants were divided into legs and assigned to specific teams on the different legs of the cruise according their current place of work and interests.

The cruise consisted of three legs. The first one was carried out in the central part of the Black Sea deep-water basin. This area was first investigated during the 1991 TTR Cruise, and the initial results were published (Ivanov, Limonov, and Woodside, 1992). However a rising interest to the Black Sea mud volcanoes made us to return to this area for further detailed investigations of some already known structures. The principal proponents for this area were Dr. Tj. C.E. van Weering and Dr. M.K. Ivanov.

OCEAN DRILLING PROGRAM SITE SURVEY

Three proposals for future scientific ocean drilling in the Mediterranean Sea are highly ranked by the international advisory panels of the JOIDES (Joint Oceanographic Institutions for Deep Earth Sampling) organization. Three proposals are currently being assessed, revised and reassessed by the Panels for possible drilling during the 1995 or 1996 campaigns of the Ocean Drilling Program (ODP). They propose drilling cruises in the Alboran Sea, on the Mediterranean Ridge and on an east-west transect from Gibraltar to the Levantine margin. The three proposals must retain their high scientific ranking in competition with proposals for drilling in each of the major oceans. Also they must be backed by sufficient geophysical survey data from each of their proposed sites to satisfy strict criteria laid down by JOIDES to ensure that the scientific objectives can be met by ODP drilling and that there are no safety and pollution risks associated with the potential locations. International collaboration among proponents within Europe has attempted to combine existing geophysical data sets from a number of institutions in support of these proposals. Nevertheless, new surveys are needed to define some of the key sites in each proposal and proponents have enlisted "ships-of-opportunity" to complete the survey data packages. The R/V *Gelendzhik*, with its impressive suite of geophysical and sampling equipment, is an ideal platform from which to carry out these investigations.

Proponents of the drilling suggested that the TTR programme might be interested in an opportunity to involve its students in "cutting-edge" international geoscience.

The second leg of the TTR-3 cruise in the Eastern Mediterranean Sea was scheduled to carry out investigations on the Mediterranean Ridge. Sites relevant to two of the Mediterranean drilling proposals could potentially be surveyed.

The principal objective was the Mediterranean Ridge mud volcano programme. Much information within this programme has been obtained already in the planned study area during the four previous cruises of the Italian R/V *Bannock* (1988-90), and the current cruise could refine the existing data package on the proposed Olimpi mud volcano site (MEDRIDGE MV-1).

One ODP proposal is to drill a series of shallow penetration sites on pelagic highs in an east-west transect from the Alboran to the Levantine Basins. This is in order to study the formation of organic rich (sapropel) layers that exist within the sediment sequences on longer time scales than are possible using conventional sediment coring. As a contribution to this "Mediterranean Sapropels" proposal (Zahn & others), R/V *Gelendzhik* carried out surveys and sampling at a site on the Inner Plateau of the Mediterranean Ridge (MEDSAP 2B) and another to the east on Eratosthenes Seamount (MEDSAP 1). The main proponents for the second study areas were M.B. Cita and R.B. Kidd.

The second ODP proposal is to drill a number of site transects at right angles to the Mediterranean Ridge to investigate the tectonic processes that have been active in this accretionary wedge of sediments during the continental collision of Africa against southern Europe. It is also proposed to drill deep sites on the Eratosthenes Seamount, a supposed old Tethyan fragment caught up in this collisional setting. R/V *Gelendzhik* was to carry out ODP site surveys to define sites on Eratosthenes Seamount (the MEDRIDGE ESM sites). The Eratosthenes Seamount was the object of the third leg of the cruise, the principal proponents for which were A.H.F. Robertson, R.B. Kidd, and J.M. Woodside.

During the port call at Izmir after the completion of the first leg, a two-day Workshop took place at Dokuz Eylul University. Lectures on geology of the Black and Mediterranean Seas and related mud volcanism were given by Tj.C.E. van Weering, M.K. Ivanov, M.B. Cita, A. Camerlenghi, and others. The geological excursion to the Karaburun Peninsula was organized under the leadership of Prof. Dr. M.K. Düzbastilar.

About 40 seminars, lectures and new data presentations were carried out aboard the shipby both members of scientific team and students.

Table I

List of participants of the Third UNESCO-ESF Training Through Research (TTR-3) Cruise

<u>First leg (8-22 June 1993)</u>: Black Sea mud volcanoes
<u>Second leg (24 June-7 July)</u>: Mediterranean Ridge mud volcanoes, survey of MEDSAP 2B and MEDRIDGE MV-1 ODP Sites
<u>Third leg (7-17 July)</u>: Eratosthenes Seamount, survey of MEDSAP 1 and MEDRIDGE ESM ODP sites

	Legs		
The Netherlands			
Tj.C.E. van Weering* [The Netherlands Institute for Sea Research (NIOZ), Texel]	1		
J.M. Woodside* (Free University, Amsterdam)		2	3
A. Pierrot-Bults (University of Amsterdam)	1		
C. Beijdorff (Free University)		2	3
W. van der Werff (NIOZ)		2	3
R. van der Meer (Free University)		2	3
M. Pott (Free University)		2	3
P. Bogaard (Free University)			3
T. van Soest (Free University)			3
Spain			
E. Ramos (University of Barcelona)	1		
F. Perez (Instituto de Ciencias del Mar, Barcelona)	1		
G. Ercilla (Instituto de Ciencias del Mar)	1		
T. Vazquez Garrido (University of Cadiz)	1		
P. Basquets (University of Barcelona)	1		
J. Galindo Zaldivar* (University of Granada)	1	2	3
A. Moncada (University of Barcelona)		2	
L. Nieto (University of Granada)		2	3
N. Vera (University of Barcelona)		2	
B. Alibés (University of Barcelona)			3
M. Carmen Campo (University of Barcelona)			3
J. Fraile Maseras (University of Barcelona)			3
United Kingdom			
N.H. Kenyon (Institute of Oceanographic Sciences, Godalming)	1		
Ch. Forster (University of Southampton)	1		
J. Pike (University of Southampton)	1		
G. O'Sullivan (University of Wales, Cardiff)	1	2	3
R.B. Kidd* (University of Wales)		2	3
A.H.F. Robertson* (University of Edinburgh)			3
S.J. Wakefield (University of Wales)		2	3
L. McMurrey (University of Wales)		2	3
R. Flecker (University of Edinburgh)			3
C. Glover (University of Edinburgh)			3
Italy			
M.B. Cita* (University of Milano)		2	
E. Erba (University of Milano)		2	

R. Lucchi (University of Milano)		2	
Turkey			
M. Ozerler (Dokuz Eylul University, Izmir)	1		
H. Eronat (Dokuz Eylul University, Izmir)	1		
Tunisia			
M. Ouakad (Universite de Tunis 2, Bizerte)	1		
Russia			
M. Ivanov* (Moscow State University)	1	2	3
P. Rozov (Yuzhmorgeologiya)	1	2	3
Yu. Gubanov (Yuzhmorgeologiya)	1	2	3
B. Rubtsov (Yuzhmorgeologiya)	1	2	3
V. Tsyganenkov (Yuzhmorgeologiya)	1	2	3
Yu. Yakovlev (Yuzhmorgeologiya)	1	2	3
A. Pavlov (Yuzhmorgeologiya)	1	2	3
L. Meisner (Yuzhmorgeologiya)	1	2	3
V. Fomenko (Yuzhmorgeologiya)	1	2	3
A. Matveenko (Yuzhmorgeologiya)	1	2	3
A. Guselnikov (Yuzhmorgeologiya)	1	2	3
A. Ziberov (Yuzhmorgeologiya)	1	2	3
S. Korkovidov (Yuzhmorgeologiya)	1	2	3
I. Prokof'ev (Yuzmorgeologiya)	1	2	3
A. Shanin (Yuzhmorgeologiya)	1	2	3
A. Ovcharov (Yuzhmorgeologiya)	1	2	3
V. Vasil'ev (Yuzmorgeologiya)	1	2	3
A. Koshman (Yuzhmorgeologiya)	1	2	3
P. Lygin (Yuzhmorgeologiya)	1	2	3
V. Trofimov (Moscow State University)	1		
A. Limonov (Moscow State University)	1	2	3
V. Gainanov (Moscow State University)	1	2	3
E. Basov (Moscow State University)	1	2	3
A. Volgin (Moscow State University)	1	2	3
V. Babushkin (Moscow State University	1	2	3
I. Korotkov (Moscow State University)	1	2	3
I. Korneva (Moscow State University)	1	2	3
E. Kozlova (Moscow State University)	1	2	3
K. Ivanova (Moscow State University)	1	2	3
A. Lototskaya (Moscow State University)	1	2	3
E. Akent'eva (Moscow State University)	1	2	3
V. Mironova (Moscow State University)	1	2	3
E. Kameneva (Moscow State University)	1	2	3
S. Polikarpova (Moscow State University)	1	2	3
G. Akhmanov (Moscow State University)	1	2	3
S. Buryak (Moscow State University)	1	2	3
A. Grobushkin (Moscow State University)	1	2	3
R. Al'mendinger (Moscow State University)	1	2	3

*National coordinators

1. METHODS

The description of the methods of data acquisition and processing has been published earlier (Limonov et al., 1993). Only new methods and specification, which have been changed, are given below.

1.1. SEISMIC PROFILING

V. Gainanov

EQUIPMENT

Seismic profiling equipment and technology used during this cruise were in principle the same as during the TTR-2 Cruise (1992), with several changes.

An IMPULSE-1 air gun has been used instead of a SHIP air gun because of technical problems with the latter. It is more powerfull, but generates a seismic signal with multiple pulses and a lower frequency range. Parameters of the "IMPULSE-1" air gun are as follows:

Working volume................................3.0 l
Working pressure..............................12.0 MPa
Signal frequency range........................10-250 Hz
First positive pulse amplitude
at a distance of 1 m ....0.3-0.4 MPa
First positive pulse duration.................7-11 ms

The hydrophone streamer was also modified and had the following parameters:

Receiving length..............................75 m
Numbers of receiving sections.................6
Section length................................10.5 m
Number of hydrophones per section.............21
Type of hydrophones...........................PDS-7
Distance between centres of sections..........12.5 m
In-line offset
min...................................400 m
max...................................475 m

SHIPBOARD SEISMIC DATA PROCESSING

Data recorded by the GROT acquisition system have been processed in two steps. The first step was carried out by a shipboard processing complex, consisting of an ES-1011 computer, convolvers, and special output equipment. In the second step digital data have been processed with an 486-DX computer.

The first stage included the following procedures:

REFORM - reformatting field records from the GROT format to the computer format (ES-1011);

KINAPL - normal moveout corrections;

COMPLX (DECON, FILT, BALA, GAIN) - deconvolution, filtering, balancing, and gain regulation of traces;

STATED - static correction - normalizing the time sections to a single time;

WGSTACK - stacking of traces;
RESTSA - amplitude recovery;
COLPLT - preparing data for display on the plotter.

The personal computer-based processing included a predictive deconvolution and the Stolt migration (in the f-k-domain). This step of processing took place between the RESTSA and COLPLT procedures. The predictive deconvolution was applied to diminish or eliminate the airgun bubble effect. To improve seismic data recorded in complex seismo-geological conditions, the Stolt migration was used. This procedure resulted in partial removal of diffraction hyperbolae produced by steep relief features of the bottom and subbottom structures.

The output of the first channel on a plotter was made after the REFORM procedure to provide preliminary data control. After the complete processing, the final time sections were used for a geological interpretation.

1.2. UNDERWATER TV

Ch. Forster

The Deep-sea Videozond TV system is designed for surveys at a water depth of up to 6000 m. It can be operated independently or as a part of various underwater systems and units. In combination with other methods, Videozond can be used for the observation of surface structure, sediment colour, sediment composition and bottom conditions.

Videozond primarily consists of three rigidly-connected units (Fig. 1), the central one being composed of a TV camera, video-recorder and the controlling electronics. A receiving transducer is mounted in the upper part of the unit. A spacer contains a pressure sealed connector for connection to the communication line and a feedthrough for connection to the external battery. Two side units contain halogene lights and batteries. The link between Videozond and the shipboard section is carried out through a conductor cable KGP1-150 and a cable windlass. The units guarantee the safety and functioning of all this equipment at great depths.

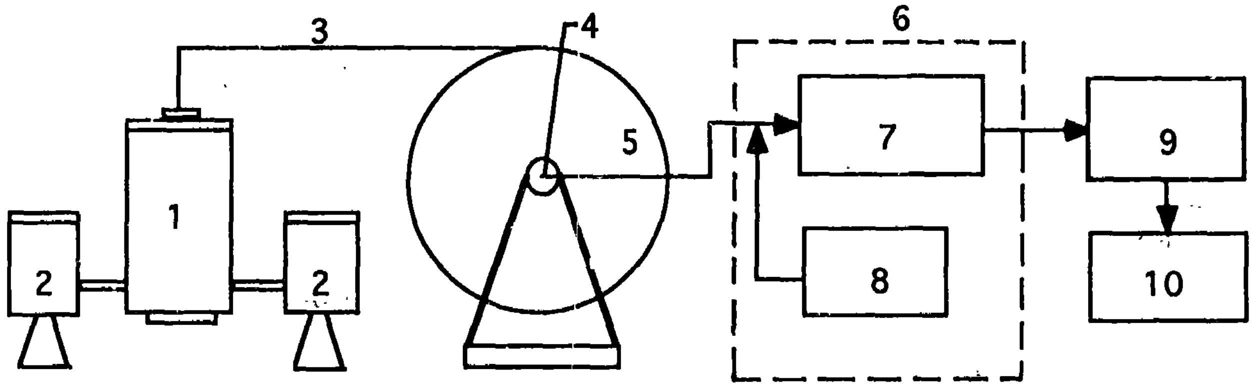

Fig. 1. Underwater TV system
1- unit - video-camera and recorder; 2 - storage for batteries (lights); 3 - communication line; 4 - spindle; 5 - reel; 6 - control unit; 7 - cable amplifier corrector (compensator); 8 - remote control console; 9 - VCR; 10 - TV monitor

---

Shipboard units incorporate the control console, the video-recorder and the TV monitor. The control console consists of a cable amplifier-corrector and a remote control. The cable amplifier-corrector provides corrections and necessary amplification for reconstruction of the video signal level and other electric parameters. With the using of up to 7 km of cable KGP1-150, it is possible to transmit coloured pictures by cable. A system of remote control is used to turn the equipment on and off.

A TV survey is carried out at a distance of from 0.5 to 3 m above the bottom surface. A scout-weight is operated to control this distance. Focusing and colour control is automatic and colour determination testing is carried out aboard the ship before launching the system. Colour video recording is undertaken on the Videozond, however, contemporaneous black and white pictures are relayed back to the ship. (See Table II for specifications).

Table II

Specifications and working parameters of the deep-sea Videozond system

Camera system	
Working pressure	600 atm (about 60 MPa)
Dimensions	1.2x1.2x0.5 m
Weight	60 kg
TV unit	
Resolution	350 lines
Number of grades	7
Necessary minimum illumination of the object	10 lx
Lighting	
2 halogene lights	12V 50W
Power unit	
External Storage battery	12V 14A/h
Communication line	
Conducting tow-cable	KGP1-150
Length	10 km
Record	
Video-recorder	VHS system
Time of continuous record	3 hrs

1.3. GEOLOGICAL SAMPLING

R. Kidd, G. O'Sullivan, and A. Limonov

Geological sampling during the 1993 Cruise almost always was carried out after preliminary MAK-1 sidescan work. The sampling sites were chosen on the basis of information obtained about bottom morphology. A satellite navigation system and echosounder were used to locate the correct sampling position.

The sampling was performed using conventional methods. The main device for this purpose was a gravity corer, up to 7 m long, 168 mm inside diameter (i.d.), and with a weight of up to 1500 kg. A detachable plastic core liner, 6.1 m long and 137 mm inside diameter, made it easier to extract cores. For this cruise such cores are designated TTR 3 xx-G, where xx refers to the sequential number of the sampling station, and G indicates use of the gravity corer.

Box cores were obtained using a Reineck corer with a 20 x 30 cm box. Such cores are designated TTR 3 xx-B, with xx being replaced by the sequential station number and B referring to the box corer. Surface preservation was good in all retrievals. Sub-sampling of the box core was carried out using 1 x 15 cm (i.d), 1 x 10 cm (i.d) and 1 x 6 cm (i.d) core tubes, which were subsequently used for sedimentological description, pore water extraction and solid phase archive material respectively (see Section 2.4).

Kastenlot core samples were obtained using a 4 m long stainless steel barrel having a square cross-section of 15 cm by 15 cm. Such cores are designated TTR 3 xx-K in the core nomenclature. The procedure of sediment extrusion from the barrel enables a number of similar whole core samples to be obtained which can then be used for a variety of shore-based and shipboard determinations. This is achieved by the corer having a false bottom which provides a mechanism for raising the core in stages. Thus when laid out horizontally with the top side removed a complete core length is revealed with coherent stratigraphy. Two complete core length samples are taken using 1 m lengths of 5 cm by 5 cm cross-sectional area 3 sided "trunking", which is fully pushed down into the sediment; these provide an archive and a sampling sub core for the Cardiff repository. Between these sections 60 ml syringes are used to extract samples from which pore waters are obtained (see section 2.4). These syringes should be removed to the Constant Temperature Room (CTR) as a matter of priority. Using T bars screwed into the base of the barrel, the false bottom is then raised approximately 5 cm to expose the base of the trunking. These can then be removed using a cheese wire to cut them out cleanly. This then exposes another fresh face from which further trunking, vials or X-radiography slabs are taken. A complete core will provide 1 set of X-ray slabs, 4 lengths of trunking and 1 set of syringes plus associated samples for bulk density determinations. The order in which these various sub samples are taken from any one Kastenlot core will be determined by the scientific priorities of the cruise programme. However, such methodology results in the maximum utilization of the core material.

1.4. GEOCHEMICAL SAMPLING

S. Wakefield, G. O'Sullivan, and L. McMurrey

The geochemical analyses carried out on material obtained on this cruise were based upon sub-samples taken from box cores. The sub-sampling procedure was as follows.

The box core with the preserved sediment/water interface was lowered gently onto the deck. Such gentle lowering was essential to ensure that the upper poorly consolidated sediment layers were not homogenized by coring procedures. When the core was secure, sub-sampling was carried out using 104 mm diameter plastic tubes. The lower ends of these tubes are sharpened and the tubes are gently pushed into the sediment. When the plastic tube reached the base of the box core the top of the plastic tube was sealed. A number of plastic tubes can be inserted into the box core enabling a large amount of sample to be taken. After sealing they were labelled, removed and stored at a constant temperature laboratory.

In the constant temperature laboratory the tubes containing the sample were placed under a glove box, where a mechanism enabled the sample to be screwed up through the base of the glove box into the overlying glove bag. As the sediment is screwed up through the base it can be cut off and placed in sample vessels; this enables very accurate determination of the location of the sample with respect to the sediment water interface.

This glove bag is connected via a high pressure hose and gas regulator to a cradle of compressed nitrogen gas bottles which are used to fill the glove bag; an oxygen meter monitors atmosphere inside the glove bag to ensure that it is oxygen free. It is essential that the sub sampling of marine sediments to be used for geochemical analyses is carried out in an oxygen free environment to prevent the aerobic decay of the sediments.

Pore waters were obtained by placing a sample in a centrifuge tube and centrifuging the sample in a refrigerated centrifuge set at the temperature of the sea floor. The pore waters obtained were stored in plastic bottles and contained in refrigerated facilities. Silica, phosphorus, barium, nitrate, nitrite, sulphur and oxygen determinations will be determined by wet chemistry ashore. Analyses well be made upon a Perkin Elmer Ultra Violet and Visual light Spectrophotometer (UV-VIS).

The sediments will be prepared for geochemical analyses by oven drying at 50°C followed by hand grinding using an agate mortar. Major element analyses will be carried out by X-Ray Fluorescence (XRF) on fused beads; minor elements will be determined by XRF on pressed powder beads. Marine standards will be routinely run along with the samples.

Biogenic silica determinations will be made using the sequential leach extraction method of Demaster (1981); the biogenic silica in leach to be determined by UV-VIS. Organic phosphorus determinations will be made using the hot acid to be determined by UV-VIS. Biogenic silica and organic phosphorus have previously been determined in sediments using X-Ray Diffraction (XRD) techniques; however, as both biogenic silica and organic phosphorus are amorphous such a method is not considered to be satisfactory.

Total carbon determinations will be determined by dry combustion, carbonate was determined by coulemetry, the difference between these two figures constitutes the organic carbon content of the sediment. $\delta^{13}C$ isotope analyses were determined using the method of Fontugne and Deplessey (1978), measurements were made using mass spectrometry.

2. BLACK SEA MUD VOLCANO AREA (STUDY AREA 2)

2.1. GEOLOGICAL SETTING

SEDIMENTARY STRUCTURE AND MUD VOLCANISM

Tj. van Weering , A. Limonov, L. Meisner, and G.O'Sullivan

The present Black Sea represents a unique environment in that it is a relatively large, deep, intracontinental, anoxic basin. The Black Sea is connected via the Bosporus sill with the Mediterranean, thus forming a semi-stagnant basin with anoxic conditions from about ~100 m waterdepth to the bottom. These conditions were firstly described some 100 years ago by Androusov (1890), and have attracted considerable scientific attention since then.

Structurally, the Black Sea consists of the slightly elongated East and West Black Sea Subbasins, separated by the regional Androusov Ridge.

Post-Mesozoic sedimentation in both subbasins is enormous. The sedimentary sequence consists of 12-15 km of highly reflective, well stratified, uninterrupted and hardly faulted strata. Only off the Crimean Peninsula and the Caucasus, compressional thrusting has resulted in faulting and uplift of the Neogene formations.

The mud volcano area is situated on the abyssal plain below 2000 m depth, in the eastern West Black Sea Subbasin. The abyssal plain in the study area is characterized by a generally flat topography between 2100-2200 m depth. Between the mud volcanoes the seabottom has microrelief features like ridges or other irregular features (see Section 2.2.b).

Paleocene and Eocene sediments have a thickness of 6 km here, and the Oligocene-Lower Miocene (Maikopian) sediments are more than 5 km thick. Quaternary sediments also reach a considerable thickness, the base being at maximum 1.7-1.8 s TWTT (1500-1600 m) below the seabed.

This area was studied during both the 1991 and 1993 cruises (Fig. 2). It has rather limited dimensions (about 80 x 80 km) and differs from the rest of the West Black Sea Subbasin by the presence of low amplitude folds, flexures and faults in the upper part of the sedimentary cover (below ’00 ms TWTT).

Mud diapirs in the Black Sea and in the Sea of Azov have been studied over a long period by geologists and geochemists from various institutions in Russia, most notably from Moscow State University, the former USSR Ministry of Geology, the Academy of Sciences and the Research Institute for Geology and Mineral Resources of the Ocean in St.Petersburg.

The presently known mud volcanoes seem to be randomly distributed and do not show alignment. T ..e (Malyshev, Kornev, and Goncharov, see Fig. 2) are situated on a large structural high at the top of the Maikopian, which extends in a SW-NE direction. Some mud volcanoes may be associated with intersecting regional faults (Yuzhmorgeologiya, unpublished data).

During the 1991 Training through Research Cruise and in earlier cruises by Yuzmorgeologiya and Moscow State University, mud volcanoes have been described and studied from an area SSW of the Crimea (Ivanov et al., 1992).

Their forms resemble craters with rims consisting of extruded mud and mud breccia and with large mud flows at their slopes. They rise 40-120 m above the seabottom. The volcanoes in the study area have a diameter ranging from 300 to 2000 m (at the seabed). Some of them have a depression at their top resembling a crater like structure and with rims at the margins extending up to 15 m above the crater floor level. One of the mud volcanoes showed collapse structures at its margins. In 1993 this mud volcano was investigated in detail and named Tredmar. A single profile recorded across the Vassoevitch mud volcano indicates probable collapse structures there as well (see Section 2.2.a, Fig. 5).

On multichannel seismic sections the mud volcanoes show an absence of coherent seismic reflections in a zone that may differ in width from several hundred meters up to 3.5 km. Vertically this zone can be traced from the sea bed down to depths of 7-9 km. However the precise level of their roots is not known. Around the upper feeder channel (in Quaternary sediments), the seismic reflectors are bent down. This may be caused by collapse of the sedimentary layers due to eruption activity, but on the other hand, may result from a velocity anomaly because the feeder channels contain relatively low velocity water- and gas-saturated sediments. The latter is supported also by the apparent down-bending of the reflector at the top of the Eocene deposits, underneath the volcano. In the Mio-Pliocene section, the seismic reflectors, on the contrary, bend upwards at the margins of the volcanic channel.

The 1991 seismic (sparker) records showed many indications for the local subsurface presence of gas in the form of bright spots, discontinuous high amplitude reflectors, or acoustic masking effects within the seismic sequence. Although recent studies by deep-tow sidescan sonar (by Yuzhmorgeologiya, 1992 [unpubl. data] and during the present cruise) revealed that extensive mud flows including blocks and clasts are characteristic features of the mud volcanoes, it is not yet clear in how far this reveals recent activity. However, active gas seepage has been reported recently (Polikarpov et al., 1989; this cruise), and gas hydrates have been sampled previously and also during the present cruise to a limited extent, the gas consisting for over 90% of methane.

The eruptive products of the Black Sea mud volcanoes consist of grey or brown-grey viscous mud with abundant inclusions of mud breccia. The mud locally is highly saturated with gas. The mud breccia is made up of fragments of unconsolidated Quaternary sediments, Pliocene sandstones, (pieces of) siderite concretions, and fragments of the Maikopian clays (which usually predominate in the mud breccia). No fragments older than Maikopian were found so far in the mud breccia, although the analogous mud volcanoes in the Kerch and Taman Peninsulas erupt mud breccia of even Cretaceous-Jurassic age (Shnyukov et al., 1971). On the basis of the composition of the mud breccia from the Black Sea mud volcanoes and there seismic signatures, one can conclude that they principally are related to the thick homogenous Maikopian clays.

RECENT SEDIMENTS

The laminated sediments of the Black Sea were discovered during one of the first scientific cruises to the area some 100 years ago (Androusov, 1890). But only after the Atlantis II cruise in 1969 the general features of the sedimentology of the Black Sea became widely known in the West (Ross et. al., 1970; Degens and Ross, 1972; Ross and Degens, 1974).

The essential stratigraphy (Section 2.2.d, Fig. 25) is that the Recent facies (unit 1) consists of alternating light and dark laminae. The formation of these laminae depends upon seasonal variations in the generation and transport of particles in the basin; the light laminae are almost entirely comprised of the nannofossil *Emiliania huxleyi*; whereas terrigenous material largely comprises the darker laminae (Hay and Honjo, 1989). Organic carbon values in this unit vary, reaching a maximum of around 4% by weight (Calvert and Fontugne, 1987). The $\delta^{13}C$ signature for modern Black Sea marine plankton is -23‰, this figure not being affected by varying amounts of phyto- and zooplankton. The $\delta^{13}C$ signature of unit 1 shows that the origin of the organic matter varies from about 25% terrestrial to about 50% terrestrial and 50% marine.

Very fine grained turbidites (up to 20 cm thick, but generally less) occur in this unit. Although these turbidites do not seem to be laterally extensive, they highlight the importance of lateral transport processes in the basin.

Underlying this coccolith ooze is a sapropel (unit 2). The boundary between the two units is often abrupt (Ross and Degens, 1974). The sapropel contains more than 14 (weight) % organic carbon (Calvert and Fontugne, 1987). Unit 2 also includes turbidites. The sapropel unit displays very heavy $\delta^{13}C$ signatures, with the sharpest peak coinciding with the maximum accumulation of organic carbon, close to the -23‰ of modern marine Black Sea plankton. This indicates that the organic matter in the sapropel has an almost entirely marine origin. The $\delta^{13}C$ signature shows increasing proportions of terrestrial organic matter towards the base of the sapropel. This continues down into unit 3 unit.

Below the sapropel is a series of laminated moderately calcareous clays, with turbidite intercalations characterized by a low organic carbon content (unit 3).

At the base of the laminated coccolith marl a chemically and mineralogically well-mixed layer with consistent organic carbon values is considered a mudflow or slump deposit (Calvert and Fontugne, 1987).

The average geochemical composition of the three Black Sea sedimentary units can be seen in Table III. These data confirm the distinction of the three lithological units in the Black Sea.

Unit 1 shows slight enrichment in mixed marine and terrestrial organic carbon, as well as moderate enrichments in Mo and U.

Unit 2 has higher levels of S and Mo, but similar levels of U and V compared to unit 3 and is enriched in marine organic carbon. The sapropel has significantly higher concentrations of

Mo, U and V. Enrichments of Mo, V and U associated with organic carbon enrichments are believed to be due to reduction with subsequent scavenging of reduced species by organic matter for Mo, V and U or by iron sulphides for Mo; or to reduction followed by the formation of insoluble compounds such as Mo sulphides and V (IV) and U (VI) hydroxides (Calvert, 1976, 1990; Anderson et al., 1989; van der Weijden et al., 1990). The distinctive geochemical signature of the second unit has been compared by Middelburg et al., (1991) to organic carbon rich radioactive shales formed at times of marine transgressions.

Table III

Average geochemical composition of Black Sea sediments

Unit	C_{org}	S	Fe	Mo	V	U
1	1.8	1.3	3.9	30	123	3.9
2	6.3	1.4	4.0	71	231	3.6
3	0.6	0.7	3.8	5	138	3.6

C_{org}, S and Fe values are in wt%, Mo, V and U are in ppm. Data from Calvert (1990), U data from Cagatay et. al., (1990).

Unit 3 has organic carbon with a $\delta^{13}C$ signature that is terrestrial in origin and with Mo and U concentrations close to average shales (Middelburg et al., 1991). The lacustrine facies unit 3 would have been deposited at a time when the Black Sea would have been isolated from the Mediterranean by glacio-eustatic sea level lowering.

Following climatic amelioration and reconnection to the Mediterranean some 9000 years before present, the Black Sea would have experienced an influx of saline water leading to displacement of nutrient-rich deep waters into the photic zone resulting in a pulse of increased marine productivity marked by unit 2, the sapropel. Finally fully marine conditions were established as unit 1. The coccolithophorid species *Emiliania huxleyi* would have invaded the Black Sea following reconnection to the Mediterranean.

Sapropel deposition is believed to have commenced across the Black Sea some 6000 years ago, deposition ended in the shallow waters some 4000 years ago, persisting in the deep waters until 1600 years ago (Calvert and Fontugne, 1987; based on ^{14}C dating). Based on varve counting, sapropel deposition began 5100 years ago and persisted until 1000 years ago (Hay, 1988). A sapropel is not accumulating in the Black Sea today due to a decrease in the marine productivity associated with an increase in terrestrial input.

2.2. RESULTS

2.2.a. SEISMIC REFLECTION PROFILING

A. Limonov and L. Meisner

Seismic reflection profiling in Area 1 was carried out along four lines crossing three mud volcanoes (Fig. 2). The recording range was 2 s (TWTT), which allowed the structure of the sedimentary cover to be observed to a depth of more than 1500 m with a resolution of about 20 m.

Judging from the isopach map by Tugolesov et al. (1985), all sections recorded outside the mud volcano area display primarily a Quaternary sequence. Pliocene sediments presumably can be seen in some places in the lowermost part of the seismic sections.

Line PR-248A runs in a south-north direction. The line starts 6 km to the south of Tredmar mud volcano[1] and crosses it. The sedimentary sequence is clearly divided into two members. The upper one is horizontally layered, undeformed and is displayed as a set of rare, strong and continuous parallel reflectors separated by semitransparent units. The lower member is often disturbed by faults and gentle folds and looks like a series of frequent, strong and continuous reflectors.

The Tredmar mud volcano was crossed by seismic line PS-248A along the center (Fig. 3). The volcano shows an asymmetrical cone, with a collapsed northern rim. The reflectors in the Pliocene-Quaternary sediments are more deformed nearer the mud volcano. Away from the axis of the mud volcano the deformation is expressed as normal faults which develop only in the lower part of the seismic section (1 sec TWTT and more below the seafloor). The nearer the mud volcano, the younger the faults are, however they do not penetrate into sediments shallower than 500 ms. The apparent fault offsets are 20-40 m. Because the faults form a quite symmetrical pattern on both sides of the mud volcano, this fault system is probably concentric and is related to the general collapse of the sedimentary layers in the volcano feeder channel. Between the faults and the volcano feeder channel, the layers of the host sediments sharply bend down for the same reason. The mud volcano feeder channel itself is characterized by chaotic seismic reflection configurations, widening downsection in a cone like form. Its apparent width in the visible lower part reaches 3 km as compared with about 1 km near the bottom surface. No signs of bright spot reflections were found in the vicinity of the Tredmar mud volcano.

Short line PR-249 is at right angles to the previous one and is oriented from west to east. The remarkable feature of this line is a zone of tectonic disturbance near time mark 20^{15} (Fig. 4). This disturbance affects only the lower, well-stratified part of the hemipelagic sequence and does not penetrate into the

---

[1]This mud volcano was discovered during the TTR-1 Cruise (see Ivanov et al., 1992) and was left unnamed then.

Fig. 2. Location map for Area No 1
1 - MAK-1 line; 2 - seismic line; 3 - sampling stations; 4 - underwater TV runs. The general position of the study area is shown in the inset

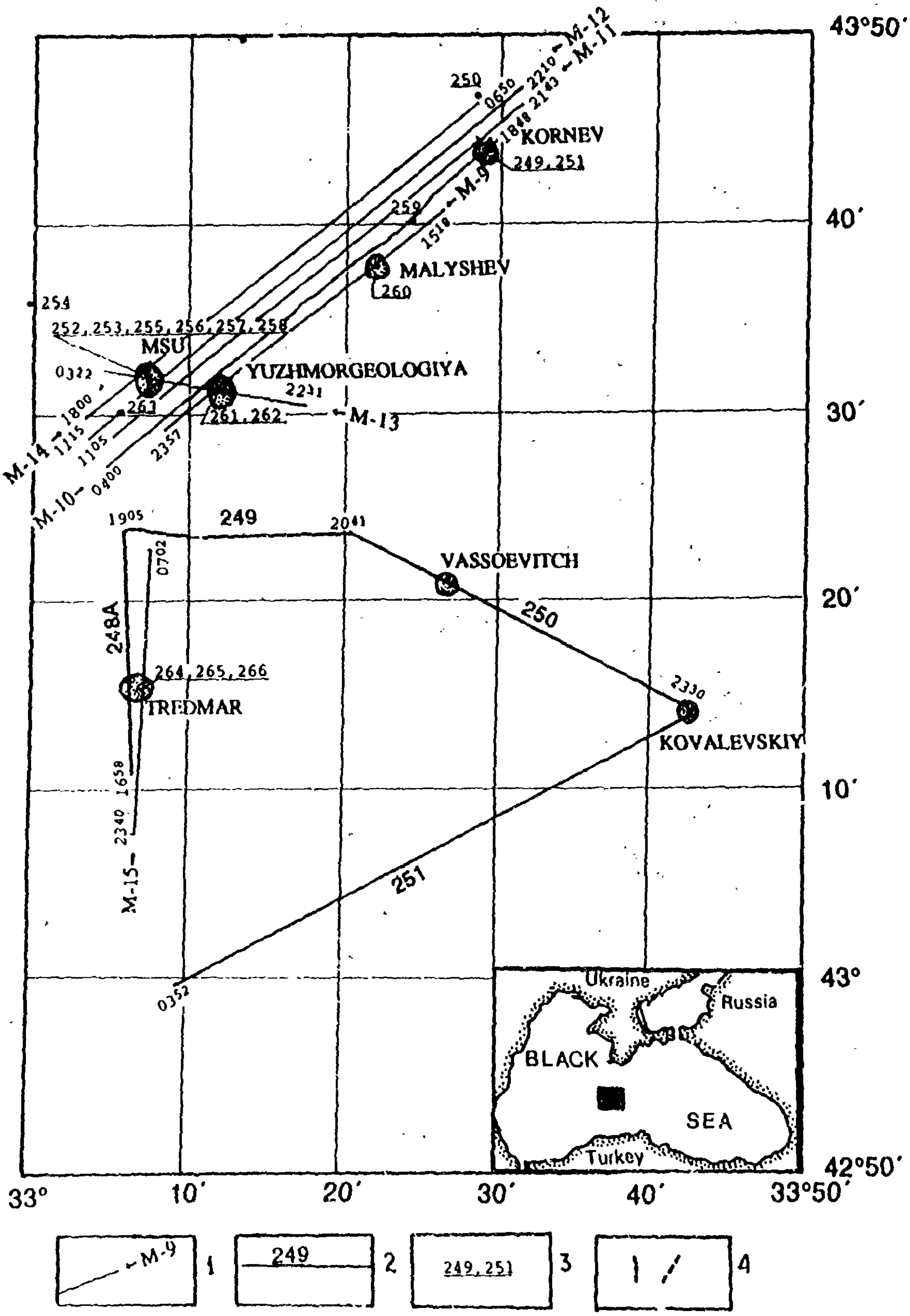

semitransparent member. The apparent width of the zone is about 1.5 km, remaining constant through the entire section. The zone is topped by a 70-80 m thick lens, with chaotic inner seismic reflection configurations. Because this zone is situated more than 15 km away from the nearest (known) mud volcano, it is unlikely to have any relation to it.

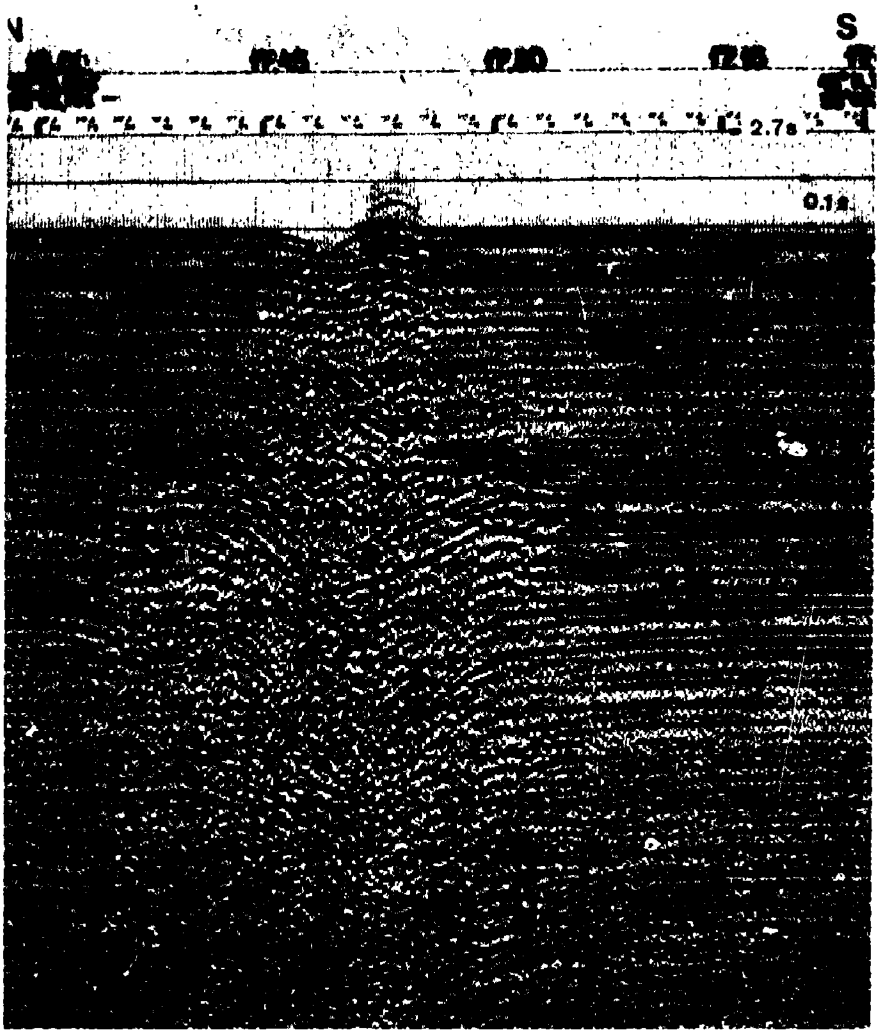

Fig. 3. Seismic profile (PR-248A) across the Tredmar mud volcano. Note two different seismic members (LM and UM) and the reflector separating them. The large faults do not penetrate into sediments of the upper seismic member

Morphologically the zone of tectonic disturbance has many features common with mud volcanoes (boundary faults, downbending of the surrounding sedimentary layers toward the center, and cone like summit). Therefore, one can conclude that the line has crossed an edge of a presently inactive mud volcano which is buried beneath approximately 400 m of sediments. Bright spot reflections are seen right above this structure and near time mark 20^{20} at a depth of 650 and 730 ms below the seafloor.

Fig. 4. Assumed buried mud volcano (arrow) on seismic profile I

Line PR-250 runs NW-SE, across the Vassoevitch mud v[illegible] o and ends at the center of Kovalevskiy mud volcano. The Vassoevitch mud volcano was not crossed exactly over its center. Its feeder channel looks like a 1.5 km wide vertical column in the upper seismic member and is about 2.5 km wide in the lower seismic member (Fig. 5). It has a structure resembling the

Tredmar mud volcano, although the boundary faults are not so clearly displayed. The record across a part of the Kovalevskiy mud volcano has a similar appearance. It also looks like vertical zone with chaotic seismic reflections, somewhat wider in the lower member. A collapse pattern in the form of sharp downbending of the host sediment layers is very distinct in the semitransparent member.

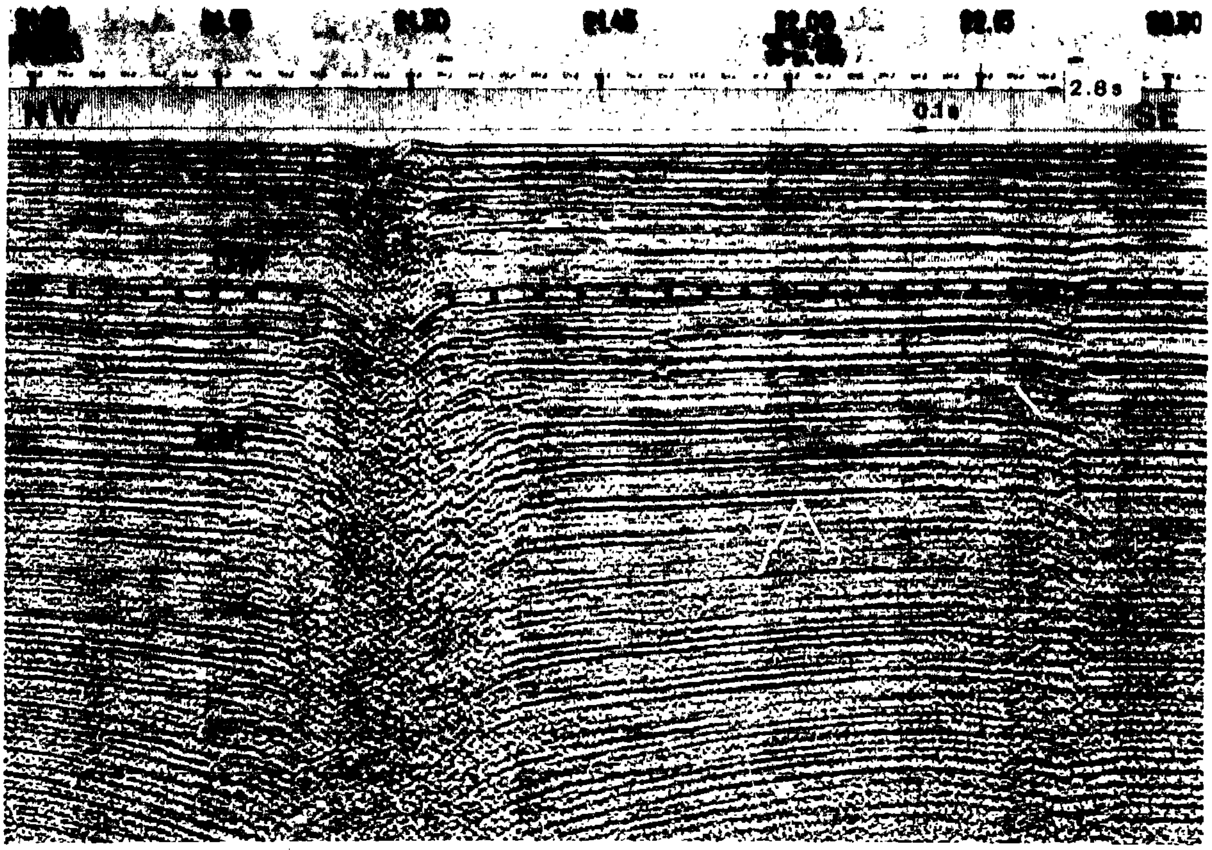

Fig. 5. The feeder channel of the Vassoevitch mud volcano (seismic line PR-250) is seen to be wider in the lower seismic member

---

The host sediments of the lower member form a very gentle anticline between the two mud volcanoes. At two places (22^{20} and 22^{50}) there are up to 1 km wide fault zones, with a 20-30 m vertical offset. One of these zones, situated to the northwest, is the only recorded fault zone which is to some extent reflected in the upper seismic member; the reflectors at the bottom of this form low amplitude (about 10 m) gentle flexure, quickly disappearing up the section.

Line PR-251 runs to the northwest from the Kovalevskiy mud volcano. The seismic record shows a normal sequence of hemipelagic sediments divided into the semitransparent and well-stratified members. No mud volcanoes were recorded along this line. The lower member is cut by normal faults near time marks 00^{15}, 00^{25}, 00^{50}, 01^{00}, and 02^{35}.

The interface between the well-stratified and semitransparent members seems to be an important boundary in the Quaternary history of the Black Sea Basin, marking a sudden activation and then quick cessation of tectonic movement. Because all the revealed faults have a constant vertical offset throughout the whole recorded section and reach only the top of the well-stratified member, they apparently belong to post-sedimentary deformations which took place after accumulation of this member. A significant decrease of the width of volcanic channel in the upper semitransparent member may indicate a sharp decrease of the mud volcano activity after this boundary.

2.2.b. SIDESCAN SONAR SURVEY

OKEAN SONOGRAPHS

N. Kenyon and A. Limonov

Four OKEAN sidescan sonar lines were recorded in the region south of our MAK-1 survey and near to the deepest part of the basin (Fig. 2). Only the starboard side was functioning, with a range of about 7 km.

The seabottom gradients here are very low, apart from the mud volcanoes.

Broad bands of relatively strong backscatter are mapped crossing the swaths. They are about 600-800 m wide and have a variety of trends. One has a crenulate edge (Fig. 6).

Fig. 6. Backscatter pattern on the OKEAN record from the deepest part of the Black Sea Basin (line 249). Such acoustic features may correspond to sand deposits. The swath range is about 5 km

They resemble high backscattering features seen on Gloria sonographs from similar areas, such as the bottom of the Mississippi Fan, adjacent to the Florida abyssal plain (Twichell et al., 1991). Such acoustic features were found to correspond, in that instance, to sands in cores. The sands were a few metres below the seabed and were both graded turbidites and debrites (Twichell et al., 1992). If the patterns here represent sand deposits they would have been carried by flows coming from the continental margin to the north and west.

A large feature with a high backscatter, which bears much resemblance to the OKEAN images of the Mediterranean mud volcanoes (see Section 3.2.b), was recorded on line 251. Its has irregular borders and visible dimensions of about 12 x 4.5 km , thus it would be the greatest mud volcano discovered in the Black

Sea (Fig. 7). However no signs of mud volcano feeder channel is visible on accompanying seismic section PR-251, except for a set of faults on the east flank of the feature. Two explanations are possible:

1. The mud volcano feeder channel is situated to the south of line PR-251, and only thin mudflow on its slope highly saturated with mud breccia was reflected on the OKEAN sonograph.
2. The feature could be a mass flow accumulation which came from the Turkish margin.

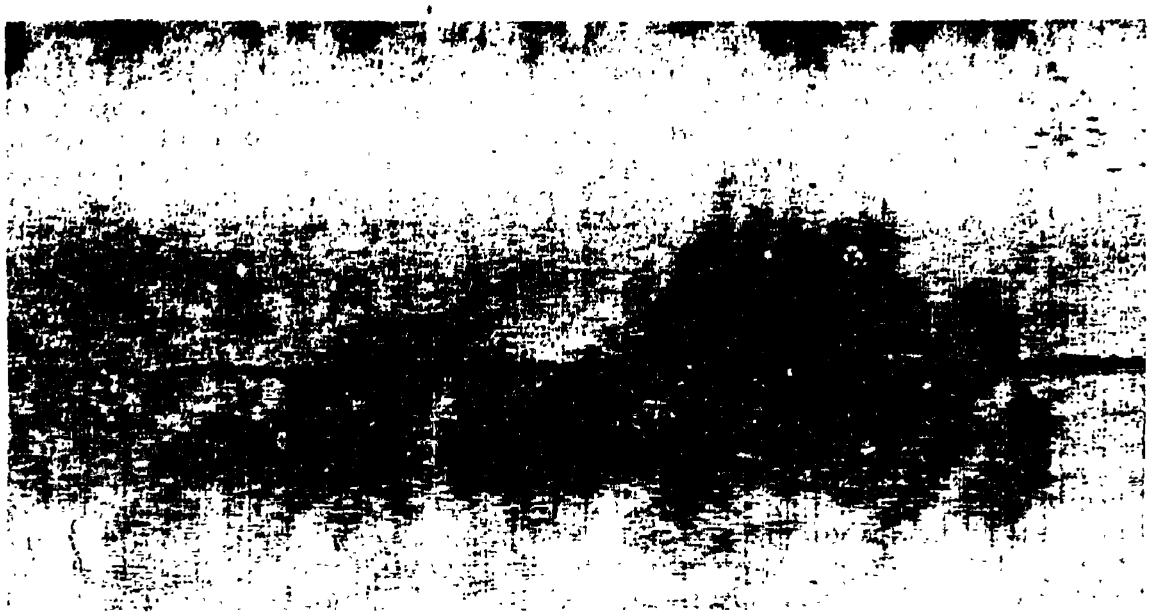

Fig. 7. A feature with strong backscatter which could be a flank of large mud volcano or a sand accumulation. The swath range is about 7.5 km. Line 251

MAK-1 SONOGRAPHS AND PROFILES

N. Kenyon, Tj. van Weering, Yu. Gubanov, A. Limonov, G. Ercilla, T. Vazquez, and F. Perez

Introduction

Five lines were run using the 30 kHz sidescan sonar on the MAK-1 system. They form a mosaic that runs in a northeast-southwest direction (Fig. 2) and which includes four of the mud volcanoes. An additional 30 kHz MAK-1 line was obtained over the Tredmar volcano. A high resolution line, with the sidescan operating at 100 kHz, was made across the Yuzhmorgeologiya and MSU volcanoes. This viewed the seabed at a scale that is four times the scale of the 30 kHz record and enabled a comparison to be made.

The data was analyzed by dividing the records into acoustic facies on the basis of their appearance on the sidescan and the 5.5 kHz profiler. Each facies is given a subjective, geomorphological name if this was considered to be justified by the data. The facies are chosen on the basis of location, relationships with their surroundings and acoustic character in plan view and profile.

Mud volcanoes

The mud volcanoes studied in more detail during this leg were the Moscow State University (MSU) (Fig. 8), Yuzhmorgeologiya (Fig. 9), Malyshev, Kornev, and the Tredmar volcano (Fig. 10).

Of this group of volcanoes, MSU and Yuzhmorgeologiya are by far the largest, with diameters at the seabed from 2-2.3 km, and an elevation above the surrounding seafloor of 80-112 m. Kornev and Malyshev have a diameter at the seabed that varies from 1.6-1.8 km, and reach a height above the surrounding seafloor of 40-75 m. While the former have a complexly shaped top with a crater like structure and a well-defined rim, the latter two have a conical shape and are almost circular at their basis. The Tredmar volcano has the most irregular shape; it consists of a steep, irregular rimmed southern and southwestern margin which rises 30 m above the sea bed, and a depressional collapse structure at its eastern and northeastern margin. The depression's floor is at 40 m below the seabed and shows evidence of slumping at its northern margin.

It is evident from the MAK-1 profiles that MSU and Yuzhmorgeologiya have been built up over a long period as a result of, most possibly, successive, massive mudflows that spread from eruptive center(s) in the crater over the rim and across the flanks. Where the mudflows - characterized by a somewhat transparent acoustic character on the profiles and a generally irregular topography - intercalate with the normal, well-layered, continuous abyssal plain sediments, the latter show an onlap character, resulting in a smoothening of smaller scale topographic irregularities (5-8 m) that characterize the flank and craters of these volcanoes.

The flanks of both the Yuzhmorgeologiya and MSU volcanoes are covered with numerous large and small, stacked and superimposed mudflow deposits. These may show a massive character (in which case they have a number of arcuate wrinkles at their lower boundaries parallelling the outline of the flow). Or, the mud flows have been transported via radiating, bifurcating or parallel channels at the outer margin of the flow. Within these flows there are local irregularities that probably indicate the presence of blocks and breccia.

Retreating, successively partially overlapping mudflows along the flanks of both MSU and Yuzhmorgeologiya volcanoes indicate that at present no massive mudflows reach far away from the rim of the crater and a decrease of activity in the course of time. This observation is further supported by the acoustic profiles over their summits which show that the relief is subdued due to the presence of recent sediments. The 1993 sampling results confirm this interpretation. In fact it seems that recent mudflows are confined within a smaller area of the crater and result in local irregularities. These have a random orientation, as can be seen in the high resolution MAK-1 profile of part of the MSU volcano. The active part here is a cone at 12-15 m above the surrounding mudflow.

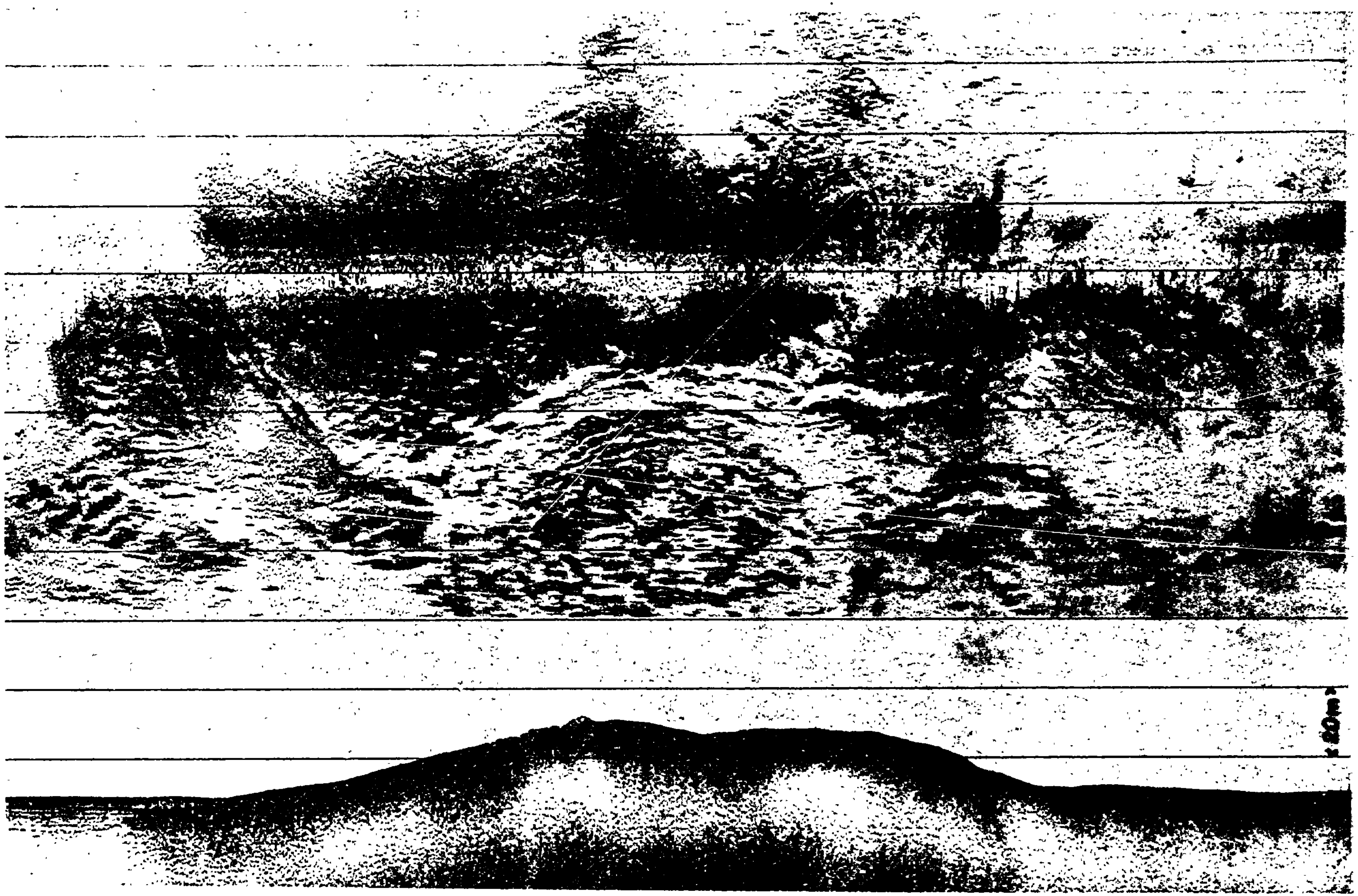

Fig. 8. The MSU mud volcano with extensive mud flows spread down the slopes. The swath range is 2 km. (MAK-1 line 14)

Fig. 9. The Yuzhmorgeologiya mud volcano acting as obstacle to material transported downslope (arrows). The swath range is 2 km. (MAK-1 line 9)

Relatively small circular or oval structures within the crater may indicate small, local vents and seeps.

The Kornev and Malyshev volcanoes both have a relatively steep, only partially smoothened cone and probably are at a less mature stage of development than MSU and Yuzhmorgeologiya. Both have slopes characterized by radial, small channelized mudflows, and lack the massive flows described before. This most possibly indicates that they have less deep feeder channels and/or that local pressure conditions are different.

Fig. 10. The Tredmar mud volcano. Note a collapsed rim and massive mud flows concentrating mainly in crater. The swath range is 2 km. (MAK-1 line 15)

The Tredmar volcano has a strongly irregular topography at its southern and southwestern margin, suggesting that post eruption sedimentation on top of the rim is relatively little. The acoustic profile and the 1993 sampling results confirm this conclusion.

Submarine slides

The submarine slides are seen as seafloor with complex patterns of mesotopographic features. Their relief is fairly low, rarely exceeding 10 m, and they occur in that part of the continental rise where the overall gradient is about 1 in 200. A variety of patterns were distinguished in the slide areas. They are:

1. *Arcuate steps with stronger backscatter.* These are always concave downslope. Usually there are several crescentic features joined together to form a feature up to 700 m long. The width of the strongly backscattering crescents is fairly constant implying a fairly constant depth to the steps of between 4 m and 7 m (Fig. 11).

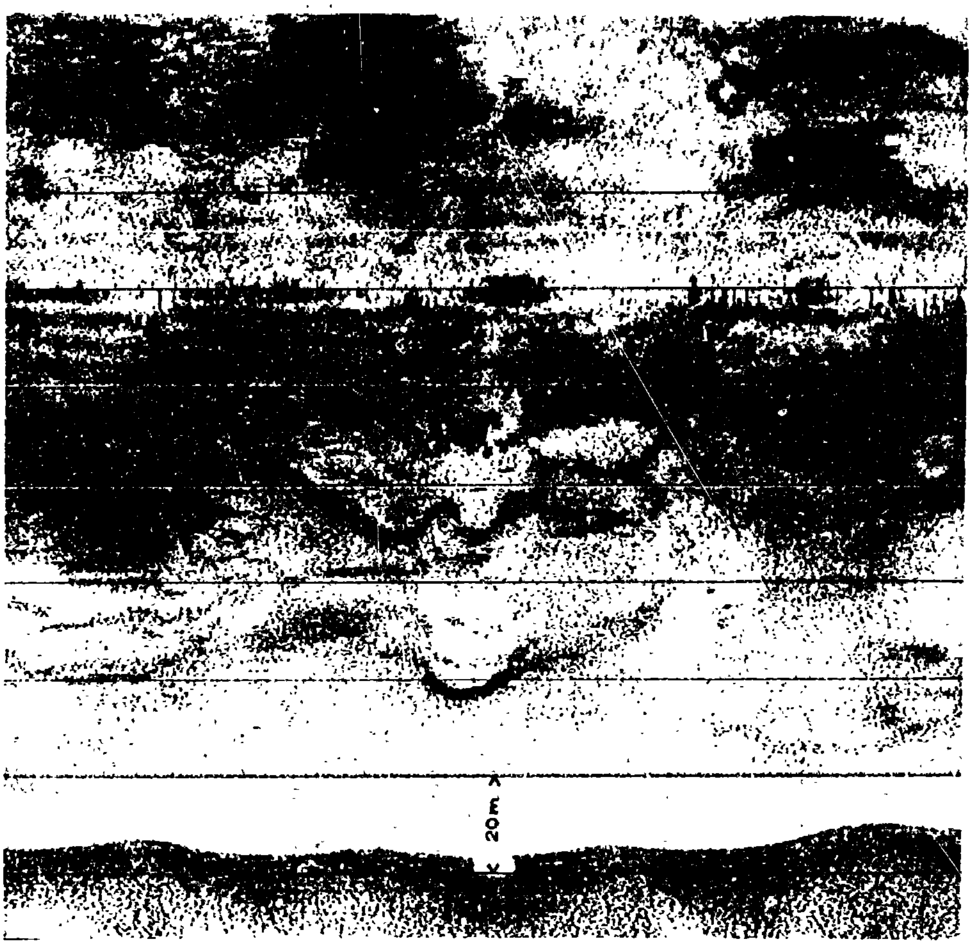

Fig. 11. MAK facies 1. Arcuate steps with stronger backscatter. The swath range is 2 km. (MAK-1 line 11)

They are thought to be large scour holes eroded by strong turbulent flows. Such holes have been seen in a variety of deep sea situations, e. g. channel floors (Shor et al., 1990), channel overbank (Normark et al., 1979) and channel mouth (Kenyon et al., in press). There is little evidence for the depth in the succession at which this type of scours occurs.

2. *Arcuate features with weak backscatter.* They are usually concave downslope but are longer than type 1 (up to 1500 m). There is less evidence for them being stepped relief.

These may also be scours. They may appear as fainter images because they are more deeply buried, probably below 4 to 5 m of sediments.

3. *Longitudinal deeps.* They are up to 6 m deep and sometimes have concave downslope crescents at their upslope ends. They are aligned parallel to the line of greatest slope.

These are also considered to be scour holes. The most prominent one, which has a depth of 5 m, but has one side higher than the other, is thought to be guided by a normal fault as the beds are at different levels on either side.

4. *Circular and oval deeps.* These are up to 7 m deep and when oval are longitudinal features, i.e. aligned downslope. They range in size up to 300 m by 150 m (Fig. 12).

Two possible causes considered are scour holes and pockmarks, the latter due to gas escape but modified by scouring flows to cause the asymmetry.

5. *Small equidimensional blobs.* They are of similar size (up to 80 m across) and tend to occur in groups (Fig. 13).

They may be blocks that have slid into place, small mud volcanoes or pockmarks. The latter perhaps due to water escape from rapidly deposited sediments or to deep seated methane gas escape.

6. *Broad bands of contrasting backscatter.* They are between 200 m and 500 m wide and aligned longitudinally (Fig. 14).

These are perhaps some sort of flow banding, where the deposits from the flow(s) have travelled at different speeds and/or at different times.

7. *Obstacle marks.* The Kornev and Yuzhmorgeologiya volcanoes have acted as obstacles to material transported down slope, resulting in parallel streaks to either side and downflow (Fig. 9).

The slide area has been subdivided into a northern, central and southern zone on the basis of the different proportions of the mesotopographic features that they display.

Northern slide area. The two main features seen in the region of our survey are types 1 and 2. There appears to be a cover of about 4 m of fairly continuous, parallel bedded sediment over a more complex level (Fig. 15).

Central slide area. This is a region of subdued backscatter patterns, mainly smooth with a few examples of type 4. There is a cover of about 9 m of continuous, parallel bedded sediments. No obvious complex level was identified.

Southern slide area. This has many different kinds of mesotopography. Types 2, 3, 4, 5, 6, and 7 are found. A cover of up to 4 m of continuous, parallel bedded sediment is present over part of the area but is missing in places. Beneath is a complex sequence up to 5 m thick. The beds are discontinuous, sometimes transparent and sometimes bedded, with a layered fill in deeps in the underlying topography. Beneath there is a parallel bedded sequence, about 25 m thick with a prominent reflector at the base.

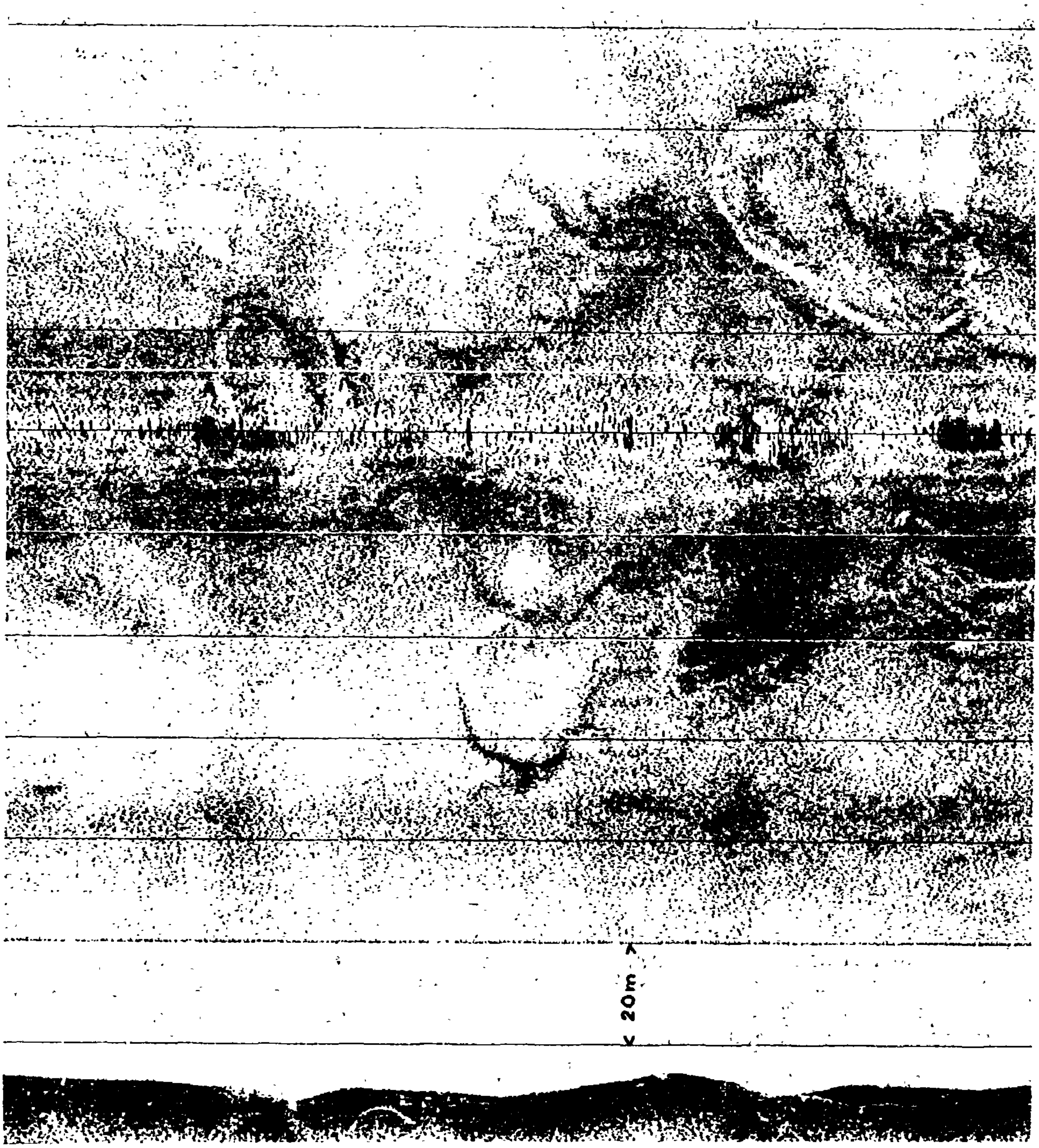

Fig. 12. MAK facies 4. Circular and oval deeps. The swath range is 2 km. (MAK-1 line 11)

Basin floor - smooth

The southern part of the region of study has a much lower gradient less than 1 in 500) than the area of the slides. Part of this area appears as uniformly weak backscattering on the 30 kHz sonographs, but on the higher resolution 100 kHz sonographs there are unusual narrow lines (see below). There is good penetration by the profiler and continuous, parallel bedding.

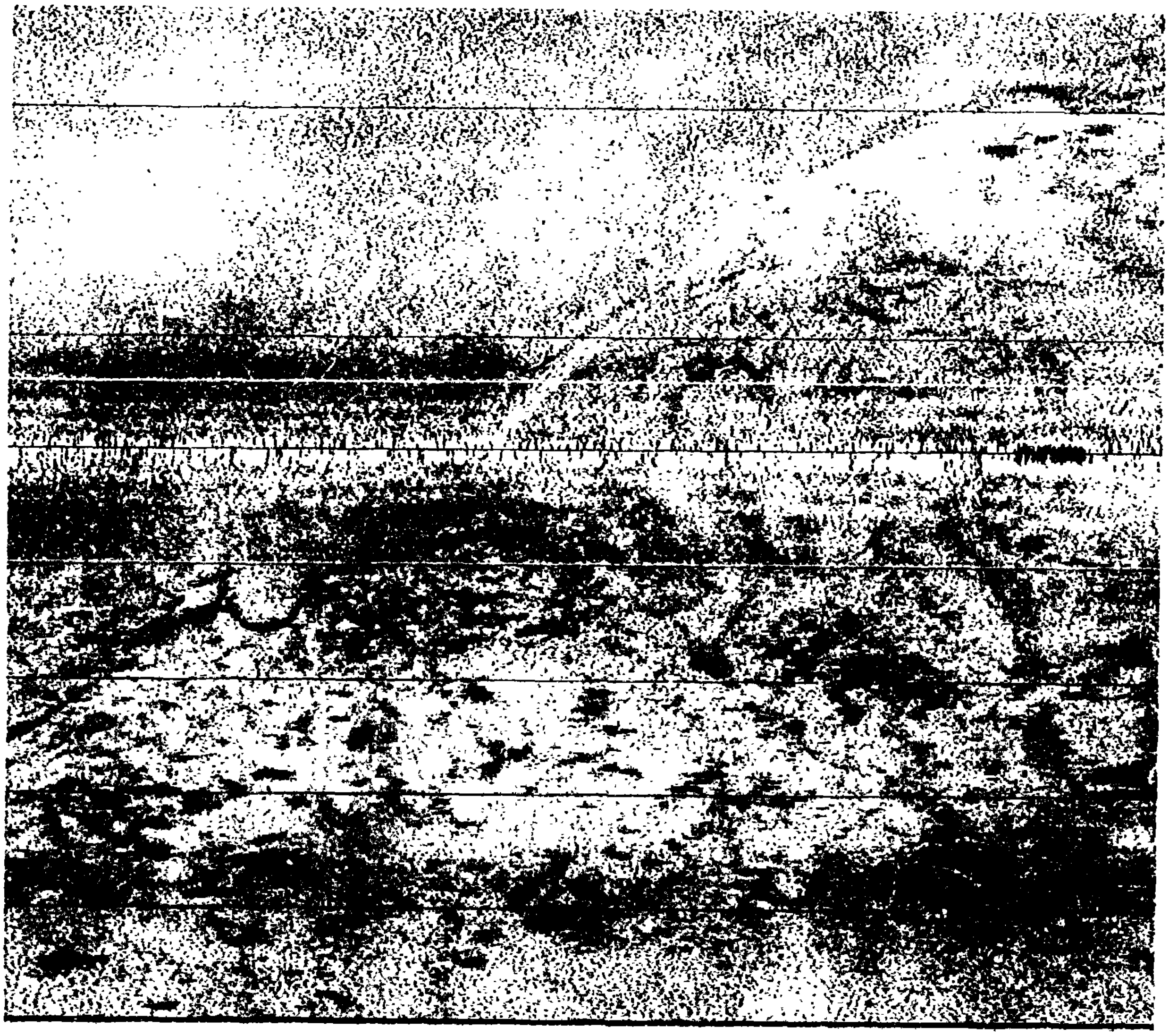

Fig. 13. MAK facies 5. Small equidimensional blobs. The swath range is 2 km. (MAK-1 line 12)

Basin floor - streaked

Both longitudinal streaks and shorter transverse features occur in the southernmost part of the region of study. They are regular bedforms. The streaks are between 50 and 250 m apart and much longer than they are wide. The transverse features resemble

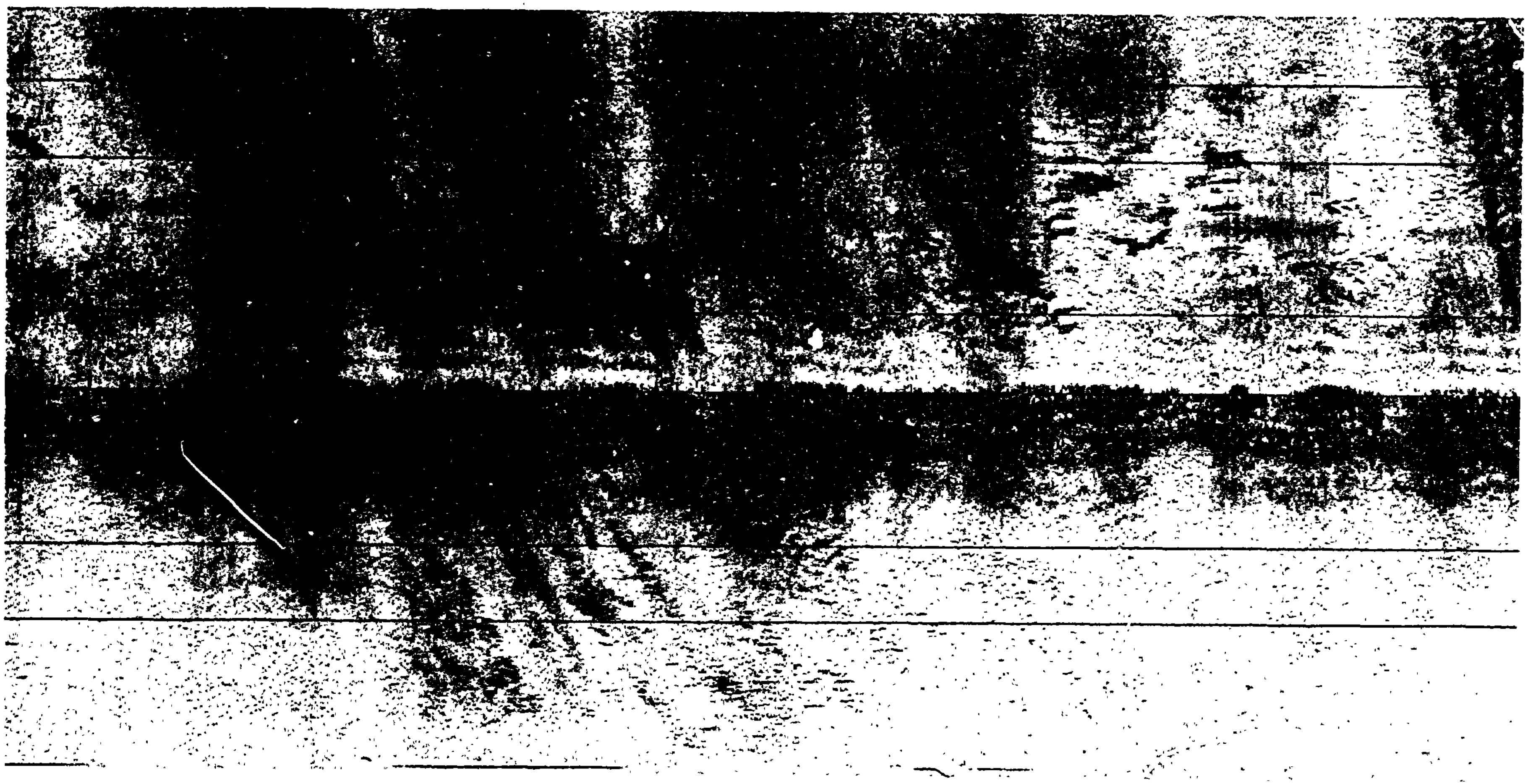

Fig. 14. MAK facies 6. Broad bands of contrasting backscatter. The swath range is 2 km. (MAK-1 line 10)

Fig. 15. Northern slide area. Acoustically turbid layer, which is the evidence for shallow gas occurrence, is clearly seen on the subbottom profile. The swath range is 2 km. (MAK -1 line 12)

sediment waves, having a wavelength of 25-50 m. Relief was not detected on the profiles. The two main trends for the streaks are N-S and WNW-ESE. There is poor penetration by the profiler. The streaks resemble current parallel bedforms such as tidal sand ribbons and trains of small sand waves (Belderson et al., 1972). One core in the area stopped in a sand bed.

Criss-cross lines

These are found on the high resolution sonograph away from the craters of the mud volcanoes, i.e. they are on the basin floor and the flanks of the mud volcanoes. The lines show moderate levels of backscatter, have a constant width of 3-5 m and are mostly straight with a few that are curved (the lines can be bent by up to 80°). The lines form an even network, with a spacing of about 50 m and a wide spread of trends, although there is a slight predominance of trends in the directions of N40°E, N65°E and N140°E (Fig. 16).

A number of widely differing possible origins were considered:

1. Faulting

No obvious faulting is seen on the profiles. However possible displacements are seen on the video runs outside of the crater of MSU volcano. These appear as groups of narrow white lines. Complex fault trends may be due to normal faulting associated with rim subsidence and uplift of the two adjacent diapirs.

Fig. 16. Criss-cross lines on high resolution (100 Khz) sonograph in the vicinity of the Yuzhmorgeologiya mud volcano (on the right). The swath range is 500 m. (MAK-1 line 13)

2. Tool marks

There are many types of tool that can cause such a pattern but some, such as trawling or naval activity are ruled out in this part of the Black Sea. Deep diving animals make widespread marks in the eastern Mediterranean (Kenyon, unpublished observation), but the marks are shorter and animals can not live in this deep and H_2S-saturated water. Iceberg plough marks have similar trends but they are more closely spaced; in addition, the waterdepth and geographical latitude of Area 1 make this impossible. Turbidity current caused tool marks are ruled out by the trends, some of which are across the direction of the nearby flows and by the occurrence of the criss cross features up on the flanks of the volcanoes.

2.2.c. UNDERWATER TV

Ch. Forster, E. Ivanova, A. Lototskaya, and H. Eronat

INTRODUCTION

During Leg 1 of the TTR-3 cruise an underwater television camera was lowered to the seabed on two separate occasions in order to record continuous video coverage over two of the mud volcanoes situated in the study area. The first of these studies was undertaken on June 12^{th} at 15^{13} for test of the equipment. Then the underwater camera was lowered at 16^{26} to scan a continuous track over the Kornev mud volcano until 17^{26} (Figs. 2, 17 and 18). The second study involved a two hour recording of video images over the MSU mud volcano on June 14^{th} starting at 16^{00} (Fig. 2 and 19). The following is a summary of the usage of the underwater television system and of the preliminary results of the respective studies.

DESCRIPTION AND INTERPRETATION OF BEDFORMS

Bedform 1: white strips

These pale features occur commonly on the tracts of seafloor scanned by the underwater video system. They are commonly 15-30 cm in width (although the width varies along the length of the features and the strips may even pinch out to scanty white filaments of only a few centimetres width). They typically have very little relief from the surrounding dark grey clay sediments and have a grainy surface texture. They are often seen in parallel sets of two or three strips which appear to be laterally continuous (Fig. 20). Strips are periodically seen to intersect but most of them are parallel features. Along the video section covering the MSU mud volcano these strips appear to be orientated in a SW-NE direction. Along the video covered section of the Kornev volcano there is no apparent underlying trend to these linear features although groups of strips share similar orientations.

The interpretation of such features is slightly subjective as it is largely based upon visual analysis of video footage. Therefore two possible explanations of the features are suggested[1]. The first is that the material is the result of bacterial growth, which is aligned with dominant current directions. The second interpretation is linked to a scouring mechanism in the basin, whereby the upper grey hemipelagic layer is removed to reveal a white coccolith-rich sub-layer. The latter interpretation is preferred because it was noted that during the video recording the camera caused certain current activity which disrupted the seabed sediments to reveal clay/coccolith layers. Discontinuous strips (such as those seen at 16^{10} and at 17^{31} in the MSU volcano track) may indicate saltation effects - possibly

---

[1]See the previous section for further suggestions.

caused by the motion of currents and debris on the abyssal plain (Fig. 21).

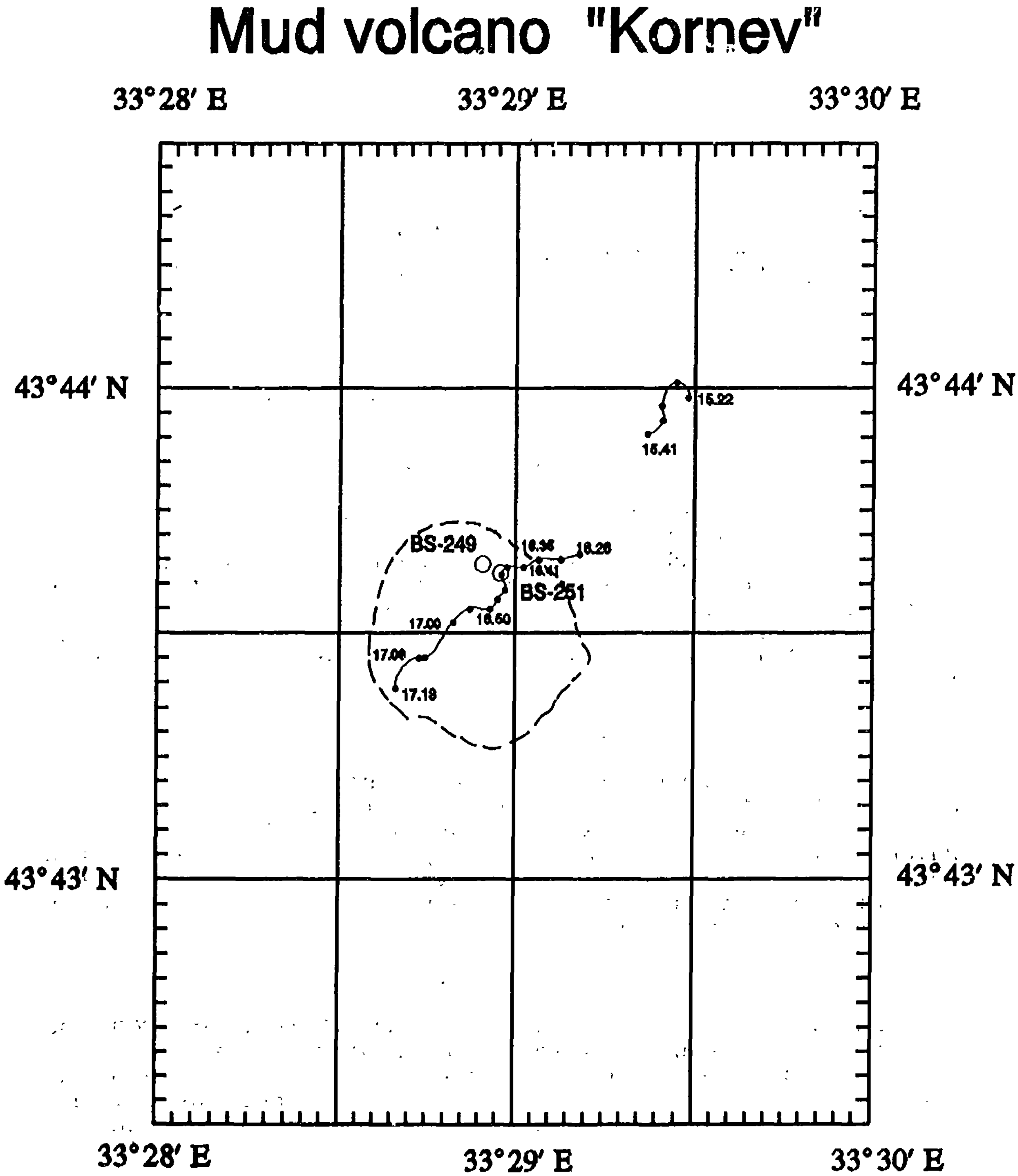

Fig. 17. Location of TV-1 track over the Kornev mud volcano

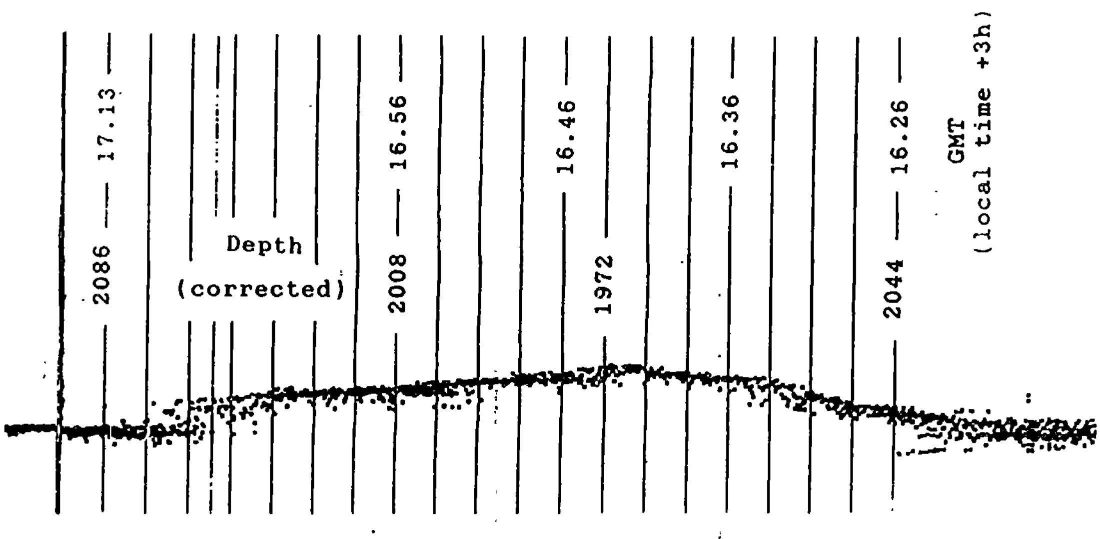

Fig. 18. The Kornev mud volcano. Bathymetry recorded during the TV-1 video track across the feature

Bedform 2: scars

These features were encountered on the outer slopes of both of the filmed sections of Kornev and MSU mud volcanoes. The bedforms commonly show evidence of sediment removal producing either elongate or arcuate scars on the surface of the seabed. These scars sometimes appear to be filled with dark clay layers. The scars are interpreted as the resultant gullies caused by submarine slumps. Fig. 22 shows a clear example of this type of feature.

Bedform 3: Blocky relief

These are perhaps more precisely described as ridges which protrude from the generally flat sediments of the basin-plain. They are composed of a more resistant and consolidated material which only have a fine clay covering. These are interpreted as relief which forms the flanks of the mud volcanoes, probably following breccia deposition by expulsion of various clay and sand fragments from the vent (Fig. 23).

Gas bubbles

During the two video scans of the Kornev and MSU mud volcanoes, it was apparent that bubbles of gas were rising from the sediment layers below the video-camera in certain areas. These bubbles represent expulsion of gases (such as methane) which filter through the sediments forming the mud volcanoes.

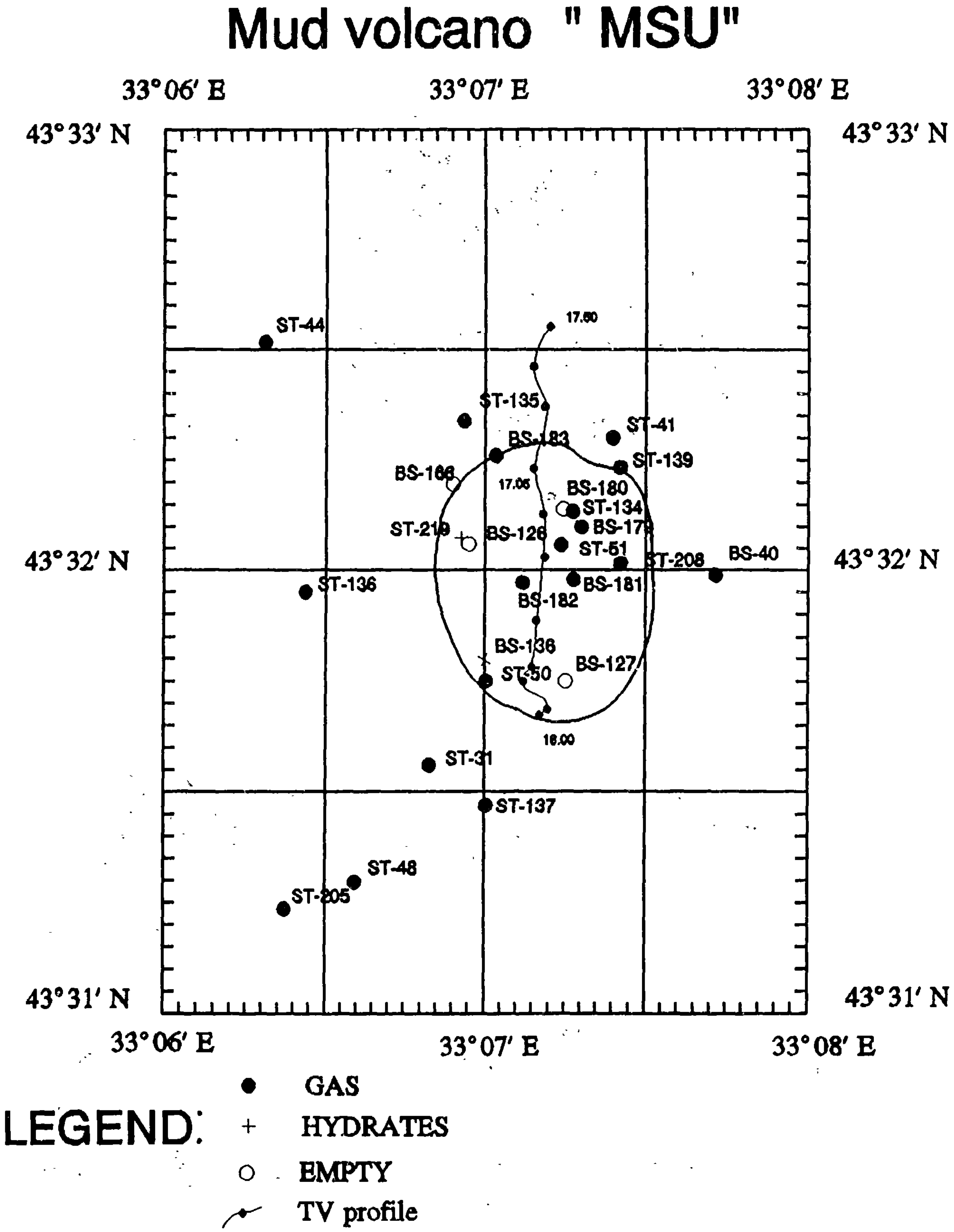

Fig. 19. Location of TV-2 track over the MSU mud volcano

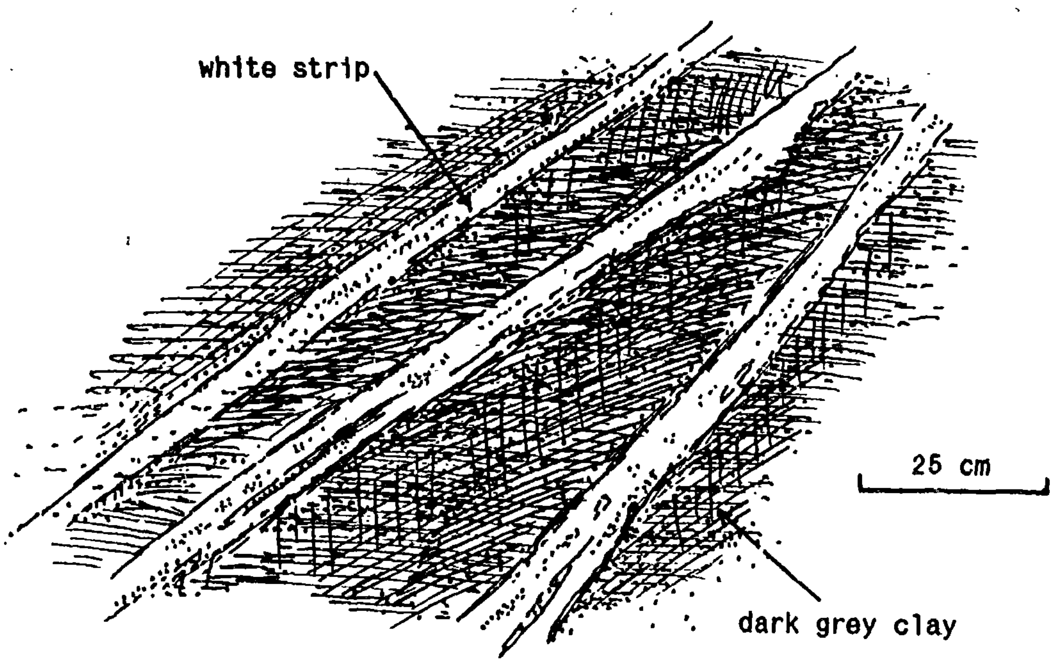

Fig. 20. Aligned grouping of white strips

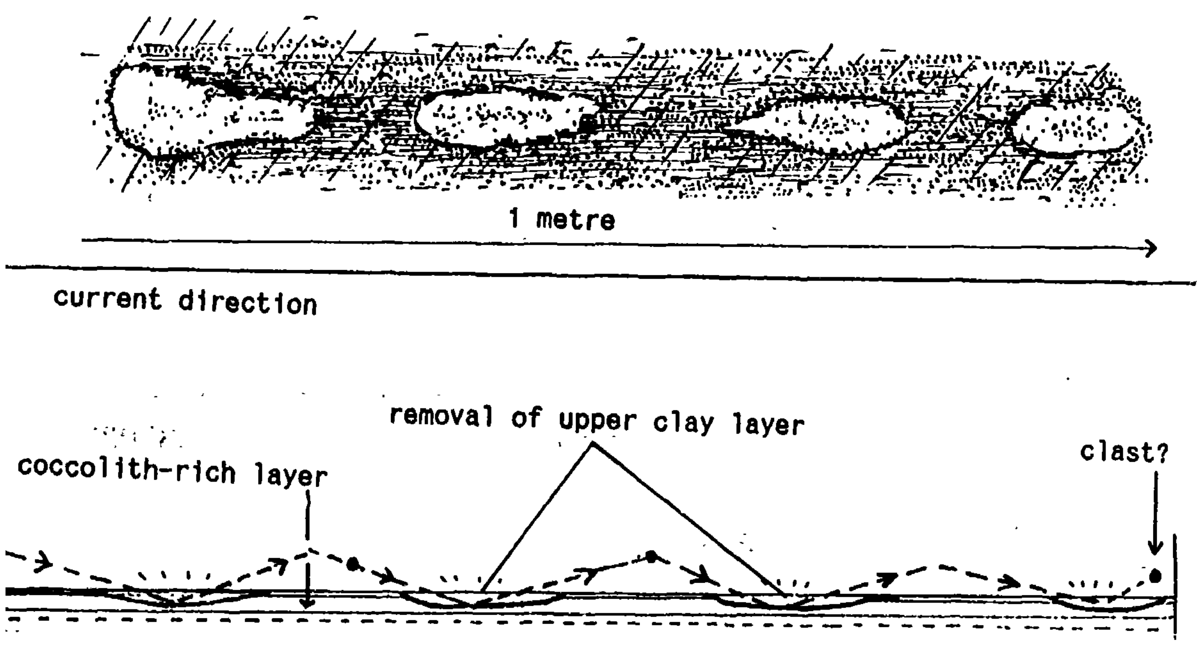

Fig. 21. Possible interpretation of discontinuous patchy strips

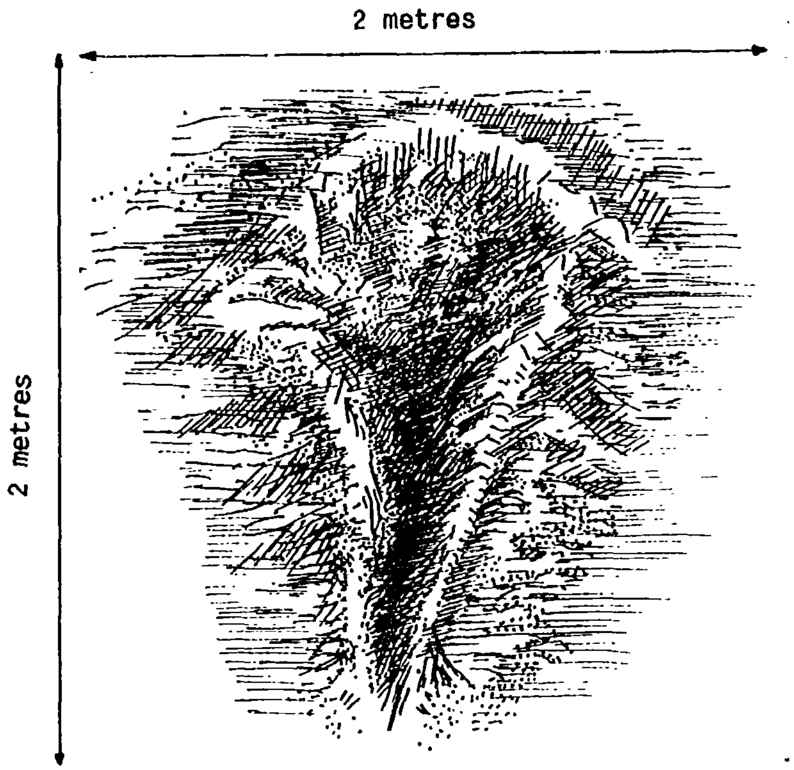

Fig. 22. Submarine slump (MSU track, 19[50])

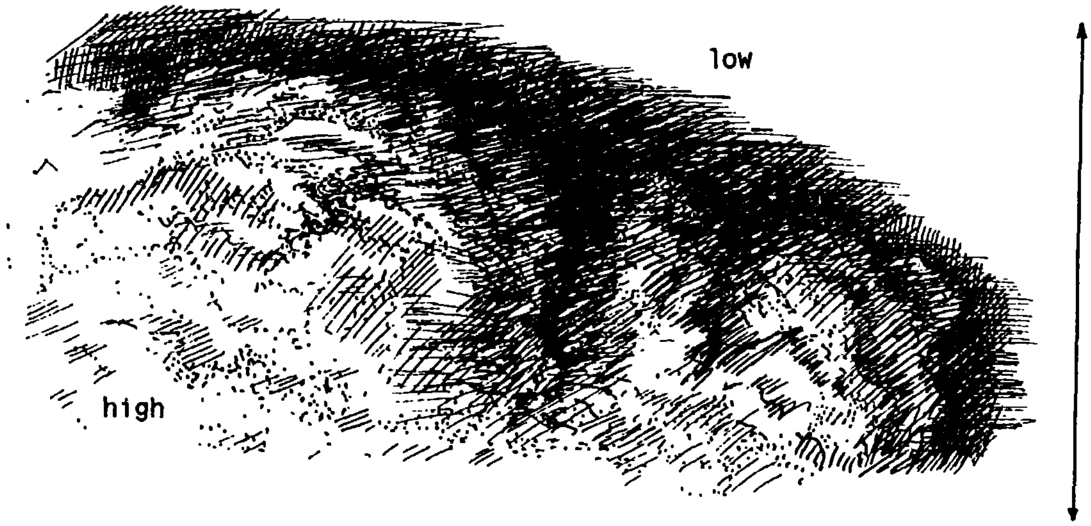

Fig. 23. Blocky relief (flanks of mud volcano)

It was noted that the dominant areas of gas expulsion on the Kornev volcano occurred between 17^{10} and 17^{12} representing an active zone to the southwest of the Kornev vent. A profusion of gas bubbles was also noted during the video recording of the MSU mud volcano site between the video-runs times 17^{17} and 17^{20}. During these times the video-camera scanned an area of gas expulsion on the MSU mud volcano which represents a zone bounding the margins of the volcano's northern slope. Gas bubbles were also observed (from 16^{20} to 16^{30}) in a second area to the south of the present day crater - away from the most recently deposited mud volcano sediments. This is close to a zone in which gas hydrates have been cored. Sapropels were not found in cored material and so, from this evidence, it is likely that this area of the MSU volcano is still unstable, with active gas-seeps and associated sediment processes.

2.2.d. BOTTOM SAMPLING

GENERAL DESCRIPTION OF THE GRAVITY CORES

J. Pike, Ch. Forster, M. Ivanov, E. Basov, I. Korneva, M. Ozerler, and E. Kozlova

Sampling stations were located on the abyssal plain, on the slopes of the volcano cones, and in the volcano craters (Fig. 2 and 24; Table IV). The area was mapped by MAK-1 profiling before sampling, and station localities were determined after interpretation of these data. Eighteen cores were obtained using gravity coring techniques and standard descriptive methods were applied. Samples were taken for further investigation onshore. In addition, breccia pebbles were washed and their composition was examined on board. The cores recovered were from the upper Pleistocene and Holocene. Fig. 25 shows how the Djemetinian, Kalamitian, Bugazian-Vityazevskian and Novoeuxinian stratigraphic beds are related to the lithological units described below. This correlation is based on the detailed lithological description. These stratigraphic and lithological units are widespread, both on the abyssal plain and in the craters of the volcanoes (Fig. 26). However, the full stratigraphic sequence of the Upper Pleistocene and Holocene sediments was described from the abyssal plain stations (BS-254, BS-250, BS-259, and BS-263) only (Fig. 27). The mud volcano craters (e.g. BS-255 to BS-258) only contain the uppermost part of this succession (Fig. 28).

Five main lithological units, including the three units described in the Recent Sediments Section (2.1), could be recognized:

Unit 1. The top of this unit is very water-saturated and sloppy. Some cores show a thin horizon of pale-grey structureless mud at the very top (BS-250, BS-256, and BS-259). This mud was approximately 15 cm thick in the mud volcano craters (BS-259) and 2-3 cm thick on the abyssal plain. Below this mud, a finely laminated (usually less than 1 mm) sequence of alternating white coccolith-rich laminae, sapropelic mud and pale-grey mud ranged in thickness from 10-45 cm. The lower boundary was very sharp.

Unit 2. This unit is characterized by sapropels and sapropelic muds, interbedded with very soft, pale-greenish grey muds. One such mud bed was always found directly below Unit 1. The upper part of the first sapropel contains a few very fine coccolith ooze laminae, and the sapropels sometimes contained fish and plant remains.

Unit 3. This unit represents thickly laminated, grey muds. These laminations, or fine beds, were shown by slight colour variations between shades of grey.

Unit 4. This unit comprises black to dark grey muds which are very rich in reduced iron, or hydrotroilite. These can be either massive or show a colour banding caused by a variable concentration of hydrotroilite.

Table IV

Summary of sampling data in Area No 1

CORE	COORDINATES	WATER DEPTH m	SETTING	RECOVERY cm	LITHOLOGY	AGE
BS-249	43°43,64 33°28,90	2050	Top of Kornev m.v.	86	Fine laminated Breccia	Holocene Mixed
BS-250	43°46,90 33°28,50	2086	Abyssal plain north of Kornev m.v.	506	Fine laminated Sapropel Mud with hydrotroilite Hydrotroilite Mud	Holocene Late Pleistocene
BS-251	43°43,62 33°28,96	1999	Top of Kornev m.v.	50	Fine laminated Breccia	Holocene Mixed
BS-252	43°31,85 33°07,03	2121	Top of MSU m.v.	207	Fine laminated Sapropel Breccia	Holocene Mixed
BS-253	43°32,06 33°07,23	2118	Top of MSU m.v.	206	Fine laminated Sapropel Breccia	Holocene Mixed
BS-254	43°36,14 32°59,67	2176	Abyssal plain 13 km N-W of MSU m.v.	568	Fine laminated Sapropel Mud with hydrotroilite Mud	Holocene Late Pleistocene
BS-255	43°31,59 33°07,13	2120	The rise on the crater of MSU m.v.	165	Fine laminated Sapropel Breccia	Holocene Mixed
BS-256	43°32,05 33°07,39	2143	Top of MSU m.v.	165	Fine laminated Sapropel Breccia	Holocene Mixed
BS-257	43°32,12 33°07,44	2116	Top of MSU m.v.	242	Fine laminated Sapropel Breccia	Holocene Mixed
BS-258	43°32,08 33°06,94	2180	Top of MSU m.v.	160	Fine laminated Sapropel Breccia	Holocene Mixed

Table IV (cont.)

CORE	COORDINATES	WATER DEPTH m	SETTING	RECO-VERY cm	LITHOLOGY	AGE
BS-259	43°40,06 33°24,08	2099	Abyssal plain between Kornev and Malyshev m.vs.	620	Fine laminated Sapropel Mud with hydro-troilite Mud	Holocene Late Pleistocene
BS-260	43°37,97 33°21,92	2096	SW slope of Malyshev m.v.	220	Fine laminated Mud with hydro-troilite Breccia	Holocene Late Pleistocene Mixed
BS-261	43°31,14 33°11,77	2085	Top of Yuzh-morgeologiya m.v.	150	Fine laminated Sapropel Breccia	Holocene Mixed
BS-262	43°31,07 33°11,85	2077	Top of Yuzh-morgeologiya m.v.	248	Fine laminated Sapropel Breccia	Holocene Mixed
BS-263	43°30,20 33°05,65	2182	Abyssal plain between Yuzhmor - geologiya & MSU m.vs.	253	Fine laminated Sapropel Mud with hydro-troilite Sand Mud	Holocene Late Pleistocene
BS-264	43°14,89 33°06,20	2157	Top of TREDMAR m. v.	279	Breccia	Mixed
BS-265	43°15,39 33°06,32	2223	Top of TREDMAR m. v.	325	Breccia	Mixed
BS-266	43°14,90 33°06,21	2172	Top of TREDMAR m. v.	294	Breccia	Mixed

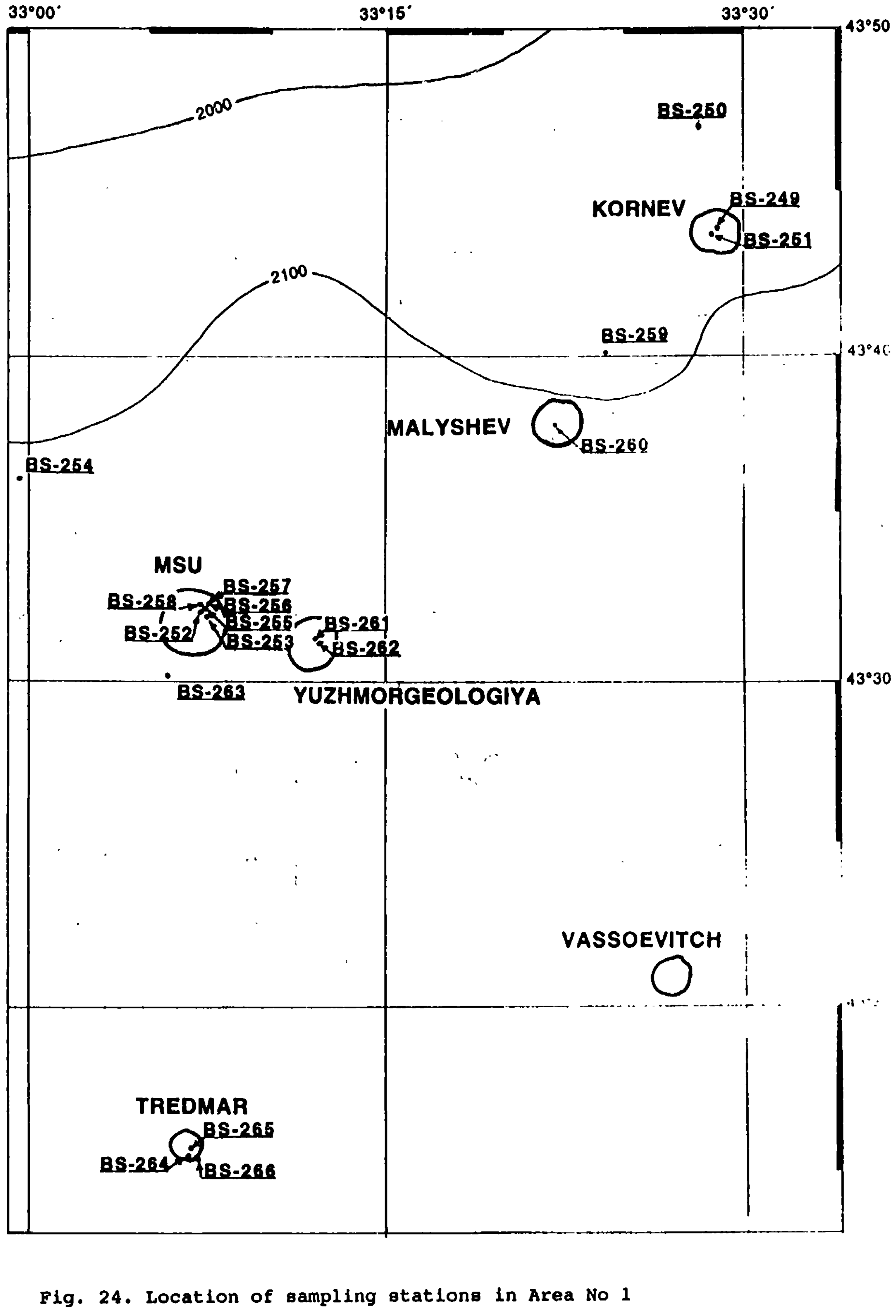

Fig. 24. Location of sampling stations in Area No 1

Unit 5. This unit is characterized by grey, finely bedded muds, with occasional fine silt laminae and spots of black hydrotroilite. Down this unit the silts become thicker (a few centimetres) and show sharp, erosive bases and grade downwards into muds. This unit may also contain debris flow deposits.

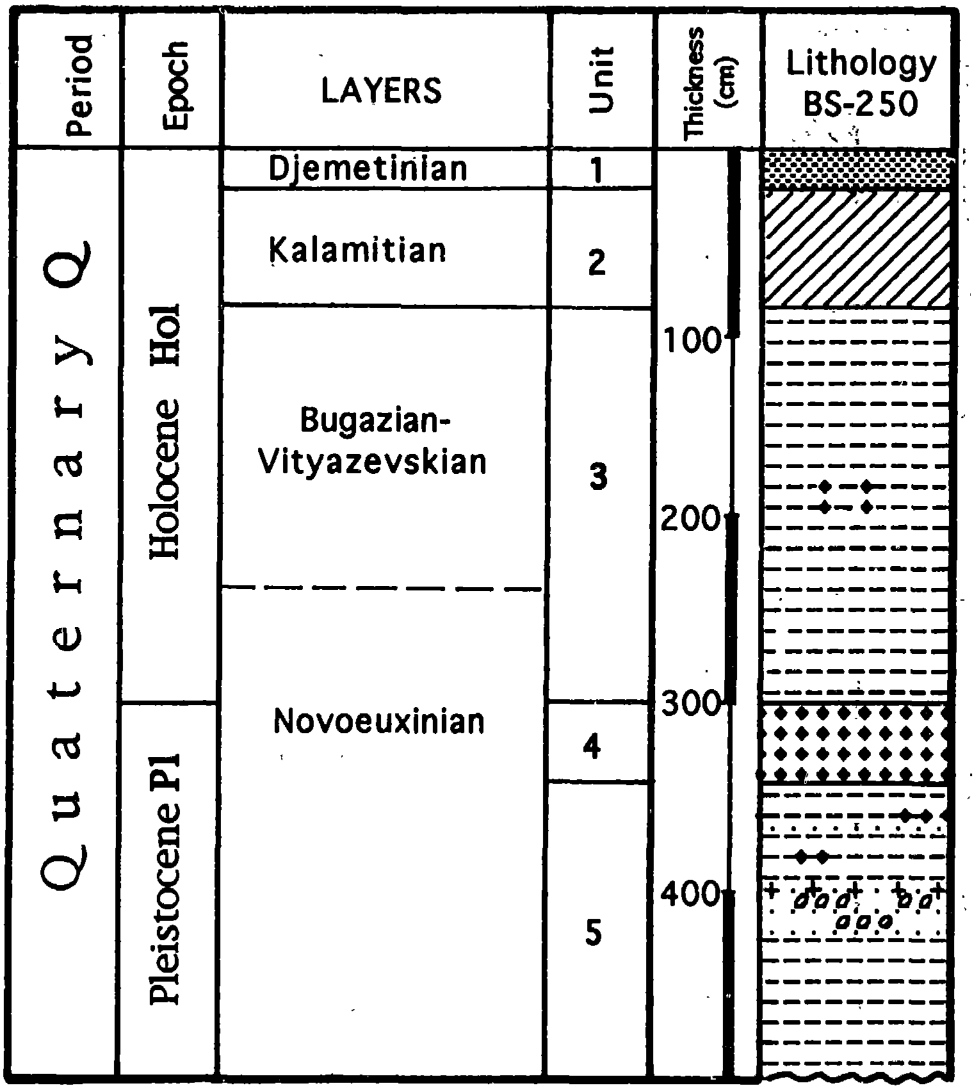

Fig. 25. Relation of the traditional Black Sea upper Quaternary stratigraphic beds to the sedimentary units described in the text

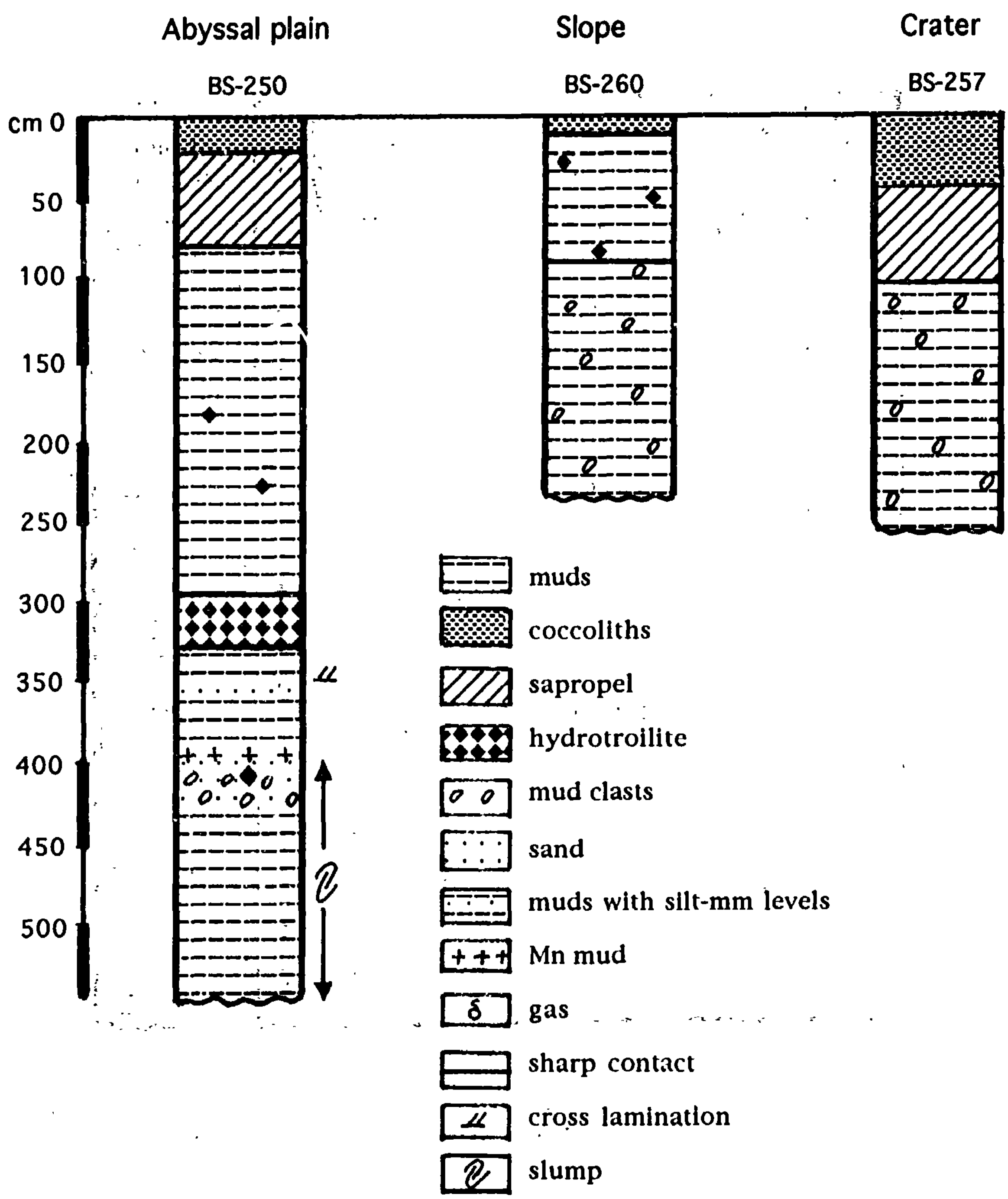

Fig. 26. Typical core sections from different morphological zones of Area No 1

Units 1, and to a variable extent Unit 2, were always present in sequences from the mud volcano craters, except for cores from the Tredmar volcano crater. In one core (BS-258) a thin sand, rich in pyrite and marcasite, was seen at the contact between unit 2 and the mud breccia (Fig. 29). Its matrix is a dense, grey mud and contains pebbles and smaller clasts which are dominantly composed of mudstones, but also with siltstones, sandstones and carbonate crusts with ostracods. These clasts range in size from 7-8 cm to a few millimetres. The mudstone clasts can be either grey, brown or contain carbonate, and may be laminated or structureless and sometimes contain pyrite. The sandstones and siltstones contain quartz, feldspar, pyrite, glauconite, and mica.

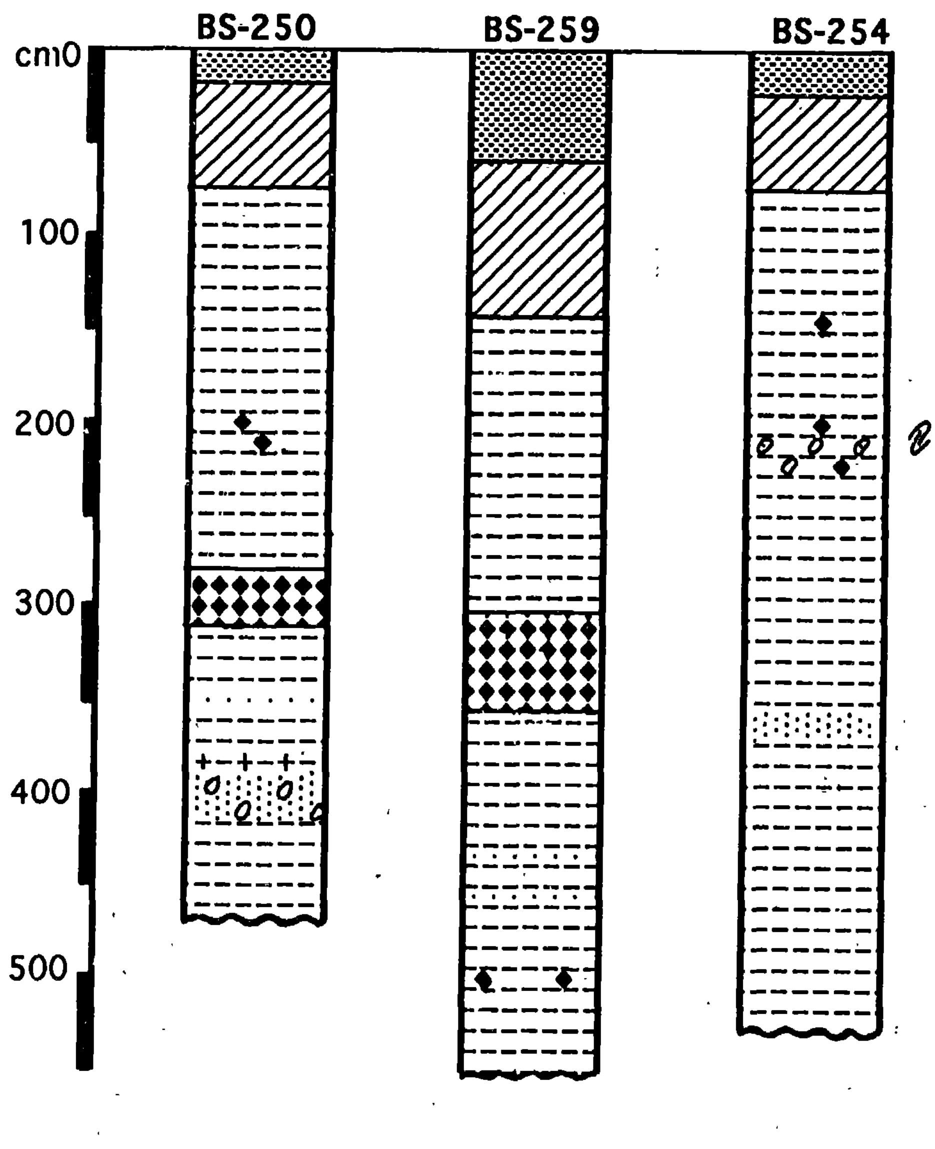

Fig. 27. Cores from the abyssal plain stations. (See the legend in Fig. 26)

In core BS-260 from the southwest slope of Malyshev volcano, two separate breccia units were seen. Many gas escape structures were seen on the surfaces of the core. Gas hydrate was recovered from the Tredmar volcano crater (Fig. 28).

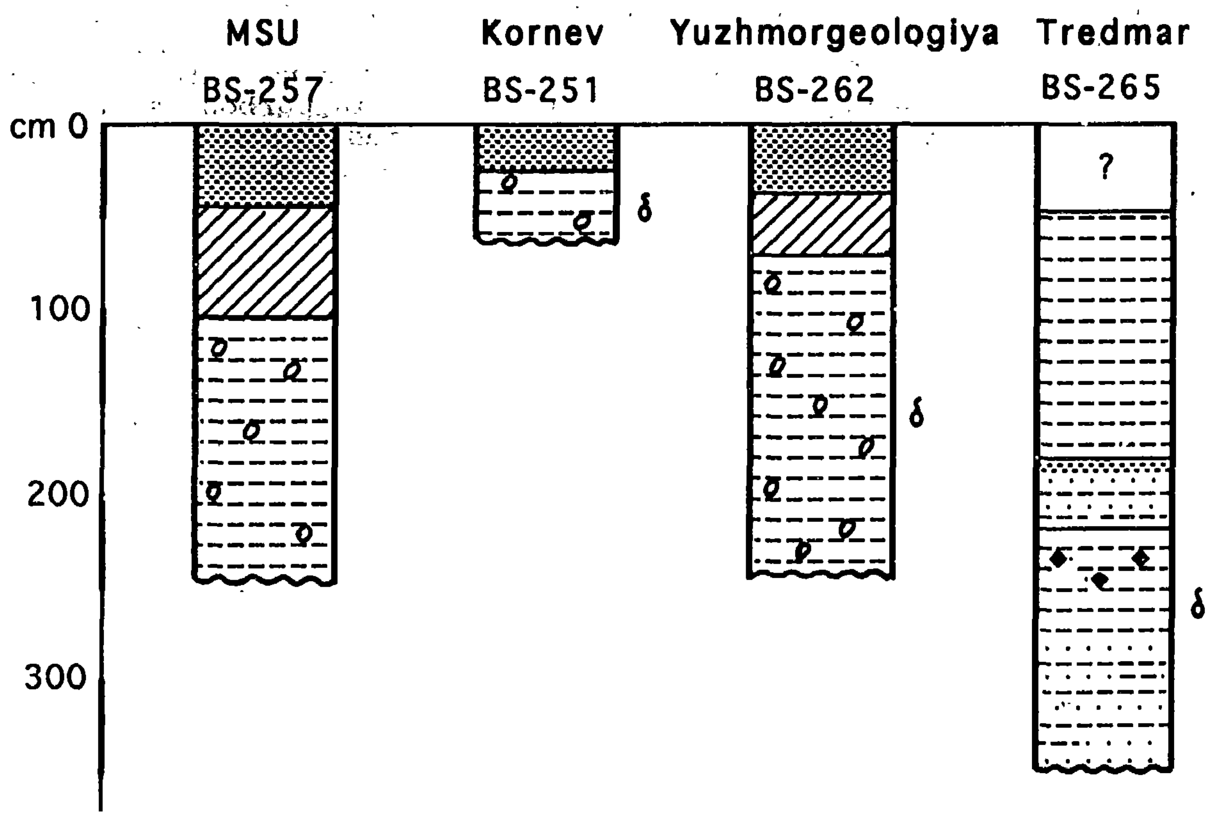

Fig. 28. Cores from the mud volcano craters. (See the legend in Fig. 26)

The grey muds of Unit 3 represent high terrigenous and shelf input into the deep basin, under the oxic conditions prevalent during deglaciation.

The hydrotroilite of Unit 4 has a complicated and poorly understood origin. There are a number of hypotheses regarding the genesis of this reduced iron-rich sediment. Here it is suggested that the fine grained hydrotroilite represents diagenetic enhancement of reduced iron-rich sediments in the deep basin. Coarser grained deposits may represent redeposition of hydrotroilitic sediments from the basin slopes.

The lowest stratigraphic unit (5) represents the deposition of laminated muds and thin, distal turbidites during the Late Pleistocene times at low water levels. The continental shelf/slope to the northwest probably provided a source for the coarser clastic material.

The data discussed allow the following main conclusions to be drawn:

1. All cores, to some extent, show a very similar stratigraphic succession.

2. Differences occur in cores taken from the mud volcano craters where a thick breccia unit is present.

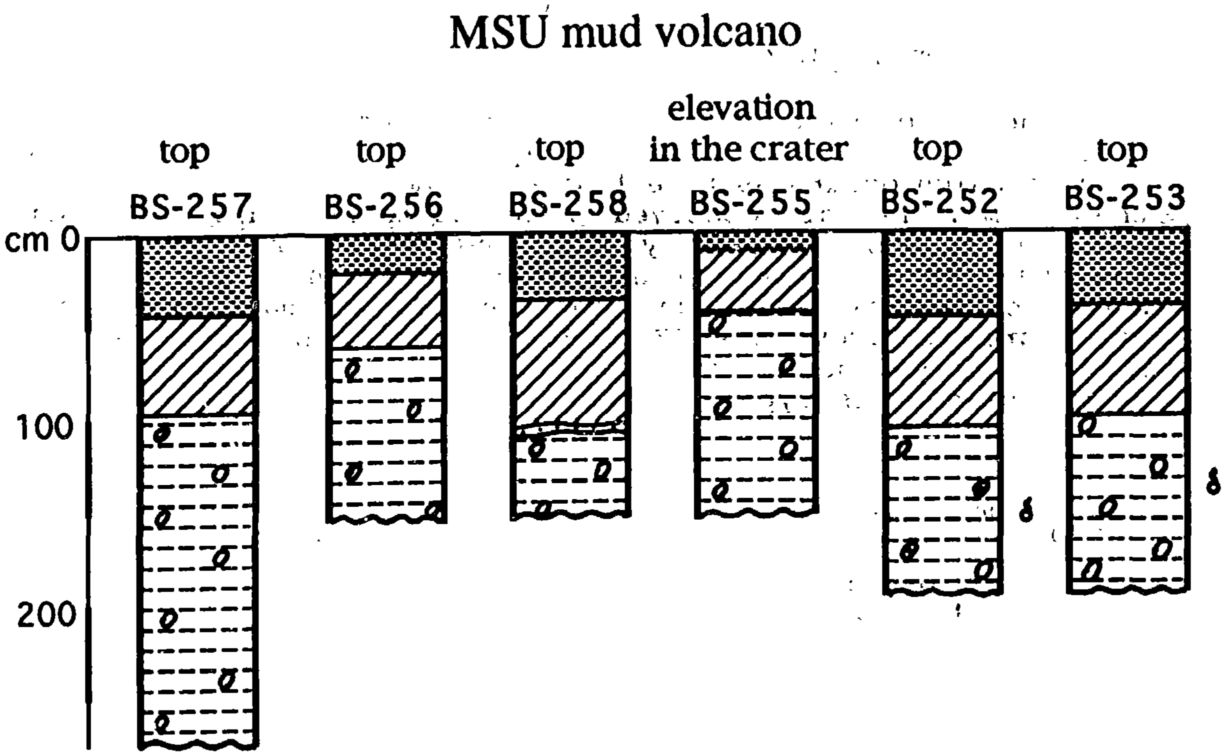

Fig. 29. Cores from the MSU mud volcano. (See the legend in Fig. 26)

3. The successions described allow the recognition and interpretation of depositional patterns in the study area, which reflect the changing tectonic, climatic and oceanographic regimes.

A SUMMARY OF GRAVITY FLOW DEPOSITS

Ch. Forster

Amongst the sites cored during Leg 1 of the TTR-III cruise, three gravity cores were taken from the abyssal plain in the study area. At these sites (BS-250, BS-254 and BS-259) gravity flow sediments were recovered in varying amounts. Through visual analysis of core material, four distinct types of deposit can be summarized - ranging from very fine-grained turbidites to a coarse debris flow deposit. The following descriptions highlight these "types" of redeposited sediment.

Type 1a (mud turbidites)

Characteristically, these very fine-grained turbidites contain no silt (Fig. 30). They are composed purely of mud (clays) and therefore grading is not apparent to the naked eye. The beds are typified by very sharp boundaries at their bases which is reflected by a gradation in colour from light grey mud at the base of the deposits to a dark grey mud that marks the top. Organic fragments are occasionally present in the bottom few centimetres of some of the beds (e.g. BS-259, 270-271 cm).

Type 1b (silt-laminated mud turbidites)

These deposits differ from the type 1a mud turbidites observed in core BS-259 because they contain a certain proportion of silt which occurs as fine laminae (commonly as a layer of less than 2 mm). They are observed in the cores from all three sites and are the most frequently occurring gravity flow deposits in the study area. Fining upwards grading is generally limited to a band of no more than 2 cm above the silt laminae which fine to structureless grey muds (Fig. 31). These muds are redeposited hemipelagic sediments and comprise the majority of the turbidite thickness of this type.

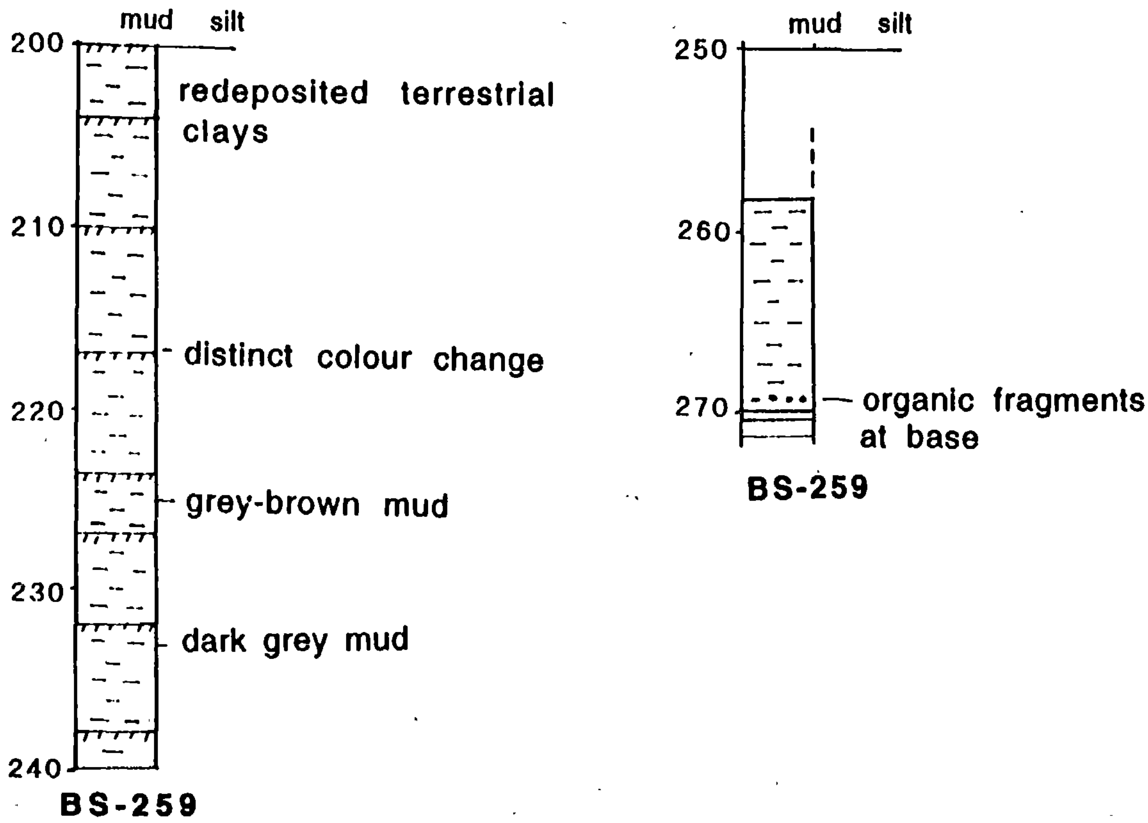

Fig. 30. Mud turbidites

Type 1c (silt turbidites)

These gravity flow deposits were identified in cores BS-250 and BS-259, however the core taken from the former site revealed perhaps the most interesting features. Typically these sediments consist of basal silt layers of between 2 cm and 5 cm which are often erosive - cutting down into the softer muds of the previous beds. A gradational fining to silty-mud is sometimes apparent, however this is not always the case. The relatively thick silt layers often show sedimentary structures such as parallel laminae and cross-lamination - the latter being occasionally highlighted by very thin muddy drapes which separate the ripple foresets. An abrupt contact with hemipelagites above the silt is common (Fig. 32).

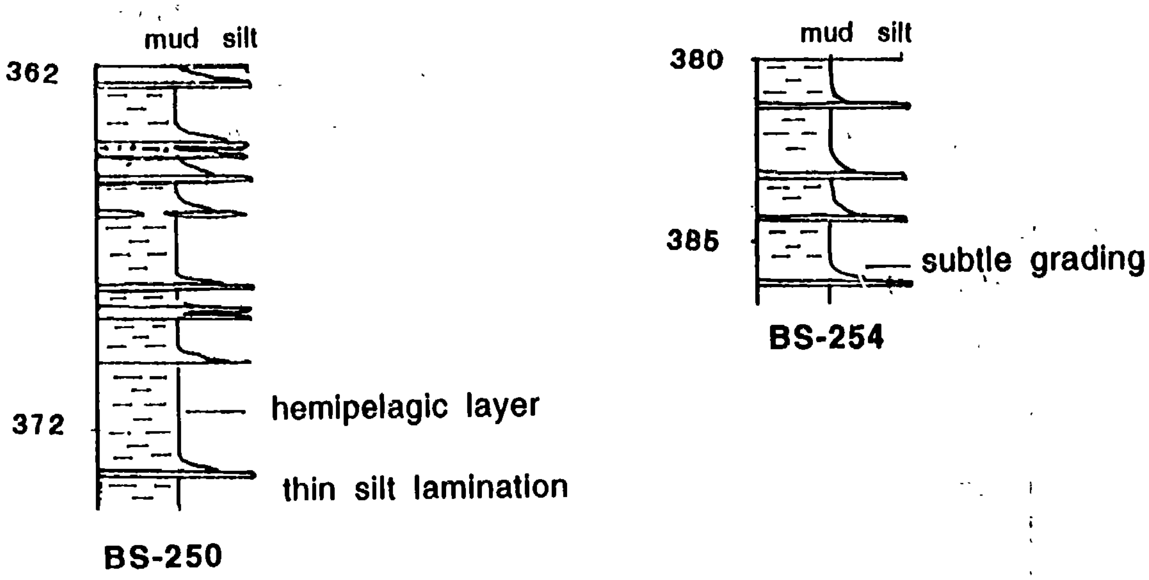

Fig. 31. Silt-laminated mud turbidites

Type 2 (debris flow deposit)

Although only one such bed was identified in the cores studied from the basin-plain, it is sufficiently different from the other gravity flow deposits to warrant a separate "type" classification. The deposit consists of a chaotic matrix-supported breccia. It has an erosive base, dominantly composed of hard, silty-mud fragments which appear to have some degree of orientation (Fig. 33, BS-254, 252-245 cm). The clay-rich matrix is variably silty and supports intraclasts with compositions ranging from a coccolith-rich sapropel to brown, terrigenous silty-muds. The clay bands above the deposit seem to down-cut into their respective underlying layers. This unit is interpreted as a debris flow deposit and is probably the result of a catastrophic mass-flow event such as slumping of slope sediment.

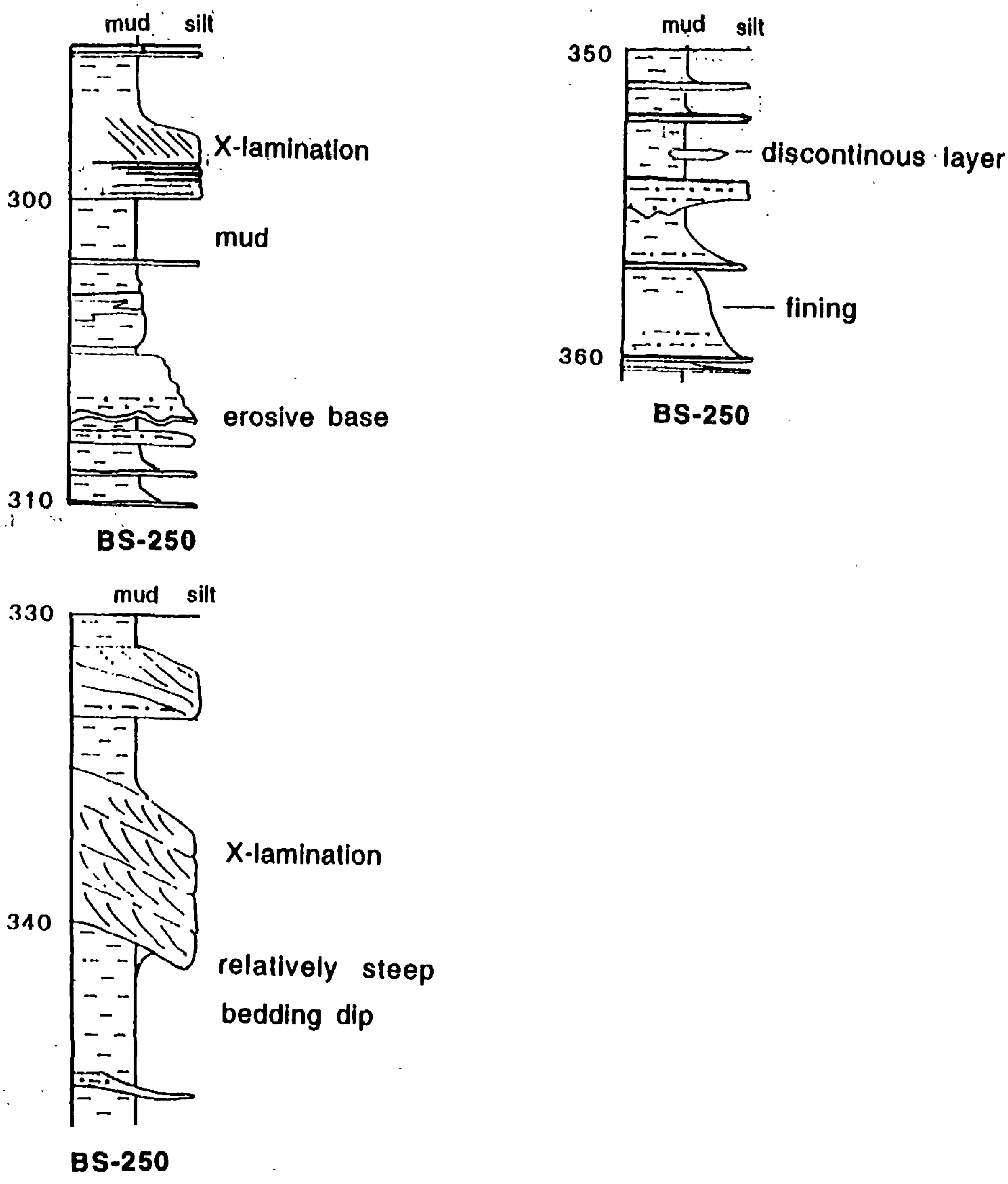

Fig. 32. Silt turbidites

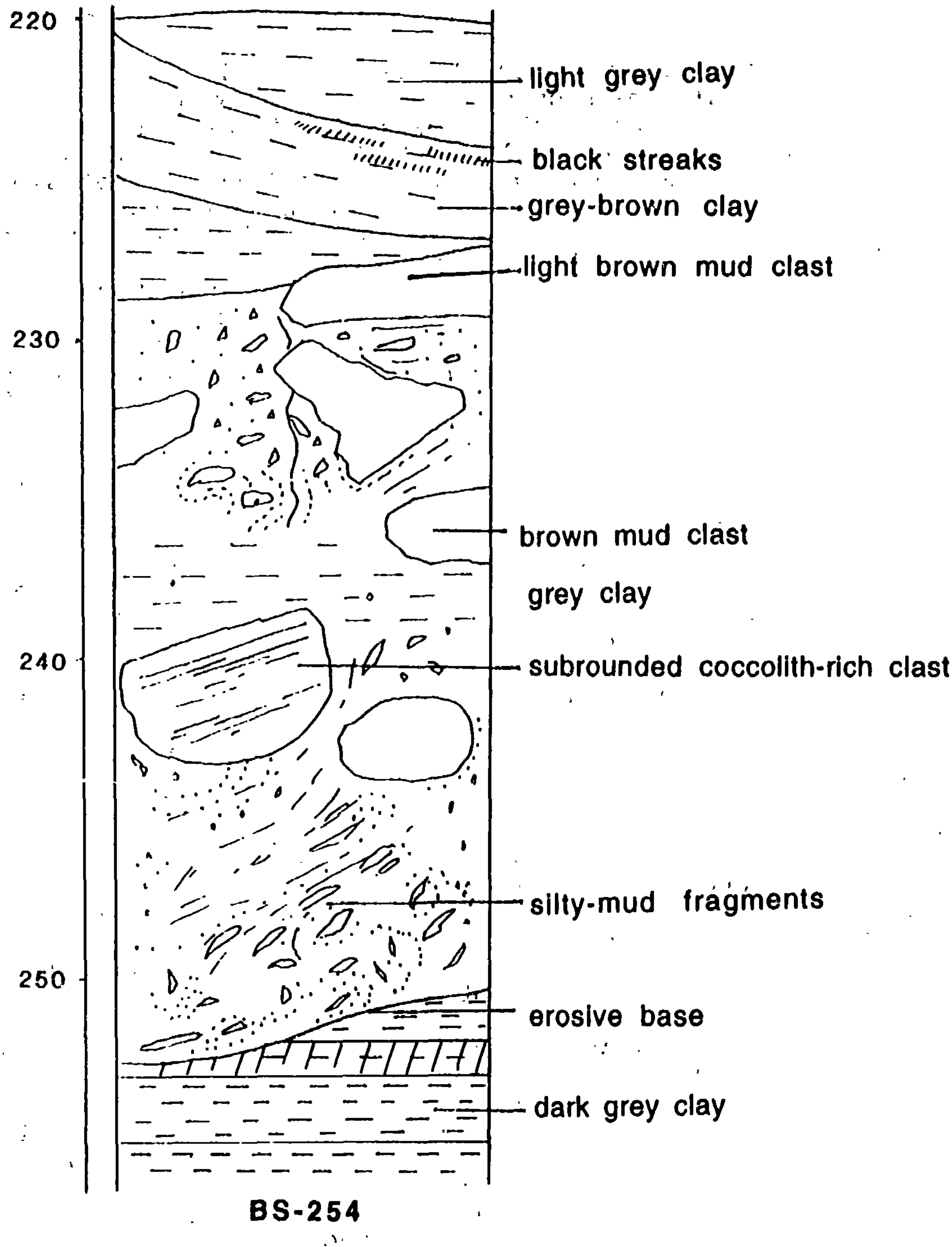

Fig. 33. Debris flow deposit

2.3. GENERAL INTERPRETATION

A. Limonov, M. Ivanov, Tj. van Weering, and L. Meisner

The data obtained during the Black Sea Leg of the TTR-3 Cruise show the following:

1. Mud volcanism in the Black Sea developed only in limited areas. So far, only one proven area is known (about 80 x 80 km) SSW of the Crimean Peninsula, where the investigations were carried out during the 1st and 3rd TTR Cruises. A second area is expected to exist near the Crimean southeastern base-of-slope, although mud diapirs are widespread along the northeastern periphery of the Black Sea Basin. Such a distribution of the mud volcanism is possibly related, in addition to composition and thickness of sediments, to the specific tectonic setting of the area. Our survey area is situated on the southeastward continuation of the great West-Crimean dextral wrench fault (Finetti et al., 1988). These authors have directly pointed out the relationship between the West-Crimean Fault and deep-seated volcanism. However they wrongly interpreted the structure seen on seismic line BS-1B as "normal" volcanics, originated from the basaltic basement in the fault zone. This seems to be a typical large mud structure, either a mud diapir or a growing mud volcano. The rest of the mud volcanoes appears to be related to the secondary auxiliary faults recorded on all seismic sections. All these faults are normal, indicating a dominant tensional tectonic regime in the area. This is possible if the suggestion by Boccaletti et al. (1988) is accepted that there has been anticlockwise rotation of the Crimea along the West-Crimean Fault. Parts of the faults, particularly in the immediate neighbourhood of the mud volcanoes, are undoubtedly the consequence rather than the cause of the mud volcanism because they probably were created by sediment collapse during eruptions.

2. Enormous rates of sedimentation in the Black Sea, estimated for the Pliocene-Quaternary, for example, to have been not less than 10 cm/kyrs, resulted in accumulation of very thick sedimentary members. Fast burial prevented pore waters from escaping from the sediments. Furthermore, the Maikopian Formation, consisting of dark clays, is rich in organic matter and contains abundant syngenetic gas accumulations on land. The weight of the overlying sediments in combination with the low permeability of the Maikopian clays has created an excess pore fluid and gas pressure which was released along weakness zones represented by faults.

3. The mud volcano activity likely has not been continuous. During the Quaternary, it was episodic and decreased with time. The mud volcanism seems to have been governed by faulting activation. The first recorded active period of the mud volcanism ceased at the level of the reflector between the upper and lower seismic members (see Section 2.2.a). Because all large faults have a constant vertical offset and none of them penetrates into the upper seismic member, this implies that tectonic activity was suddenly renewed at this boundary (presumably in the end of the Early/beginning of the Middle Pleistocene) and similarly suddenly decreased. This confirms the assumed relations of the mud volcanism with faulting.

For most of the Black Sea mud volcanoes studied so far the mud breccia is overlain by either the Lower Holocene (Bugazian-Vityazevskian) or, more rarely, the Upper Holocene (Djemetinian-Kalamitian) sediments. Thus, the next episode of decrease of the mud volcano activity occurred at the boundary between Pleistocene and Holocene. The third one took place at the beginning of the Upper Holocene. According to the traditional Black Sea Quaternary stratigraphy, these boundaries can be dated as 7 kyrs and 3,5-4 kyrs respectively (Kuprin, 1982). Some mud volcanoes are still active, displaying abundant gas seepages, as was shown by the underwater television recording. The Tredmar mud volcano is thought to be one of the most active. This mud volcano has a very irregular morphology with steep relief features. Its mud breccia crops out at the seafloor and is highly gas-charged; about 2 l of gas was easily obtained from a core section approximately 40 cm long and 14 cm in diameter. Gas hydrate crystals were found in some core sections from this mud volcano.

3. OLIMPI MUD VOLCANO AREA (STUDY AREA 3)

3.1. GEOLOGICAL SETTING

M.B. Cita and A. Limonov

The Olimpi area is situated on the Mediterranean Ridge, about 150 km south of Crete. The Mediterranean Ridge is the largest structural element of the Central and Eastern Mediterranean, stretching from the Calabrian Rise in the west to the Florence Rise in the east over a distance of some 1500 km (Fig. 34). The Ridge is of the order of 150-300 km wide and has an arcuate convex southward shape. To the north the Mediterranean Ridge is bounded by a number of trenches forming part of the Hellenic Trench System. They are from west to east: the Matapan Trench with the maximum depth of over 5000 m, the Gortis Trench (-3585 m), the Pliny Trench (-3630 m), and the Strabo Trench (-4450 m) (IOC-UNESCO, 1981; Le Pichon et al., 1982a, b). The southern boundary of the Mediterranean Ridge is delineated by narrow and flat abyssal plains whose depths decrease in general from west to east. This series of abyssal plains (A.P.) consists of the Messina A.P. (-4200 m), the Sirte A.P. (-4150 m), and the Herodotus A.P. (-3225 m) (Cita and Camerlenghi, 1990). Directly south of Crete the abyssal plain is narrowed to a trough where the Ridge and the African margin north of Cyrenaica are in contact.

The average depth of the Mediterranean Ridge is about 2.1-2.2 km, varying between 1200 m and more than 3000 m. Its topography is characterized by small closely spaced depressions and ridges (with a relief of 50-100 m and a wavelength of 0.5-2 km) oriented mostly parallel to general trend of the Ridge. Such a pattern produces a hummocky hyperbolic acoustic reflection when using conventional echosounding devices. After Hersey (1965) it is known as "cobblestone topography".

The first descriptions of the Mediterranean Ridge have been probably published in two papers by Giermann (1966, 1969), who summarizing his notions about this structure, wrote: "It is most evident that the Eastern Mediterranean Ridge is an outer Alpine mountain belt, folded up during later Miocene times". (Giermann, 1969, p. 606).

The majority of researchers agrees that the Mediterranean Ridge is a young structure which originated as a result of the African and Eurasian plates convergence, but interpretations of this structure are controversial. Thus, Stride et al. (1977) suggested the Mediterranean Ridge to be the outer ridge of the Hellenides similar to the lithospheric flexure found on the outer side of the Pacific deep-sea trenches, but suffering a compressional stress. The outer swell concept was also supported by Hsü and Ryan (1973).

The hypothesis that the Mediterranean Ridge is a buried outer volcanic arc was declared by Hsü (pers. commun., 1992).

The third hypothesis suggests the Ridge as a pile of imbricated sheets of sediments, possibly also including basement nappes, which were scraped off from the African margin as it underthrusted beneath the Aegean Plate (Dewey et al., 1973).

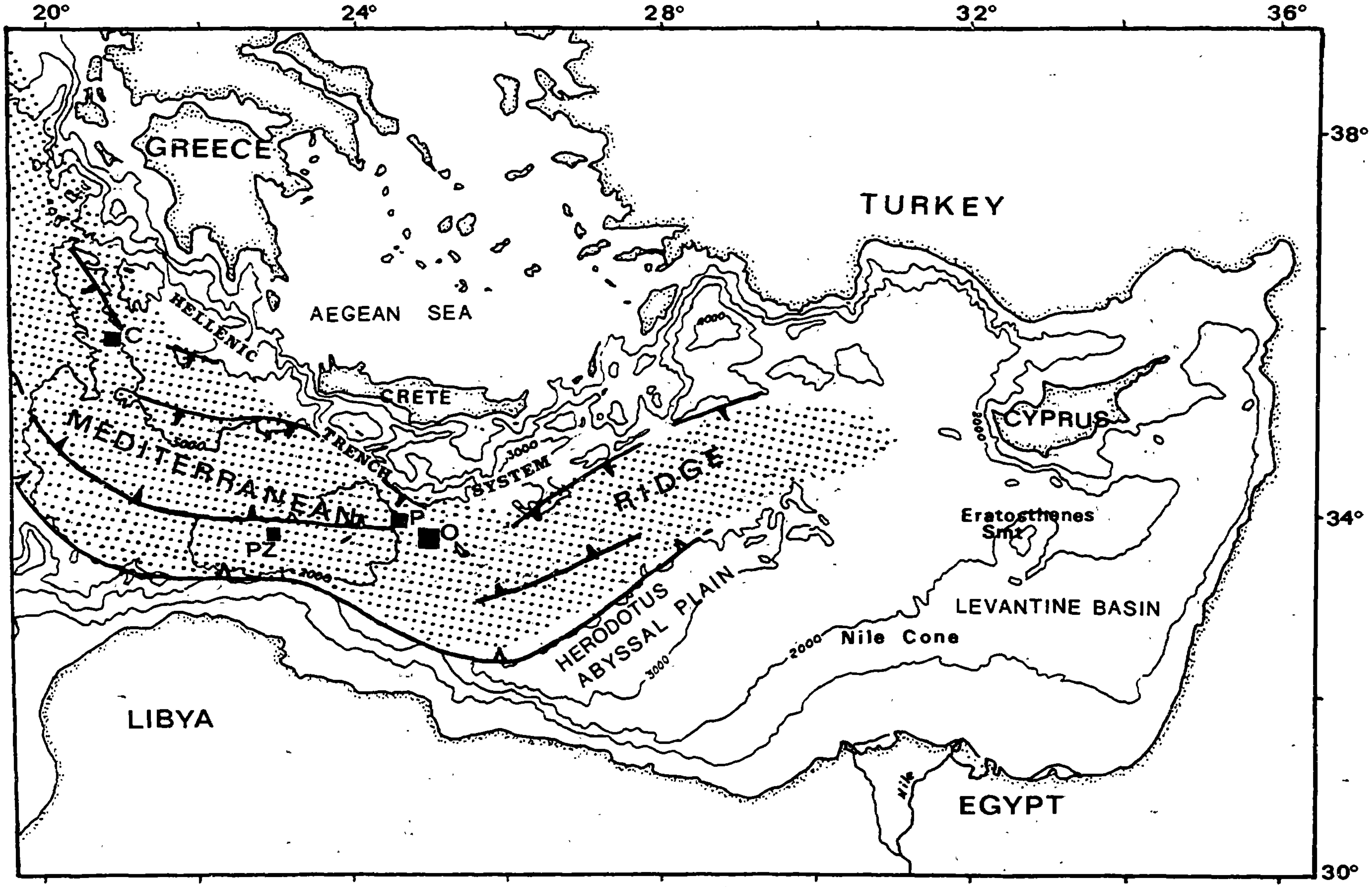

Fig. 34. Location of the Mediterranean Ridge in the Eastern Mediterranean Sea (dotted area). Also shown are the localities of mud diapirism known before the TTR-3 Cruise (C - Cobblestone area, PZ - Pan di Zucchero area, P - Prometheus 2 area, and O - Olimpi area). Black triangles indicate major thrust fronts and open triangles indicate the outer deformation front. (After Cita and Camerlenghi, 1990)

There were also a number of other hypotheses varying from a mid-ocean ridge to a giant olistostrome (see a summary in Cita and Camerlenghi, 1990).

On the basis of comprehensive investigations carried out in 1978, Le Pichon et al. (1982b) concluded that only the lower part of the African margin sedimentary cover is involved in subduction under the European plate, the upper part being scrapped off, forming the Mediterranean accretionary Ridge under strong compressional stress. Ryan et al. (1982) came to the conclusion that the décollement surface occurs at the base of the pile of off-scrapped sediments and becomes progressively stratigraphycally deeper towards the Hellenic Arc, coinciding at last with the Aptian plastic shale. The Hellenic Trench is thought to be a fore-arc basin representing a downfaulted margin consisting of Mesozoic carbonates.

At present the Mediterranean Ridge is considered to be a young Neogene to Recent intra-Mediterranean chain, with ongoing rapid deformation due to incipient collision produced by the relative motion of the African and European Plates and Aegean Microplate. This collision is of a continental type.

Unlike other accretionary prisms, the aroward edge of the Mediterranean Ridge accretionary complex is deeper than the seaward edge. Such a pattern is explained by asymmetric sediment supply: the entire north African sedimentary discharge is trapped at the relatively narrow seaward edge of the Ridge where it is intensively deformed. The fore-arc region on the European side receives much less sediments, which are trapped by the Black and Aegean Seas. As a consequence, the fore-arc basin (Hellenic Trench System) is significantly deeper than the "oceanic" trench situated in the region of the peri-African abyssal plains (Cita and Camerlenghi, 1990).

The southern boundary of the Mediterranean Ridge accretionary complex is marked by well-displayed deformation fronts (Belderson et al., 1970, 1978), contrasting to almost horizontally stratified sediments on the neighbouring abyssal plains. Several imbricate thrust sheets, also suggested to be the inner deformation fronts of the Ridge, were defined from seismic reflection profiles (Finetti, 1982). One can suppose that a compressional stress spreads quite far southward of the Mediterranean Ridge because a regional thrust was found from seismic reflection profiles also on the Sirte Rise (Limonov et al., 1992a).

A peculiar character of the Mediterranean Ridge is the presence of the Messinian evaporites at a shallow subbottom depth (100-400 m). They strongly influence the interstitial fluid migration, pore water pressure, the pattern of structural deformation, and the bottom topography creating the diapiric and dissolution structures (Cita and Camerlenghi, 1990). Their presence also leads to the appearance of deep-seated brines in small anoxic basins situated in the outer part of the Ridge (Cita et al., 1989b).

On the Mediterranean Ridge, four mud diapir and mud volcano areas have been documented before the TTR-3 Cruise: the Cobblestone (or Prometheus) area (35°51′ N/20°48′ E), the Pan di Zucchero area (33°47′ N/22°48′ E), the Prometheus 2 area (33°50′

N/24°26′ E), and the Olimpi area (33°43′ N/24°48′ E). All of them are located in the crestal zone of the Mediterranean Ridge, in the depth range between 1400 and 3000 m (Camerlenghi et al., 1992) (Fig. 34).

Geological and geophysical exploration of the Olimpi area was carried out by the Marine Geology Research Group of the University of Milano and associated scientists through discrete cruises with the R/V *Bannock* (1988-1990). The first cruise, in September 1988, led to the unforeseen discovery of three mud diapirs, well visible on the 3.5 kHz echosounder record (Fig. 35), during a transit from Rhodes to a target research area on the Mediterranean Ridge crest. Brief but intense field work resulted in:

a) the creation of a detailed bathymetric map of an area of approximately 100 km^2 (Fig. 36);

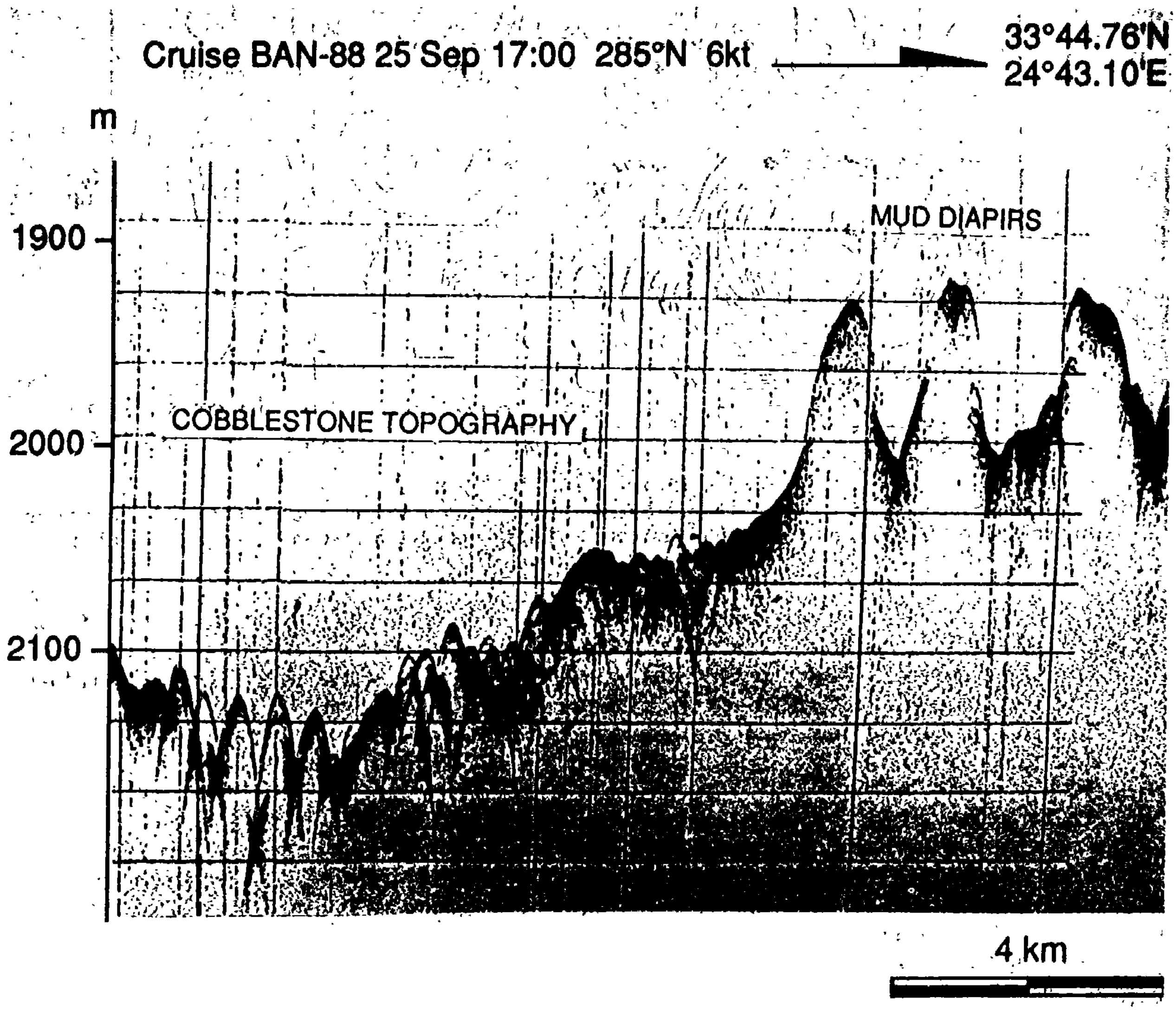

Fig. 35. Mud diapirs recorded on the 3.5 kHz echosounder profile during the R/V *Bannock* Cruise in 1988 (BAN-88)

b) the identification of five dome-like structures;
c) the recovery of four gravity cores precisely located with reference to the very complex bottom configuration; and
d) the identification of a mud breccia at or beneath the surface of the diapirs (Cita et al., 1989c).

The second cruise (April 1989) was dedicated to geophysical exploration of the area by single-channel seismic profiling, but unfavourable weather conditions prevented completion of the planned survey. During this survey, a dome-like structure larger than any of those documented previously was discovered in the southwestern corner of the diapiric field.

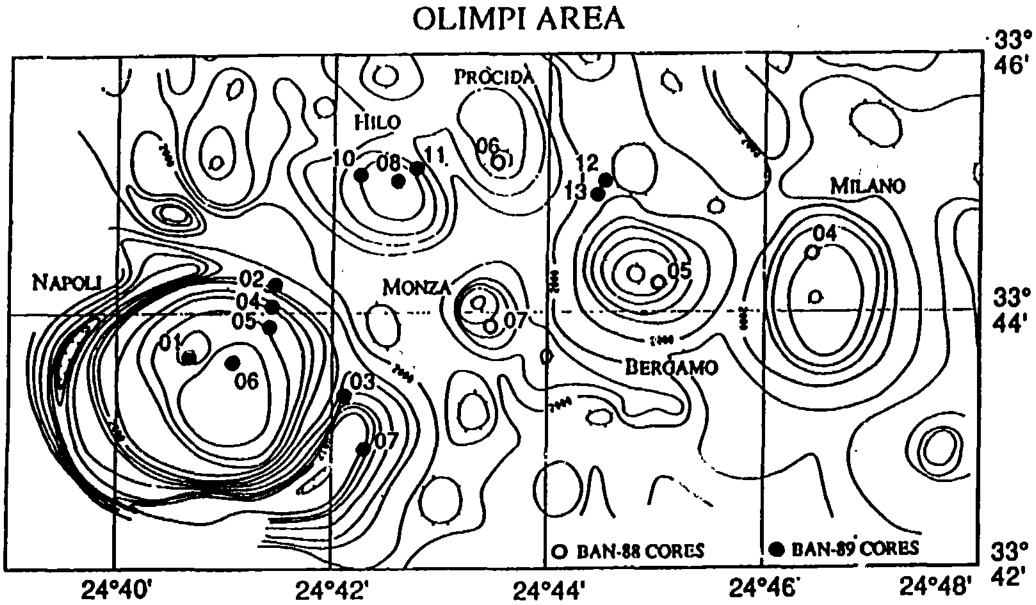

Fig. 36. Bathymetric map of the Olimpi area with location of cores taken during the BAN-88 and BAN-89 Cruises. (After Cita and Camerlenghi, 1990)

It should be explained that the name "Olimpi" derives from the Olympic games, which occurred in the week of the discovery in September 1988, and that the various domes were named after the hometowns of the main researchers involved, i.e.:
Milano dome after the hometown of M.B. Cita;
Bergamo dome after the hometown of A. Camerlenghi;
Monza dome after the hometown of E. Ebra;
Hilo dome after the hometown of F.W. McCoy;
Procida dome after the hometown of the master of R/V *Bannock*,
and Napoli dome (discovered in 1989) after the hometown of L. Mirabile, chief scientist of the spring 1989 cruise.

The third cruise (September 1989) was dedicated to geological and geophysical (heat-flow) research and resulted in a more detailed bathymetric survey, in additional coring, especially on the Napoli dome, and in numerous heat-flow measurements (Cita and Camerlenghi, 1990; Camerlenghi et al., 1992).

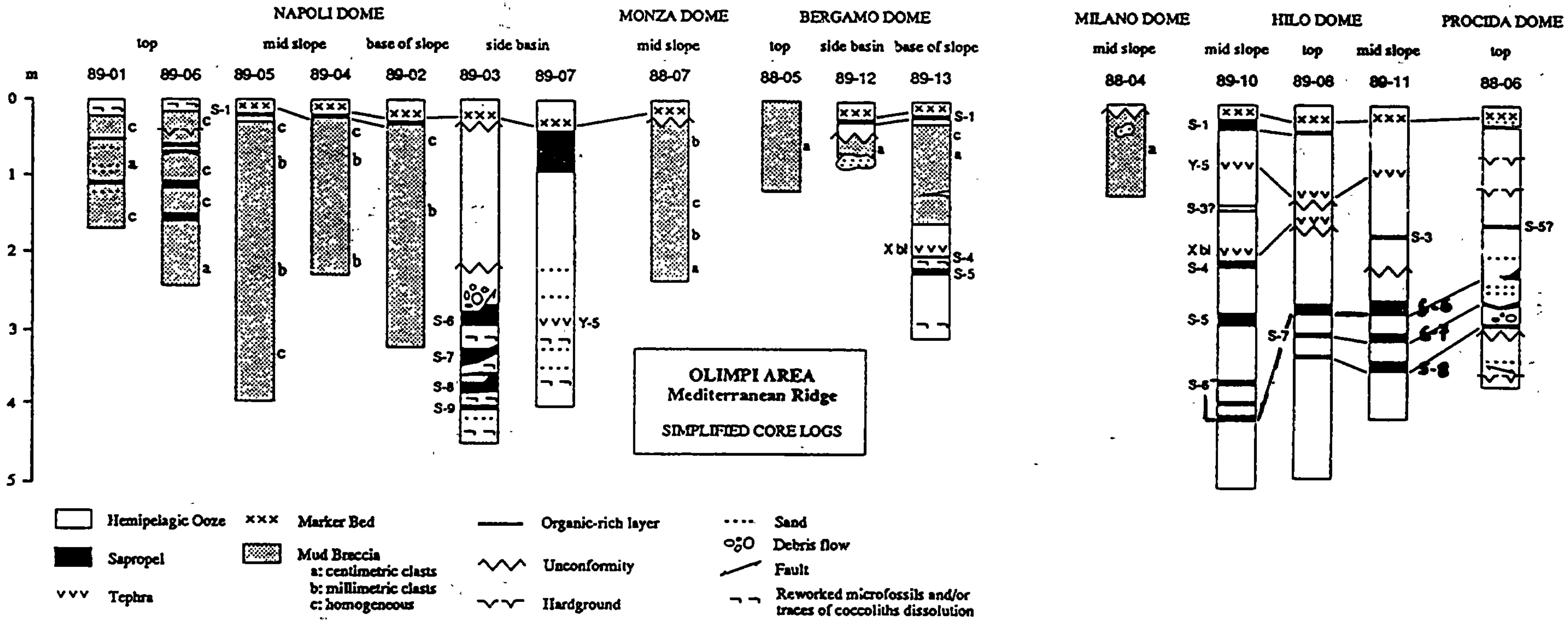

Fig. 37. Cores recovered in the Olimpi area during the BAN-88 and BAN-89 Cruises. (After Camerlenghi et al., 1992)

The fourth cruise carried out in 1990 completed the planned high resolution seismic survey, which was intended as a site survey for ODP Drilling Proposal 330 (Mediterranean Ridge) with special reference to proposed Site MV1 (Mud Volcano).

Sixteen cores were obtained from the Olimpi diapiric (or, more exactly, mud volcano) field: seven from a transect across the Napoli dome, the others from other domes, mainly from their tops (Figs. 36 and 37).

The domes examined during the exploration display two typical morphologies:

Subconical (mud cones) with a vertical relief not exceeding 100 m above the regional level, and a basal diameter of approximately 1 to 2 km;

Large flat topped (mud pies) with a depressed rim at the base, a vertical relief of up to 200 m, and a basal diameter of up to 4 km.

The depths of the summits of the mud volcanoes and diapiric structures range between 1900 and 1920 m, and are considered relevant to the emplacement mechanism.

The mud volcanoes and diapiric structures typically contain a matrix-supported mud breccia of a deep provenance, that can be intruded or extruded. The host sediments consist of hemipelagic marls (dominant lithology) deposited at a low sedimentation rate, intercalated with sapropels and tephras (minor, isochronous lithology).

The mud breccia is matrix-supported, with clasts up to several centimeters in size. The composition of the clasts is fairly monotonous, including mudstones, sandstones, calcarenites, and quartz arenites (Staffini et al., 1993).

Microfossils from the mud breccia are scanty and mixed in age, with a dominance of the Middle to Early Miocene taxa. They include some older forms that might be reworked in the essentially terrigenous formations which are supposedly the source of the mud breccia itself.

The mud breccia displays several typologies that have been subdivided as follows (Cusin et al., 1992; Staffini et al., 1993).

Type A Massive is further subdivided in:

A-1 with centimetric and pluricentimetric clasts;
A-2 with millimetric clasts;
A-3 homogenous, very fine-grained. Within this type we found a "mousse" sub-type which is soft, expanding, and rich in subspherical cavities related to gas escape.

Type B Organized is further subdivided in:

B-1 layered with millimetre to centimetre scale layers displaying a horizontal bedding in the cores;
B-2 graded with upward increase in matrix/clast ratio and upward decrease in grain size;
B-3 patchy/cloudy with patches or clouds of different colours in a fine-grained matrix.

Carbonate content of the mud breccia ranges from 10 to 35%, with the higher values recorded in the type A-3 breccia (Staffini et al., 1993). Clay is a major component of the mud breccia; the mineral composition is characterized by a high smectite content (29 to 66%) suggesting the Nile Cone as source area (Cusin et al., 1992). Dolomite (up to 12%) was detected by X-ray diffractometery only in the Napoli dome (Cita and Camerlenghi, 1990).

Gas composition of the mud breccia was measured from cores raised at the Napoli dome. It includes methane and higher hydrocarbons indicative of a biogenic, but also partially thermogenic origin (Camerlenghi et al., 1992).

Heat flow measured in the Olimpi field is low (12-30 mW/m^2) and decreases away from the field (Camerlenghi et al., 1992).

The sediments overlying the mud breccia, and the youngest part of the stratified column in general, where the volcanism and diapirism are recorded, are characterized by a black, centimetric marker bed (MB) consisting of Mn micronodules of bacterial origin (Cita et al., 1989a). Mn is related to flux expulsion from the accretionary wedge as a discrete event, possibly related to the Santorini eruption of the Bronze age.

3.2. RESULTS

3.2.a. SEISMIC REFLECTION PROFILING

A. Limonov

The seismic reflection profiling in Area No 2 was carried out along lines PS-106 to PS-116 (Fig. 38).

The first line PS-106 starts on the Cretan continental slope, about 75 km south of Gaidhouronisi Island, and is oriented in a NE-SW direction. It was designed in order to cross the deformation front, related to a backthrust in the inner part of the Mediterranean Ridge, and the Olimpi mud volcano/mud diapirs area.

From the beginning of the line (at 15^{22}) till 19^{00}, the seafloor dips gradually towards the Hellenic Trench. The topography of the seafloor is irregular. Between the beginning of the line and 16^{50} the seafloor profile has a step-like form. The Alpine basement of Crete Island lies at a depth of 80-300 ms (TWTT) from the seafloor. It is broken by normal faults with vertical offset of up to 200 ms. The sedimentary cover is represented mainly by relatively weakly deformed Pliocene-Quaternary deposits with continuous low-amplitude reflectors.

The presence of the M-reflector may be observed between 16^{10} and 16^{40}. After 16^{50} the bottom topography becomes more irregular, and the thickness of Pliocene-Quaternary sediments decreases. The Alpine basement possibly outcrops at the seafloor in some places.

The Hellenic Trench is V-shaped in the crossing point. Its northern slope has no significant Pliocene-Quaternary sediments; and on the southern slope their thickness does not exceed 150 ms. The underlying surface is very irregular and is displayed as a series of overlapping hyperbolic reflections.

The deformation front was crossed at 22^{15}. It is expressed as rather steep (about 8°) step with a relative high of about 380 m. The inner structure of the deformation front is not seen, but it may be comprised of a number of backstop thrusts (Cita and Camerlenghi, 1990). The width of the deformation front on line PS-106 is about 12 km.

Two high (150 m each) dome-like structures were recorded between 22^{40} and 23^{00}. Their apparent width is more than 1 km. On the OKEAN image it is seen that these structures are related to curved ridges oriented obliquely to the line.

The point on the line corresponding to time mark 23^{25} is the closest point to the proposed ODP Site MEDSAP 2B. The distance between them is about 4 km. The thickness of the Pliocene-Quaternary sediments at this point is 130 ms (about 110 m). They are represented by a semitransparent unit with only a few weak discontinuous reflectors. The underlaying member is thought to be of the Messinian age. The apparent thickness of this member is 200 ms, but the bottom is not clearly seen. The member is displayed as number of strong but poorly-correlated reflectors. From the reflection pattern one can conclude that it is likely made up of carbonate-sulfate varieties of evaporites. The member is folded and faulted. No reflectors were recorded beneath this member.

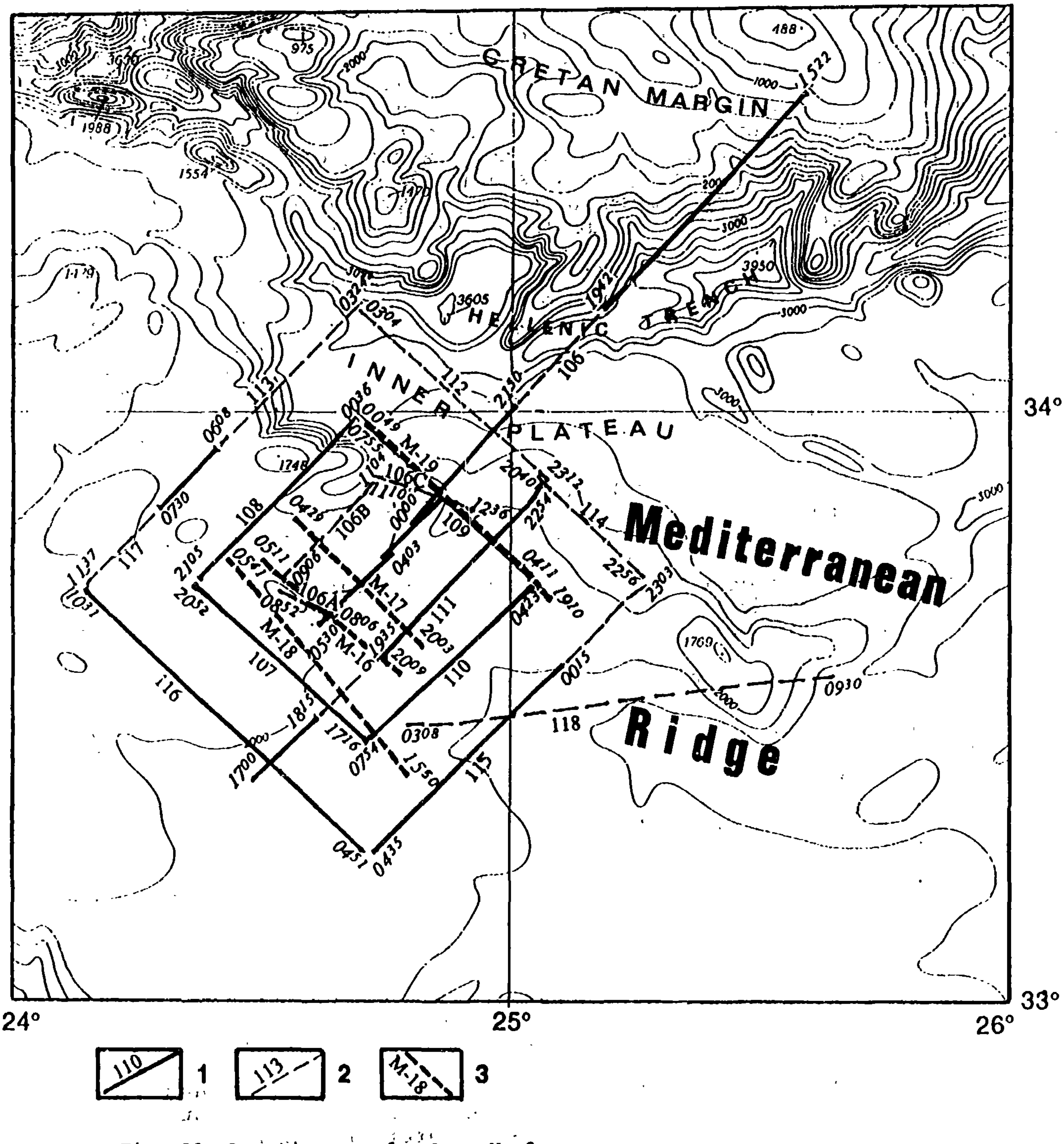

Fig. 38. Location map for Area No 2
1 - seismic and OKEAN line; 2 - OKEAN line; 3 - MAK-1 line. (The bathymetry is from IOC-UNESCO, 1981)

A dome-like structure is clearly seen near time mark 01^{55}. It has the appearance and seismic signature of a typical mud diapir (mud volcano) (Camerlenghi et al., 1992).

Starting from 02^{10} and continuing till 04^{40} (considering the break in record between 02^{22} and 04^{03} for airgun repairs and restarting the line), the seismic line runs across the Olimpi mud diapirs/mud volcanoes field where it crosses the Monza and the eastern part of the Napoli dome. The thickness of Pliocene-Quaternary sediments in this area varies between some tens of milliseconds and 150 ms. The thickness of the underlying Messinian layer possibly does not exceed 30-40 ms. In some locations Pliocene-Quaternary sediments seem to be underlain directly by the pre-Messinian Miocene. The deepest reflector is recorded at a depth of about 480 ms below the seafloor.

Seismic line PS-107 was laid down in order to define, together with the OKEAN swath survey, the southern and southwestern limits of the area of mud diapirism and volcanism. The line runs in a SW-NE direction, southwest of the Olimpi area.

The bottom topography along the line is characterized by small irregularities up to 50 m high. Their wavelengths vary between 600 to 700 m and 1000 m. The penetration is rather shallow, not more than 250 ms.

The general feature of this seismic section is a quite constant thickness of a transparent Pliocene-Quaternary unit (a little more then 100 ms) and a very complex relief of the underlying surface. This surface is disturbed by numerous folds and faults. Amongst the latter one can suggest the presence of both normal and thrust faults with a vertical offset of up to 100-120 ms. The deformations are quite young and most of them are well-displayed in the bottom morphology (Fig. 39). This indicates that the Mediterranean Ridge are still in the stage of development. The Messinian seems to occur between time marks 18^{18}-19^{05} and 20^{00}-20^{52} (the end of the line).

Line PS-108 runs from the southwest to the northeast. A relatively weakly disturbed sedimentary section is recorded on the first half of the line. The Messinian is the deepest unit seen in the record. Its thickness is about 100-150 ms. The Messinian is overlain by a transparent layer of Pliocene-Quaternary sediments, up to 200 ms thick.

This pattern is disrupted suddenly at 22^{45} where the deformation front begins (Fig. 40). The front looks in the cross-section as a large swell with dome-like structures complicating its surface. Only short uncorrelatable reflectors are visible inside this rock pile, and the general seismic pattern is chaotic. The deformation front on the profile is separated from the Inner Plateau by a narrow trough. The elevation of the uppermost point of the deformation front above the trough floor is about 1300 m at this place and the angle of the slope is about 8-10° toward the northeast.

The wall of the deformation front is not as high and steep on the next NW-SE running line PS-109, but the general structure remains very similar. The Pliocene-Quaternary sediments almost appear to be absent from the deformation front, or, if present, they may be so intensively deformed that they do not differ in seismic character from the underlying deposits.

The Upper Plateau (Mediterranean Ridge) is characterized by an alternation of areas with almost undeformed upper sedimentary section ($02^{15}02^{45}$, 03^{50}-04^{15}) and folded Neogene-Quaternary sediments (02^{45}-03^{50}). The folds are perfectly reflected in the seafloor topography, forming a typical "cobblestone" pattern (Fig. 41). The folds are very closely spaced and have a height of 30-40 m and a wavelength of 800-900 m. The thickness of Pliocene-Quaternary sediments averages 130 ms, and that of the Messinian (?) is 200 ms.

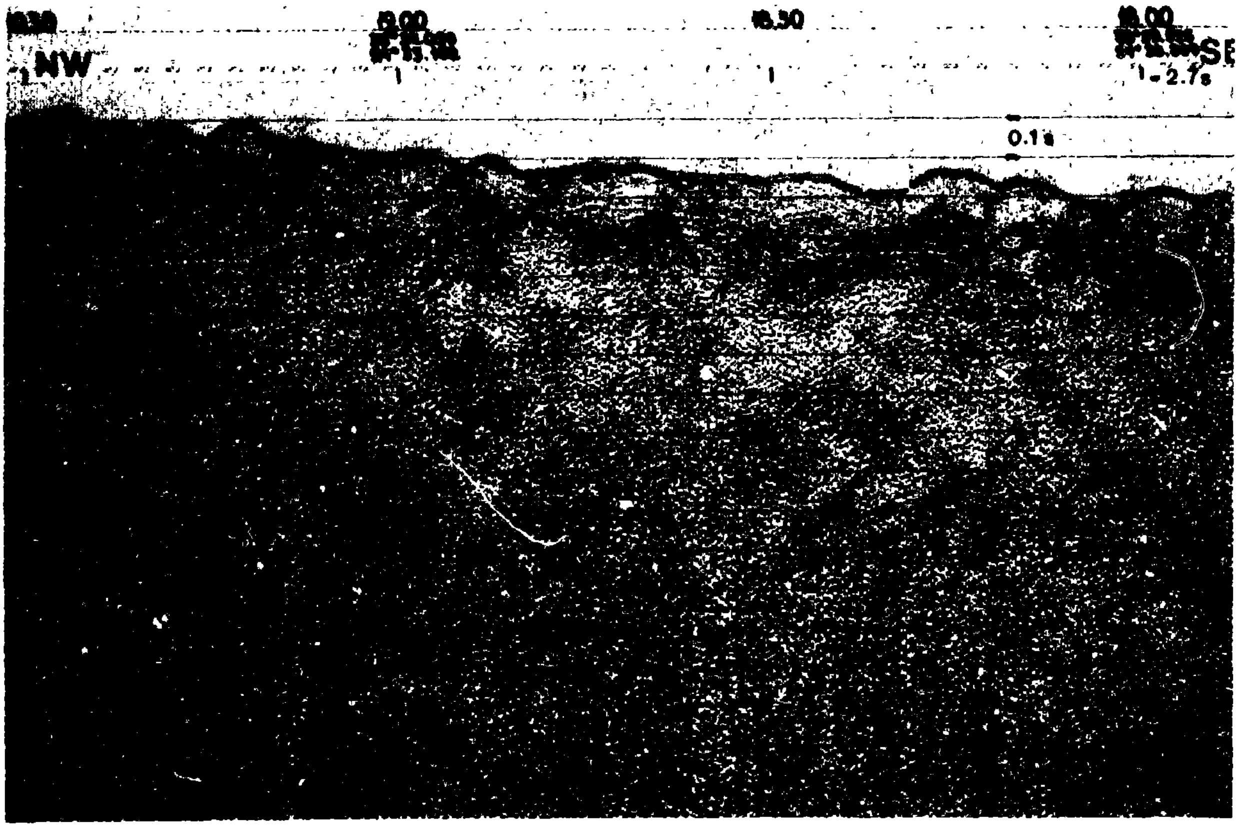

Fig. 39. Young deformations displayed in the seabottom morphology of the Mediterranean Ridge. This pattern is evidence of the continuing activity of Ridge. (Line PS-107)

Line PS-110 closes the square, three sides of which are formed by the previously described seismic lines. It is oriented in a NE-SW direction.

The picture seen in the seismic section is very similar to that recorded on the Mediterranean Ridge along line PS-108. The difference is an increased thickness of the assumed Messinian layer (up to 250 ms) and Pliocene-Quaternary sediments (up to 200 ms).

A structure similar in appearance to a mud dome is recorded near the end of the line (07^{40}). It is a gentle swell, more then 4 km in diameter at the base, with an elevation of about 130 m. Any inner reflections in this structure are absent. Geological sampling on this structure proved its diapiring origin by recovering mud breccia, and, in keeping with the naming convention for this region described in Chapter 3.1, it was named "Toronto" (after the hometown of John Woodside) (Fig. 42).

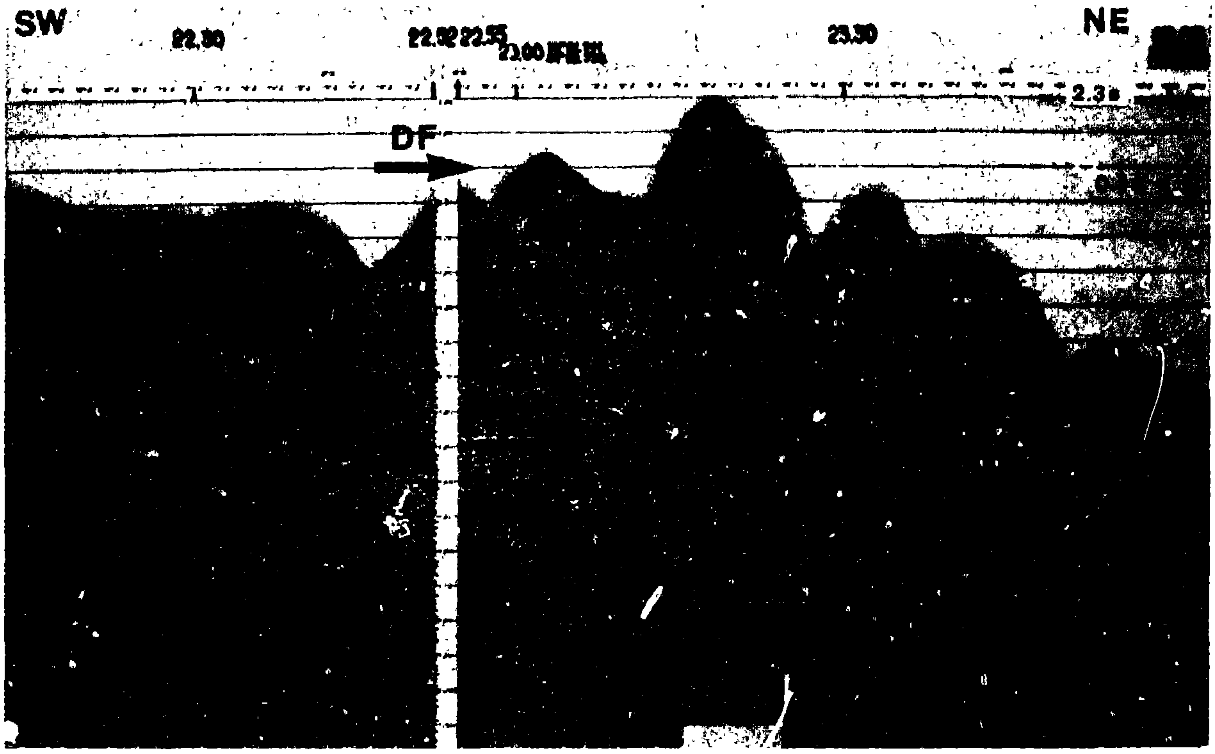

Fig. 40. Seismic image of the inner deformation front (DF) of the Mediterranean Ridge. (Line PS-108)

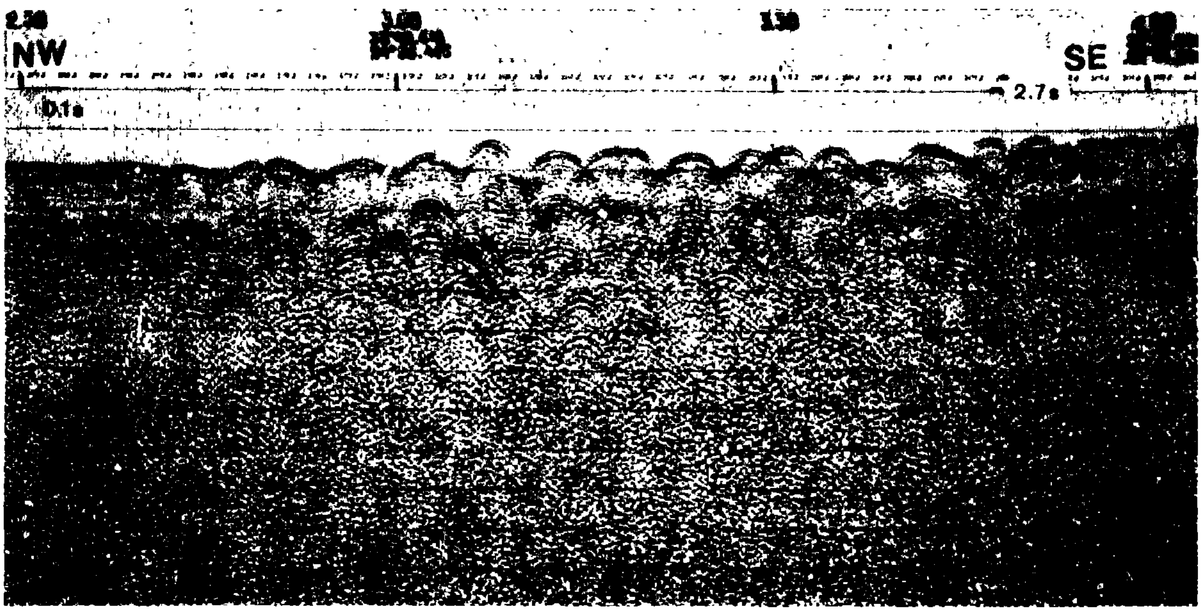

Fig. 41. Cobblestone topography of the Mediterranean Ridge formed by small and frequent folds. (Line PS-109)

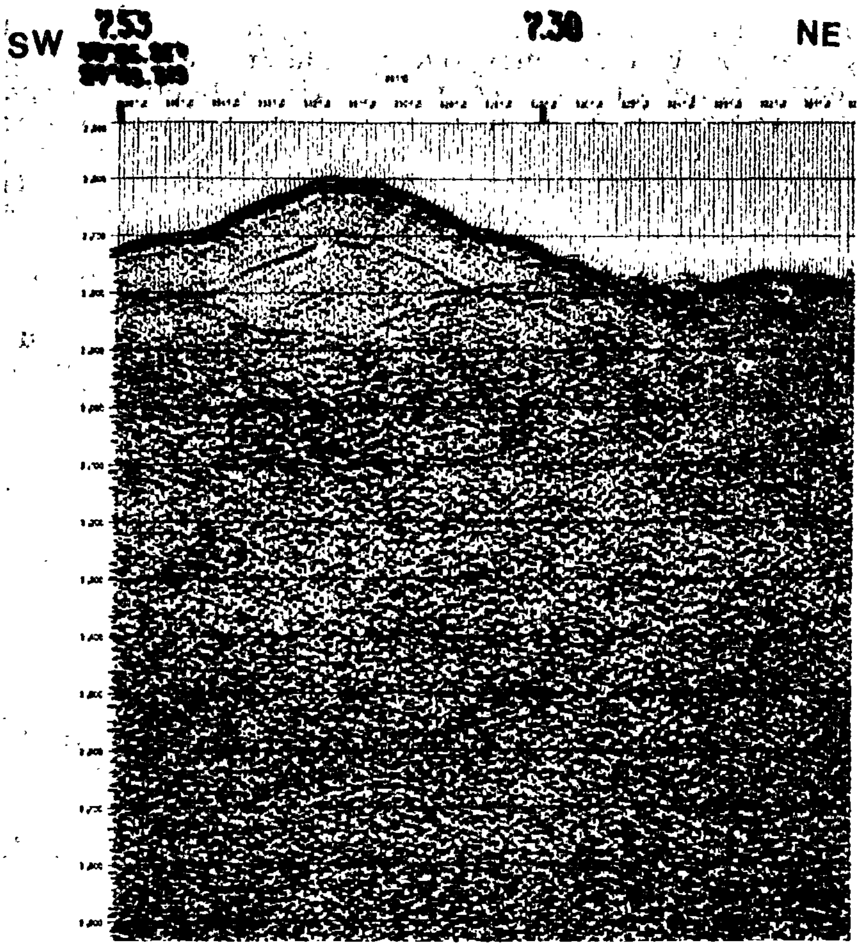

Fig. 42. Seismic image of the Toronto mud dome. The reflector at about 100 ms below the seafloor is an artifact produced by secondary triggering of the air gun. (Line PS-110)

Line PS-111 was dedicated to filling the gap between seismic and OKEAN lines PS-106 and PS-110. It runs parallel to them in a SW-NE direction. The line is discontinuous because of the air gun malfunction between 17^{58} and 19^{36}.

From the beginning of the line to 17^{20}, the Messinian and Pliocene-Quaternary sediments occur almost undisturbed; but after this time mark, there is a wide zone (till the break of recording at 17^{58}) of tectonic disturbance with a complex surface topography and uncorrelatable subsurface reflectors. The zone is displayed at the seafloor as a broad gentle rise.

After the break in recording and to 21^{20} the appearance of the Messinian and Pliocene-Quaternary sediments in line PS-111 becomes again almost horizontal, with low amplitude and short wavelength undulations. However the Messinian layer is broken by numerous normal faults with vertical offsets of a few tens of meters. The thickness of Pliocene-Quaternary sediments is 150-200 ms and of the Messinian is about 200 ms, although the base of the

Messinian is not clearly seen.

By the end of this line segment, the penetration significantly increases and attains almost 0.9 s, but deep reflectors can be traced only over a short distance.

The next zone of the tectonic disturbance is recognized between 21^{20} and 22^{20}. It is also expressed as a very gentle rise in the seabottom topography. The whole zone is characterized by chaotic seismic reflection configurations, so that the Pliocene-Quaternary layer can not be separated from the underlying sediments.

After the second deformation zone and till the end of the line, there is a tendency for the Pliocene-Quaternary to thicken from 80 ms to more than 200 ms. The base of the underlying Messinian is not defined. The sediments are slightly folded and occur with weak northeastern inclination towards the trench.

Seismic reflection profiling was also carried out along the last third of line PS-113, from 06^{04} to 07^{28}. This part of the line is characterized by a complex seabottom topography, with a relief of 330-350 m. No continuous reflectors were recorded along the line. The upper 300 ms of the seismic section has a semitransparent acoustic pattern. The lower part is displayed as chaotically bedded, with frequent, short and uncorrelatable reflectors.

The rough topography seems to be conditioned by the present of a number of mud domes. One of them stands separately at time mark 06^{25}. It has a basal width of about 1.6 km and a height of 80 m (Fig. 43).

A huge rough dome seen between 06^{40} and 07^{28} looks like a dark grey spot more than 10 km in diameter on the OKEAN record. It is proposed that this is a great mud volcano or, more likely, a field of very closely spaced mud volcanoes with overlapping mudflows. The sampling at Site 101 inside this dark spot recovered mud breccia under a thin cover of hemipelagic sediments. This patch of mud volcanoes was called "Gelendzhik", after the hometown of several Russian cruise participants.

Seismic profiling was carried out along line 115 from 00^{45} to 04^{41} (the end of the line). The topography seen in the profile has a typical "cobblestone" pattern with a relief of up to 150 m. From the corresponding OKEAN image it is evident that larger topographic features are oriented parallel to the line direction. The penetration is shallow and does not exceed 250 ms.

The upper transparent Pliocene-Quaternary layer has a thickness of 50-100 ms. The M-reflector is well-displayed between 02^{00} and 04^{41}. On the rest of the profile there is quite gradual transition from the transparent Pliocene-Quaternary unit to the underlying chaotically-bedded member.

The last line PS-116 is the southernmost line in Area No 2. It crosses the crest of the Mediterranean Ridge in a SE-NW direction. As well as the common topographic and seismic stratigraphic features already described for other seismic lines across the Mediterranean Ridge, there are some peculiarities to be mentioned. First of all, the reflector beneath the Pliocene-Quaternary layer between 05^{50} and 06^{05} bends down sharply, forming a pattern very similar to that shown for mud diapirs/mud volcanoes, although no signs of this phenomenon are seen on the seafloor (Fig. 44).

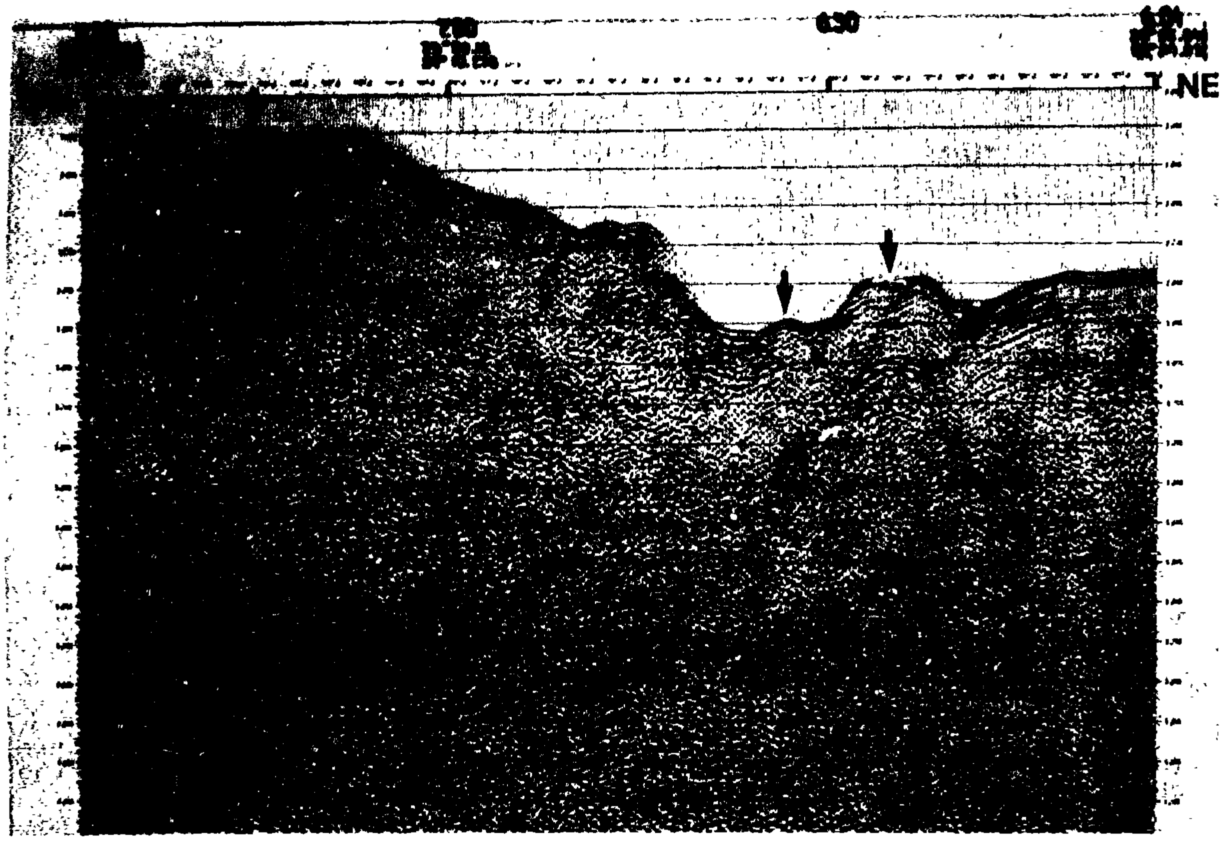

Fig. 43. A number of possible mud domes (arrows) recorded along seismic line PS-113

One more structure which is suspected to be a mud dome is recorded near time mark 07^{50}. It represents rather a gentle and flat-topped dome, about 1 km in diameter and 60 m high. Two similar structure between 09^{30} and 10^{00} could be the crests of elongated ridges seen on the corresponding OKEAN record.

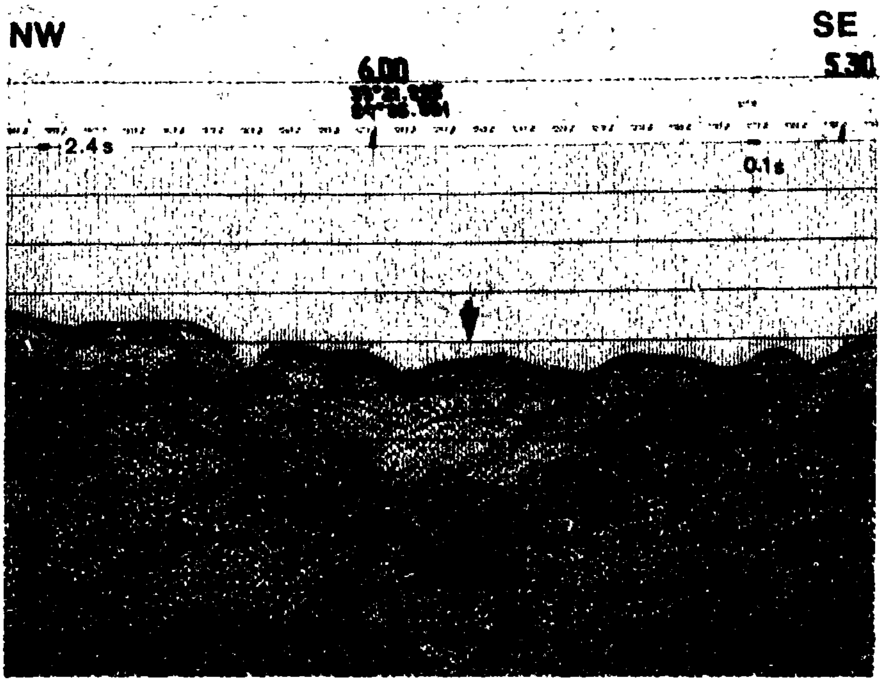

Fig. 44. A feature resembling a mud diapir by its inner structure (downbending pattern of the subbottom reflectors) but without the characteristic topography on the seafloor. (Line PS-116)

3.2.b. SIDESCAN SURVEY

OKEAN SONOGRAPHS

J. Woodside and V. Fomenko

The area was crossed from northeast to southwest by the first line (Line 106) to provide the general setting. The line started on the Cretan margin, continued across the Hellenic Trench, an Inner Plateau region and inner deformation front, and across the Olimpi mud diapir/mud volcano area between Milano and Napoli mud domes.

On the Cretan side of the Hellenic Trench are of tilted fault blocks inferred to be composed of sedimentary rocks. The edges of strata in these blocks give some of the strongest return signals of the entire survey area. The southern side of the trench axis also has an area of high amplitude backscatter which could be from large debris or possibly mud diapirs and volcanoes having a layer of mud breccia near the sea floor (see below). The absence of equally strong shadow regions which might be associated with rubble, and the presence of some circular features with what appear to be flow lobes emanating from the inferred cone, suggest the second interpretation is more likely. On the other hand, some coarse material would be expected in the vicinity of the trench.

Recognition of mud breccia

One of the most striking features shown by the OKEAN records are large irregular patches of very high reflectivity having no directly obvious relationship to the bathymetry. The first two bottom samples taken were from adjacent areas where the seafloor reflectivity observed by the OKEAN system showed the greatest contrast: a very black patch (very high reflectivity) and a very light patch, almost white (very low reflected backscatter). The core taken on the dark patch (core 79G) contained mud breccia at 75 cm from the seafloor, but mud breccia was not found from the core from the area of low reflectivity (core 80G) (Fig. 45).

A tentative correlation of the coarse material in the mud breccia with the higher reflectivity characteristics of the OKEAN record proved later to be correct. It was clear that the OKEAN sidescan sonar is affected by the sediment composition and grain size within the upper metres of sediment on the seafloor. This was also true of the deep-towed higher resolution MAK-1 sidescan system, but to a slightly different degree because of the different transmission characteristics for the two systems; and this difference provides the possibility of calibrating the depth to the mud breccia with slightly more precision.

It is clear from a cursory examination of both the MAK-1 and the OKEAN records that there are variations in level of reflectivity associated with what appear to be separate flows of mud breccia from mud volcanoes. In the case of Moscow mud volcano, there are two variations in the level of reflective backscatter in the OKEAN record which appear to be related to different flows as observed on the MAK-1 record for the same area. On the MAK-1 records, however, there are more shades of grey in the reflectivity indicating greater resolution in the determination of different flows of different ages.

The survey area was mapped on the basis of the correlation observed between high reflectivity patches and the presence of mud breccia. Without fail, all cores confirmed this correlation for the region. Obviously this is not a universal correlation: high reflectivity can be caused in many other ways (e.g. changes in angle of backscatter where strong reflections come from surfaces facing the source and receiver and weak reflections or shadows from bottom surfaces facing away at various angles from the source and receiver, the presence of hard surfaces such as the near-surface or outcropping sedimentary rocks in the Hellenic Trench, coarse material such as debris which has come from steep slopes, etc).

Mud diapir and mud volcano field

Within a surveyed region of more than 6000 km^2 we identified a number of large and small new diapirs and volcanoes on the basis of morphology and reflectivity (see above) (Fig. 46). It seems clear that more such features lie outside the area as well. Swath bathymetric mapping is required to observe many diapirs and volcanoes which lie within areas of high reflectivity because the more subtle reflections defining their morphology are obscured by the high reflectivity. Thus, areas characterized by near-surface mud breccia may contain a number of diapirs and volcanoes that the OKEAN can not see. The MAK lines (see the next section) provided more morphological details as well, but were restricted to only four relatively short lines in the area.

The focal point of the survey area was the Olimpi field surveyed originally by Cita et al. (1989c). The original survey and subsequent mapping (see, for example, Cita et al., 1989c and Camerlenghi et al., 1992) defined a close grouping of mud diapirs. Such a density of diapirs could not be observed elsewhere in the region using OKEAN. It is not clear whether the Olimpi field is in fact the central part of the broader region or simply a part of the belt of diapirs. OKEAN mapping did indicate that folds in the surrounding southern half of the region seems to encircle the region with the Olimpi field in the centre. The folds are best developed on the southeastern and southwestern lines with some also visible in the extreme southern part of the region. The impression given by this distribution of folding is of a broad regional outward compression from within the Olimpi area. This suggests that the investigated diapirs and volcanoes are superposed on a broader (and possibly expanding) regional dome which could be inscribed by the folds.

It seems to be pertinent to the evolution of this large diapir belt that its location lies just to the southwest of the Pliny Trench which is terminated by a series of southwest to northeast directed backthrusts. Camerlenghi et al. (1992) indicate that the diapirs may originate from fluid mud which becomes overpressured near the backthrust and beneath a sealing layer of salt. The presence also of some strike-slip faulting southwest from the Pliny Trench might provide zones of weakness (or broken seal) through which the mud could rise. This idea obtains some support from the apparent presence of another concentration of mud diapirs and volcanoes southwest from the analogous Strabo Trench further east along the ridge crest. This latter region of diapirs is inferred from the OKEAN line 118 which was run east from the survey area along the ridge crest, and has not been checked with coring (Fig. 47).

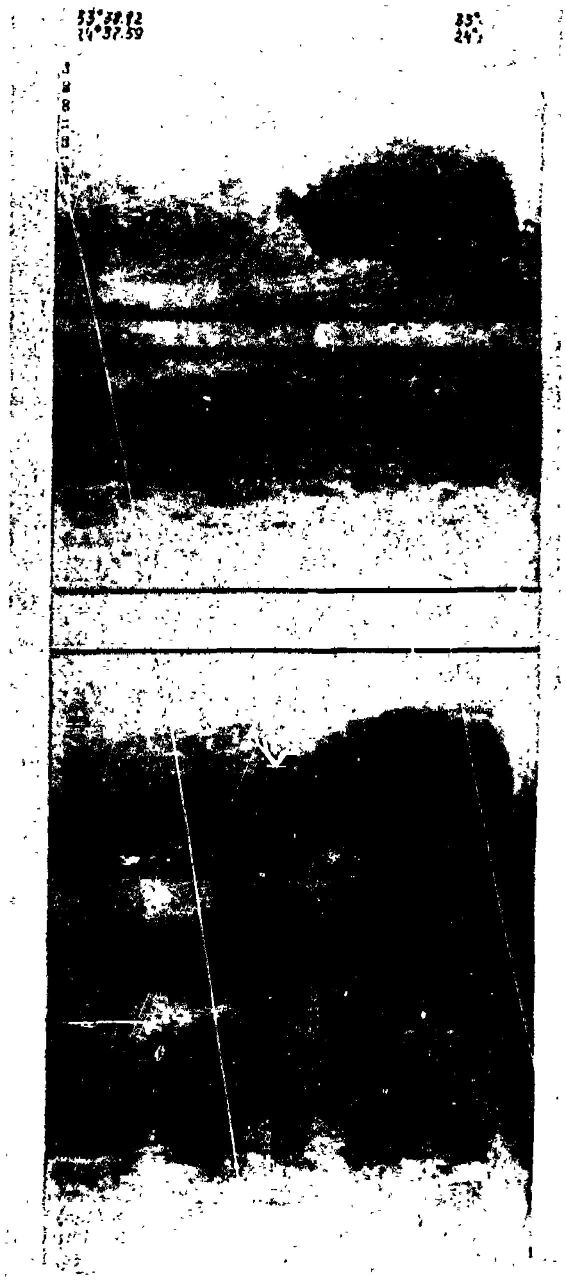

Fig. 45. OKEAN record of the Moscow mud dome with locations of sampling sites 79 and 80. Core 79G contained mud breccia at 75 cm from the seafloor; the mud breccia was not found in core 80G (see Fig. 57). Unprocessed (above) and processed (below) sonographs. The swath range is about 15 km. (Line 106A)

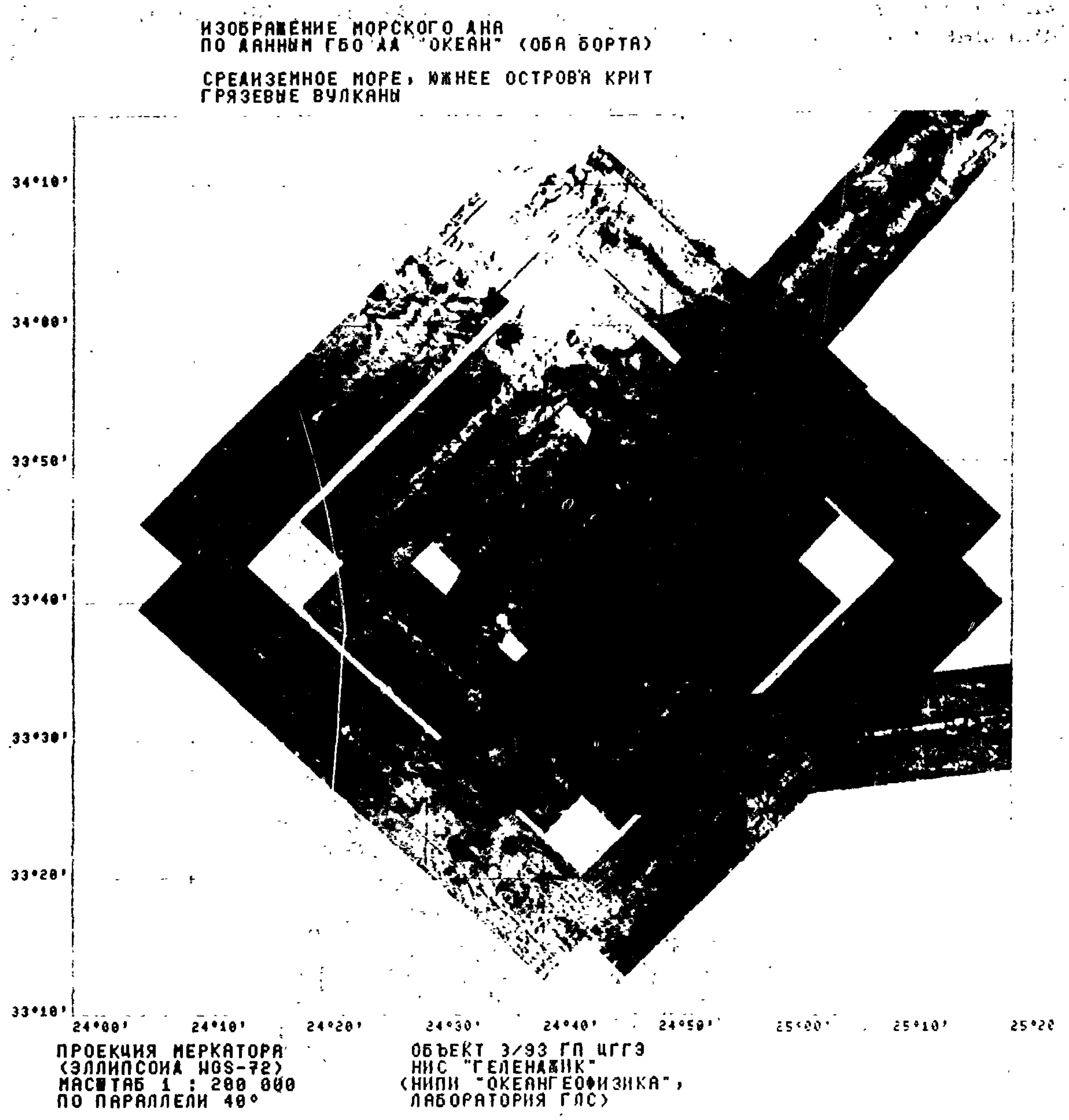

Fig. 46. OKEAN mosaic showing most of the mud domes around the Olimpi area. Smaller domes are not seen because of a small scale of the mosaic. (Compiled by V.B.Podshuveit, Yuzhmorgeologiya, on the base of digitized data)

In summary, the OKEAN sidescan sonar was of fundamental importance in mapping out not only the individual centres of diapirism and mud eruption but also the unexpected large extent of what can be called the Mediterranean Diapiric Belt. Furthermore it provided some evidence that this diapiric belt may itself represent a regional doming which is creating superficial folds around its perimeter. With the regional mapping completed with the OKEAN it was then easier to focus on specific areas of interest with the tools for detailed investigation of the target features.

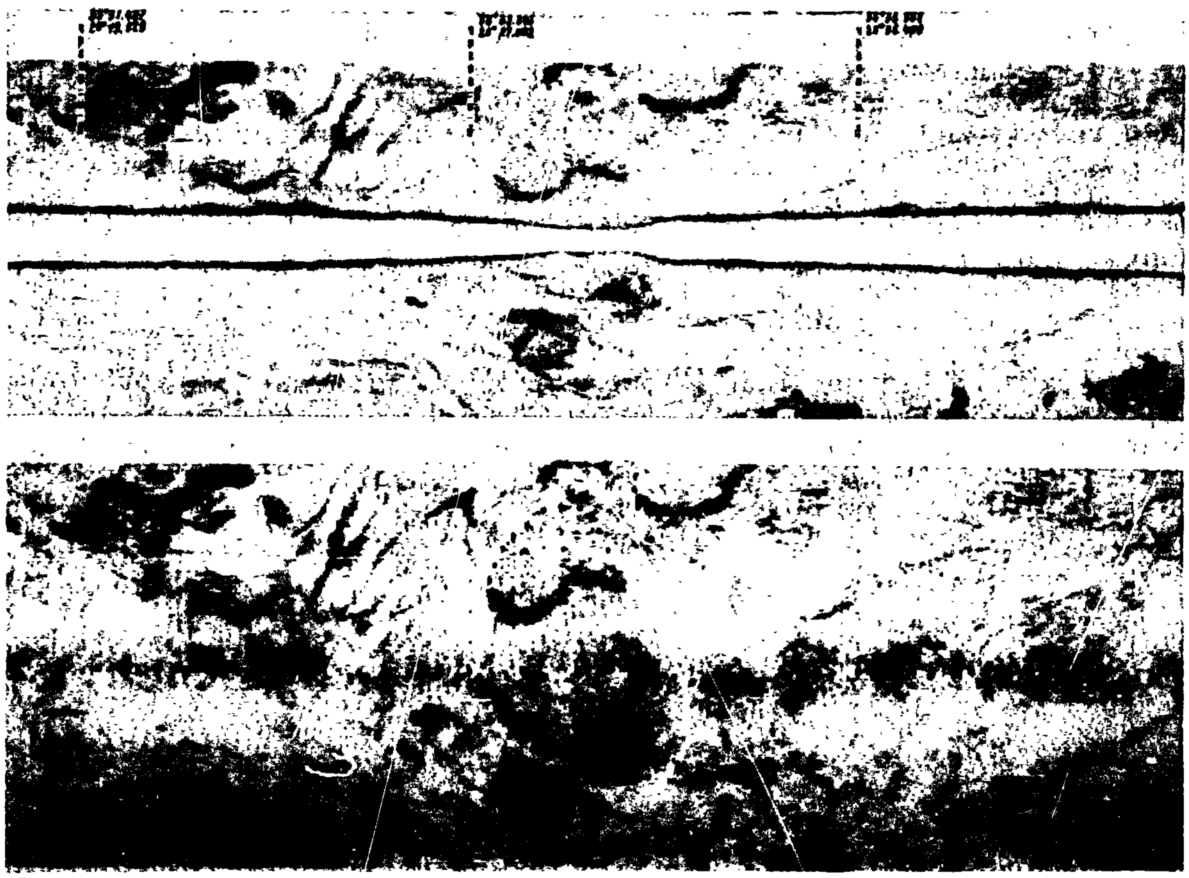

Fig. 47. Possible mud domes (rounded patches) recorded along OKEAN line 118. Unprocessed (above) and processed (below) sonographs. The swath range is about 15 km

MAK-1 SONOGRAPHS

W. van der Werff, C. Beijdorff, Yu. Gubanov, N. Vera, J. Galindo-Zaldivar, A. Moncada, and L. Nieto

During the 2nd leg of the TTR-3 Cruise, 4 MAK-I 30 kHz transects (16, 17, 18, 19) were acquired which all trend in NW-SE direction and are spaced between 5 to 20 km apart (Fig. 38). The total length of the MAK-I recorded lines is 150 km. In contrast with the OKEAN mosaic, these transects do not overlap, but allow for a more detailed interpretation of structural and sedimentary features.

The lines cover a number of significant mud volcanoes and undulating fold and fault structures which either may be associated with the evolution of the accretionary complex or the mud diapir field. In addition, marked changes in reflectivity and structural lineations, pockmarks, collapse holes, flow structures and other unidentified structures have been mapped. These features will be described below according to their acoustic facies in MAK-I swath profiles, and their structural trends.

Description of structural and sedimentological elements

Type I: The Mediterranean Ridge is characterized by a surface composed of undulating folds that consist of open anticlines and synclines. Two different fold orientations have been recognized that respectively have a NNE-SSW and E-W trend. The wavelength varies from 300 m to 1 km, and the amplitude is generally less than 50 m. The lengths of the hinge lines are generally greater than 2 km. Axial surfaces of these folds are mostly subvertical. In some areas of the MAK-I surveys, it is possible to recognize periclinal ends of folds and "en echelon" arrays of folds. Anticlines can be divided into two distinct groups, respectively *Type IA* and *IB*. *Type IA* shows folding of highly reflective sediments composed of pelagic materials (Fig. 48). *Type IB* anticlines are characterized by pelagic materials that define the flanks of the folds, possibly intruded by diapirs distinguished by acoustically opaque seismic facies (Fig. 49). These diapirs may be composed by mud breccia. Diapiric intrusions occur associated with normal faults in the core of the folds.

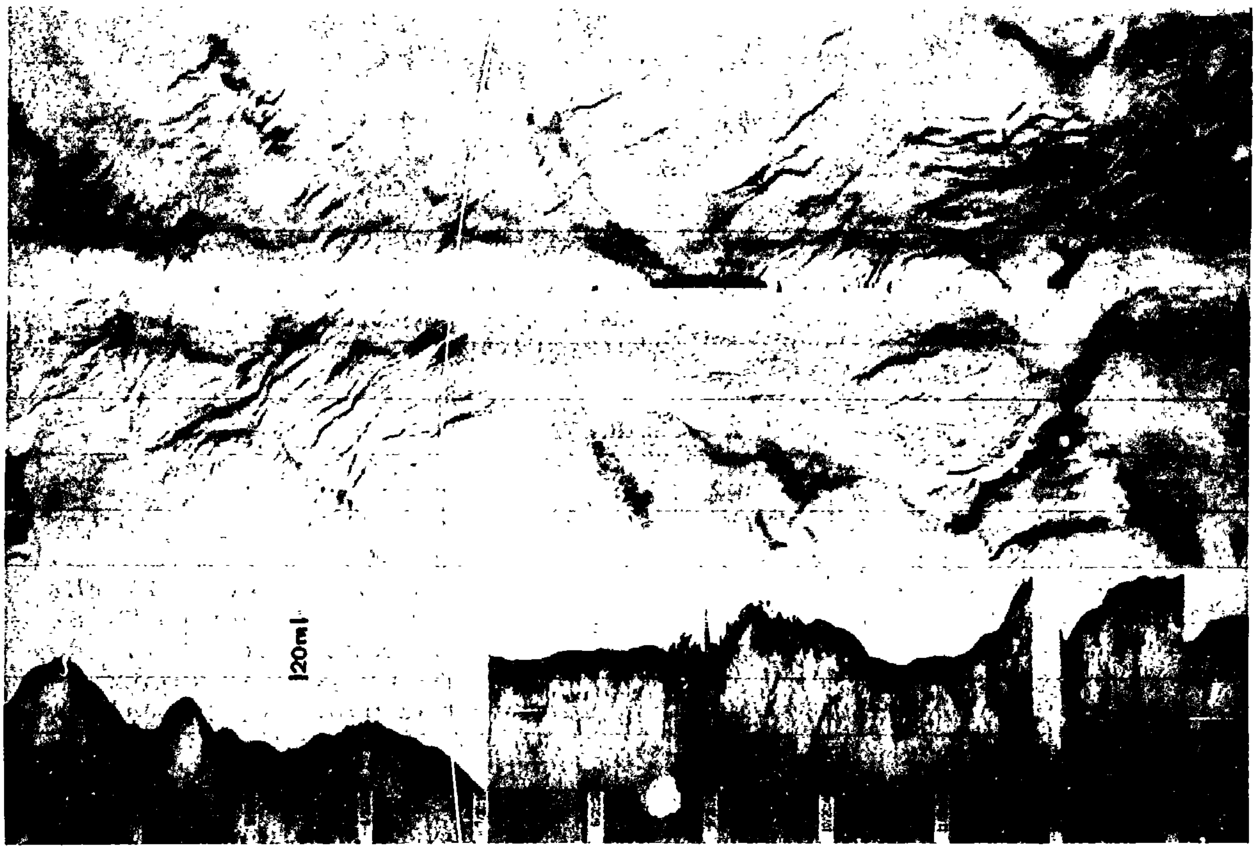

Fig. 48. MAK facies 1A. Folding in highly reflective sediments. (MAK-1 line 19)

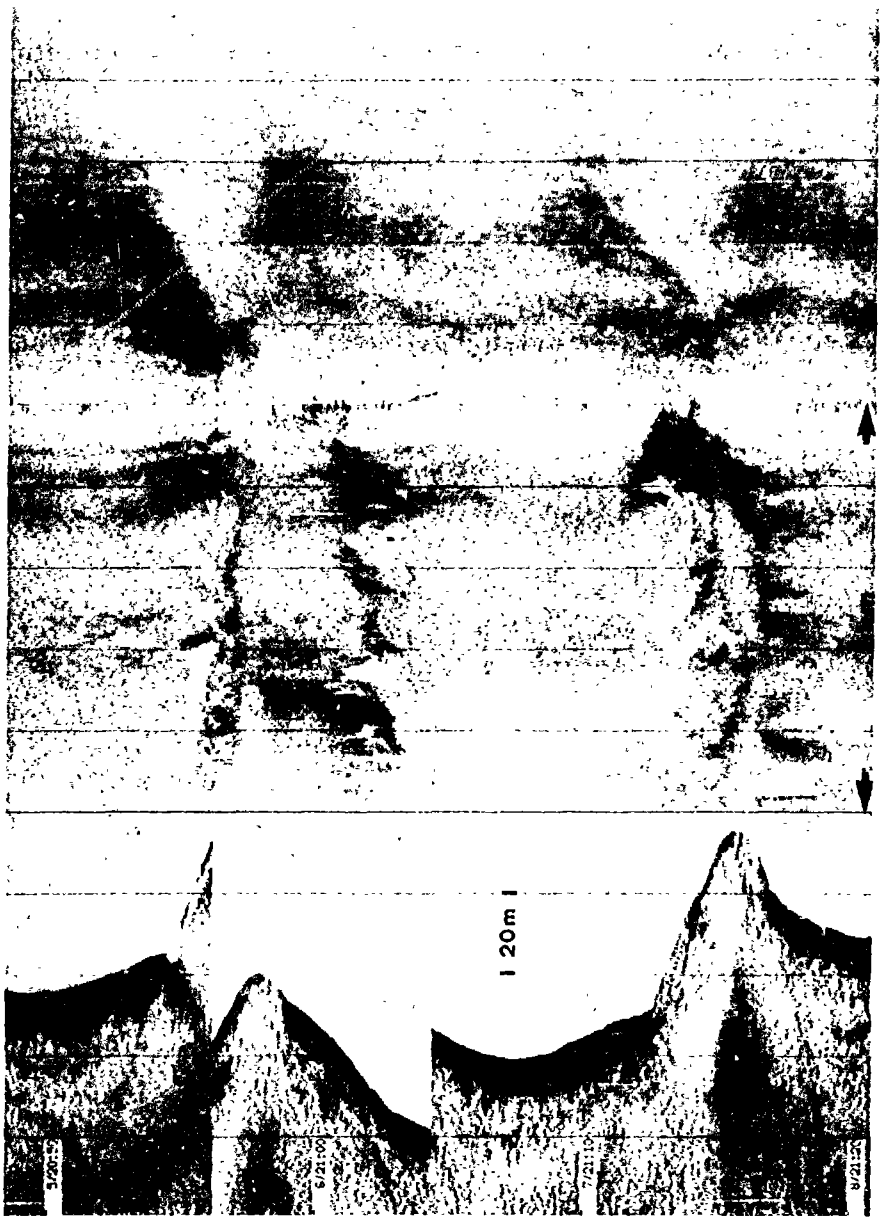

Fig. 49. MAK facies 1B. Folds possibly protruded by diapirs. (MAK-1 line 17)

Type IIA: Mud volcanoes and mud flows are identified in profiles 16, 17 and 18 (Fig. 50). The reflectivity of the mud breccia is higher than that of the autochthonous pelagic sediments. The boundary between the low- and high- reflective sediments is very sharp.

The shape of the mud volcanoes is generally circular with a maximum radius of about 3.5 km. The mud volcanoes are characterized either by a rather flat topography ("mud pies") or by a typical "Mexican hat" topography with a synclinal rim developed around the center. The presence of a highly-reflective seismic facies together with semicircular lineation patterns may represent debris flows composed of mud breccia, that erupted from the top of the mud volcanoes. Circular rims are identified around and inside the mud volcano complex and may represent local "cones".

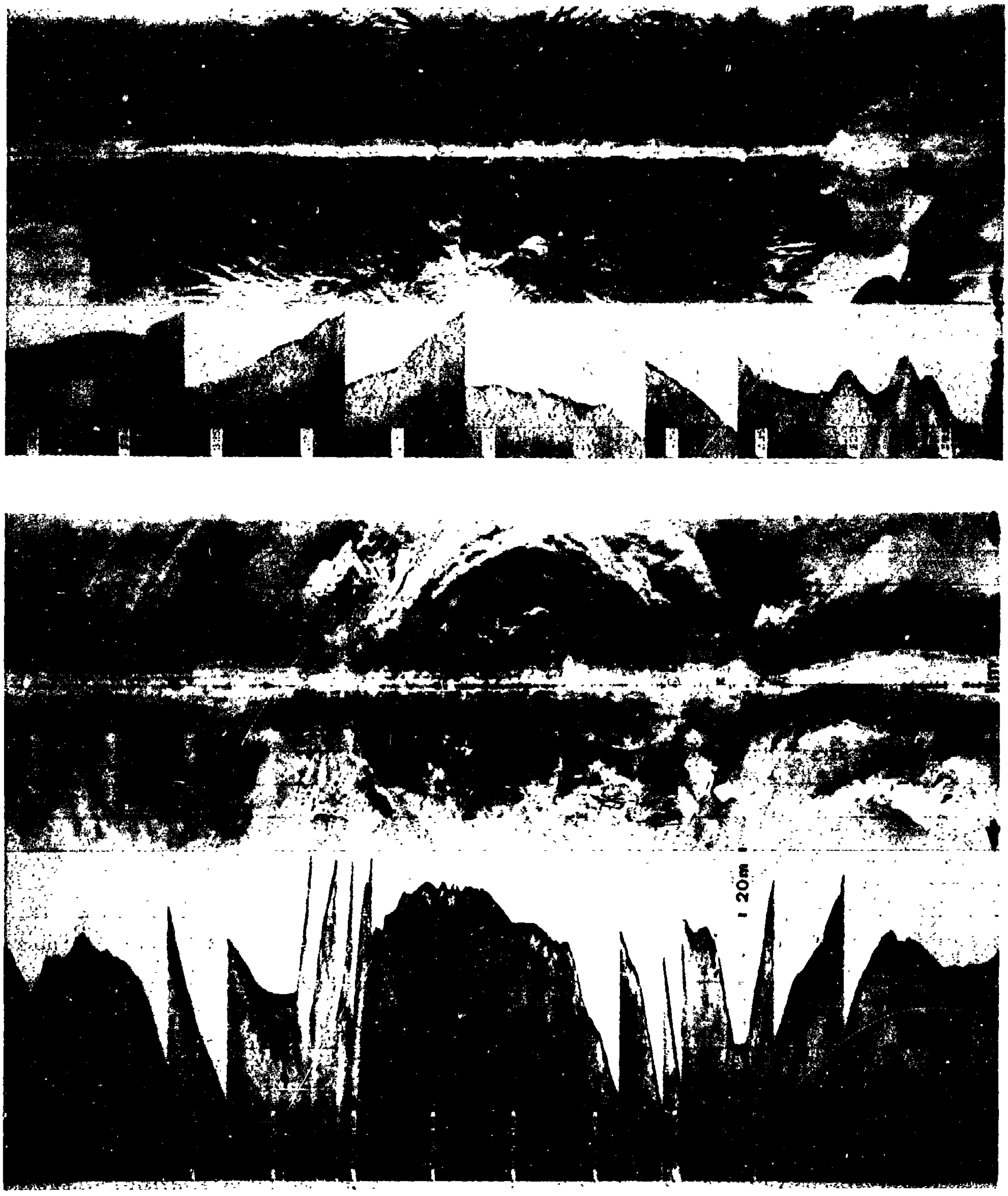

Fig. 50. MAK facies IIA. Mud volcano and mud flows. A: the Toronto Dome (MAK-1 line 17); B: the Napoli Dome (MAK-1 line 18)

Type IIB: Several smaller sized "dome" structures with varying surface expressions and a lower reflectivity have been mapped (Fig. 51). The diameter of these concentric structures varies from 100 m to more than 1 km. These features possibly represent smaller vents. In some areas it is also possible to identify nearly circular holes of about hundred meters in size which may be related to dissolution or in some cases may represent brine pools (Fig. 52).

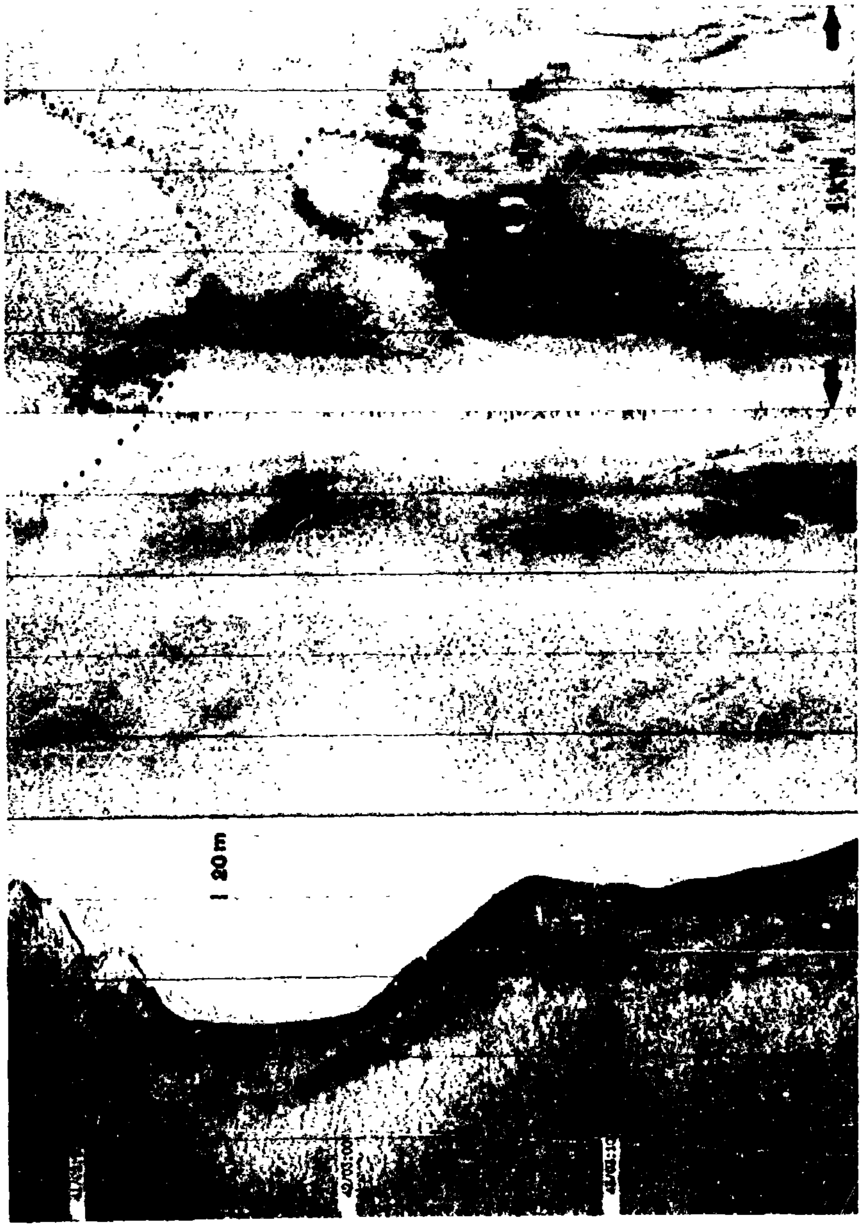

Fig. 51. MAK facies IIB. Smaller sized "dome" structures (MAK-1 line 16).

Type III: Low-reflectivity areas with thin linear features.
This type of facies is shown e.g. in a part of the 19 MAK-I line (Fig. 53). The thin lines are generally short (few kilometres) and gently sinuous. These features can be interpreted as small folds or fractures. In these areas the acoustic profile shows up to 60 m of well-layered sediments.

Fig. 52. MAK facies IIB. Circular structures which may be related to dissolution (brine pool?). (MAK-1 line 18)

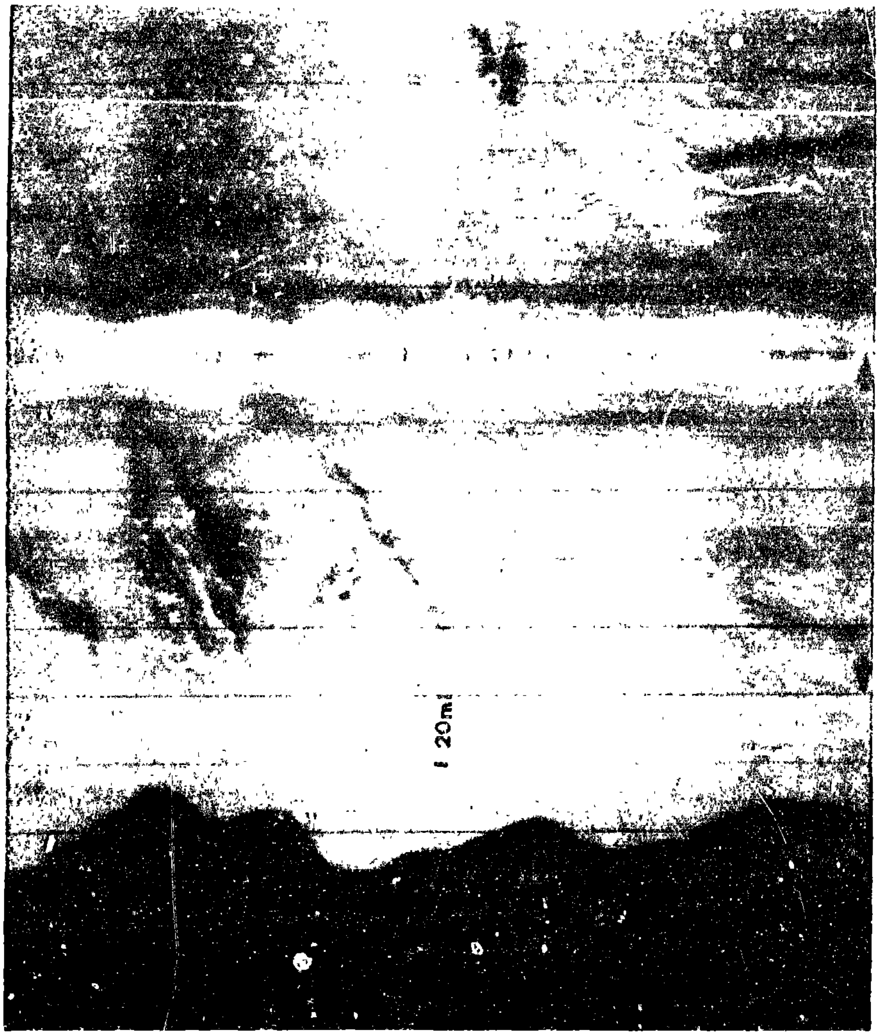

Fig. 53. MAK facies III. Small folds and fractures. (MAK-1 line 19)

3.2.c. UNDERWATER TV

E. Ivanova and A. Lototskaya

Two underwater video runs were made across the Napoli and Moscow mud volcanoes in the Olimpi area. The first one crossed the Napoli Dome from the depression along the southeast side (33°42.906'N/24°41.684'E), up the slope and across the volcano crater in the northwest direction, ending on the opposite slope (33°43.844'N/24°40.586'E) (Fig. 54). The duration of the recording was 2 hours 28 minutes. The second line crosses the Moscow volcano from the southwest to the northeast between the points with the coordinates 33°39.780'N/24°30.546'E and 33°40.825'N/24°30.601'E. The duration of this recording was 2 hours 39 minutes. The Napoli dome was chosen because it is the ODP target, and the Moscow mud pie was selected on the basis of the interesting results from the Napoli dome and apparent similarities between the two features.

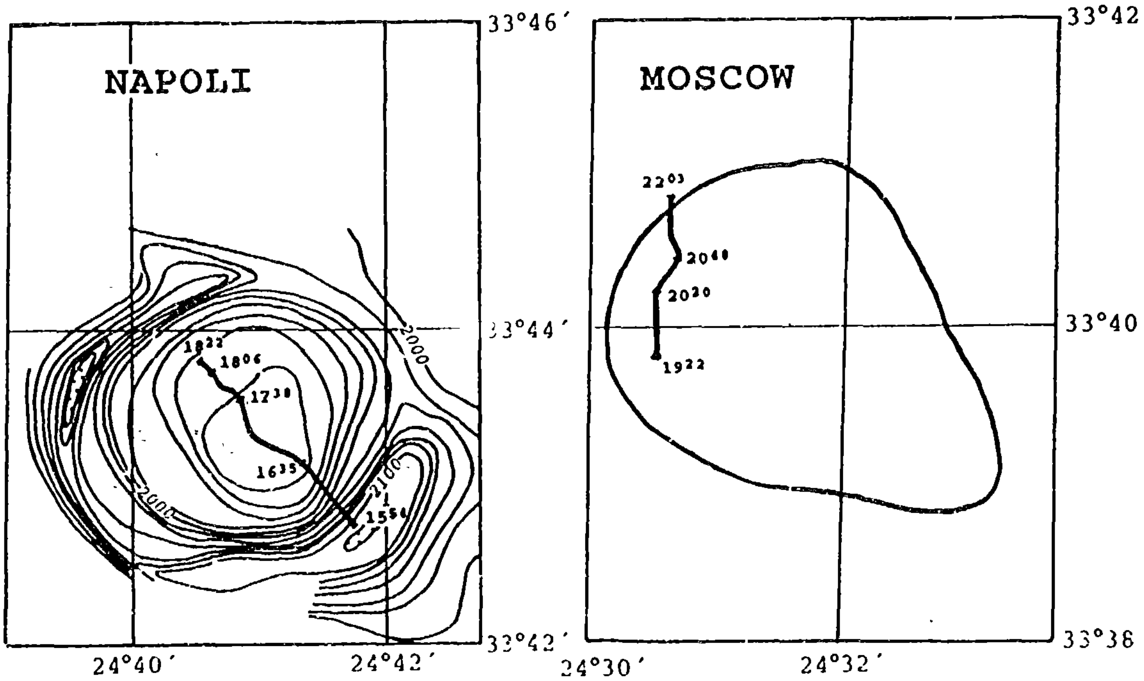

Fig. 54. Location of the underwater TV profiles on the Napoli and Moscow mud domes. (The bathymetry of the Napoli dome is after Camerlenghi et al., 1992)

The bottom sediments are represented generally by yellowish-brown mud which is common to the tops of most of the cores taken in the area. An unconsolidated, water-saturated thin layer which is easily removed by the slightest movements of the bottom water (caused, for example, by movement of the video camera apparatus) covers this mud in many places. The following bottom features were observed also; and some preliminary ideas about their nature are given which should be discussed with the specialists such as biologists.

(1) In some areas of the Napoli Dome in particular, there occur patches, strips and fields of dark grey to black heterogeneous material which tends to be comparatively coarse, even gravelly. These patches have sharp boundaries with basal light sediments and seem to fill in the bottom depressions. They could be the result of mud breccia flowing down the volcano slope.

(2) On both domes there are black holes of two types:

(a) The first type is of a small diameter (less than 10 cm) and circular in shape. Sometimes the holes are surrounded or covered by white matter. Most often, the white material on the rims is absent from one quadrant of the circular structure, giving a "horseshoe" appearance. Occasionally the white material lies only along two sides of the hole like two parentheses. In these cases the holes look elliptical, and the long axis is assumed to be in the direction of the slope of the dome. The holes are occasionally aligned in rows which seem to be roughly parallel to the dip of the slope (assuming that the camera was towed up dip at these times); and in places they form groups or fields. Bubbles of gas in the water column are often observed, associating with these features.

(b) The second type is represented by holes of a larger size than the first type (approximately from 50 cm to a metre scale). They are irregular in shape. Their rims also may have a white coating. Active gas bubbling is observed simultaneously with the appearance of these structures. In most cases, sediment is being expelled from these holes. We infer that fluids are actively being vented here, bringing away some surrounding sediment with them. In so doing, the vents enlarge and deepen to form larger pits. Possibly the process of expelling mud breccia into the water column acts to winnow out the gravel-sized clasts which form the dark patches described above.

(3) Tracks up to a metre long and 5 to 10 cm across are observed on both domes but they are more prevalent on the Moscow Dome. They are inferred to represent the traces of bottom fauna activity (e.g. holothurians?).

(4) Blocky structures sometimes arise in or around the pits created by the most active vents. They give the appearance of a rough hard black rim in places, or a step inside the depressions. Shadows from the camera lights indicate that these rims are elevated a few centimetres above the seafloor. They are accompanied by cracks and holes in areas characterized by abundant fluid vents. It might be speculated that they are formed either by some precipitation at the vents or by the build-up of organic material (see next feature).

(5) White, dark brown, reddish-brown, and greenish-blue crusts are observed covering the blocky structures described above, as well as the margins of the holes. We speculate that

they might be bacterial mats which derive their feeding from the material emitted from vents. The favourable environment for various communities of organisms in the vicinity of the vents is suggested by the presence also of areas with a high density of shells and what appear to be worm tubes. The later features have the appearance of randomly bent and twisted wire, or loose black string dropped on the seafloor.

(6) Abundant shells are often observed near the vents. Light brown mud on the sea floor in these areas also records the tracks of various unidentified organisms which form a dense pattern of light lines.

(7) The presence of man is never to be forgotten: on the Moscow mud dome we observed a wine bottle.

Four main types of areas are formed by different combinations of the described features:

(a) The yellowish-brown sediment with holes and traces of bottom fauna characterizes lower parts of the slopes of both volcanoes. Gas bubbles are usually observed rising through the water in these areas.

(b) Dark-grey patches, strips, and fields of mud breccia were noticed mainly on the slopes. A lighter fine-grained fraction of sediment was probably carried further down the slope where it was found as unconsolidated dark layer above basal light sediments.

(c) Areas of extended depressions with irregular blocky margins, holes of large size and cracks, all covered by inferred bacterial mats can be interpreted as the most active zones. They were found only on the Napoli mud volcano, but are expected to be present on the Moscow mud volcano as well because of similarities in the character of the MAK-1 records. They coincide obviously with the locations of the most active fluid emission.

(d) Fields covered by shells and different features of organic origin seem to surround the most active parts of the Napoli volcano.

We consider the most important contribution of this part of the study is the evidence for active and extensive emission of fluids from the Napoli dome. Multiple gas bubbles in the video records indicates that the sediments of the dome are extremely saturated with gas constantly escaping to the seawater. It was confirmed by bottom sampling of a mud "mousse" full of vesicles from gas bubbles and small conduits. The OKEAN and MAK-1 sidescan sonar records show the Napoli Dome to be light in colour, in contrast to most of other domes which exhibit high level of backscattering suggesting the presence of subsurface mud breccia. There are, however, highly reflective spots and irregular patches which are thought to be caused by vents and pits containing vents. The same sonar pattern was observed on the Moscow mud dome but the video line there did not cross any active vents.

3.2.d. BOTTOM SAMPLING

M.B. Cita, E. Erba, R. Lucchi, R. van der Meer, M. Pott, and L. Nieto

A total of 25 cores (1 Kastenlot core, 3 box cores and 21 gravity cores) were collected during Leg 2 of the TTR-3 Cruise in the Eastern Mediterranean (Fig. 55). The total recovery is 61.59 m; the longest core recovery is 491.5 cm (core 97G from the plateau), whereas the shortest core recovery is 81 cm (core 96G from the deformation front) (Table V).

The shipboard investigations included splitting of the cores, photographing them, detailed lithologic description and sampling for micropaleontology and sedimentology. Coring was focussed on the Napoli Dome (discovered and previously sampled during cruises BAN-88 and BAN-89) and on new domes discovered during the present cruise, situated on the plateau and inner deformation front north of the mud diapir/mud volcano belt. The results are here synthesized by areas.

NAPOLI DOME AREA

Three cores (84G, 85G, 86G) were taken from the Napoli Dome area (Fig. 56). They all contain the mud breccia overlain by a veneer of pelagic sediments (Holocene oozes). The mud breccia is very fine grained, not organized and belongs to the facies A-3. The peculiar mousse-type mud breccia (A-3b) is characterized by a strong smell of H_2S and abundant millimetric voids due to gas expansion. It is always overlain by a homogeneous, very fine grained, soupy mud breccia (A-3a), fading upwards into pelagic marls. The boundary between the Holocene ooze and the mud breccia is marked by an oxidized interval up to 10 cm thick.

MOSCOW DOME AREA

Six cores were collected from the Moscow Dome area (Fig. 57). The dome is a new mud-pie discovered during the present cruise and named after the home town of co-chief scientist Michael Ivanov.

In Fig. 57 the cores are reported along a NW-SE transect including two cores taken from outside the Moscow Dome boundary. Cores 89G, 90G, 91G and 79G contain the mud breccia and pelagic sediments. Cores 88G and 80G contain pelagic sequences with some hiatuses (see below). The mud breccia of the Moscow Dome is characterized by a massive structure and a very sticky matrix with millimetric to pluri-centimetric clasts of semi-lithified to indurated sediments (calcarenites, sandstones and siltstones). Both facies type A-1 and A-2 are identified. In core 90G, the mud breccia is overlain by a veneer of recent oozes, while in core 79G the entire Holocene section is represented. Sliding of pelagic sediments along the slope is documented in core 91G, where the Holocene sequence is disturbed and repeated three times due to slumping. In core 89G, two intervals of the mud breccia are interbedded with pelagic sediments testifying to multiple injections or flows of extrusions. The upper boundary between the mud breccia and the pelagic sediments is always transitional and

Table V
Summary of bottom sampling data in Area No 2

CORE	DATE	TIME AT BOTTOM*	WATER DEPTH (m)	COORDINATES		SETTING	RECOVERY (cm)	LITHOLOGY	FACIES	AGE
TTR3-78K	27-6-93	17:40:12	2213,6	33°50.31'	24°53.23'	Plateau	197,0	MARKER BED MARL SAPROPEL S-1 TEPHRA Y-5	Pelagic Pelagic Euxinic Volcanogenic	HOLOCENE LATE PLEISTOCENE
TTR3-79G	28-6-93	11:26:05	1967,7	33°39.23'	24°32.61'	Moscow -dome	276,0	MARKER BED SAPROPEL S-1 MARL MUD BRECCIA	Pelagic Euxinic Pelagic Diapiric type A (massive)	HOLOCENE LATE PLEISTOCENE MIXED
TTR3-80G	28-6-93	14:11:17	1920,3	33°39.00'	24°34.71'	Close by "white area"	499,0	MARKER BED MARL SAPROPEL S-1, 5 & 6 TEPHRA Y-5	Pelagic Pelagic Euxinic Volcanogenic	HOLOCENE LATE PLEISTOCENE MIDDLE PLEISTOCENE
TTR3-81G	28-6-93	15:20:37	1903,9	33°40.68'	24°36.42'	Top of Sivor-dome	318,0	MARKER BED Dark X-4(?) TEPHRA MARL MUD BRECCIA	Pelagic Volcanogenic Pelagic Diapiric type B-3 (patchy cloudy)	HOLOCENE LATE PLEISTOCENE Mixed
TTR3-82G	28-6-93	16:46:11	2042,2	33°37.61'	24°41.08'	Mudstone-dome	235,0	PTEROPOD OOZE MUD BRECCIA	Pelagic Diapiric type A-2 (massive)	HOLOCENE Mixed
TTR3-83G	30-6-93	10:17:57	1971,0	33°46.92'	24°36.53'	Milford Haven-dome	218,0	MARL MUD BRECCIA	Pelagic Diapiric type A-1 (massive)	HOLOCENE Mixed
TTR3-84G	30-6-93	12:06:41	1949,4	33°43.47'	24°41.13'	Top of Napoli-dome, at location of rounded feature, visible on MAK-1	311,5	MARL VENEER MUD BRECCIA Some dark layers	Pelagic Diapiric type A-3 (mousse) Type B-1 (layered)	HOLOCENE Mixed
TTR3-85G	30-6-93	13:05:24	1950,4	33°43.46'	24°41.10'	Top of Napoli-dome	211,5	MARL VENEER MUD BRECCIA	Pelagic Diapiric type A-2 (massive) and diapiric type A-3 (mousse)	HOLOCENE Mixed
TTR3-86B	30-6-93	14:19:30	1770,3	33°43.47'	24°41.11'	Top of Napoli-dome	52,0	MARL VENEER MUD BRECCIA	Pelagic Diapiric type A-3 (homogeneous)	HOLOCENE Mixed
TTR3-87G	1-7-93	11:14:40	1810,6	33°43.82'	24°27.63'	Top of mystery dome	395,5	MARKER BED MARL TEPHRA Y-5 SAPROPEL X-4(?)	Pelagic Pelagic Volcanogenic Euxinic	HOLOCENE LATE PLEISTOCENE MIDDLE PLEISTOCENE
TTR3-88G	1-7-93	12:37:48	1937,1	33°41.18'	24°30.11'	Flank of Moscow-dome	482,5	MARKER BED SAPROPEL S-1 TEPHRA Y-5 SAPROPEL X-4(?) SAPROPEL S-5	Pelagic Euxinic Volcanogenic Euxinic Euxinic	HOLOCENE LATE PLEISTOCENE MIDDLE PLEISTOCENE

CORE	DATE	TIME AT BOTTOM*	WATER DEPTH (m)	COORDINATES	SETTING	RECOVERY (cm)	LITHOLOGY	FACIES	AGE
TTR3-89G	1-7-93	13:40:14	1859,8	33°41.15' 24°30.81'	Base of slope of Moscow-dome	368,5	MARKER BED MUD BRECCIA TEPHRA Y-5	Pelagic Diapiric Volcanogenic	HOLOCENE LATE PLEISTOCENE Mixed
TTR3-90G	1-7-93	15:28:40	1847,9	33°40.50' 24°31.42'	Top of Moscow-dome	113,0	MUD BRECCIA	Diapiric type A-1	Mixed
TTR3-91G	1-7-93	16:44:00	1922,0	33°39.10' 24°31.82'	Base of slope of Moscow-dome	361,0	MARKER BED (3 times) SAPROPEL S-1 (3 times) MUD BRECCIA	Pelagic Euxinic Diapiric	HOLOCENE Mixed
TTR3-92G	2-7-93	15:33:44	1920,1	33°47.16' 24°39.06'	Top of Leipzig-dome	112,0	MUD BRECCIA	Diapiric type A-1 & A-2	Mixed
TTR3-93G	2-7-93	16:34:11	2053,4	33°46.40' 24°39.51'	Base of Leipzig-dome		MUD BRECCIA SAPROPEL S-1 MARL MUD BRECCIA	Diapiric Euxinic Pelagic Diapiric type A-1 & A-2	Mixed HOLOCENE
TTR3-94G	2-7-93	17:28:21	1987,2	33°46.81' 24°39.25'	Mid slope of Leipzig-dome	180,5	MUD BRECCIA	Diapiric type A-1	Mixed
TTR3-95G	3-7-93	15:16:08	2247,3	33°52.50' 24°50.57'	Jaen-dome, mid slope of deformation front	277,5	MARLS MUD BRECCIA	Pelagic Diapiric type A-1 & A-2	HOLOCENE Mixed
TTR3-96G	3-7-93	16:28:01	2187,1	33°53.[illegible] 24°49.58'	Flat top of deformation front	81,0	MARL & STONE	Pelagic	HOLOCENE MID & EARLY PLEISTOCENE
TTR3-97G	3-7-93	17:58:13	2209,5	33°50.3[illegible]' 24°53.23'	Plateau	491,5	MARKER BED MARLS SAPROPEL S-1 ,4 ,4*,5 & 6 TEPHRA Y-5 & X-4	Pelagic Pelagic Euxinic Volcanogenic	HOLOCENE LATE PLEISTOCENE MIDDLE PLEISTOCENE
TTR3-98B	3-7-93	19:10:06	2211,6	33°50.31' 24°53.23'	Plateau	24,0	MARL SAPROPEL S-1	Pelagic Euxinic	HOLOCENE LATE PLEISTOCENE
TTR3-99B	3-7-93	21:08:43	2211,1	33°50.30' 24°53.44'	Plateau	35,5	MARL SAPROPEL S-1	Pelagic Euxinic	HOLOCENE LATE PLEISTOCENE
TTR3-100G	4-7-93	17:01:45	1832,0	33°49.86' 24°16.48'	Gelendzhik plateau	409,0	MARKER BED MARL SAPROPEL S-1, 4, 5(?) & 6 TEPHRA	Pelagic Pelagic Euxinic Volcanogenic	HOLOCENE LATE PLEISTOCENE MIDDLE PLEISTOCENE
TTR3-101G	4-7-93	18:32:16	1952,9	33°53.78' 24°18.69'	Gelendzhik-dome	178,0	PTEROPOD OOZE MUD BRECCIA	Pelagic Diapiric type A-1 & A-2	HOLOCENE Mixed
TTR3-102G	5-7-93	4:34:14	199[illegible],8	33°27.12' 24°44.32'	Toronto-dome	84,0	PTEROPOD OOZE MUD BRECCIA	Pelagic Diapiric type A-2	HOLOCENE MIDDLE & LATE CRETACEOUS

* Ship Time

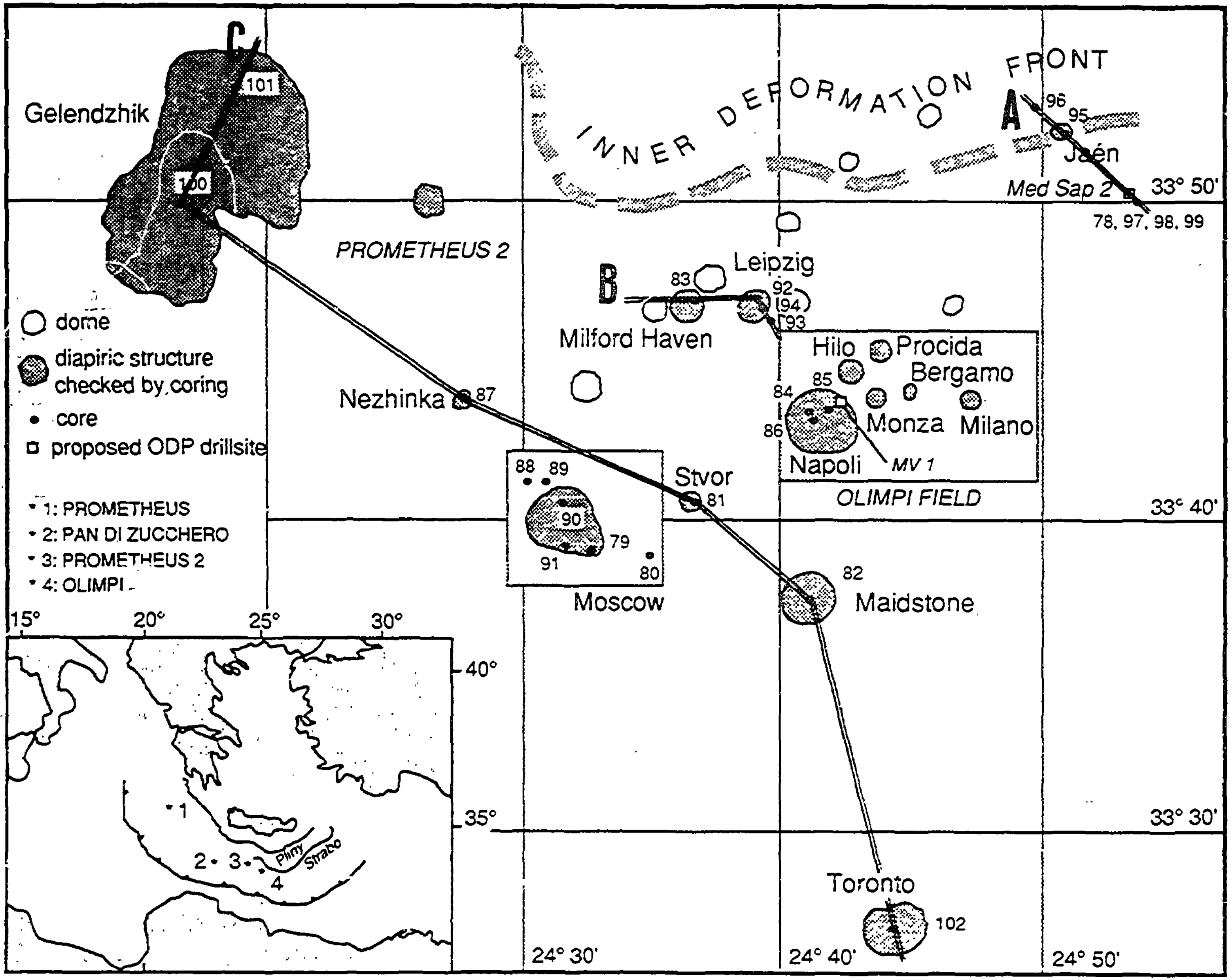

Fig. 55. Location of the mud domes and sampling stations in Area No 2

marked by an oxidized interval up to 20 cm thick. The lower boundary of the mud breccia in core 89G is sharp and the oxidized interval was not observed.

TRANSECT A (JAÉN DOME AND PLATEAU)

During survey across the inner deformation front, a small dome was discovered on the middle part of the slope. The two cores collected from this area are illustrated in Fig. 58.

Core 96G had a 81 cm recovery of Holocene and Late Pleistocene oozes overlying very stiff sediments of Early Pleistocene age. At the boundary between the two lithologies calcareous crusts were found. The crusts consist of limestones, dolomites, calcarenites with foram sands infilling burrows, and they indicate hiatuses and hardground formation. Mud breccia was sampled at the Jaén Dome with core 95G. It contains millimetric to centimetric clasts of partially lithified to indurated sediments and is massive in structure (types A-1 and A-2). The upper boundary to the pelagic sequence is gradational and marked by a 20 cm thick oxidized band. Pelagic sedimentation is represented by 2 m of Late Pleistocene to Holocene oozes, with an interbedded tephra layer (Y-5) and sapropel (S-1). The Marker Bed was not observed.

The plateau north of the Olimpi area was sampled with four cores (1 Kastenlot core, 1 gravity core and 2 box cores) in order to recover a thick, undisturbed pelagic sequence of Holocene to Pleistocene age. Core 97G has the longest recovery (491.5 cm) and reached the Middle Pleistocene. The sequence includes from top to bottom: the Marker Bed, sapropel S-1, tephra Y-5, tephra X-4, sapropel S-4, sapropel S-4 bis, sapropel S-5, sapropel S-6, and tephra V-1. Microfaults occur in intervals above tephra X-4 and just underlying sapropel S-4. Core 78K recovered the upper part of the sequence including the Marker Bed, sapropel S-1 and tephra Y-5. Both box cores 98B and 99B recovered the Holocene section including the sediment/water interface, but did not reach the base of sapropel S-1.

TRANSECT B (MILFORD HAVEN AND LEIPZIG DOMES)

This W-E-SE transect includes four cores collected from the Milford Haven Dome (core 83G) and the Leipzig Dome (cores 92G, 93G, and 94G; Fig. 59). All cores contain mud breccia overlain by pelagic sediments with a transitional boundary between the two lithologies. The upper boundary of the mud breccia is marked by an oxidized band in cores 83G and 94G, whereas oxidation was not observed in cores 92G and 93G. The mud breccia is massive, contains millimetric to pluri-centimetric clasts of partially lithified to very indurated sediments (types A1 and A2). Only the matrix of core 92G is characterized by a strong smell of H_2S.

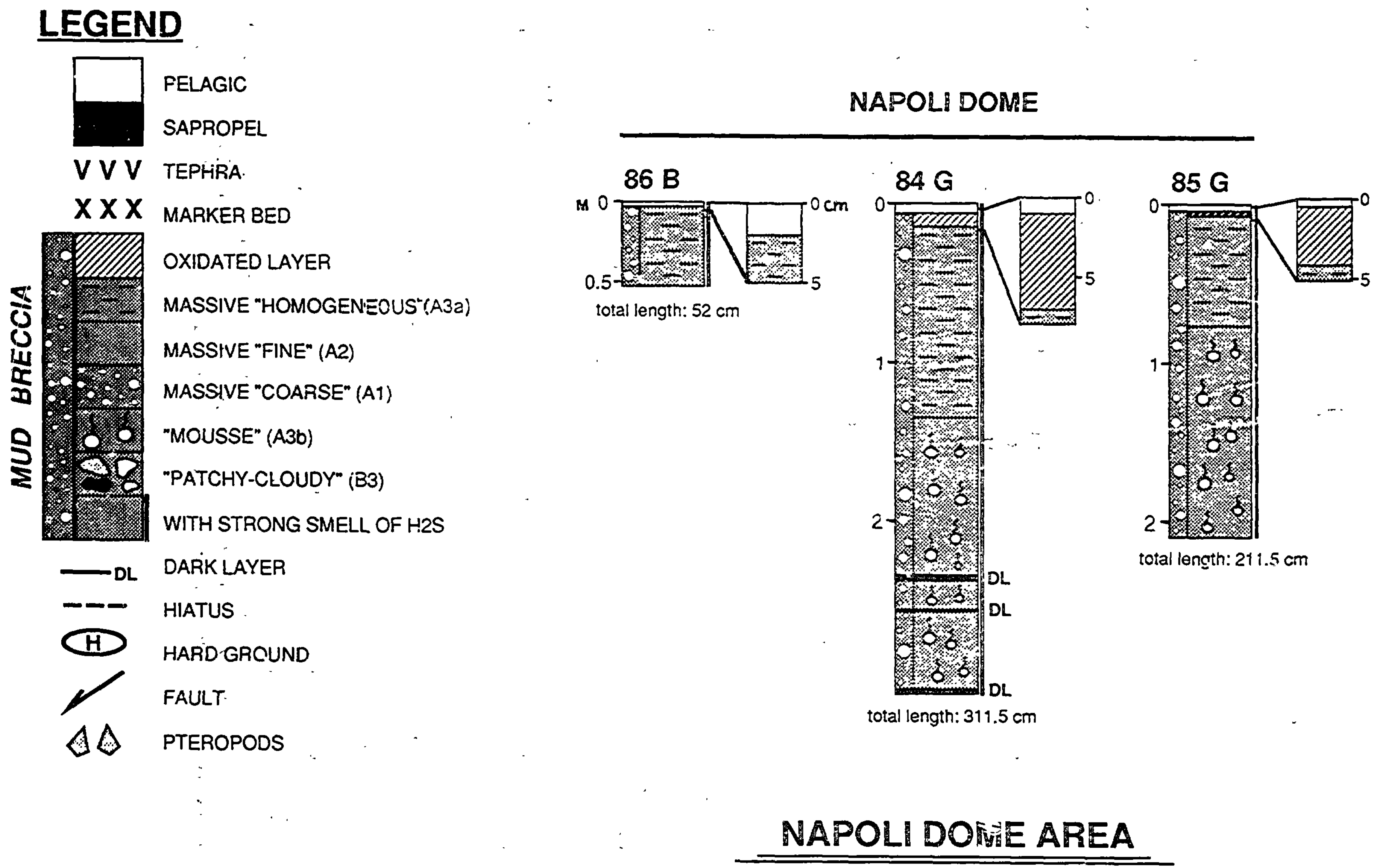

Fig. 56. Cores from the Napoli Dome area. (See the location in Fig.55)

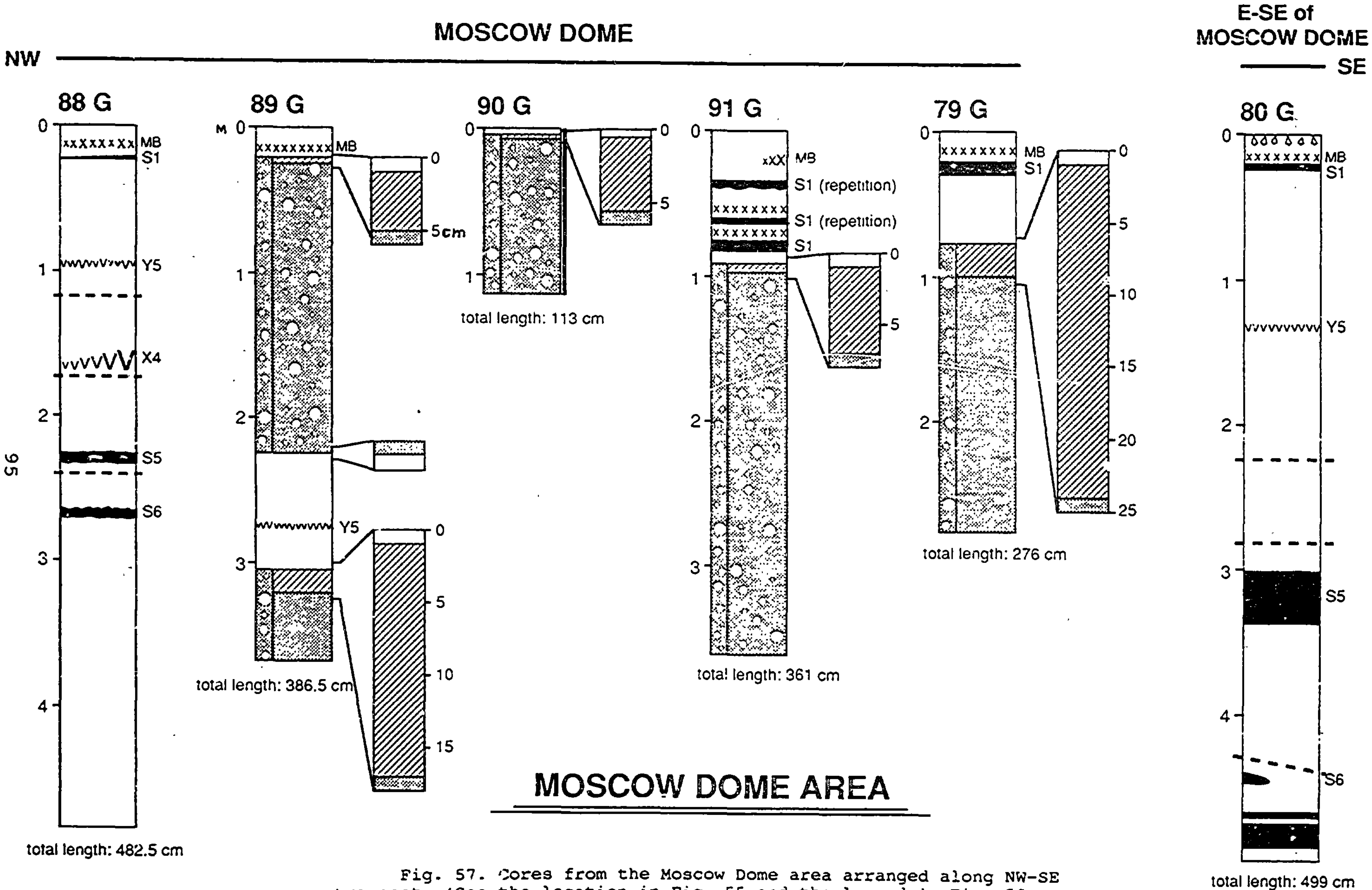

Fig. 57. Cores from the Moscow Dome area arranged along NW-SE transect. (See the location in Fig. 55 and the legend in Fig. 56)

In both cores 92G and 93G (Leipzig Dome), the upper part of the mud breccia contains 1 cm thick layers of Holocene oozes. Core 93G recovered two intervals of mud breccia separated by the latest Pleistocene to Holocene pelagic sediments. The upper mud breccia shows a spectacular basal contact with sapropel S-1, marked by a thin, pyrite-rich, very dark grey, silty layer. Foraminiferal assemblages within sapropel S-1 are nicely preserved and tests do not show breakage.

TRANSECT C (GELENDZHIK DOME, NEZHINKA DOME, STVOR DOME, MAIDSTONE DOME, AND TORONTO DOME)

Transect C is a long NW-SE transect with cores taken from the Gelendzhik, Nezhinka, Stvor, Maidstone and Toronto domes (Fig. 60). Mud breccia was recovered from all the domes, with the exception of the Nezhinka Dome where a pelagic section with some hiatuses was cored (core 87G, see below). A pelagic section was also sampled in core 100G (see below), raised from the Gelendzhik southwest of the core 101G. The mud breccia of these domes is massive and fine- to coarse-grained. Several pluri-centimetric clasts (sandstones, siltstones and calcarenites) were observed at various levels. Only the matrix of the mud breccia recovered in core 102G (Toronto Dome) is characterized by a strong H_2S smell. Calcareous nannofossils from the matrix of the mud breccia sampled at the Toronto Dome are common and moderately to well preserved. Unlike all other mud breccia cored on various domes of the diapiric/mud volcano belt surveyed during cruise TTR-3 Leg 2, the matrix contains exclusively Cretaceous nannofossils. Further investigation is foreseen to better precise the age of the mud breccia from the Toronto Dome. However, the occurrence of *Eprolithus floralis* and *Rhagodiscus angustus* indicates that the matrix cannot be older than the Late Aptian and therefore is mid- to Late Cretaceous in age.

The upper boundary of the mud breccia to the overlaying pelagic sediments is always marked by an oxidized interval up to 20 cm. In cores 101G (Gelendzhik Dome), 82G (Maidstone Dome) and 102G (Toronto Dome) the pelagic sedimentation is represented by a few centimetres of pelagic oozes, while in core 81G (Stvor Dome) the mud breccia is overlain by more than 2 m of pelagic sediments of Holocene to Late Pleistocene age.

THE MUD BRECCIA

Sixteen cores out of 22 collected during cruise TTR-3 Leg 2 contain the mud breccia, the type-sediment of the Olimpi Field and Prometheus-2 diapirs and which also characterizes the domes of the diapiric/mud volcano belt surveyed during the present cruise. It is a mud-supported breccia with submillimetric to pluri-centimetric clasts of different lithologies.

The six types of mud breccia identified by Cusin et al. (1992) and Staffini et al. (1993) on the basis of their structure and texture (see Section 3.1) were also observed during this cruise.The massive type of mud breccia is the most common. Types A-1 and A-2 were recognized in all the domes cored, except for the Napoli Dome where the Type A-3 (both A-3a = homogenous and A-3b = "mousse") is found. The fine grained types are usually

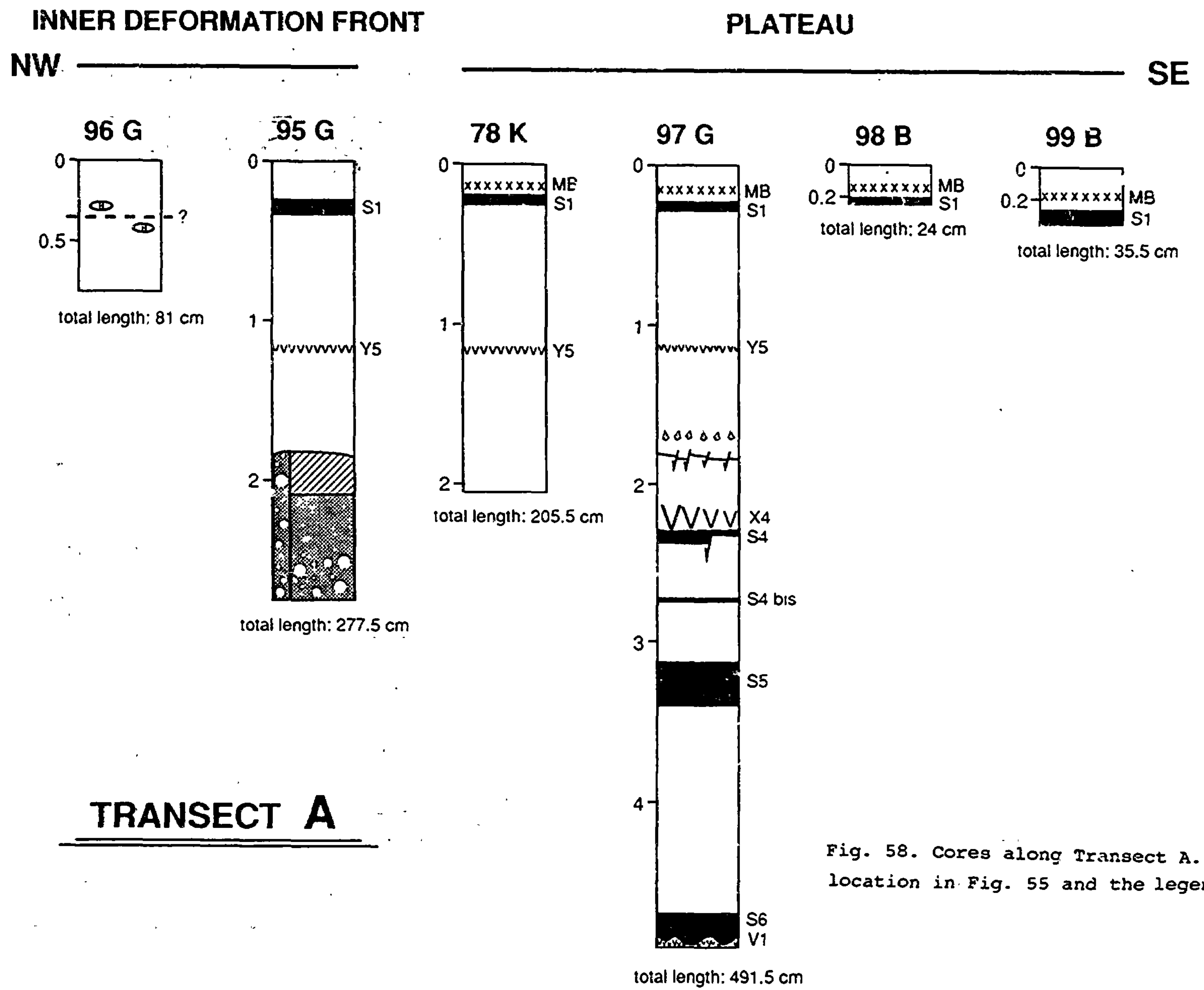

Fig. 58. Cores along Transect A. (See the location in Fig. 55 and the legend in Fig. 56)

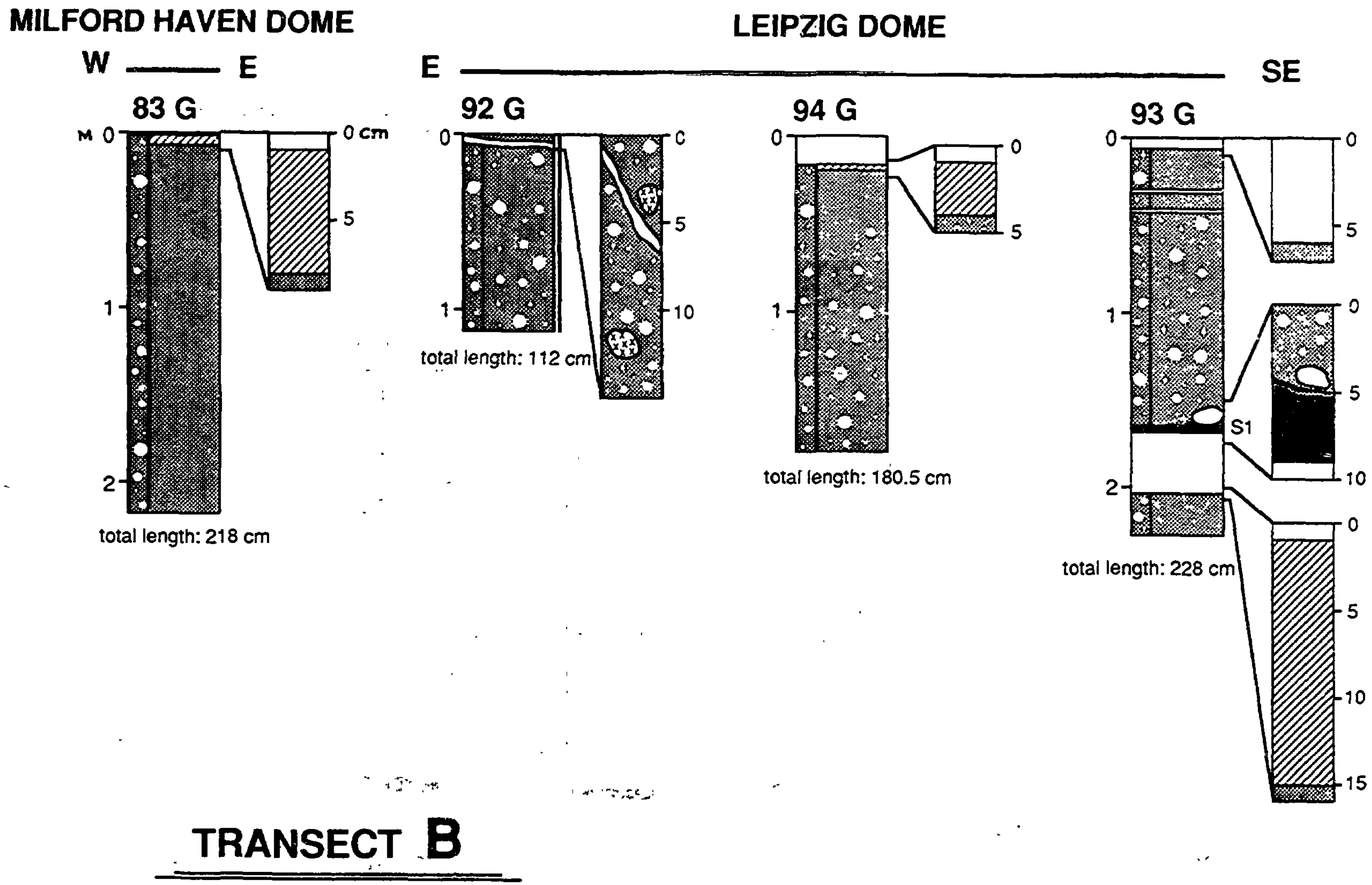

Fig. 59. Cores along Transect B. (See the location in Fig. 55 and the legend in Fig. 56)

characterized by a strong smell of H_2S when opening the cores. A shipboard study was dedicated to the characterization of the clasts (lithology and texture). The results are presented by R. van der Meer (see further on).

Smear slide investigation of several samples from the matrix of the mud breccia revealed high contents of clay, dolomite, nannofossils, quartz, and occasionally common pyrite. Calcareous nannofossil assemblages of mixed Pleistocene, Pliocene, Miocene and Late Oligocene age are characterized by high abundance and moderate to good preservation. The calcareous nannoflora of the mud breccia from the Toronto Dome is different from all the others. It is constituted of only Cretaceous taxa, without mixture of younger species. *Watznaueria barnesae* (a long ranging species) is common, but the occurrence of *Eprolithus floralis* and *Rhagodiscus angustus* indicates that the matrix is not older than Late Aptian and therefore is middle to Late Cretaceous in age. Further, land-based investigation is needed to better precise the age of the mud breccia of the Toronto Dome.

Fig. 61 illustrates the correlation of six cores from the Leipzig, Moscow, Jaén, and Stvor domes. Core 81G from Stvor mud volcano recovered the thickest pelagic section on top of mud breccia. It contains tephra X-4 and the Marker Bed. Three hiatuses were identified and are responsible for the absence of sapropels S-1 and S-4 and tephra Y-5. A strong tectonic activity results in sliding of pelagic sediments along the slopes as evidenced by the triple repetition of the Holocene section in core 91G, and by the hiatuses pointed out in core 81G.

Cores 93G and 89G recovered two intervals of mud breccia interbedded with pelagic sediments. The boundary between the mud breccia and the overlying pelagic sediments is always gradational and is marked by an oxidized band with dominant Pleistocene-Holocene foraminifers and nannofossils and low percentages of reworked older taxa. The boundary between the mud breccia and the underlying pelagic sediments is sharp, parallel to bedding plane, and lacks an oxidized band.

Grading in the mud breccia

Mud breccia textures indicate massive or organised facies which are suggestive of intrusion and extrusion/reworking processes respectively. The data reported are derived from 10 cores raised from mud domes with different morphology (Table VI). The purpose of this analysis was to study of the interface, and the texture and grading in the transitional layers, between mud breccia from single events of flow and hemipelagic mud.

From each of the sampled cores a 2 kg sample was taken from clay-rich sediment for clast analyses. Special attention was paid to the contact between the dark grey diapiric/mud volcano sediment and the hemipelagic mud, from each interval of which five to seven sub-samples were taken in a vertical spacing of 2-3 cm. Sixty-seven sub-samples were taken in dark grey mud breccia from 10 cores; and 33 of them were taken from close to the boundary with hemipelagic mud that covers the mud breccia. The clasts were removed from the adhering matrix with a 900 micrometer sieve under running water in a laboratory. Only three gravity cores were washed by hand (81G-83G). The size of the

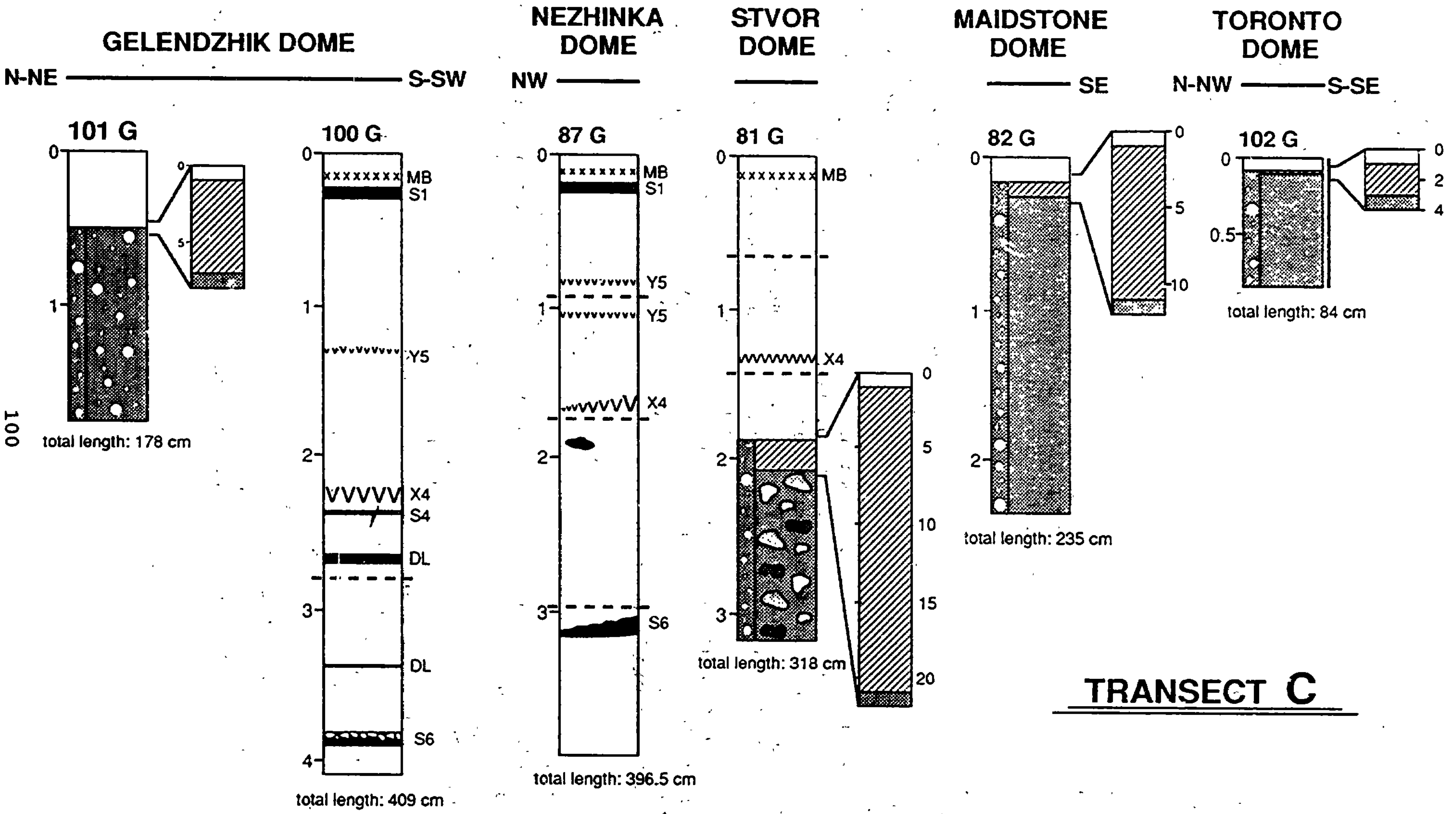

Fig. 60. Cores along Transect C. (See the location in Fig. 55 and the legend in Fig. 56).

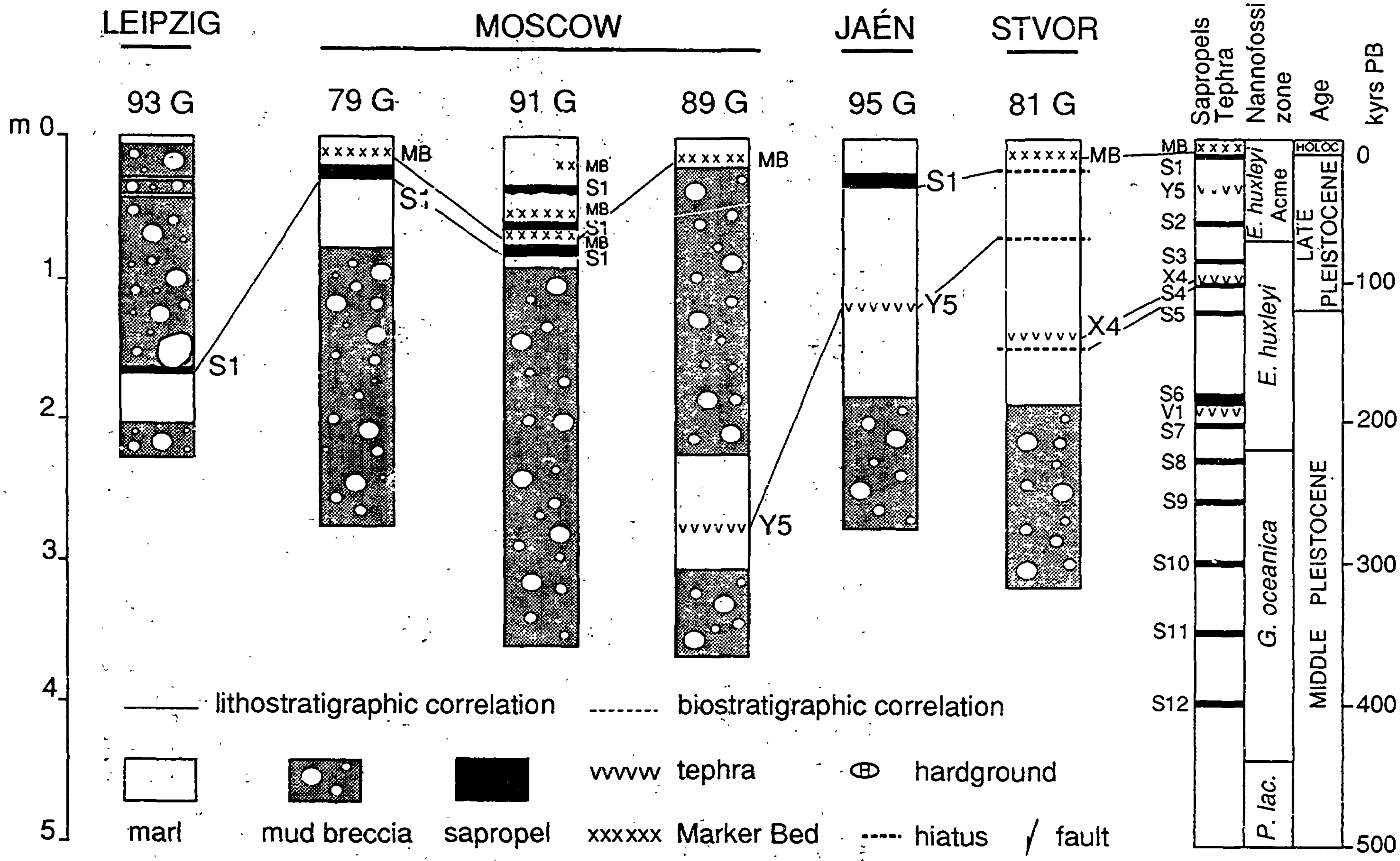

Fig. 61. Correlation of cores from the Leipzig, Moscow, Jaén, and Stvor domes. (See the location in Fig. 55)

Table VI

Cores used for the analysis of the mud breccia grading

Core No	Amount of samples	Total weight of sample (kg)	Total weight of clasts (kg)
TTR3-79G	1		
TTR3-81G	1	2	0.5
TTR3-82G	1	2	0.6
TTR3-83G	5	2	0.5
TTR3-89G	24	2	0.7
TTR3-90G	7	2	0.3
TTR3-91G	8	2	0.6
TTR3-92G	5	2	0.4
TTR3-93G	10	2	0.5
TTR3-94G	5	2	0.45
	Total: 67		

largest clast in each sample was measured along its longest axis. These results are presented in Figs. 62-66, with the diameter of the largest clast from each sample plotted against the depth. A macroscopic description of the lithology was made with the aid of the Munsell Soil Colour Charts and hydrochloride acid. Finally, the weight of clasts out of 2 kg was measured for each cores.

The mud breccia is mud-supported and contains clasts of variable size and angular shape. The colour of the clay matrix ranges from grey to dark grey (hue 2.5y n3/0-n5/0).

The composition of the clasts identifies four lithologies of which the bulk consists of dark grey mudstone (hue 2.5y n4/0). Other lithologies are white carbonate, brownish cherts, light olive-grey mudstone and light olive-grey conglomerate.

Fining-upward (F.U.) grading in clast size has been observed in mud breccia in four out of seven samples from the boundaries of the expelled mud and hemipelagic sediment. Sediment organization such as grading indicates extrusion processes. Grading was observed in the following core sections: 89G/4a, b, c, d, e; 89G/5a, b, c, d, e, f; 90G/1, 2, 3, 4, 5, and 94G/1, 2, 3, taken from the mud flows (Figs. 62b,c, 63 and 66). Grading was observed in the mud breccia in the top of the flow at the boundary with the overlying hemipelagic sediment three out of four times; and grading was noted once at the boundary with the underlying hemipelagites at the base of the mud flow. At the last case there were no signs of erosion produced by the mudflow.

The mud-supported breccia displaying grading in the studied flows consists of a massive intermediate part without any ordering in clast size either in vertical or lateral direction. The graded parts occur at the top and at the bottom within a range of about 3-12 cm of the boundary. The appearance of graded beds above and below a massive intermediate part means that a water-saturated mud flowed down the slopes of the dome with a relative high velocity depending on: the fluidity of the mud, the slope angle, the amount of expelled material (intensity of the

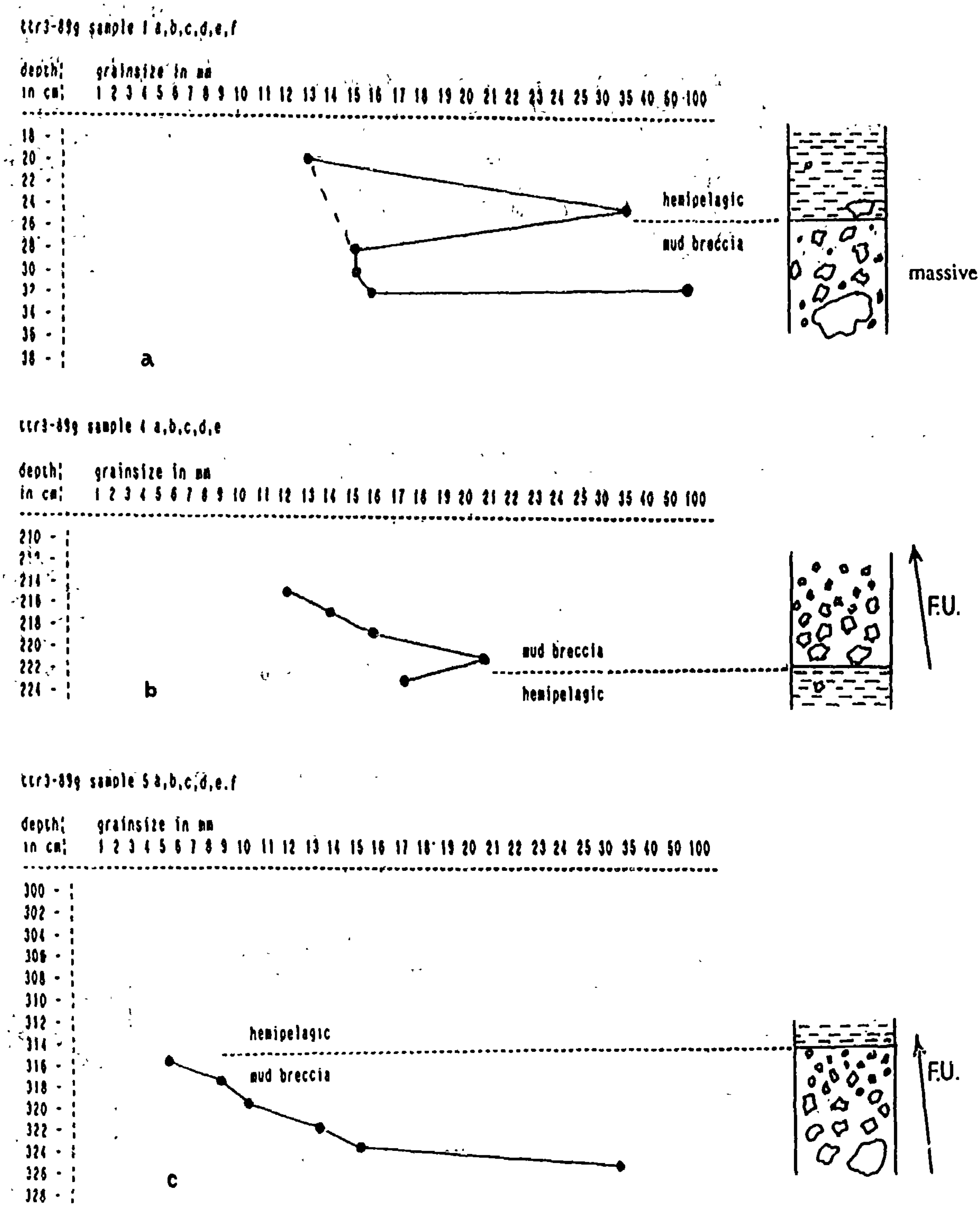

Fig. 62. Results of the mud breccia grading analysis in core TTR3-89G

eruption), the local bottom topography, and the distance of deposition area from the vent. In the case of graded beds with a thickness of 3-12 cm at the top and bottom of the mud flow and a massive intermediate part, it is most likely that immediately after the eruption, fluidity is less important than the flow velocity for producing graded beds. Near the vent, where the velocity is highest, a massive bulk of mud breccia is transported over a thin cover of fluidized sediment which is pushed in front of the flow, and grading in this part is limited to 3-5 cm, while the upper part of the mud flow is likely to have a larger thickness of grading because of an overlying turbulent water layer. Sorting out of clasts will be much easier in a turbulent mixture of water, clasts and mud than beneath a massive bulk of mud breccia. Away from the vent velocity becomes less important, and the fluidity becomes the main factor for grading in the mud breccia.

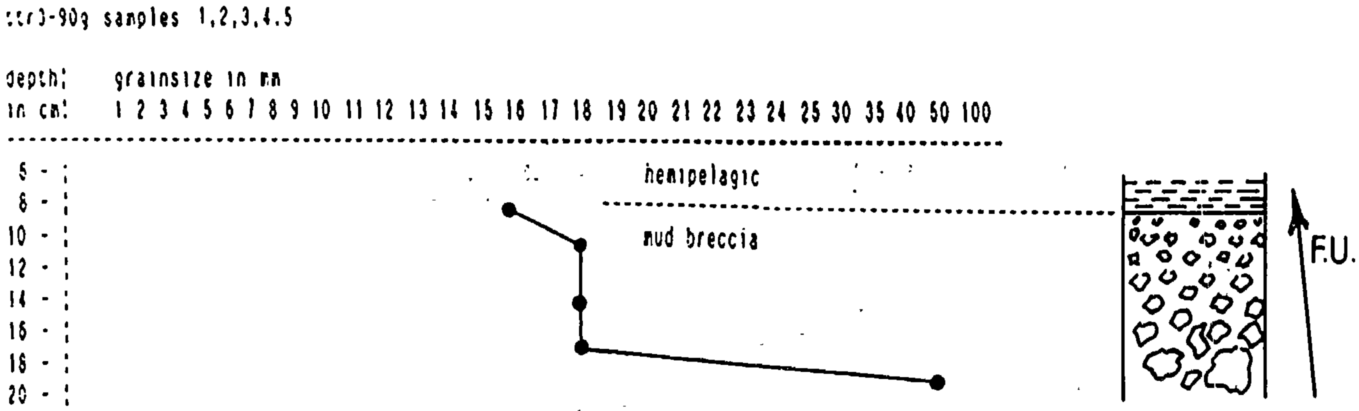

Fig. 63. Results of the mud breccia grading analysis in core TTR3-90G

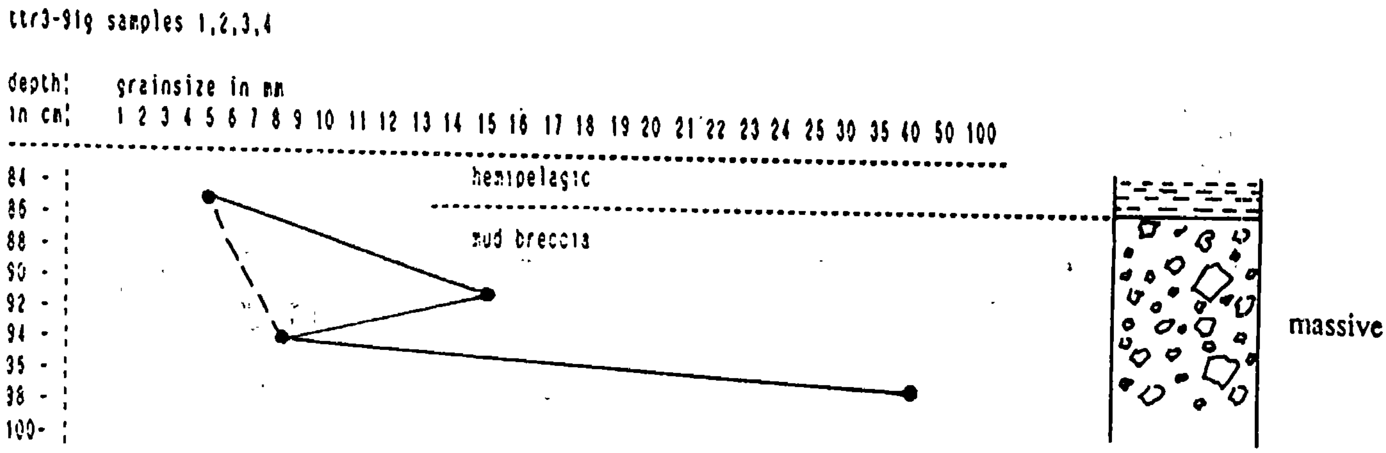

Fig. 64. Results of the mud breccia grading analysis in core TTR3-91G

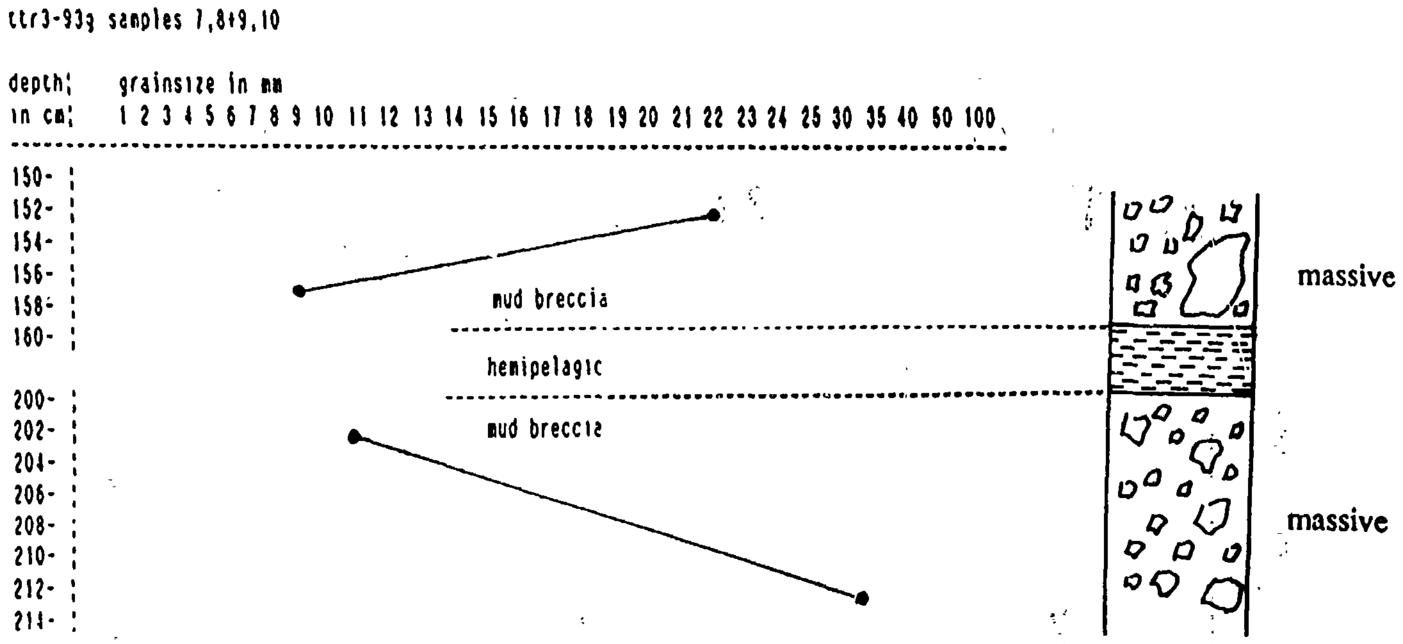

Fig. 65. Results of the mud breccia grading analysis in core TTR3-93G

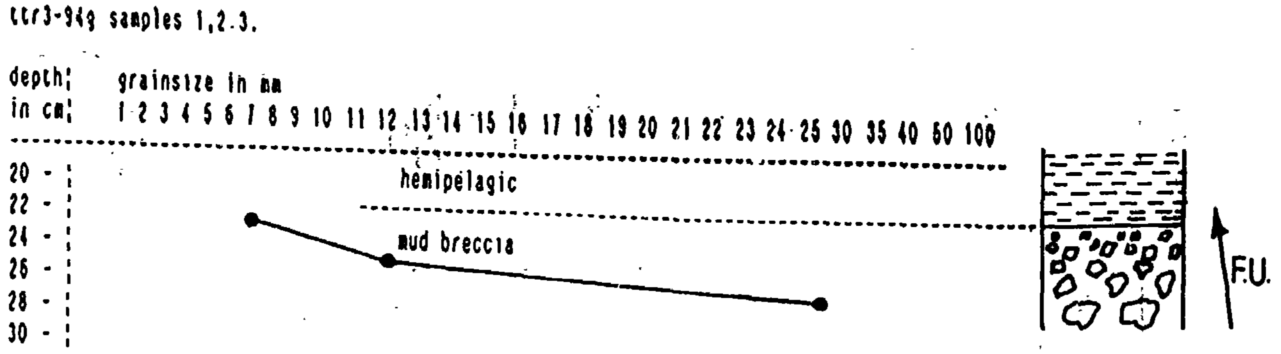

Fig. 66. Results of the mud breccia grading analysis in core TTR3-94G

THE PELAGIC CORES

Pelagic sequences of the Holocene to Middle Pleistocene age were recovered in 9 cores (1 Kastenlot core, 2 box cores, and 6 gravity cores). Fig. 67 reports the correlation of pelagic cores based on marker lithologies and calcareous nannofossil biostratigraphy. Core 97G is the reference section from the plateau: it consists of a continuous pelagic section with microfaults at the base of sapropel S-4; core 78K (Fig. 58) also recovered a 20 cm thick, pelagic sequence of the Late Pleistocene to Holocene age. Sedimentation rates were calculated for these two cores is. The average sedimentation rate fluctuates between 2 and 3 cm/kyrs, but a distinctive increase (4.4 cm/kyrs) is recorded in core 97G between approximately 100 Kyrs and 180 kyrs B.P. as documented by a very thick sapropel S-5 (50 cm).

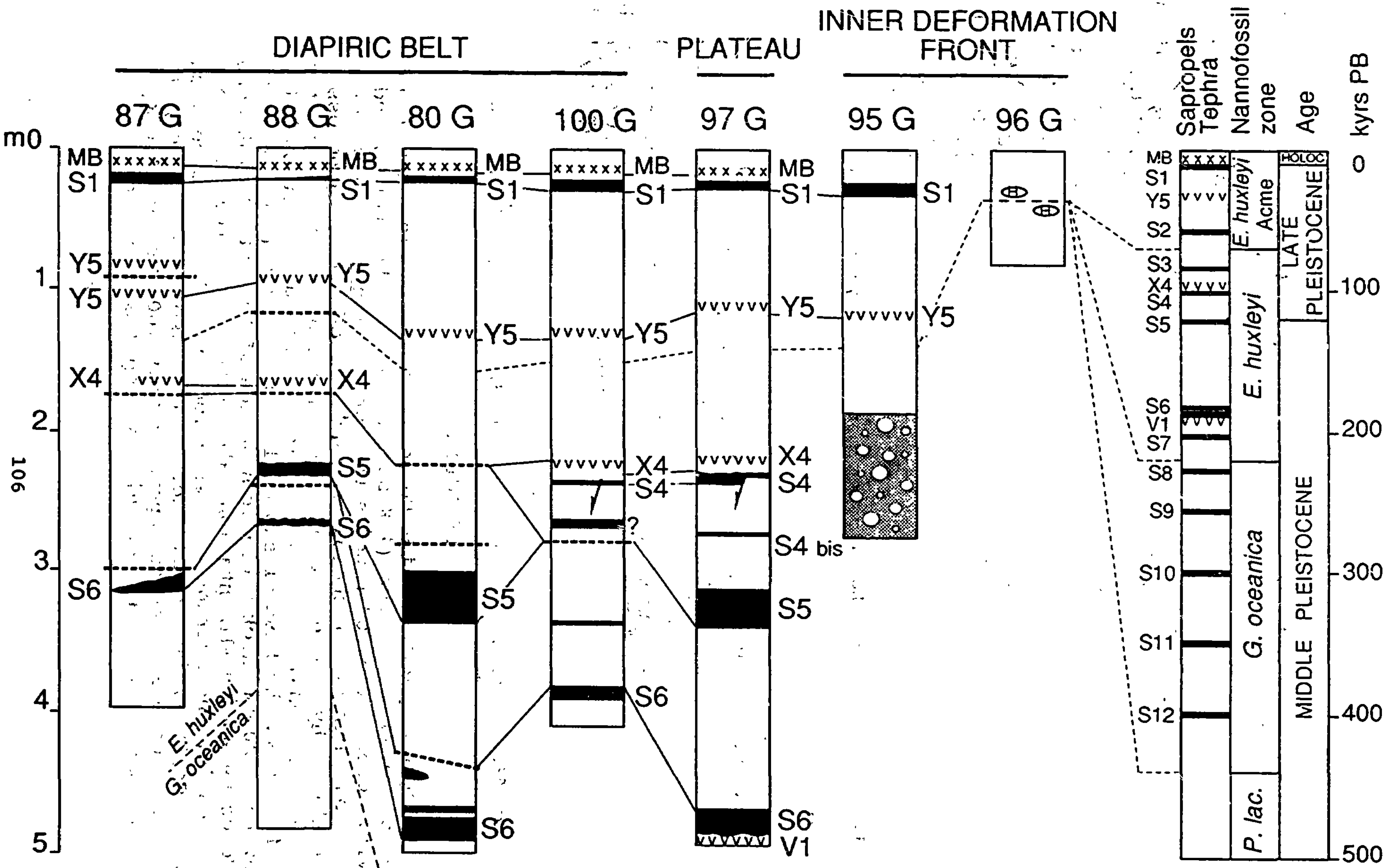

Fig. 67. Correlation of the pelagic cores from different morphological zones

Other pelagic cores were collected from various domes and none contains a continuous sequence. Several hiatuses were detected at various intervals of most cores, and microfaults were observed in core 100G. The Marker Bed and tephra Y-5 occur in most cores, whereas sapropels and tephra layers are frequently absent as a result of the strong tectonic activity of the area.

The Marker Bed (a peculiar layer dated to approximately 3.5 kyrs B.P. is a black, few centimetres thick layer consisting of Mn micronodules and containing abundant bacteria colonies) occurs in all the cores, with the exception of core 95G raised from the Jaén Dome of the inner deformation front.

Sapropel S-1 of Holocene age and tephra Y-5 (approximately 40 kyrs) are always present. Tephra X-4, usually recorded on top of sapropel S-4 (approximately 100 kyrs), occurs in all cores with the only exception of core 80G, but sapropel S-4 is documented only in core 100G from the Gelendzhik Dome.

Sapropel S-5 (approximately 125 kyrs) is very thick in core 80G from the Moscow Dome, but is thinner, heavily bioturbated in cores 88G and 80G, and is absent in cores 87G and 100G. Sapropel S-6 (approximately 180 kyrs) is present in all the cores from the domes. It is very well expressed only in core 80G from the Moscow Dome, while is relatively thin and strongly bioturbated in the other cores. In core 97G from the plateau a tephra layer (V1) was recovered at the base of sapropel S-6.

Core 96G consists of Holocene-Late Pleistocene oozes resting of very stiff marls of the Early Pleistocene age (*Pseudoemiliania lacunosa* nannofossil zone). The hiatus is marked by pluri-centimetric crusts of limestone, dolomite, and foraminiferal sands infilling burrows (hardground).

The coring results indicate that the tectonic activity was stronger in the interval between 180 kyrs and 100 kyrs B.P.

3.2.e. GEOCHEMICAL SAMPLING

S. Wakefield and G. O'Sullivan

AIMS AND OBJECTIVES

The geochemical programme in the Olimpi mud volcano area has two main aims:

1) the assessment of the diagenetic status of the sediments in general and the S-1 sapropel layer in particular.

2) a geochemical appraisal of the "mud breccia" facies.

One objective of the sampling programme is therefore to obtain high resolution quality pore water samples around a well defined S-1 layer. Analysis of these samples for redox sensitive elements will enable characterization of the present geochemical environment such that secondary diagenetic features in the sediment will be distinguishable from primary sedimentological inputs. A second objective is to obtain a number of cores of the "mud breccia" facies on which solid phase bulk geochemical and elemental partitioning analyses will be carried out. It is hoped that these geochemical data may help resolve the question regarding the origin of this facies.

METHODS

Geochemical samples for porewater analysis were taken from two types of cores: box cores and Kastenlot cores. In order to mimic the conditions on the sea floor all manipulations of the samples have to be carried out in a temperature controlled room and in nitrogen filled glove bags to avoid temperature and oxidation artifacts in the data. The system used has been developed by Cardiff and IOSDL geochemists over the past few years.

The box cores were sub-sampled by gently pushing plastic tubes into the top surface of the sediment. Three tubes were used for this purpose; a working sub-core for core description (15 cm i.d), an archive sub-core (7 cm i.d.) and a sampling sub-core (10 cm i.d). The sub-cores were removed from the box core; the archive sub-core was labelled and stored in the Constant Temperature Room (CTR), the working sub-core was given to the sedimentologists and the sampling sub-core was taken to the CTR for processing.

Sub-sampling of the Kastenlot core was carried out using 48 numbered 60 ml syringes. Two syringes were used for each sampling interval, noting the depths from which they were taken. The syringes were removed, stored in a sealed plastic bag and taken to the CTR.

SAMPLING

The sediment is introduced into the glove bag through a hole in the glove bag base. A jack mechanism was used to elevate the sediment.

After repeated inflations to obtain an oxygen content below 1%, the seal over the hole in the base of the glove bag was removed and the sediment was elevated into the glove bag. At 1 cm sampling intervals the protruding sediment was scraped off using a spatula and placed into a numbered centrifuge tube, noting the sampling interval and the tube number. The process of elevating the core and scraping off the protruding sediment was repeated until 8 centrifuge tubes had been filled.

The method for sampling the Kastenlot differed only in that the sediment is stored in 60 ml syringes. The sediment from the two syringes of each sampling interval were placed in the centrifuge tubes. The top centimetre of sediment that had been in contact with the air, and the bottom centimetre that had been in contact with the rubber plunger in the syringe were treated as contaminated and disposed of.

The filled centrifuge tubes were placed into numbered centrifuge buckets; the number of the centrifuge tube and bucket were noted. The buckets were centrifuged in a refrigerated centrifuge, chilled to 13°C (Mediterranean in-situ seafloor conditions) at 4000 r.p.m. for 30 minutes. After centrifugation the buckets were removed to the porewater filtering glove bag.

POREWATER FILTERING

The porewater filtering glove bag was inflated as before. Using a 20 ml syringe with a short piece of 3 mm internal diameter sleeving attached the porewater was removed from the sediment taking care not to introduce any sediment into the syringe. The sleeving was discarded and the amount of porewater in the syringe noted. A 5μ and a 0.2μ filter were connected to the syringe. A small amount of porewater is flushed through the filters to waste. The porewater is then filtered into 2 numbered bottles. The process is repeated for all remaining centrifuge buckets. This completes the process for the first set of 8 samples. The centrifuge buckets are removed to the sampling glove bag which is then inflated and the whole process is repeated until 24 porewater samples have been taken.

PRESERVATION

When all 24 samples have been taken the porewaters are preserved to prevent further bacteriological activity or precipitation. The 2 bottles taken from each porewater sample will be analyzed for different elements and will therefore need to be preserved in a different manner. One bottle will be used for nitrogen species determination. To prevent bacteriological activity 3 μl of $HgCl_2$ (mercuric chloride; 3.5 g/l) were added per ml of porewater to the sample using a Gilson pipette. The full sample nomenclature was written on the bottle that was then marked "N" for nitrogen. The other bottle will be analyzed for Si, P and trace metals (e.g. Mn, Fe). To keep the elements in solution 10 μl of 50% Hcl (hydrochloric acid) were added per ml of porewater. The full sample nomenclature was written on the bottle that was then marked "T" for trace metals.

The porewater samples were then stored in the CTR until analysis.

CORES PROCESSED

Two sites were occupied, the MEDSAP 2B site and the Napoli Dome. At the MEDSAP 2B site a total of 47 porewater samples were collected: 23 from a box core (99B), total penetration 29 cm, which bottomed out in the S-1 sapropel layer and 24 from a 176 cm long Kasten core (78K). These 24 samples were distributed 6 above and within the S-1 layer, and 18 at various intervals below this horizon. Such sampling resolution around the S-1 sapropel layer should enable a detailed porewater characterization of this horizon's current redox status.

At the Napoli Dome core 86B 23 porewater samples were taken from the 45 cm deep box core. Qualitatively this core consisted of a thin pelagic section overlying the "mud breccia" facies. Upon addition of the $HgCl_2$ spike to the porewaters, samples below 5 cm depth produced a brown colouration and/or precipitate. This is believed to be mercuric sulphide, (HgS_2), indicating the presence of free sulphide ions in these lower porewater samples. This sampling resolution entirely compliments core KC11 taken during the MD 69 MARFLUX expedition (1991), the central and upper part of which was highly disturbed by coring.

3.2.f. ODP SITE SURVEY FOR MEDSAP 2B

R. Kidd

In addition to the mud volcanoes exploration, an important secondary objective in the Olimpi study area during the Third TTR Cruise was to carry out surveys to define a new site on the so-called Inner Plateau for the ODP Mediterranean Sapropels drilling proposal. The requirements for the MEDSAP sites are expanded Plio-Pleistocene sediment sections in pelagic settings that could be expected to contain as full as possible a record of the sapropel layers. The proposal aims to test hypotheses for the formation of these enigmatic dark organic-rich layers (Kidd et al., 1978a, b), which seem to have been important in the paleoceanographic evolution of a number of enclosed ocean basins. It has proven exceedingly difficult to identify undisturbed sequences that could be expected to be complete records in the portion of the MEDSAP transect between Cyprus and Italy where the only potential pelagic settings are on the tectonically-elevated Mediterranean Ridge. A sparker seismic and echosounder line run from NE to SW by R/V *Bannock* in 1989 suggested that a uniquely undisturbed Plio-Pleistocene section occurs on the Inner Plateau. To complete a suitable ODP site survey package for this site (MEDSAP 2B) required crossing seismic, echosounder and high resolution seismic lines to show the continuity of the sequence at depth, a swath-mapping survey with sidescan to define the potential sediment pond in plan view and sampling to determine the presence of the upper sapropels, their sedimentation rate and geotechnical character.

On its initial run into the Olimpi area from the northeast on the $26^{th}/27^{th}$ of June, R/V *Gelendzhik* deployed the OKEAN long range sidescan system and airgun seismics and acquired a seismic and echo sounder line that crosses the Inner Deformation Front and parallels the R/V *Bannock*'89 line. This OKEAN 106 line provides a sidescan swath looking southeast at the proposed site. The airgun failed just after passing the site at 23^{46} and a short section was repeated (now processed out of the seismic profile). This airgun line suggests that there may be around 0.28 s (TWTT) of sediment thickness on this plateau area but also that there may be complications in the sequence caused by underlying features along strike from MEDSAP 2B. As indicated by the *Bannock*'89 3.5 kHz profile, our echosounder showed rough surface relief of tens of meters on the plateau which is north of the more highly variable "cobblestone topography" that is characteristic of the Mediterranean Ridge.

At the end of the OKEAN 106 line we made a second crossing of the site from SW to NE. This provided further sidescan and echosounder data with similar character but the airgun was not operational at this stage. The sidescan swaths defined an apparent sediment pond about 5 km wide, trending NNE-SSW between fold ridges and the proposed sampling site was moved approximately 2 km to the northeast nearer to the centre of the pond.

Kasten core 73K was recovered on the 27^{th} of June (35°50.30'N/24°53.23' E; water depth 2170 m). The most recent sapropel (S-1) and tephra (Y-5) were recovered in a 1.97 m core dominated by nannofossil marls. Initial nannofossil stratigraphy and correlation with existing cores in the region suggest sedimentation rates around 3 cm/kyrs before S-1 (~8 kyrs B.P.) and 2 cm/kyrs thereafter.

We crossed through the 78K core station once more with an OKEAN airgun seismic and echosounder line (OKEAN 109) on the 29th of June from NW-SE. This again suggested that the core station might be a better location for drilling than the originally selected position so the new location for MEDSAP 2A is defined by the crossing of *Gelendzhik*'93 seismic line 109 at 02^{37} on the 29th of June with the *Bannock*'89 line now at 16^{10}.

On the 2nd-3rd of July the same line was surveyed with the deep-towed short-range sidescan system MAK-1 but in the opposite direction. This not only defines the sediment pond more accurately and shows that no local slumping or debris flows influence sedimentation around the proposed site but also provides our only high-resolution seismic record over the site (78K). This record shows penetration to ~40 m subbottom and, because it is deeply towed and does not suffer from side echoes, is far more useful in this regional topography than conventional surface 3.5 kHz profiles. The sediment pond contains a well-defined sediment sequence gently sloping towards its centre. On this line Site 78K would appear to be on a slight knoll but is clearly beyond the influence of the fold ridges that can be up to 30 m high just 4 km to the southeast or the major deformation front some 6 km to the northwest. Although it was not apparent from the airgun record, the deep-towed profiler image of the upper sedimentary sequence shows that the record under station 78K might not be as continuous as that further along the MAK 19 line.

On the 3rd of July we returned to the area of station 78K and took gravity core 97G and two 15 cm square, ~30 cm long Reineck box cores, 98B and 99B, slightly to the northeast of 78K (33°50.31'N/25°53.24'E; w.d. 2173 m). Core 97G is a 4.91 m long, wide diameter gravity core that reached the S-6 sapropel (~180 kyrs). The sequence of nannofossil marls is interspersed with five sapropels (S-1, S-4, S-4*, S-5, and S-6) and three volcanic tephras (Y-5, X-4?, and W-4) and the high resolution profiler record suggests that we may be able to see the traces of the thickest of them.

The new MEDSAP 2B site (Fig. 55) as defined by these surveys and sampling (33°50.31'N/25°53.24'E; w.d. 2173 m) appears to be the most continuous and undisturbed pelagic sequence that could possibly be found in this part of the proposed east-west Mediterranean Sapropels drilling transect. Here on the Inner Plateau of the Mediterranean Ridge sedimentation has been continuous and at relatively high rates at least through the late Quaternary. The prognosis for recovery of the deeper sapropel record through to the Messinian appears good.

3.3. GENERAL INTERPRETATION

A. Limonov and M. Ivanov

The TTR-3 leg 2 has brought the most unexpected results. Everybody on the shipboard was focused on more accurate definition of the structure of the Olimpi mud diapiric field, and especially the Napoli Dome in order to obtain the data needed for the organization of the Ocean Drilling in this, one would think, well-studied region. Instead of this, we obtained principally new results on the structure of the Mediterranean Ridge. It has been proven that the OKEAN system is one of the best currently available instruments for the exploration of new mud structures on the Mediterranean Ridge. It provides the most clear indications of mud structures seen on the sonographs as dark (high reflective) isometric patches with irregular boundaries.

The new date obtained are as follows:

1. The Olimpi mud diapiric field is not a restricted area (about 100 km^2) as was thought previously, but represents a part of a large region where mud structures are widespread (the surveyed area is more than 6000 km^2). The Olimpi and Prometheus 2 Areas constitute a single zone. It is suggested that other known areas (Cobblestone and Pan di Zucchero) belong to the same zone which is referred to here as "The Mediterranean Mud Diapiric Belt". This zone seems to continue to the east because some possible mud diapirs and volcanoes were recorded along OKEAN line 118. Although only nine new structures have been checked by a direct geological sampling, there are few doubts that the rest of the more than ten structures revealed by the OKEAN and high resolution seismics are also mud volcanoes or mud diapirs. Moreover, it should be a great number of small similar structures their which are below the resolution of the OKEAN system. An example is the Haén dome which has a crestal diameter of only ~100 m and was found rather accidentally only with the help of the MAK-1 system. Thus, the phenomenon of the mud volcanism is rather the rule than exception for the Mediterranean Ridge accretionary complex as for other similar tectonic features such as the Nankai Trough accretionary prism (Taira et al., 1992) or the Barbados accretionary complex (Le Pichon et al., 1990).

2. The large structures surveyed with the MAK-1 system are not mud diapirs but mud volcanoes with mud flows spreading down their cones. The exceptions are the smallest domes (Haén, Stvor and Nezhinka), which shows no mud flows on its slopes, and possibly also the Leipzig dome. The mud domes typically have a bottom diameter of 1 to 3.5 km, but the Gelendzhik mud volcano stands apart in this respect. It is of about 10 km in diameter; however we suspect that the Gelendzhik is a group of tightly situated mud volcanoes whose mud flows overlap each other, that is the Gelendzhik represents not a single mud volcano but a mud volcano/mud diapiric plateau.

3. The dimensions of the mud volcanoes and the depth of their roots seem to increase generally southward, from the inner deformation front to the Mediterranean Ridge crest. The oldest

mud breccia (Cretaceous) was found on the southernmost mud volcano, Toronto.

4. The mud volcanoes on the Mediterranean Ridge differ very much in appearance from the Black Sea mud volcanoes. The feeder channels of Mediterranean mud volcanoes are never seen on seismic sections, whereas the feeder channels are well-displayed for the Black Sea mud volcanoes. The tectonic settings of these two groups of mud volcanoes are also different. The Black Sea mud volcanoes developed under a tensional tectonic stress, and the Mediterranean Ridge mud volcanoes were formed under a strong compressional stress. This could be the reason why the feeder channels are not seen on seismic sections. The sedimentary sequence is intensively deformed by folding and faulting, the latter including both normal faults and thrusts. The eruptive products of the Mediterranean mud volcanoes had to find their way to the seafloor along variously oriented fault planes and tilted strata. Because of this the feeder channels should not be a vertical columnar disturbance but a highly circuitous pathway within the sedimentary pile. The horizontal compressional stress also could enhance the formation of the Mediterranean mud volcanoes, squeezing out a viscous sedimentary mass to the seafloor.

A further difference between the Black Sea and Mediterranean Sea mud volcanoes is the source formations. A single source formation, the Maikopian clays, is assumed for the Black Sea case, whereas for the latter there is evidently several source formations which may vary in age from as old as Cretaceous to early Miocene (Camerlenghi et al., 1992).

5. The Messinian evaporites seem to form a rather thin (maximum about 200 ms TWTT) and discontinuous layer in the surveyed part of the Mediterranean Ridge. The seismic sections show at some places the pre-Messinian rocks under the Pliocene-Quaternary sediments. This is also confirmed by the absence of the Messinian fragments in the mud breccia recovered so far. So the Messinian can hardly play the part of the impermeable barrier creating an excess interstitial pore pressure in the underlying rock, as was suggested by Cita and Camerlenghi (1990).

6. Some mud volcanoes on the Mediterranean Ridge are active. The bottom sampling demonstrated the mud breccia actually occurring at the sea bottom without the overlying oxidated layer (Napoli and Leipzig Domes). Spectacular manifestations of gas and fluid seepages accompanied by the development of bacterial mats were recorded with underwater TV on the Napoli Dome. Since the mud volcanism on the Mediterranean Ridge reflects the general tectonic evolution of the accretionary complex, which is progressing now, we may expect the appearance of new mud structures here.

4. ERATOSTHENES SEAMOUNT (STUDY AREA 3)

4.1. GEOLOGICAL SETTING

A. Robertson, J. Woodside, and R. Kidd

INTRODUCTION

Eratosthenes Seamount is located in the Levantine Basin of the Eastern Mediterranean Sea between Cyprus and the Egyptian continental margin. A wide divergence of scientific opinion exists on the origin of this edifice which rises over 1000 m above the surrounding seafloor. A major part of R/V *Gelendzhik*'s study programme in the area of Eratosthenes Seamount was to run surveys and collect samples to define potential Ocean Drilling Program sites that could answer the continuing geological controversy on the history of this enigmatic feature and its relationship to the geology of the surrounding regions. As well as the definition of the so-called ESM drillsites with tectonic objectives, we were also planning to carry out surveys to define a site MEDSAP 1C on Eratosthenes Seamount for the Mediterranean Sapropels transect. This was to be sited where the CEC MARFLUX programme had recovered a 12 m piston core, KC20, from the summit region. Although this core recovered sapropels it was considered a condensed section and we were charged with looking for a part of the summit where sedimentation rates might be higher.

RELATIONSHIP OF ERATOSTHENES SEAMOUNT TO CYPRUS GEOLOGY

Assuming the Eratosthenes Seamount is indeed, a positive crustal feature in the process of collision with Cyprus along an active margin, there is clearly a potential tectonic relationship to the onland geology of Cyprus.

In outline, the island of Cyprus is made up of three tectonic units: the Troodos Massif in the centre, the Mamonia Complex in the southwest and the Kyrenia Range in the north. The Troodos Massif is an ophiolite, believed to have formed above a (north-dipping?) subduction zone in the Late Cretaceous. The Mamonia Complex includes the remnants of a Mesozoic (Triassic-Cretaceous) passive marginal and marginal oceanic crust (Triassic) related to opening of Neotethys in the Eastern Mediterranean area. The Kyrenia Range is dominated by a Mesozoic (Triassic-Jurassic) carbonate platform, overlain by Early Tertiary volcanics and sediments and Miocene flysch-type sediments. The three units were tectonically brought together by a combination of thrusting and strike-slip. The Mamonia Complex and the Troodos Massif had docked by the Early Tertiary, while compression and/or strike-slip movement between the Troodos Massif and the Kyrenia Range has taken place in stages, continuing into the Pleistocene (Robertson et al., 1991).

The Troodos Massif is overlain by deep-sea sediments, mainly pelagic carbonates and calciturbidites. Rapid shallowing-upwards took place in Late Oligocene-Early Miocene time. Deposition in the Miocene took place in a number of fault-controlled basins (Eaton and Robertson, 1993). In the south, a Cretaceous transform fault within the ophiolite (Arakapas) was reactivated by southward thrusting in Early-Mid Miocene time. A series of WNW-EWE trending structural lineaments were generated that can be traced offshore on shallow single-channel seismic profiles (Limonov et al., 1992b). This deformation possibly could relate either to the initiation of the present cycle of northward subduction beneath Cyprus and/or to a collision event along a pre-existing active margin, conceivably collision and transfer of the Hecateus unit from the downgoing plate to the over-riding Cyprus active margin. Following this local compressional event, the margins of the Troodos Massif underwent crustal extension in the Mid-Late Miocene to mid Pliocene, giving rise to the Mesaoria basin in north Cyprus and the Polis basin in west Cyprus. By the time of the Messinian salinity crisis, evaporites (gypsum) was precipitating in relatively shallow, small fault-controlled basins in south, west and north Cyprus. Extension continued into the Pliocene, mainly in the Mesaoria basin, where up to 750 m of marine mudstones and clastic sediments accumulated in an asymmetrical half-graben. The cause of this extension possibly was "roll-back" of the Cyprus trench and/or transtension related to crustal escape of Anatolia westwards after Late Miocene suturing of Neotethys to the east (Robertson et al., 1991).

By the Pleistocene, crustal extension had ended in Cyprus (other than in the Polis basin), giving way to regional compression and uplift. The Troodos Massif was strongly uplifted in Late Pliocene-Pleistocene, focussed on Mount Olympus. Very coarse, ophiolite-derived clastics were shed radially into shallow seas. Marine terraces developed in coastal areas. The interplay of relatively slow tectonic uplift and faster eustatic sea-level change gave rise to a flight of marine terraces and complementary land erosion surfaces (Poole and Robertson, 1991). Radiometric dating of coral suggests that uplift was most rapid in the Late Pliocene-mid Pleistocene, continuing subsequently at a slower rate. Some coastal areas have experienced recent submergence. The cause of the uplift is believed to be a combination of regional underthrusting beneath Cyprus and the hydration of ultramafic rocks of the mantle wedge which were hydrated and protruded upwards as serpentinite to form the present dome shape of Troodos.

GEOLOGICAL AND GEOPHYSICAL DATA AVAILABLE

Eratosthenes Seamount is the most striking and enigmatic feature of the Levantine Basin, in the easternmost Mediterranean Sea. Lying between Cyprus and the Nile mouth, about 100 km directly south of Cyprus, it rises to shallowest depths of less than 800 m from a surrounding moat at a depth of roughly 2000 m. In plan view it is about 50 km across, but is slightly elongated along a NNE-SSW axis. It is undergoing active deformation, as shown by several cross-cutting fault scarps (with trend of roughly E-W and ENE-WSW) and tilted strata apparently underthrusting Cyprus to the north, the Levantine basin to the south, and the Mediterranean Ridge to the west.

There exists no real consensus about its origin, history, and structure. Because of its relationship to the Cyprus arc, a focus of the 1991 TTR Cruise, as well as its inclusion among proposed sites for ODP drilling in the Mediterranean Sea, it became an important subject of this cruise.

What is known about the seamount has added to controversy over its nature. For example, during the 1987 cruise to the eastern Mediterranean of the R/V *Akademik Nikolai Strakhov* rocks as diverse as granite, limestone, and serpentinite were dredged from the southern half of the seamount (Udintsev, pers. commun., 1993).

The crustal structure of the eastern Mediterranean and Eratosthenes Seamount in particular has been the object of several geophysical experiments but the data are equivocal. Because it does not appear to be either typical continental or oceanic, it has been inferred to be both by different people, as well as a mixture of the two: intermediate or stretched continental crust (outer continental margin environment). Seismic refraction results and gravity modelling suggest that the crust thins by about 2 to 3 km along a NNE-SSW line through Eratosthenes, from a depth of about 24 to 26 km in the Levantine Basin to the east (Woodside, 1977; Makris and Stobbe, 1984). The sedimentary section, however, is perhaps as much as 15 km thick; and the seismic velocity of the underlying crust is about 6.7 km/s which is high for continental crust and would be reasonable for oceanic crust (layer 3) if it were not so thick (10 km compared to a more typical value of 5 km).

A large magnetic anomaly is associated with the Eratosthenes structure but suggests a broader deep-seated source (Ben-Avraham et al., 1976; Woodside and Williams, 1977). It ranges in amplitude from -150 nT to the northwest to 450 nT to the southeast and is elongated in the same direction as the seamount. The length of the anomaly in the NNE-SSW direction is almost 300 km between enclosing 0 nT contour lines and over 100 km in the NW-SE direction between the maximum and minimum values. Several small local anomalies superposed on the main anomaly distort the overall anomaly towards the northwest. Ben-Avraham et al. (1976) interpreted the source as basic or ultrabasic - possibly ophiolitic - material that has rotated counter-clockwise since the time of its formation; Woodside (1977) suggested that the source might be volcanic intrusions similar to those which accompanied both the NE-SW faults of the Syrian Arc in the Eocene and the NW-SE Oligocene fault system which cut through the previous faults (Said, 1962).

In strong contrast to the magnetic anomaly, the gravity anomaly is almost entirely topographic (Woodside, 1977). There is a free air anomaly of about 75 mGal that diminishes to a Bouguer anomaly of less than 20 mGal after correction for a topographic mass with an assumed density of 2.67 g/cm^3. This suggests that the seamount is supported by the crust or by forces within the upper lithosphere, because there appears to be no lower crustal root or flexural response to the topographic load. A regional westward increase in gravity by about 20 mGal just to the west of the seamount corresponds to the westward thinning of the crust by about 2 to 3 km as noted above; and to the west of the seamount lies a NNE-SSW-oriented long-wavelength linear positive residual gravity anomaly of 30-50 mGal which indicates the presence there of a major crustal discontinuity (Woodside, 1992).

Although a number of interpretations regarding the origin and development of Eratosthenes seamount have been proposed, none are widely accepted over any other. It has variously been hypothesized to be a continental fragment which has been situated just to the north of Egypt since the formation of the African margin in the Mesozoic, an oceanic plateau which became separated from others which were assimilated along the arcs to the north as exotic terranes (Rotstein and Ben-Avraham, 1985), an ophiolitic body like the Troodos of Cyprus, a large up-domed structure which collapsed to its present elevation, and a more recently (since late Miocene) elevated crustal block caused by collision of the distal part of the African rifted margin with Cyprus.

Part of the reason for the controversy over the nature of Eratosthenes is the lack of good data and clear observations. It is not easy on seismic reflection profiles to trace known reflectors from the Levantine basin across the surrounding deformation zones and onto the seamount. Most people agree that the Messinian evaporites are missing on the seamount or very thin; however, the M-reflector is interpreted to be present in some parts of the seamount by some people. This indicates that the seamount was already a positive topographic feature at least is far back as the upper Miocene; but its earlier history is unknown. Its destiny appears to be further deformation as it collides with Cyprus, eventually to become attached to or consumed by Cyprus.

TECTONIC OBJECTIVES OF PROPOSED SCIENTIFIC OCEAN DRILLING

An excellent opportunity clearly exists to integrate the results marine and land-based geology in the Eratosthenes area. Assuming Eratosthenes is, indeed, in the process of being consumed beneath Cyprus, then a fundamental tectonic process is involved that needs to be investigated by deep-sea drilling. The initial stages of continental collision remain very poorly understood and the Eratosthenes Seamount area (along with Indonesia) is an excellent location to study this problem. Two phases of ocean drilling are envisaged: i) shallow drilling (<500 m), as part of the study of the Mediterranean Ridge (ODP proposal No 330); ii) deeper drilling, including basement objectives. The first phase of shallow drilling, prior to the TTR-3 survey was not expected to reach basement, but was expected to be capable of studying the critical collapse of the seamount. Four sites were originally selected: ESM 1 was on the crest of the seamount and would determine the subsidence history; ESM 2 was on the north flank of the seamount where the sediment cover and penetration of older subsidence-related units was thought to be possible; ESM 3 was near the southern margin of the Cyprus trench and was seen as documenting faulting and seamount breaks-up (e.g. debris flows); finally, ESM 4 was sited on the terraced outer edge of the Cyprus margin and was expected to provide a contrasting sedimentation and subsidence record.

Before the first-phase of drilling could be scheduled it was necessary to obtain additional site-survey data, in the form of high-quality single-channel seismic data (or equivalent), sidescan sonar data and cores. The main objective of the third part of the TTR-3 cruise was to provide this information.

Successful results from this cruise would also help to stimulate the collection of the additional MCS and other data necessary before any deep-drilling of crustal basement objectives could be undertaken, as in the proposed phase 2 of deep drilling of the Mediterranean convergence zone.

4.2. RESULTS

4.2.a. SEISMIC REFLECTION PROFILING

A. Limonov and J. Woodside

Seismic reflection profiling in Area No 3 was carried out along tracks designed to define the principal structural features and to cross the sites proposed for Ocean Drilling (Fig. 68).

Seismic line PS-119 follows the WNW to ESE trend of the south Cyprus margin. The seismic section shows an intensively tectonized sequence with complex topography and almost no inner reflectors.

Line PS-120 are oriented from north to south. It starts on the southern Cyprus margin and crosses the Eratosthenes Seamount at its centre, passing through the three sites proposed for ocean drilling: MEDSAP 1A, ESM 2A and ESM 3A. Apart from line PS-121 which follows the foot of the northeastern flank of the Eratosthenes, the remaining lines (PS-122 to PS-127) all cross the seamount from west to east or are short joining lines.

The Cyprus margin has a rough topography and very complex subbottom seismic pattern. The thickness of Pliocene-Quaternary sediments varies from almost 0 to 220-230 ms TWTT (about 200 m). Their bottom is not clearly seen. Apparent deep reflections are probably only diffraction hyperbolas and side echoes.

The uneven slope of the Cyprus margin is changed abruptly southward by a large trough separating the Eratosthenes Seamount from the Cyprus margin. The seafloor in this trough is flat and slightly tilted toward Cyprus. The transition from the intensively disturbed rocks composing the Cyprus margin to the undisturbed Pliocene-Quaternary sediments filling the northern trough is very sharp and is marked by what could be a thrust fault. The sediments covering the northern slope of the Eratosthenes Seamount are underthrust beneath the Cyprus margin at this place.

The trough is very young, and the subsidence accompanying the underthrusting is possibly continuing. The thickness of Pliocene-Quaternary sediments increases from the Eratosthenes slope northward, from 200 ms to almost 1200 ms. Rare and low amplitude faults are seen in the lower part of these sediments section. The underlying substratum is broken by faults with the offsets of up to 220-250 ms. This substratum could be composed of the pre-Messinian Miocene and older formations because the reflector at its top differs in the seismic signature from the M-Reflector. The different seismic signature could also be caused by the deformation.

Because the faults in the substratum are not displayed in the overlying sediments, it is evident that there was a passive infilling of already existing topography. The general seismic pattern of the trough's sedimentary infilling looks like that of a fan rather that of a hemipelagic sequence. The progradational pattern with toplap and sigmoidal reflections is seen in the upper 150 ms of this sequence (Fig. 69). This pattern is evidence that the sediment input was from the Eratosthenes Seamount rather than from the Cyprus margin. In addition, the transparent seismic

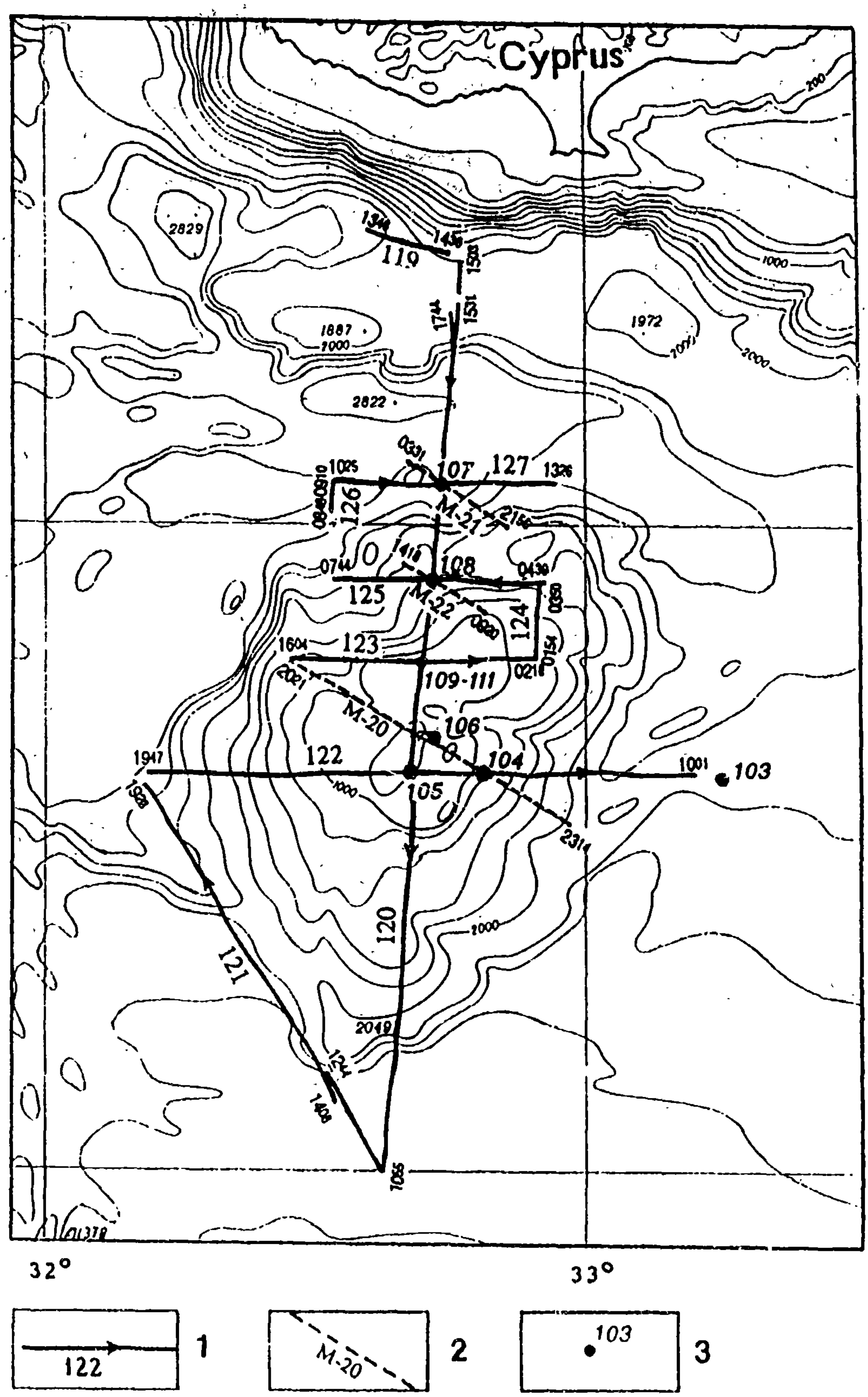

Fig. 68. Location map for Area No 3
1- OKEAN and seismic line; 2 - MAK-1 line; 3 - sampling station. (Bathymetry is from IOC-UNESCO, 1981)

members, which could be debris flow deposits, are concentrated in the southern part of the trough joining to the Seamount.

A large uplifted ridge, about 300 ms high at the base of Pliocene, is situated near time mark 19^{55}. This deformation is very young because the overlying Pliocene-Quaternary sediments have clearly post-sedimentary deformation. Their thickness over the ridge is 110-120 ms and remains almost constant both on the top and slopes of the ridge. This ridge serves as a trap for the sediments supplied by the Eratosthenes Seamount, since the level of sedimentation south of the ridge is higher than that north of the ridge (Fig. 69). The ridge was chosen as a site for ODP drilling (ESM-3A).

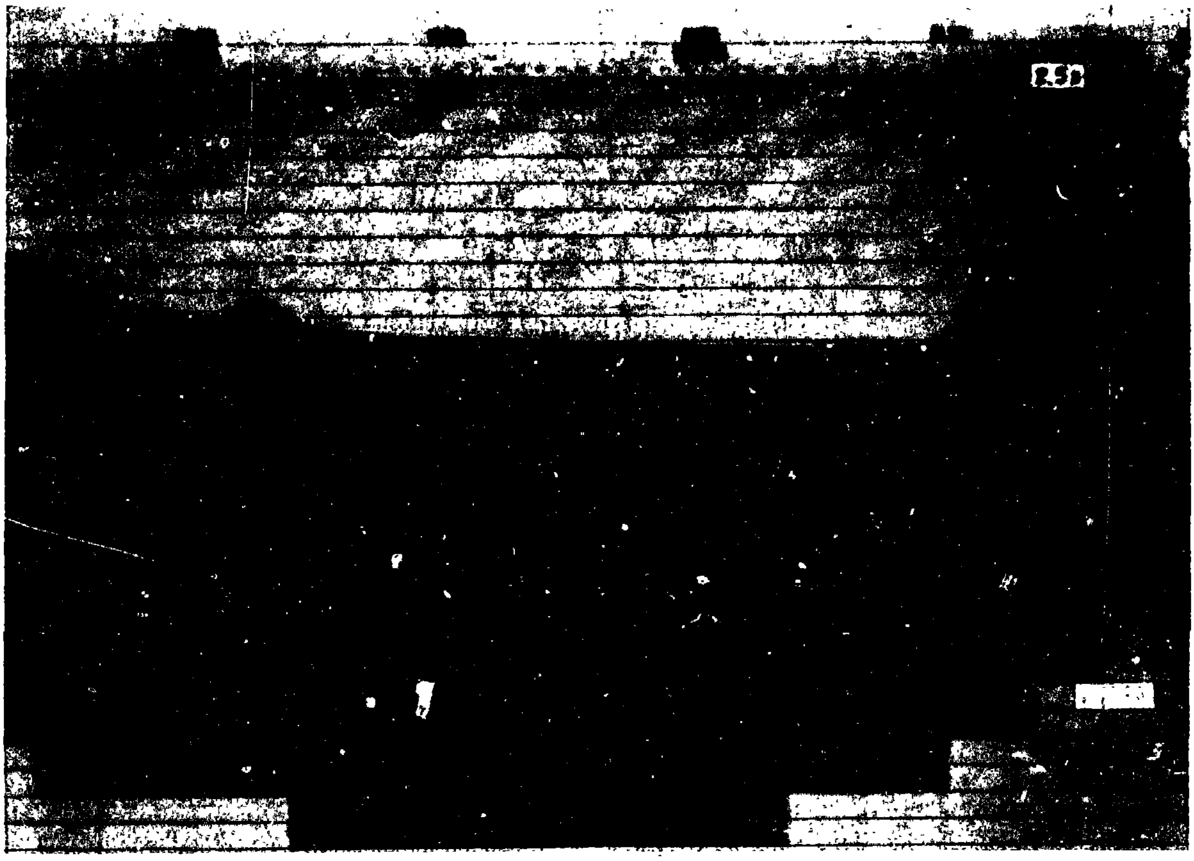

Fig. 69. A trough north of the Eratosthenes Seamount with progradational seismic pattern in the upper 150 ms of the sedimentary sequence and transparent seismic members (debris flow deposits?) in the southern part of the trough. This pattern is the evidence that the sediments came principally from the Seamount. A young ridge at 19^{55} acts as a sedimentary trap. Note the difference in the sedimentation levels north and south of the ridge. (Seismic line PS-120)

The northern slope of the Eratosthenes Seamount is a series of structural steps which were formed by normal faults with about 200-220 m offsets. Pliocene-Quaternary sediments on these steps have a thickness of 100-150 ms. They are represented by a seismically semitransparent unit of inferred hemipelagic sediments. They are absent near time mark 01^{00} possibly because of slumping, and the pre-Pliocene surface outcrops at the seafloor. This site was also proposed for ODP drilling (ESM- 2A).

The faults in the substratum seem not to penetrate into Pliocene-Quaternary sediments, indicating that the steps probably originated in pre-Pliocene time, but the Pliocene-Quaternary sediments form the flexures above the fault planes well-displayed in the bottom topography. So the faults are evidently still "alive" (Fig. 70). The pre-Pliocene surface is an erosional unconformable interface which is thought to have been formed during the Messinian sea-level drop. No coherent reflectors were recorded below this surface on the top and north slope of the Seamount.

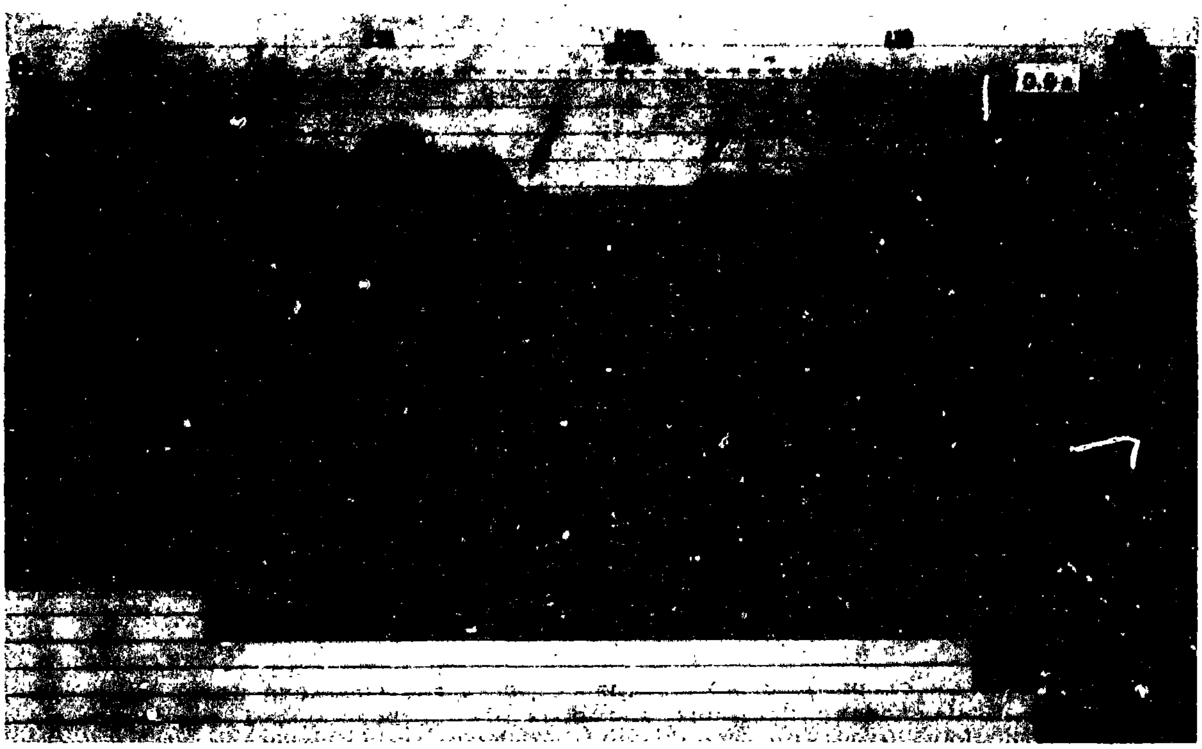

Fig. 70. Active faults (arrows) at the top of the Eratosthenes Seamount. (Seismic line PS-120)

The Eratosthenes Seamount is rather flat-topped but like the north slope is also broken by normal faults with vertical offsets of 100÷200 ms. Pliocene-Quaternary sediments which drape the fault scarps have a semitransparent appearance and a thickness of up to 150 ms.

A site structurally typical of the top was chosen near time mark 01^{25} for ODP drilling.

Inferred pre-Pliocene rock outcrops at the scarp near the uppermost part of the southern Eratosthenes slope. What could be a carbonate buildup is observed on the upper plateau just near the slope break (Fig. 71).

The southern slope is constructed simpler than the northern one. It is gentle and is not so affected by tectonic deformations. The blanket of Pliocene-Quaternary sediments increases gradually in thickness downslope from the top break to 150-180 ms, and this thickness remains almost constant throughout the rest of the slope. There is a feature resembling a large slump scar between time marks 05^{45} and 06^{10}, an interpretation confirmed by the OKEAN sidescan sonar.

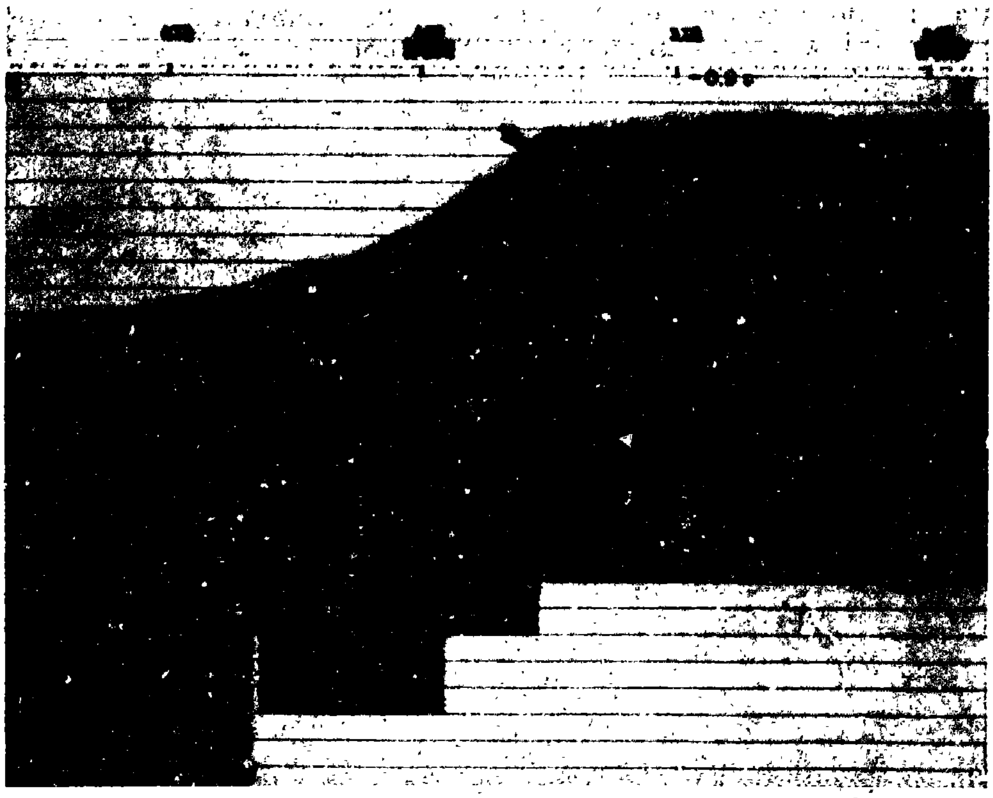

Fig. 71. Outcrops of pre-Pliocene rocks at the southern scarp near the top of the Eratosthenes Seamount and possible carbonate buildup (arrow). (Seismic line PS-120)

In contrast to the northern slope, the southern one shows a much deeper seismic penetration. The deepest reflectors are recorded at depths of 700-800 ms from the seafloor. It is suggested that Pliocene-Quaternary sediments of the southern slope are underlain by up to 200 ms thick Messinian sediments. The Messinian pinches out upslope possibly near time mark 04^{10}. The assumed Messinian layer is distinguished by continuous subparallel and weak inner reflectors and should be represented by sulphate-carbonate rocks. It is almost undisturbed, but the underlying layers are very deformed by faulting and folding.

The picture seen at the southern foothills looks almost like a mirror image of that at the northern foothills. However, the trough here is narrower and shallower. The thickness of Pliocene-Quaternary sediments in this trough attains only 450 ms.

The divergent pattern of the Plio-Quaternary reflectors demonstrates that sedimentary infilling was somewhat simultaneous with tectonic subsidence. The thickness of the Messinian seems to be the same as on the slope. Therefore the subsidence of the southern slope was quite young (possibly Middle-Upper Pliocene) and gradual, whereas in the north the subsidence started earlier and was very rapid. This is evidenced also by the variations in thicknesses of the Plio-Quaternary. Although the southern trough might be expected to receive large quantities of the Nile-derived sediments, the thickness of sediments in the southern trough is less than in the northern trough.

The southern wall of the southern trough seems to have been upthrust northward (Fig. 72) with a vertical offset of about 900 ms. The seafloor of the Levantine Basin located further south is uneven, with numerous low-amplitude undulations reflecting the structure of the subbottom sediments. They form frequent folds with an amplitude of up to 100 m and a wavelength of less than 1 km. Faults are present as well. The thickness of Pliocene-Quaternary deposits is 400-500 ms, and the thickness of the Messinian is considered to be 300-400 ms.

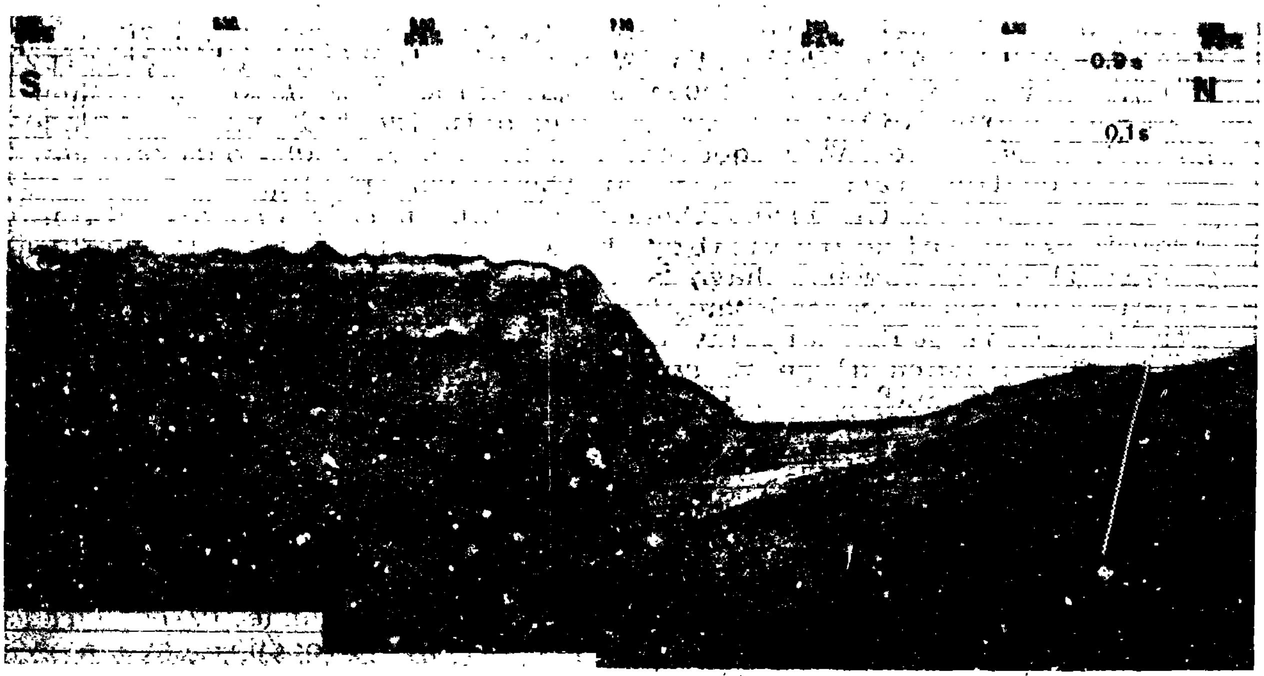

Fig. 72. Structure of the southern trough. The tectonically compressed margin of the Levantine plate (LP) overthrusts the trough. (Seismic line PS-120)

Seismic line PS-121 follows the southwestern slope of the Eratosthenes Seamount, from SE to NW. The line crosses the southwestern edge of the trough where a large projection of the sediments from the south is piled onto the southwestern slope of the Eratosthenes (15^{50}-17^{00}). This sediment pile is probably slumped from the steep southwestern margin of the trough above the underthrusted slope of Eratosthenes Seamount; and it is expected to be comprised of sediments from the Nile Cone to the south. The Messinian occurs at a depth of 600-800 ms and its bottom is not displayed.

Further northwest the seafloor gradually deepens, and the thickness of seismically transparent undisturbed Plio-Quaternary sediments increases from about 100 ms at 17^{05} to 200 ms at the end of the line. The thickness of the Messinian is interpreted to be 100-300 ms. The seismic reflection configurations of the Messinian are mostly chaotic.

Seismic line PS-122 starts at the base of the western flank of the Eratosthenes Seamount, crosses its top from west to east, and ends in the East Levantine Basin. The western slope has a rather simple structure and is almost not affected by tectonic deformations. The semitransparent Pliocene-Quaternary layer has a thickness gradually varying between 100 and 150 ms. The underlying unit on the slope is represented probably by the Messinian which has an average thickness of about 100 ms and pinches out at the upper slope near time marks 04^{50}-04^{55}. A lens like body with a chaotic stratification is seen near 20^{15}. Its lower edge is confined by a gentle rise of the underlying rocks. It is thought to be an olisthostrome or slump masses originating possibly before the lithification of the Messinian sulphate-carbonate sediments. A unit with a strong reflectivity at the top occurs at 300-400 ms below the seafloor. Weak discontinuous reflectors can be traced inside this unit. Its age is supposed to be the Oligocene. Pre-Messinian rocks outcrop near the slope-top transition like at the southern slope.

The top of the Eratosthenes is flat in this cross-section. No signs of faults are visible. Thus, the principal faults on the Eratosthenes Seamount have a sublatitudional orientation. No reflectors are recorded beneath the erosional surface underlying the Pliocene-Quaternary layer.

The eastern slope is somewhat similar in the structure to the northern one. It is intensively disturbed by normal faults and has a step like configuration. However this configuration is not a simple reflection of the structure of the pre-Pliocene rocks as it was created mostly by slump and slide processes.

The Messinian is absent on this slope, and the pre-Messinian rocks are exposed at the steepest upper part of the slope.

The topography becomes flatter toward the base-of-slope, but the relief of the deepest reflector underlying the Pliocene-Quaternary layer is very complex. Pliocene-Quaternary sediments occur discordantly draping the already existing relief, like at the northern slope.

Starting from 09^{25}, the well-layered Pliocene-Quaternary unit changes abruptly into a chaotically layered and obviously intensively deformed sediment pile about 400-600 ms thick. The underlying reflector forms here a relatively narrow depression possibly connected with the northern slope.

Seismic line PS-123 crosses the northern edge of the top of the Eratosthenes from west to east and passes through the proposed ODP Site Medsap 1A (ESM 1A). The erosional surface at this site lies at a depth of 120 ms (about 110 m) from the seafloor under the acoustically transparent Plio-Quaternary layer. Short inclined reflectors occur below at a depth of

200-300 ms from the seafloor. A large fault scarp is seen near time mark 21^{00}. The vertical offset is 260 m. Bedrocks are exposed on the steep wall formed by the fault plane.

On the next short seismic profile (PS-124) oriented in a north-south direction, the offset along the fault is the same, but the fault plane seems to be draped by a thin cover of young sediments, possibly slumped from the top.

Seismic line PS-125 runs in a east-west direction across the proposed ODP Site ESM 2A on the northern slope of the Eratosthenes Seamount. A large young normal fault with a vertical offset of 200 ms was crossed obliquely at 05^{00}. In the immediate vicinity to the ODP Site, there is a highly uplifted block which is not seen on north-south line PS-120. The block height is 270 m. It is topped by 80 ms thick cover of Pliocene-Quaternary sediments. The inner structure of the block is not clearly defined, but there is a sense of a synclinal folding of the layers inside the block. The penetration is rather deep on both sides of the block (400-500 ms), and the probable Palaeogene/Neogene boundary is visible at a depth of 200-300 ms from the seafloor.

Seismic lines PS-126 (south-north oriented) and PS-127 were laid out at the base-of-slope. Line PS-127 is also the crossline through the proposed ODP Site ESM 3A. The principal picture from this profile confirms the interpretation made for line PS-120. A large block seen at 11^{40} is an upthrust deformed sheet, and the reflectors on the northern Eratosthenes slope dip gently beneath this sheet. The underthrusting process is evidently going on now because the youngest sediments covering the block are deformed as well.

4.2.b. SIDESCAN SONAR SURVEY

OKEAN SONOGRAPHS

B. Alibes, M. Campo, J. Fraile, J. Galindo-Zaldivar, V. Fomenko and L. Nieto

Nine long-range sidescan sonar lines (119-127) were run in the area of the Eratosthenes Seamount along the corresponding seismic lines. The sonographs were studied and interpreted along with the seismic records. The following main OKEAN facies types were recognized in the study area:

Facies 1. Homogeneous facies, generally with low reflectivity. Location: mainly in undeformed basin areas.

Facies 2. Heterogeneous facies, with curved features and variable reflectivity, but usually higher than that of facies 1. Location: in the Levantine Basin south of the Eratosthenes Seamount and on the Cyprus margin.

Facies 3. Heterogeneous facies with linear features and variable reflectivity. Location: the slope of Eratosthenes Seamount.

The main structural and morphological features that can be identified in the OKEAN records are:

(i) An upthrust of the assumed accretionary wedge of the southern Cyprus slope onto the sediments infilling the trench. The thrust front has an arcuate shape, trends between E-N and NE-SW and is characterized by the change of acoustic facies 2 to facies 1.

(ii) On the northern slope of the Eratosthenes Seamount, several scarps trending between E-N in the lower part and SW-NE in the upper part are seen. The scarps are covered by sediments which form features resembling slope apron or fan (Fig. 73).

(iii) Several circular holes with a diameter of about 500 m were recorded at the top of the seamount. They have no preferential orientation. Two E-W elongated rises and NE-SW trending faults are seen in the central part of the top.

(iv) On the southern slope, there is an NW-SE trending scarp with an irregular geometry. This is cut by orthogonal canyons opening southward. A major slump about 5 km long developed on this slope. The slump scar has an arcuate shape (Fig. 74).

(v) Several high reflective patches with irregular shapes are located in the trough south of the Eratosthenes Seamount. The contact between the sediments infilling the trough and the sediments of the Levantine Basin is sharp and takes place across the thrust front.

(vi) Two fault zones with N-S and NE-SW trends are situated at the southwestern boundary of the seamount. The first one seems to be older because it does not continue across the second zone. There are also two dome structures elongated in the SE-NW direction. Their lengths are between 1.5 and 3 km.

(vii) A slumping takes place also on the eastern slope of the seamount. The deformation front of the slumped sediments is seen at the toe of the slope. Compression folds in the slumped sediments have a NE-SW trend. There are also some dome structures in this part of the surveyed area.

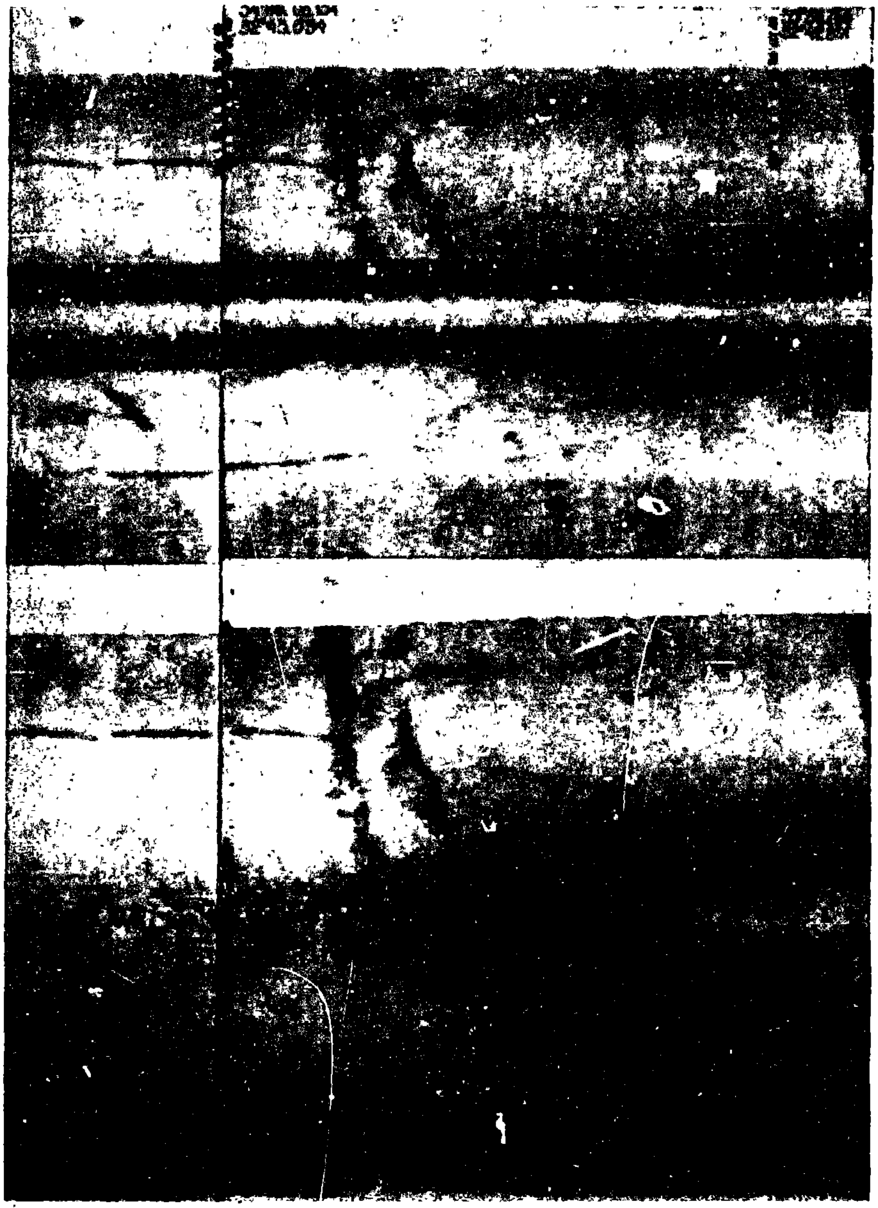

Fig. 73. Scarps (S) on the northern slope of the Eratosthenes Seamount covered by sediments which form a feature resembling a fan (F). A ridge (R) acting as a sedimentary trap (see section 4.2.a) is also seen on the left. Unprocessed (above) and processed (below) sonographs. The swath range is about 15 km. (Line 120)

MAK-1 SONOGRAPHS AND PROFILES

C. Beijdorff, W. van der Werff, and Yu. Gubanov

Three MAK-1 transects (20, 21 and 22), were run on the Eratosthenes Seamoun, each in a NW-SE direction (Fig. 68). The presently obtained deep-tow sidescan information represents the first data of this kind in the region. A total length of MAK-1 lines is 88 km.

The following features have been mapped:

Unit 1. Fault scarps. These lineaments vary in trend from E-W to NW-SE and are characterized by broad bands of a highly reflective sonograph facies (Fig. 75). Often, minor slump bodies with a width of up to 500 m are situated at the base of these scarps. Slump scars and gullies may occur occasionally at the top and across the fault scarps. Fault scarps offset major fault blocks by 150-200 m and indicate recent tectonic activity. The acoustic profiles display a homogeneous highly reflective seismic facies at the scarps. This suggests probably that possible pelagic sediments have been affected by slumping or were not deposited at all.

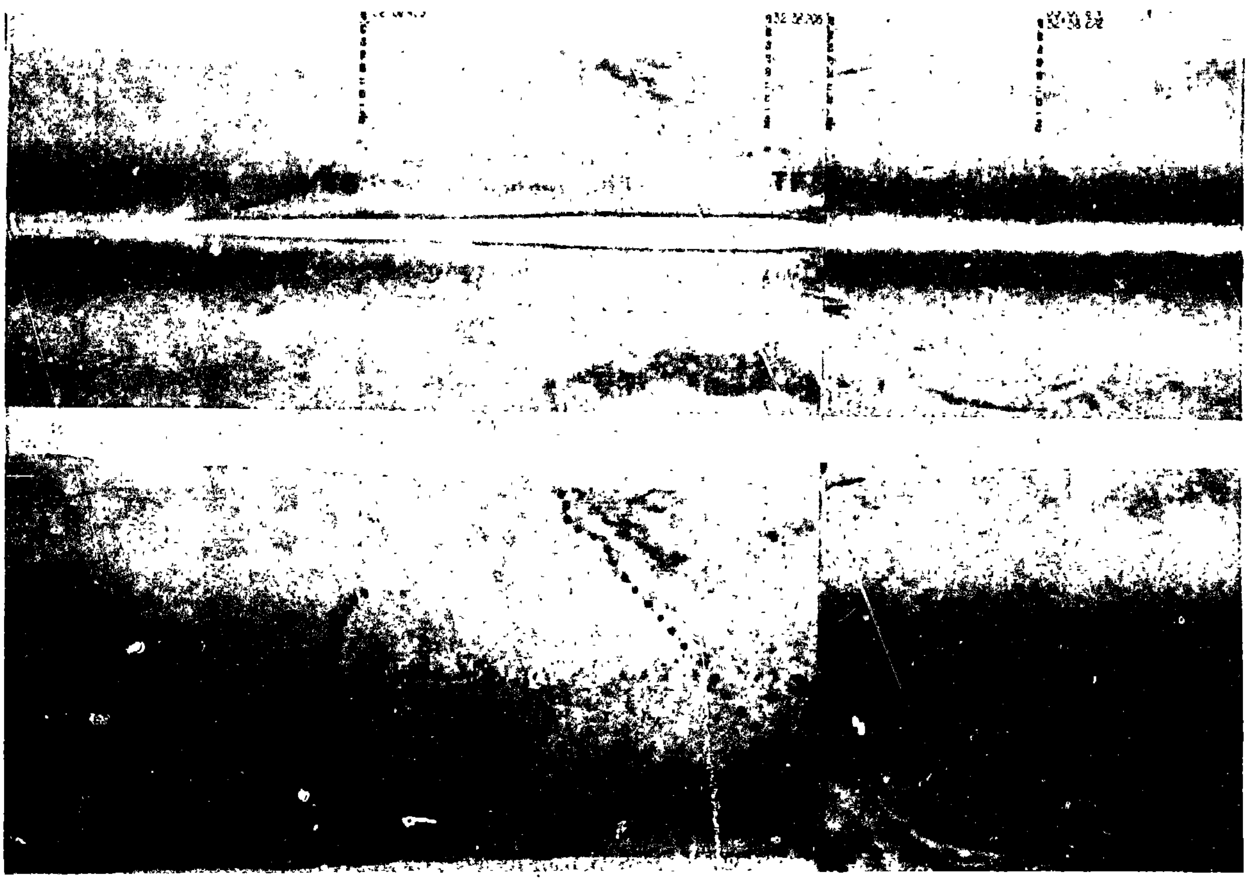

Fig. 74. A slump scar (SS) on the southern Eratosthenes slope. A thrust front (TF) separates the southern trough from the Levantine Basin. Unprocessed (above) and processed (below) sonographs. The swath range is about 15 km. (Line 120)

Unit 2. Subcircular holes (Fig. 75). These features are characterized by a diameter of some tens to 300 m and their relative depth is several metres. Most of the holes occur in the vicinity of fault scarps and are notable by high reflective rims on the side facing the MAK-1 fish. Many of them have a quite perfect circular shape. The holes could be related to karst, but more likely they originated from shallow gas or/and fluid seeps and represent pockmarks.

Fig. 75. Fault scarps with gullies and pockmarks on the top of the Eratosthenes. (MAK-1 line 20)

Unit 3. Anticlines. Anticlines are expressed on the acoustic profiles by open folds in pelagic sediments (Fig. 76), which may indicate either a regional compressive tectonic regime or, more likely, local compression because of block rotation. The folds are not seen on the sonographs because they run perpendicular to the trend of the MAK lines or because they lack a major surficial expression.

MAK line 21 runs across the outer-trench slope, trench and proto-thrust zone. An interesting aspect is shown by microfolding of the trench deposits (Fig. 77) situated in front of the proto-thrust. The folding is characterized by a type of "kinky" folding which may be caused by compression of a less competent layer on top of a more rigid "basement" during the underthrusting.

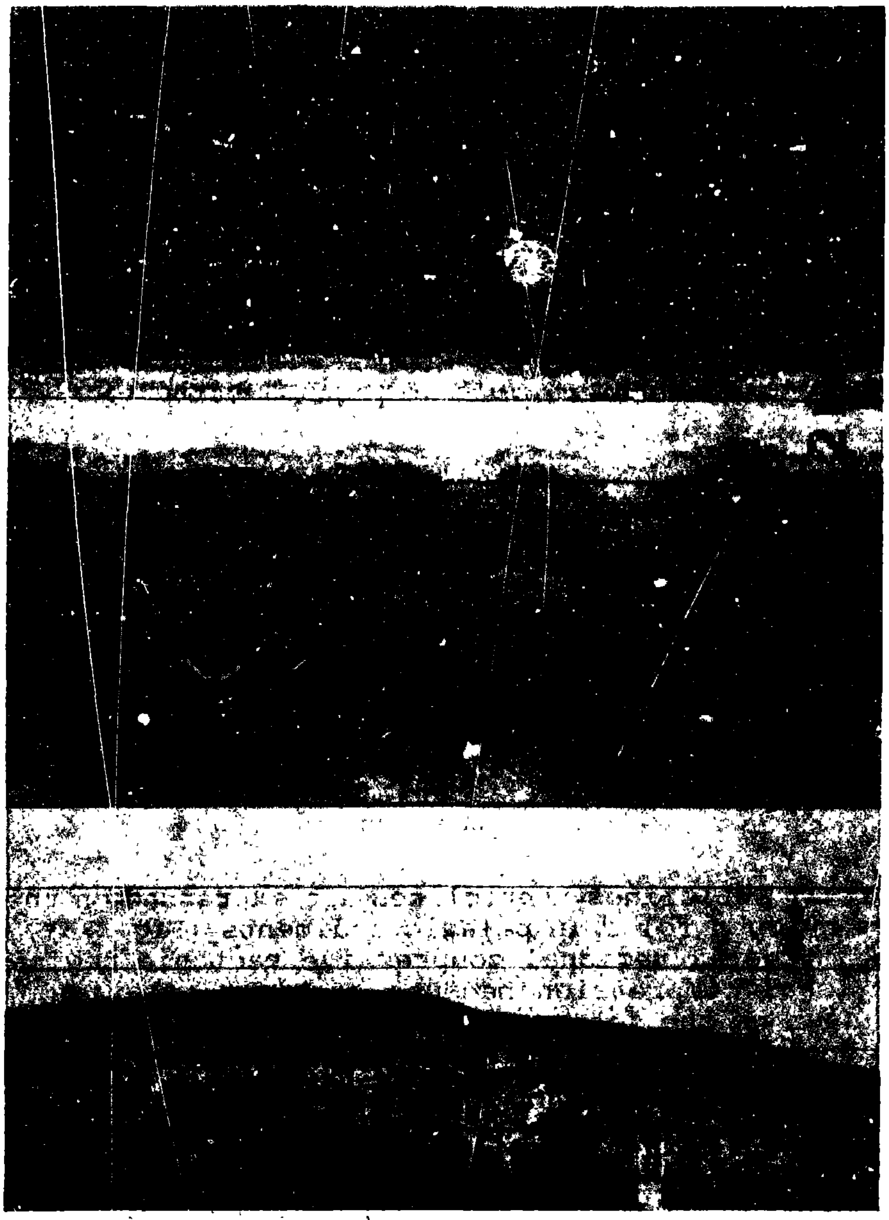

Fig. 76. Anticline folds seen on subbottom profile. (MAK-1 line 22)

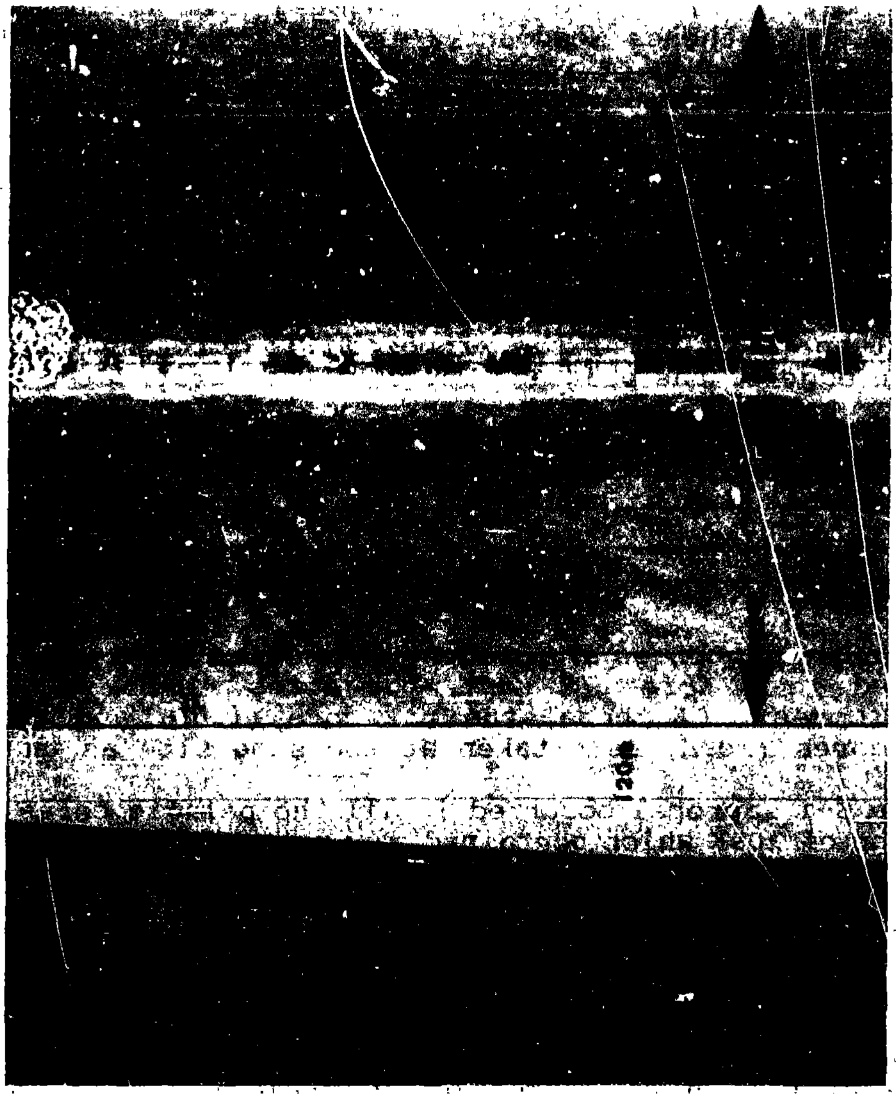

Fig. 77. Microfolding in the trench sediments seen on subbottom profile. (MAK-1 line 21)

4.2.d. BOTTOM SAMPLING

R. Lucchi, M. Pott, L. Nieto, E. Ivanova, A. Lototskaya, C. Glover, R. Flecker, E. Basov, R. Kidd, and A. Robertson

A total of 9 cores (2 Kastenlot cores, 1 box core and 6 gravity cores) were collected during Leg 3 of the TTR-3 cruise over the Eratosthenes Seamount (Fig. 68, Table VII). The total core recovery was 31.13 m. The longest core recovered was 534.5 cm (core 103G from a small ridge to the east of the eastern flank), whilst the shortest core recovered was 104 cm (core 108G from the north flank) not including the box core. The procedures carried out aboard the ship included splitting of the cores, photographs, detailed lithologic description and sampling for micropaleontological and sedimentological studies. The cores are arranged geographically into two broad transects (Fig. 78). The first runs north-south from the bottom of the north flank parallel to the line of the proposed ODP drilling sites to the southern edge of the plateau. The second is orientated east-west from the base of the east flank to the central part of the plateau. Figs. 79 and 80 show the correlation of the cores (except for the box core) along the north-south and east-west transects, based on marker lithologies and calcareous nannofossil biostratigraphy.

THE PELAGIC CORES: 105G, 106K, 109K, AND 111G

Pelagic sequences of Holocene to Middle Pleistocene age were recovered in 5 cores (2 Kastenlot cores, 1 box core, and 2 gravity cores). Of these, the box core (110B) and one of the Kasten cores (109K) were taken at the same site as the gravity core 111G.

The S-1 sapropel occurred in all the pelagic cores with the exception of 109K which contained a sapropelic horizon at the S-1 level. The upper boundary of S-1 was found between 21 and 22.5 cm from the top of every core. The thickness of the S-1 sapropel in these cores was also moderately constant, varying between 4 and 7.5 cm. The S-2 and S-3 sapropels were not identified in any of the pelagic cores. S-4 was not found in 109K, but in both the others it was identified using the microfossil assemblage. The S-4 sapropel found in 105G was finely laminated. The S-5 sapropel was identified in all three of the pelagic cores and showed traces of bioturbation in each, although 106G was particularly heavily bioturbated. The S-5 in 109K contained laminations and the bottom contact was an undulating one. Gravity core 105G also contained sapropel S-6 at a depth of 302 cm and another sapropel at 340 cm which has tentatively been identified as S-8. Neither of these sapropels were found in any of the other cores from this leg, although KC20, which was a 12.04 m core taken in 1991 during leg MD69 of the MARFLUX programme, recorded S-6, S-7 and S-8 from the plateau region. Nannofossil analysis based on the zonation of Gartner (1977) indicated that the bottom part of core 105G falls within the *Gephirocapsa oceanica* Zone and is therefore the oldest sediment recovered in this leg. The sediments in the other cores correspond to *Emiliania huxleyi* Zone and *E. huxleyi* Acme-zone.

Table VII

Summary of the bottom sampling data in Area No 3

CORE	DATE	TIME AT BOTTOM*	WATER DEPTH (m)	COORDINATES	SETTING	RECOVERY (cm)	LITHOLOGY	FACIES	AGE
TTR3-103G	9-7-93	14:04:33	2069.2	33°36.52' 33°14.40'	Top of foothill, E of Eratosthenes rise	534.5	MARL SAPROPELIC LAYER SAPROPEL S-1, 3, 4 & 5 TEPHRA Y-5 & Z-?	Pelagic Euxinic Euxinic Volcanogenic	HOLOCENE LATE PLEISTOCENE MIDDLE PLEISTOCENE
TTR3-104G	9-7-93	17:16:49	1268.8	33°36.90' 32°48.32'	Upper part of steep slope, near fault scarp	487.5	MARKER BED MARL SANDY LAYERS	Pelagic Pelagic Pelagic	HOLOCENE
TTR3-105G	9-7-93	19:01:25	803.0	33°37.99' 32°40.02'	Top of Eratosthenes rise	541.5	MARL SAPROPEL S-1, 5 & 6 TEPHRA Y-5	Pelagic Euxinic Volcanogenic	HOLOCENE LATE PLEISTOCENE MIDDLE PLEISTOCENE
TTR3-106K	9-7-93	21:09:38	910.6	33°40.60' 32°42.62'	Top of Eratosthenes rise	390,0	MARL SAPROPEL S-1, 5 & 6 TEPHRA Y-5	Pelagic Euxinic Volcanogenic	HOLOCENE LATE PLEISTOCENE MIDDLE PLEISTOCENE
TTR3-107G	11-7-93	19:25:27	2566.6	34°04.01' 32°42.79'	Top of foothill, N of Eratosthenes rise	483.5	MARL SAPROPEL S-1, 3 & 4 TURBIDITES	Pelagic Euxinic Pelagic	HOLOCENE LATE PLEISTOCENE
TTR3-108G	11-7-93	21:18:04	1528.4	33°55.15' 32°42.79'	N slope of Eratosthenes rise	104.5	MARL	Pelagic	HOLOCENE
TTR3-109K	12-7-93	20:37:18	938.7	33°47.86' 32°42.09'	Top of Eratosthenes rise	336,0	MARL SAPROPELIC LAYER SAPROPEL S-1 TEPHRA Y-5	Pelagic Euxinic Euxinic Volcanogenic	HOLOCENE LATE PLEISTOCENE
TTR3-110B	12-7-93	21:37:01	942.8	33°47.85' 32°42.07'	Top of Eratosthenes rise	29,0	MARL SAPROPEL S-1	Pelagic Euxinic	HOLOCENE LATE PLEISTOCENE
TTR3-111G	12-7-93	22:44:34	939.2	33°47.85' 32°42.07'	Top of Eratosthenes rise	296.5	MARL SAPROPEL S-1 & 5 TEPHRA Y-5	Pelagic Euxinic Volcanogenic	HOLOCENE LATE PLEISTOCENE MIDDLE PLEISTOCENE

* Ship Time

Traditionally the base of *Emiliania huxleyi* Acme-zone, defined by the sharp increase of this species, was identified as 720 kyrs, but the latest investigations for the Eastern Mediterranean (Rio et al., 1990) showed it to be an event correlated with a boundary between climatic stages 4 and 3 (approximately 53 kyrs). In the sequences this boundary is situated between the tephra Y-5 and the sapropel S-3.

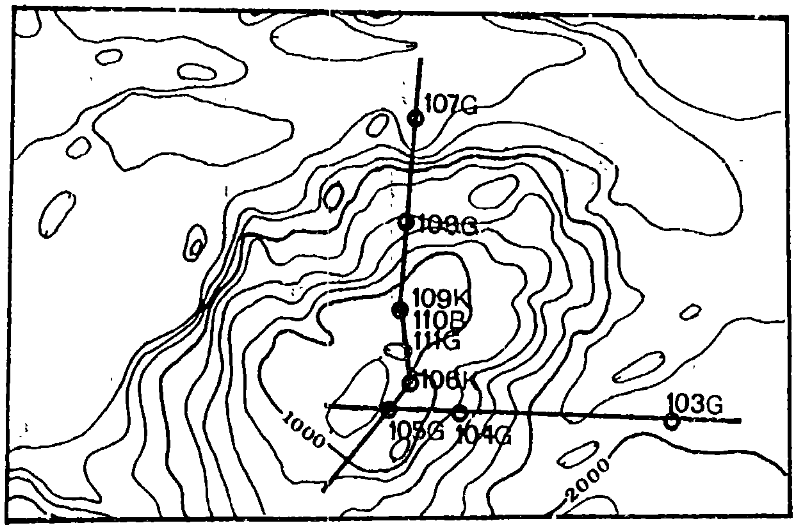

Fig. 78. Location of transects over the Eratosthenes Seamount

Smear slide analyses of gritty silt layers which showed perlitic cracks on the surface on the split cores indicated that these horizons contained abundant shards of volcanic glass. The fibrous and unaltered nature of the glass is typical of the Y-5 tephra. The Y-5 tephra has been identified in all three of the pelagic cores. In all these cores it occurs between 30 and 40 cm below the S-1 sapropel.

GEOGRAPHICAL POSITION AND INTERPRETATION

Cores 105G and 106K were both positioned on the main summit of Eratosthenes. Core 106K was obtained on the site of KC20. The S-1, S-5, S-6, S-7 and S-8 sapropels were all identified in this core, and 106G also contained S-1 and S-5 in similar positions (19 and 333 cm respectively). The log of KC20 indicated two dark layers above S-5, neither of which were given names. Above the S-5 sapropel in core 106K had only one dark layer was present which smear slide analysis revealed to be sapropelic. It has been tentatively suggested that this may represent the S-4 sapropel, but it was not clear which of the two dark layers in KC20 it might correlate.

105G was cored on the prospective ODP drilling site, ESM 1. It was located on the very highest part of Eratosthenes in an attempt to core the thickest pelagic sequence. However once the

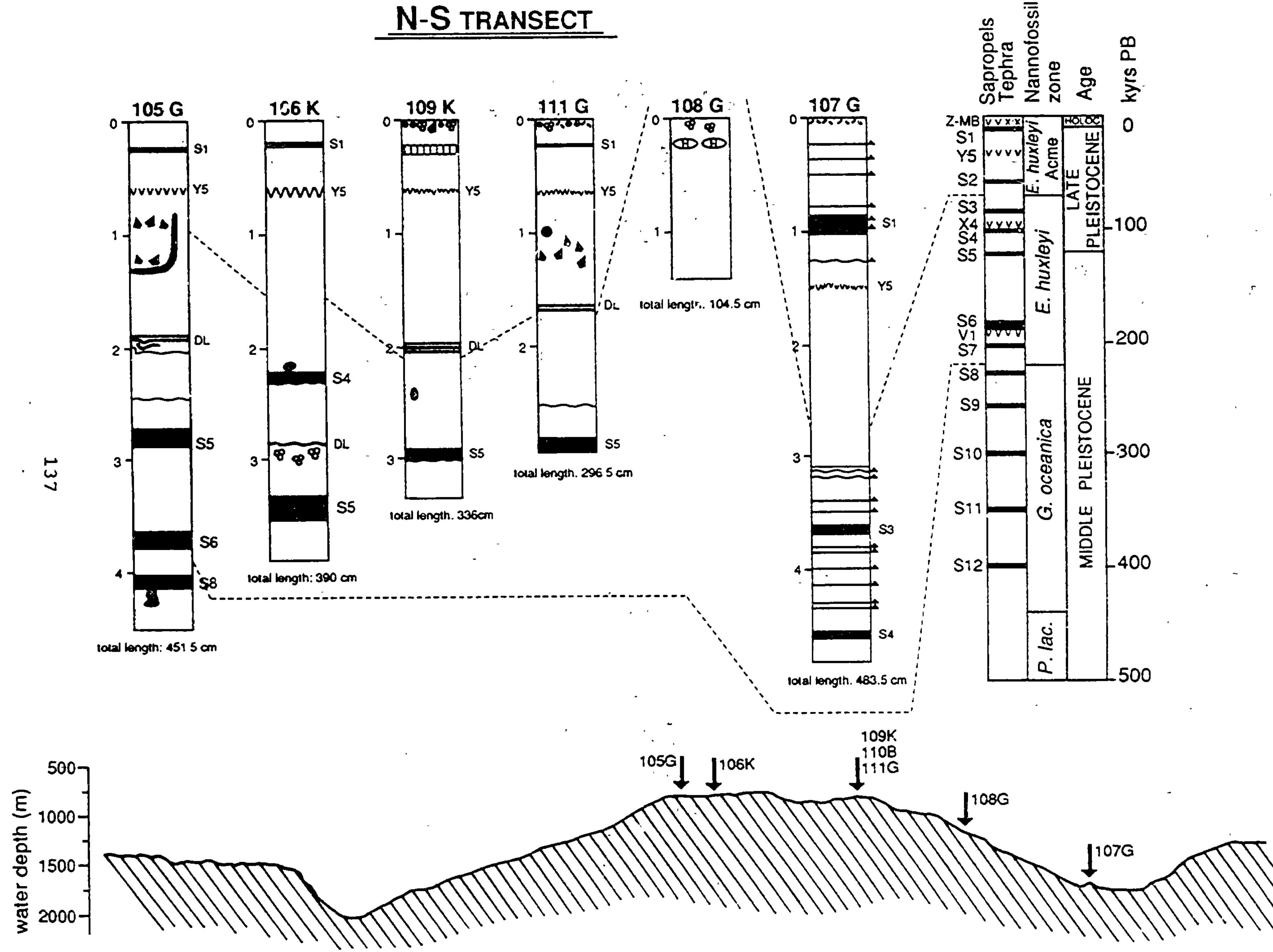

Fig. 79. Correlation of the cores along the north-south transect (see the legend in Fig. 80)

north-south seismic line had been shot and processed it became clear that a potentially thicker Plio-Quaternary sequence was located on the northern tip of the plateau. Core 109K was located at this point and although the maximum recovery from the Kasten and gravity cores taken at this site was only 336 cm, the wider spacing of the sapropels S-1 and S-5 found in it (268.5 cm from the top of S-1 to the top of S-5), in comparison with those found in 105G (230 cm), indicates that the sequence was indeed expanded at this point.

THE FLANK CORES: 103G, 104G, 107G, AND 108G

Three sites were cored on the flanks of the seamount (see Fig. 68). Cores 107G and 108G are situated on the line of proposed ODP drilling on the northern side of Eratosthenes, whilst 104G was taken from the bottom of a steep slope close to the eastern edge of the plateau. Core 103G was taken at the foot of the eastern flank (Fig. 68) and was thought initially to contain a pelagic succession. Later study of the sedimentation rate however indicates that it is probably best thought of as a flank-located core.

The location of 108G, the shortest core taken on this leg, was determined using the north-south seismic section shot over the northern flank. In the hope that an older section would be recovered, the core was positioned in an area which appeared to have no Plio-Quaternary over on account of tectonic activity and related re-sedimentation processes. The core recovery was only 104 cm, however, due to a carbonate hardground found between 16 and 20 cm depth. The hardground consisted primarily of cemented foraminifers and contained traces of boring. For the entire core the nannofossil assemblages are referable to the *Emiliania huxleyi* Zone in the Late Pleistocene.

The north-south seismic section indicates a small basin at the foot of the northern flank of Eratosthenes, bounded to the north by a topographic bulge. Core 107G was located on the southern side of the top of this topographic feature. The core recorded an expanded sequence containing a thick (16.5 cm) S-1 sapropel which consisted of five small fining upwards sequences (between 2 and 5 cm thick), indicating that much of its thickness can be attributed to redeposition by turbidity currents. Another sapropel occurred at 362 cm. This sapropel, interpreted as S-3, did not show fining upwards sequences, and its thickness (8 cm) is therefore thought more likely to represent pelagic accumulation. It did show fine scale pale coloured laminations and was bioturbated throughout. A third sapropel, 7 cm thick, was found at 461 cm and has been interpreted as S-4. It contained abundant pteropods and was heavily bioturbated, but did not show fining upwards horizons, thus it is also thought to have accumulated without much turbiditic input.

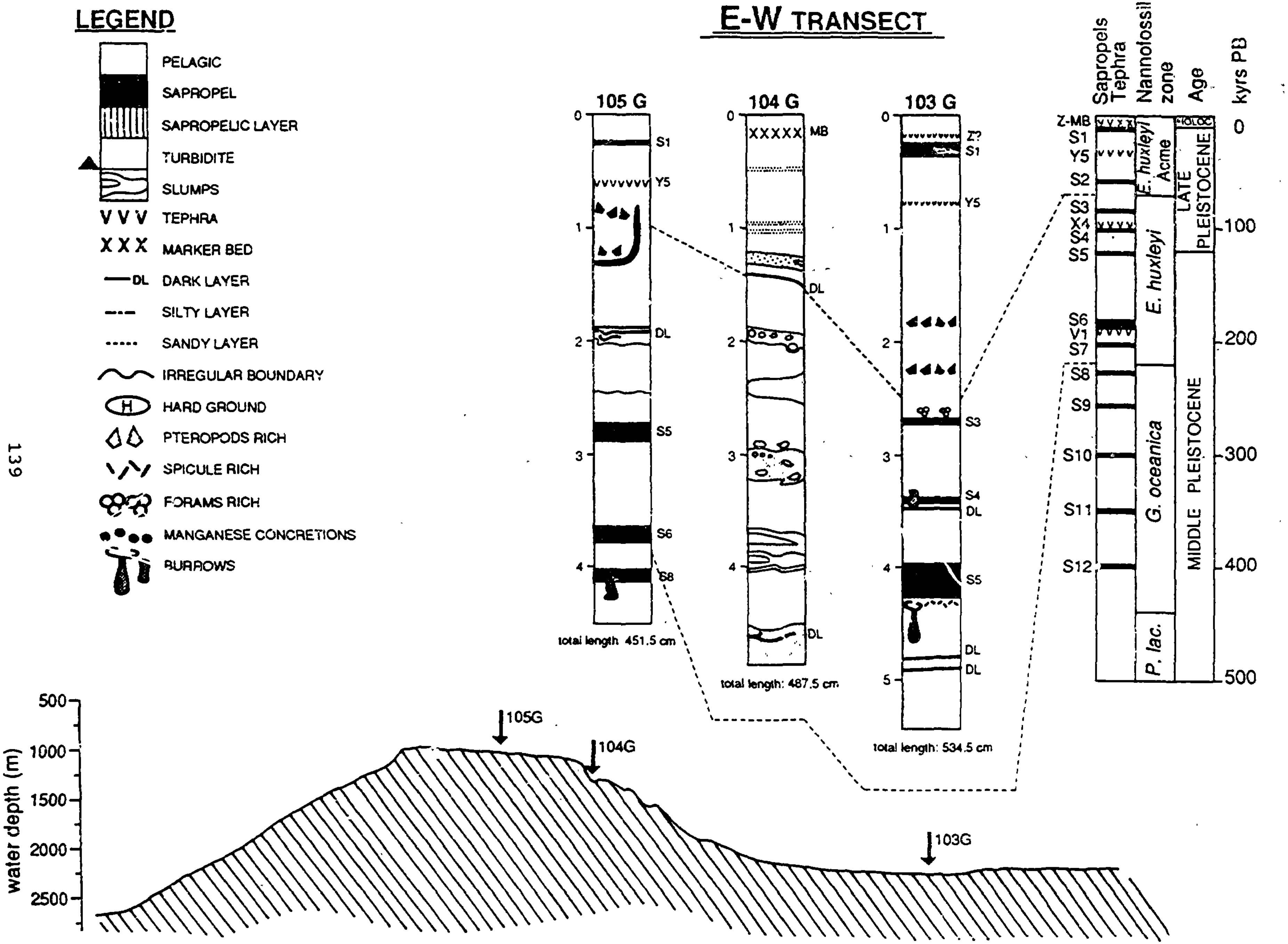

Fig. 80. Correlation of the cores along the east-west transect

The top and bottom of core 107G was dominated by two sections of fine-grained fining upwards horizons, 5-10 cm in thickness, some of which had been heavily bioturbated. These have been interpreted as mud turbidites, the coarser fraction of which is thought to have been pounded in the basin to the south of the topographic bulge. The central part of the core starting at 43 cm below the top, between the S-1 sapropel and the Y-5 tephra, and continuing downwards for 203 cm, is dominated by a stiff marl containing abundant microfossils and pteropods. Initially it was thought that this marl represented a period of pelagic accumulation, but the sedimentation rate proved to be too high not to have been affected by re-sedimentation processes. Towards the bottom of this marl section the nannofossils indicate that there is a transition from the *E. huxleyi* Acme-zone to the *E. huxleyi* Zone, so that the whole core dates from the Upper Pleistocene and the Holocene. MAK line 22 across this area shows layered sediments on the southern side of the topographic hillock, but not on its northern side. This supports the idea that periodically turbid layers poured off the northern flank of Eratosthenes, depositing almost all the traction load in, or before the basin and most of its suspended load is deposited on the south side of the topographic ridge which thus acts as a barrier. It is also evident from the corresponding seismic record which shows that the level of sedimentation is higher south of the barrier than to the north (see Section 4.2.a). Further discussion of sediment deposition mechanisms related to calculated sedimentation rates in this core will be undertaken later.

Smear slide analysis at 149.5 cm in core 107G showed that this horizon contained abundant shards of volcanic glass. This was identified as the Y-5 tephra.

Steep slopes immediately to the east of the seamount's plateau are interpreted from seismic and MAK-1 records as fault scarps. Core 104G is located at the base of one of these fault scarps quite close to the plateau region. The bulk of the core is made up of debris flow units which in conjunction with the seismic profile recorded across this area have been interpreted as slump units from the fault scarps. The debris flow units began at 163 cm from the top of the core and are all assigned to the *Emiliania huxleyi* Zone of the Early Pleistocene. They contain reworked nannofossils of Oligocene and Miocene age. A sequence of pelagic sediments with an original sedimentary dip are found above the debris flows and are interpreted as in situ slope deposits. This pelagic sequence consisted almost entirely of planktonic foram-rich marls, but 12 cm from the top a dark bioturbated layer was found which contained pteropods and manganese nodules similar to the "marker bed" found during Leg 2 of the cruise. It is not clear why these nodules should be found in this core and not in any of the other cores in the Eratosthenes area, but it is thought that it may be due to the formation conditions required being affected by micro-topographic variation.

The S-1 sapropel found in 103G was considerably thicker (12.5 cm) and occurred a few centimetres lower down the core than the S-1 sapropels found in the pelagic cores. Lower down the cores the marker sapropels and the Y-5 tephra are all displaced downwards relative to the pelagic cores, indicating that a significantly higher sedimentation rate affected 103G than that affecting the pelagic cores on the plateau. Neither the pelagic nor the flank cores contain the S-2 sapropel and 103G is the only core in which sapropel S-3 has been found in this Eratosthenes region. It occurred at a depth of 260 cm, was bioturbated and contained abundant foraminifers. S-4, in core 103G showed a spectacular vertical burrow which extended from the overlying marl through the 6 cm of sapropel, down into the underlying marl. The infilling material was a dark soft mud which contained organic material which might have been derived from the sapropel. Surrounding the base and lower sides of the burrow a violet chemical front was visible which gradually joined the sides of the burrow in its upper parts. The S-5 sapropel was not visible in 103G, probably because the core did not penetrate deep enough.

The Y-5 tephra was clearly identified in 103G, 40 cm below S-1. It was underlain by a series of marls some of which were particularly rich in pteropods. Smear slides showed the boundary of *E. huxleyi* Acme/*E. huxleyi* Zones lies towards the bottom of this sequence, at 245 cm, above S-3.

103G was taken from a small bathymetric ridge at the base of the eastern flank of Eratosthenes. It was originally thought to be a pelagic sequence because it did not appear to contain any of the re-sedimentation features that characterize the cores taken on the flanks, e.g. the fining upwards horizons visible in 107G which have been interpreted as mud turbidites and the debris flow units which were found in 104G. It is probable however, that the expanded nature of this core, in comparison to the cores taken from the plateau region of the sea mount, was due to the accumulation of fines which may have originated from the slump activity and faulting on the eastern flank which was so clearly visible in 104G and in the east-west seismic section across this area. Layers which contained abundant pteropods could be interpreted as the coarsest part of the suspended fines to reach this far east.

SEDIMENTATION RATES

Overall sedimentation rates calculated from the lowest present sapropel unit to the present day (t=0) vary between and 1.8 cm/kyrs and 4.6 cm/kyrs. The pelagic cores vary systematically from 1.8 cm/kyrs on the summit to 2.4 cm/kyrs on the lowest terrace. Sedimentation rates in the Mediterranean as a whole are recorded as 2-3 cm/kyrs. It is to be expected that the sedimentation rates observed on the Eratosthenes are lower than this general rate as it is raised into the intermediate water layers where current regimes are known to be strong. Overall flank rates are 4.6 cm/kyrs and 3.4 cm/kyrs.

Within the pelagic cores (105G, 106K, 109G) sedimentation rates vary from 1.5 cm/kyrs to 6.2 cm/kyrs (Fig. 81a). All three cores show a uniform sedimentation rate of 1.8 cm/kyrs from the

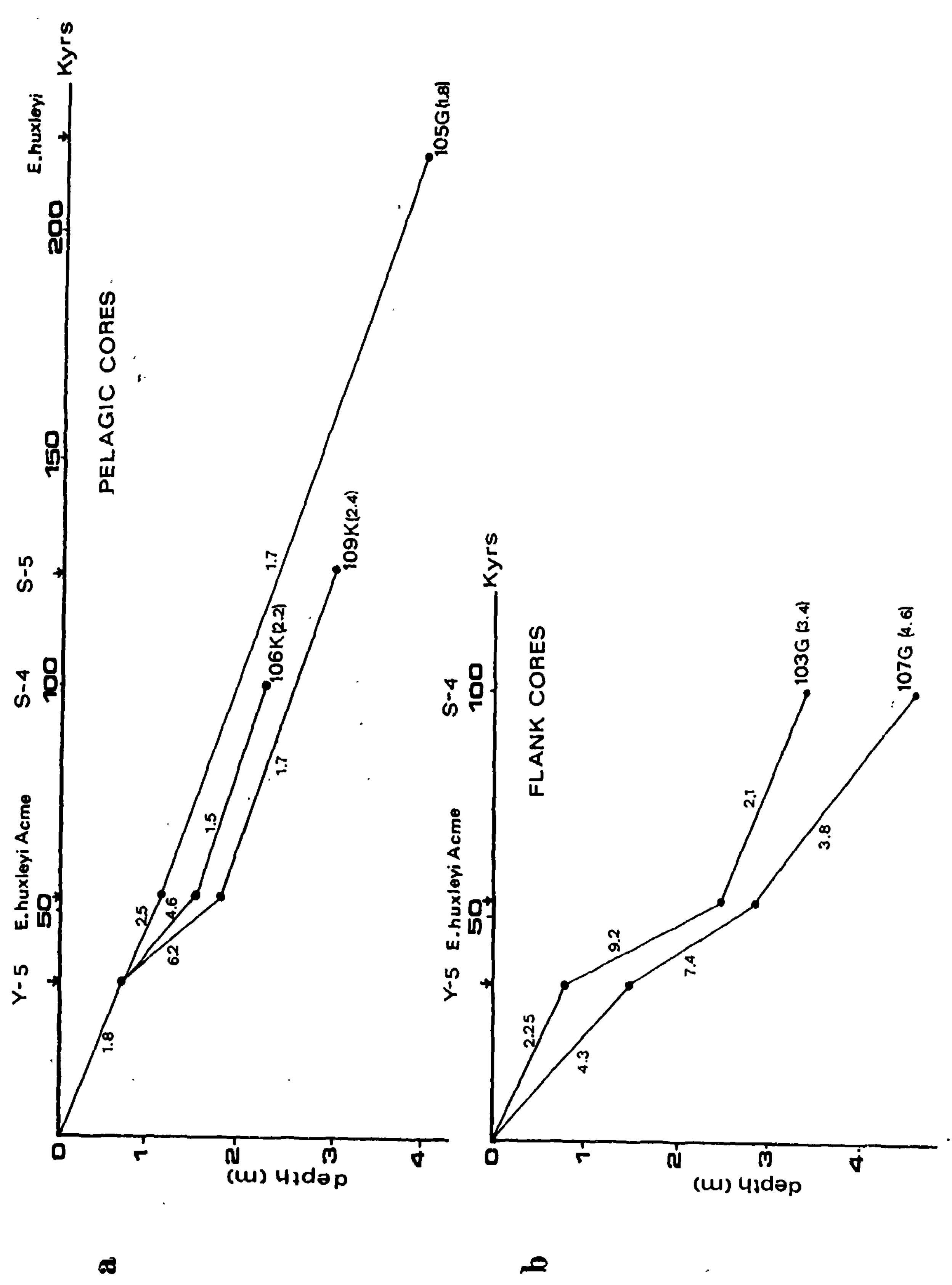

Fig. 81. Sedimentation rates during the Late Quaternary in the area of the Eratosthenes Seamount
2.1 - rate in cm/kyrs. Figures in brackets represent sedimentation rate over the entire section

Y-5 tephra up to the present day. Between the Y-5 and the *E. huxleyi* Acme boundary sedimentation rates are higher and vary between 2.5 cm/kyrs and 6.2 cm/kyrs. Core 105G, which has the most uniform sedimentation rate, is situated at the highest point of the summit and the small increase in sedimentation rate seen between the Y-5 and the *E. huxleyi* Acme boundary is probably not significant. It is a condensed section reaching the S-8 sapropel at only 4 m depth. Between the Y-5 and *E. huxleyi* Acme boundary foram-rich layers are seen, particularly in the lower part. Core 106K is some 100 m bathymetrically lower than 105G; and core 109K, which has a rate of 6.2 cm/kyrs, is located on a summit terrace which is 350 m below the highest point. Core 109G contains abundant pteropod fragments within the zone of high sedimentation.

Throughout the flank cores (103G, 104G, and 107G) much higher sedimentation rates are seen than in the pelagic cores (Fig. 81b), with background sedimentation rates varying from 2.03 cm/kyrs to 4.3 cm/kyrs. In cores 107G and 103G these increase to 7.4 cm/kyrs and 9.2 cm/kyrs respectively, between the Y-5 and *E. huxleyi* Acme layers. Of all the cores, 107G has the highest sedimentation rates throughout. It is situated at the base of the seamount on a small rise, beyond pounded, coarse sediment and receives mud turbidites which are visible in the 3.8 cm/kyrs and 4.3 cm/kyrs regions. The central (Y-5 to *E. huxleyi* Acme) zone, however, contains marl with darker laminations and sparse pteropods but has a sedimentation rate of 7.4 cm/kyrs. Core 103G displays undisturbed pelagic sections post- Y-5 and pre-*E. huxleyi* Acme but has elongated mottles and two distinct pteropod layers between the Y-5 and *E. huxleyi* Acme Zone where sedimentation reaches 9.2 cm/kyrs.

It must be noted that sedimentation rates cannot be taken as absolute but must be considered as an indication of rate. The position of the changes in gradient are entirely artificial, due to the predetermined position of dated horizons. However, the sediment distribution in cores 103G and 107G, in particular, indicates that between the Y-5 and *E. huxleyi* Acme boundary one may indeed be observing a distinct sedimentological regime. Y-5 has been taken as 35 kyrs, *E. huxleyi* Acme as 53 kyrs, S-4 as 100 kyrs, S-5 as 125 kyrs and *E. huxleyi* as 220 kyrs. The given age for Y-5 is 35-40 kyrs, the effect of using 40 kyrs instead of 35 kyrs for Y-5 is to further increase the sedimentation rates in the central zone. Errors in the absolute age determinations of the nannofossil boundaries and sapropel layers are not currently available to us. Errors for the position of the nannofossil boundary are always below the level indicated and range from up to 21 cm in 106K to 41 cm in 105G but are probably considerably lower. The effect of lowering the boundary position is also to increase the sedimentation rates observed in the central sections. Thus, despite the errors inherent in this method of calculating sedimentation rates, the trends indicated appear to be valid.

Core 108G contains no dated boundaries and thus sedimentation rates cannot be calculated. Core 104G is not plotted because the debris flow and missing S-1 and Y-5 layers indicate that the position of the *E. huxleyi* Acme layer immediately above the debris flow layers is not the true position of the boundary. If it is, the calculated sedimentation rate is 2.5 cm/kyrs. Core 111G is considered to be identical to 109K.

DISCUSSION

It can be seen that high sedimentation rates occur in all areas between the Y-5 tephra and the *E. huxleyi* boundary (except in 105G). These regions are typified by good preservation of pteropod fragments and laminations and/or mottles. This general increase in sedimentation rate could be attributed to a number of factors: increased terrigenous sediment input, increased productivity, current reworking, sediment drift, tectonic resuspension of sediment, or tectonic downfaulting of blocks. Changes in terrigenous input and productivity are most likely to be the result of climatic variation. However the size and periodicity of the changes recorded in the cores is not compatible with that known for climatic change during the Pleistocene and this mechanism must be overruled. It is probable that combinations of all the other factors are responsible for the trends seen.

In the pelagic cores it is probable that a certain amount of ponding, contourite and drift formation occurs on the lower terraces of the summit region. The condensed nature of 105G on the highest point of the Eratosthenes seamount confirms this; and the foram-rich layers above the *E. huxleyi* Acme boundary suggest that this layer has been winnowed, particularly in the early stages of the central section. If, at this time, tectonic activity increased somewhat, resuspension of sediment accompanied by down-faulting of the terrace blocks may cause a general movement of sediment off the flank areas and onto the lower terrace regions.

On the flanks, instability caused by tectonic tremors, together with higher suspended sediment levels would cause frequent turbid flows. This should give high sedimentation rates characterized by layering but not showing the classic fining-up sequences of turbidites. This model can certainly be applied to 103G in which the zone of high sedimentation is characterized by elongated mottles and distinct pteropod layers.

Core 107G needs more careful consideration because of its rather special location. As previously described, the core sits on a bulge, probably caused by thrust faulting along a decollement at the base of the flank fault. The central section of high sedimentation rate consists of a marl with sparse pteropods and darker laminations. Either side of this are muddy turbidites. The muddy turbidites can be interpreted as the remnants of turbiditic flows, whose coarse fraction was deposited in the depression at the base of the slope and ahead of the rise. A possible interpretation of the higher sedimentation rate of the central section is that during a period of increased tectonic activity the rise was lifted out of range of the turbiditic bottom layer but was still within the range of a thickened turbid upper layer. With time the basin to the south was partially filled with turbiditic material until the turbidites could once again reach the summit of the small rise. Alternatively, during a period of higher tectonic activity the turbidites would have been thicker and faster, bypassing the rise altogether and leaving just a thick layer of suspended sediment to deposit on the southern slope and summit.

In conclusion, it appears that the increased sedimentation rates seen in all cores between the Y-5 tephra and the *E. huxleyi* Acme boundary can best be explained by a period of increased tectonic activity, causing down-faulting of tectonic blocks, sediment ponding and current reworking on the new topography, re-suspension of sediment and frequent downslope movement of turbid layers.

MICROFOSSIL ANALYSIS

Analysis of foraminifers assemblages was used for identification of tephra and sapropel layers and to estimate the age of the sediments. All the Eastern Mediterranean sapropels were formed under poorly oxidized bottom conditions. However there is evidence of different temperature and salinity conditions (Ryan and Cita, 1977; Kidd et al., 1978a, b; etc.) which can be also identified by ecological groups of planktonic foraminifers. Sapropel S-1 (8 kyrs B.P.) (Oggioni and Zandini, 1987) was deposited during a Holocene warm trend and is represented in the cores mainly by warm-water assemblages of planktonic foraminifers: *Orbulina universa*, *Globigerinoides ruber*, *Globigerinoides sacculifer*, and *Hastigerina siphonifera*. Sapropel S-3 (80 kyrs B.P.) seems to be formed under cooler temperature conditions but is also represented mainly by warm-water species. It contains a large number of *O. universa* and less abundant *H. siphonifera* and *Gs. ruber*. *Gs. saccullifer* was not found in the S-3 interval. Species from cold-water assemblages such as *Globigerina bulloides* and *Neogloboquadrina eggeri* are more abundant then in the S-1 interval. Sapropel S-4 (100 kyrs B.P.) is represented by both warm- and cold-water fauna. Most abundant of the first group is *Gs. ruber*, and *Turborotalia quinqueloba* is the most abundant of the second. *T. quinqueloba* forms most of fine fraction of the samples. S-5 (125-120 kyrs B.P.) was formed under very warm temperatures conditions. Planktonic foraminifers fauna from the S-5 layer consists of warm-water *O. universa*, *Gs. ruber*, *Gs. sacculifer*, and *H. siphonifera* of a very large size, and contains no cold-water representatives, Sapropel S-6 (185 kyrs B.P.) contains a fauna of completely opposite type. It is represented by *N. eggeri* - *G. bulloides* fauna which consists either of cold water species like *G. bulloides*, *T. quinqueloba*, and *Neogloboquadrina pachyderma* or of low-salinity indicators - *N. eggeri*. One sapropel layer was identified as S-8 (225 kyrs B.P.) by the nannofossils. It contains very warm-water fauna of planktonic foraminifers including such tropical species as *Gs. sacculifer*. The tephra layer Y-5 (35-40 kyrs B.P.) usually contains a sparse, cold-water fauna of planktonic foraminifers. Transparent sharp-shaped volcanic glass makes up the majority of the samples.

4.2.f. ODP SURVEY

R. Kidd

In the limited time available, we were to attempt to survey four sites in support of tectonic objectives of the Mediterranean Ridge ODP drilling proposal, Eratosthenes Seamount component, sites ESM 1 to 4; and one site in support of the Mediterranean Sapropels drilling proposal, MEDSAP 1C. In the event, the results of the initial part of our studies of Eratosthenes Seamount led us to revise the positioning of the sites and to suggest a possible combination of MEDRIDGE and MEDSAP drilling objectives into a single site (see Sections 4.1 and 4.3).

We launched the OKEAN sidescan and airgun seismic equipment off the Cyprus coast around midday on the 7th of July along line 119 (see Fig. 68). The longest line to be run with these systems was a roughly north-south line set to parallel the existing multichannel seismic (MCS) line, MS-54. This line, 120, was ~4 km to the west and provided a sidescan image over all of the sites on the MS-54 line and a seismic profile over ESM 1, which was located near the summit of the Seamount, but not actually on the MCS line. Problems with the airguns meant that two portions of this line 120 were repeated.

On the 8th/9th of July we continued with a west to east line across the Seamount through ESM 1, imaging with sidescan the MEDSAP 1C site, which had been chosen at the location of the 12 m long piston core collected by the MARFLUX programme. Two repeats occurred on this line. On the 9th of July we also recovered gravity core 105G, from the ESM 1 site (33°38'N/ 32°40'E; uncorrected water depth 781 m) and Kasten core 106K (33°40.6'N/32°40.6'E; uncorrected water depth 887 m) from the MEDSAP 1 site. These cores recovered very similar pelagic sequences to 4.41 m and 3.90 m subbottom respectively. Both recorded sapropels through to the S-5 although in neither were all present and the longer core reached the S-8 at age 225 kyrs. Sedimentation rates are generally low, between 1.5 and 1.8 cm/kyrs. Thus shipboard analysis of the summit cores suggests that both are pelagic nannofossil marl sections, somewhat condensed and with indications of missing sapropels. We decided to continue with our initial notion to try to locate an alternate, more expanded section on the summit, for the sapropels drilling.

Overnight and through much of the 10th of July, a MAK-1 deep-towed sidescan sonar and profiler survey line, 20, was run across the summit, which passed through the proposed MEDSAP 1C. This showed clearly the intersecting normal fault scarps which are a feature of the OKEAN and seismic lines and are very apparent in the Udintsev's multi-beam bathymetry map. Also seen were patches of circular depressions of uncertain origin (see Section 4.3). In the meantime, analysis of the seismic profiles so far collected indicated clearly that there was Plio-Quaternary sediment cover across the entire top of the Seamount. Consequently, the proposed ESM 2 becomes unviable as a "window" to the older sediment sequences, and time constraints were already making surveys over the lowest priority site ESM 4 unlikely. On the other hand, interesting potential drilling targets were visible on the north slope that could both serve the deeper objectives of ESM 2 and introduce the possibility of penetrating with drilling an upthrust sheet and its underlying decollement zone. In addition, a thickened Plio-Quaternary cover was evident near the top of the north slope as a possible alternate MEDSAP site. We elected to obtain the survey data needed to define these three as alternative drilling targets.

On the $10^{th}/11^{th}$ of July we ran further OKEAN and seismics lines, 123 through 127, to provide east-west crossing profiles with sidescan over possible new sites: MEDSAP 1D on line 123, ESM 2A on line 125, and ESM 3A on line 127 respectively.

Gravity cores 107G and 108G were recovered on the 11^{th} of July from ESM 3A and ESM 2A respectively. The latter, core 108G defining ESM 2A (33°55.15'N/32°42.79'E; uncorrected water depth 1492 m), revealed a thin calcareous hardground over 1 m of stiff pelagic marls. Core 107G (34°04.01'N/32°43.52'E; uncorrected water depth 2510 m) from the south face of a knoll on top of the inferred thrust sheet recovered a 4.8 m long core containing two sequences of thin mud turbidites between which are marls containing the Y-5 volcanic ash.

Next we ran two consecutive MAK lines to allow us to obtain high resolution seismic crossings of the ESM sites, recognizing that there was no time to do the same at the new MEDSAP 1D site. MAK line 21 provides an oblique SE-NW crossing of ESM 3A/107G and illustrates remarkably well the local tectonic and sedimentary setting around the foot of the Seamount's north slope and the inferred thrust sheet hill beyond. MAK line 22 passed obliquely over ESM 2A/108G and demonstrates that there is indeed a "window" to older sequences there, between possible limestone blocks that appear to have detached by gravity sliding on the slope.

We completed our survey effort with a suite of cores taken at the alternate MEDSAP ID site (33°47.8'N/32°42.1'E: uncorrected water depth 915 m). Gravity core 109G, Kasten core 111K and box core 112B define a pelagic sequence with only slightly higher overall sedimentation rates than at MEDSAP 1 but again high rates (here up to 6.2 cm/kyrs) in the period below the Y-5 ash and again some gaps in the sequence of sapropels.

In summary, the ODP site surveys carried out over Eratosthenes Seamount by R.V. *Gelendzhik* have revised the locations and provided seismics, sidescan and sampling data for three tectonically-oriented drilling targets for the proposed Eratosthenes drilling transect; and have also provided the necessary survey data to define one target and an alternate for the eastern end of the Mediterranean sapropels transect.

4.3. GENERAL INTERPRETATION

A. Robertson, J. Woodside, A. Limonov, and R. Kidd

The results of the recently completed, dedicated ODP site-survey during the TTR-3 Cruise add very significantly to understanding of the structure and tectonic setting of the Eratosthenes Seamount.

The objective of this final section is to highlight findings from the last leg of the cruise, in the light of existing information, relevant to the geological and tectonic setting of Eratosthenes. The objectives were determined by the needs to obtain ODP site survey information from three or four sites. It was a measure of the effectiveness of the shipboard data collection, that it was possible early on in the cruise to show that two of the previously selected sites were either unsuitable, or could be bettered. Without the rapid availability of high quality, processed seismic data the revised ODP sites could not have been selected at sea.

In the following sections, the main features of Eratosthenes investigated are summarized.

ERATOSTHENES PLATEAU AREA: THIN SEDIMENTS ON A BASEMENT

The airgun seismic records add very considerably to knowledge of the structure of the upper levels of the Eratosthenes Seamount (Fig. 82). The following features are particularly important. First, the Plio-Quaternary sediment cover is very much thinner than had been assumed, based on study of earlier multichannel seismic data (e.g. MS-54, B28). A prominent reflector can be traced beneath the entire plateau area of the seamount. This is suggested to mark the base of the Plio-Quaternary succession, which assuming a seismic velocity of 1800 m/s, is inferred to range from thickness of less than 50 to ca. 200 m. The Plio-Quaternary succession is very well-layered and relatively uniform in thickness, although the cover thins markedly near the edges of the seamount and thickens somewhat on occasional swells. The reflector beneath the Plio-Quaternary succession is assumed to be a Messinian erosional surface. Underlying layers are not clearly imaged on the new airgun data, but the basement is seen to be cut by a series of high-angle faults. The Plio-Quaternary succession is draped over these faults with little signs of disturbance. However, faulting of the cover is indicated on the high resolution seismic data (MAK-1; see below).

Further evidence of deformation of the plateau area is provided by the OKEAN and MAK-1 data. A detailed swath bathymetric map produced from the earlier *Akademik Nikolai Strakhov's* survey reveals a number of prominent ENE-WSW trending linear features within the plateau area, that generally step downwards towards the north and northwest. The northern and northwestern margins show the maximum evidence of faulting and break-up, while the southwestern, southeastern and northeastern margins, although faulted are less dramatically affected. Small elongate depressions are present between several of the ridges

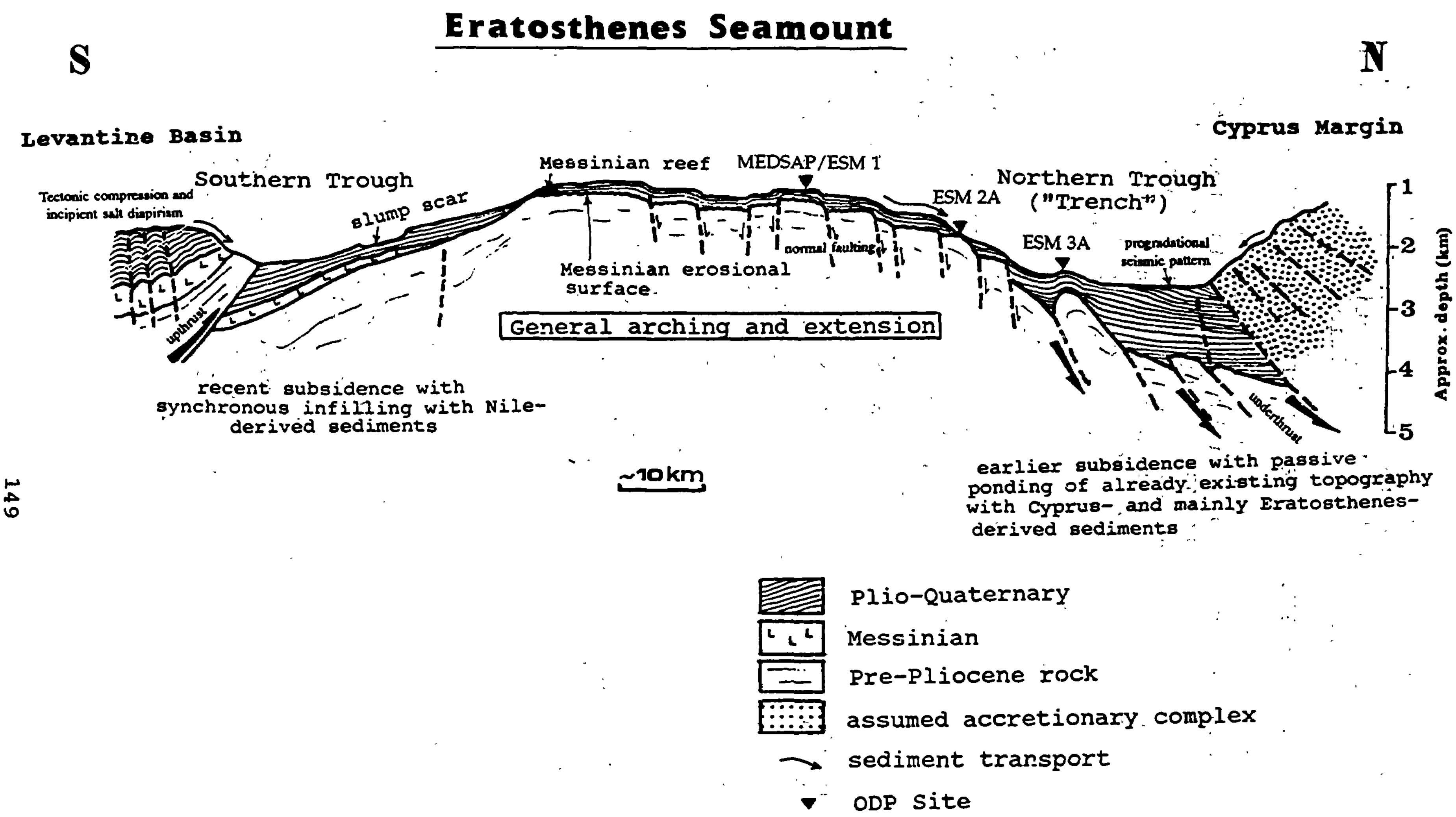

Fig. 82. General geological interpretation of the Eratosthenes Seamount shallow structure along seismic line PS-120

on the plateau. The OKEAN data confirm that these linear features are fault scarps, typically up to 500 m wide. The MAK-1 data further suggest that these faults have been active recently, with evidence of slumping and sediment redeposition.

ERATOSTHENES MARGINS: ACTIVE FAULTING AND BREAK-UP

The swath bathymetric map shows that Eratosthenes is roughly quadrilateral shaped, being bounded by very rectilinear fault scarps. Slopes are steepest and most irregular along the NW and NE margins, suggesting that the seamount could be foundering in this direction. The TTR-3 airgun data confirm that the edges of the seamount are indeed, fault scarps. The OKEAN sidescan records reveal that the faults are created by downward stepping fault blocks beneath the Plio-Quaternary succession. Most of the faults are parallel or subparallel to the adjacent margins of the seamount. However, locally along the SW margin N-S trending faults on the OKEAN records appear to terminate against SW-NE trending fractures. The OKEAN records also allow the trends of individual fault scarps to be determined, especially when combined with the swath bathymetry. The most dramatic fault scarps along the upper slopes of the northern seamount margin are estimated as being 110-120 m high and can be traced more than 2-3 km as individual segments, on the OKEAN and MAK-1 records. The MAK-1 records also show that the thin Plio-Quaternary sediments above the fault blocks are deformed into large-scale (hundreds of meters wavelength) upright folds. These could be explained, by one or a combination of, compression transmitted from the basement, buckling of soft sediments above the hanging wall of rotated fault block, or the effects of gravity sliding above a deeper-level decollement that was not imaged. The second explanation seems to be the most suitable. In other areas (e.g. east and west flanks) the Plio-Quaternary sediments are seen to be folded above small downward-stepping fault blocks. In this case, these folds are most likely to reflect soft-sediment deformation above the footwall of brittally deforming basement rocks.

EVIDENCE OF SEDIMENT INSTABILITY

Sediment instability is well-documented, particularly along the marginal fault scarps and on various parts the slope (Fig. 83). Sediment instability is most dramatically imaged on the north margin, where debris flows were cored (see below). Large-scale gravity movement is also imaged on the south margin with slumped units up to 5 km long on OKEAN record. The MAK-1 record of the faulted southern edge also reveals numerous small fault controlled conduits that serve to funnel soft sediments downwards onto the slope. Subcircular depressions in the seafloor near these locations could result from collapse, as lower sediment levels foundered downslope (see below). In addition, extensive sliding has taken place on the east flanks, associated with the development of gravity folds, locally trending NW-SE.

Fig. 83. Debris flows (arrows) on the northern Eratosthenes margin. (MAK - 1 line 21)

EVIDENCE OF UNDERTHRUSTING BENEATH THE CYPRUS MARGIN

The airgun profiles confirm earlier suggestions (e.g. Kempler and Ben-Avraham, 1987) that the Eratosthenes Seamount is in the process of being actively underthrust beneath the Cyprus margin to the north. This is important because in some earlier interpretation, the seamount has been inferred to be an old collisional structure, possibly inactive since the Miocene or earlier. Our new data clearly show that a thick Plio-Quaternary succession is being actively underthrust beneath Cyprus. The presence of confused reflectors in the overlying wedge, indicates that this area is highly deformed, and it is tentatively interpreted as a wedge of older sediments that has been uplifted and accreted (i.e. a subduction complex). Minor downslope gravity motion of sediments into the Cyprus trough is imaged; however, the bulk of the sedimentary fill is interpreted as turbidites, largely derived from the Eratosthenes Seamount to the south.

NORTH MARGIN: EVIDENCE OF A YOUNG DECOLLEMENT

Further important evidence of active underthrusting was found near the foot of the northern slope of the seamount. There, a small wedge of Eratosthenes-type basement is being actively thrust beneath the Cyprus trough. This ridge is shown to be laterally continuous for at least some kilometres on the OKEAN record. Also, the fact that this features is effective at ponding sediment implies that it is, indeed, a laterally extensive feature. The actual decollement plane can be traced downwards to an estimated depth of 1000 m beneath the small upthrust ridge. Viewed obliquely on the nearly E-W crossing seismic line, the decollement plane is seen to be markedly stepped, suggesting that lateral ramps may be present. The basement sliver is overlain by a deformed drape of Plio-Quaternary sediments (Fig. 84). Further information on this structure is provided by the MAK-1 narrow beam profiler and high resolution profiler. The sediments within the small basin behind the upthrust ridge are deformed by trains of upright folds, estimated at 400-500 m in wavelength and up to 10 m in amplitude. The folding is inferred to result from compression transmitted laterally as the sediments enter the trench. In addition, the basinal sediments near the contact with the upthrust ridge appear to be rotated upwards, which may have resulted from frictional drag during tectonic uplift. Small-scale folds are also present on the adjacent lower slope of the seamount. The MAK-1 record suggests that these could be either tectonic folds, similar to those in the small trough, or the results of large-scale sliding or creep along a decollement plane that was not imaged.

EVIDENCE OF UNDERTHRUSTING ALONG THE SOUTH MARGIN

One of the most striking discoveries from the TTR-3 seismic data is the presence of a discrete zone of underthrusting of the southern flank of Eratosthenes, beneath the more elevated Levantine Basin to the south. Previously, this was thought of as a high-angle fault zone, or possibly the site of a relict northwards-dipping subduction zone. However, the TTR-3 airgun seismic data clearly show that the Plio-Quaternary succession of the southern trough is being thrust beneath the Levantine Basin. The decollement plane was clearly imaged on the NS airgun seismic profile and this surface can also be seen on the NW-SE trending run (Fig. 85). The reflectors thicken southwards beneath the underthrusting zone, suggesting that this a very young basin undergoing extremely rapid subsidence. In support of this interpretation, sediments on the lower part of the southern flank of the seamount appear to be markedly slumped, leaving sediment starved slump scars on the higher reaches. Also, evidence of normal faulting is observed along the southern flank. The over-riding Levantine Basin is strongly deformed by what appears to be a combination of compression and salt diapirism. Notably, serpentinite was dredged by the R/V *Akademik Nikolai Strakhov* from near the base of the Levantine Basin slope. This could be oceanic layer three material that has been upthrust and/or diapirically intruded from beneath the Levantine Basin. Such an origin would, in turn, suggest that Eratosthenes was originally separated from the North African continental margin, at least by stretched continental crust, with ultramafics at relatively shallow levels.

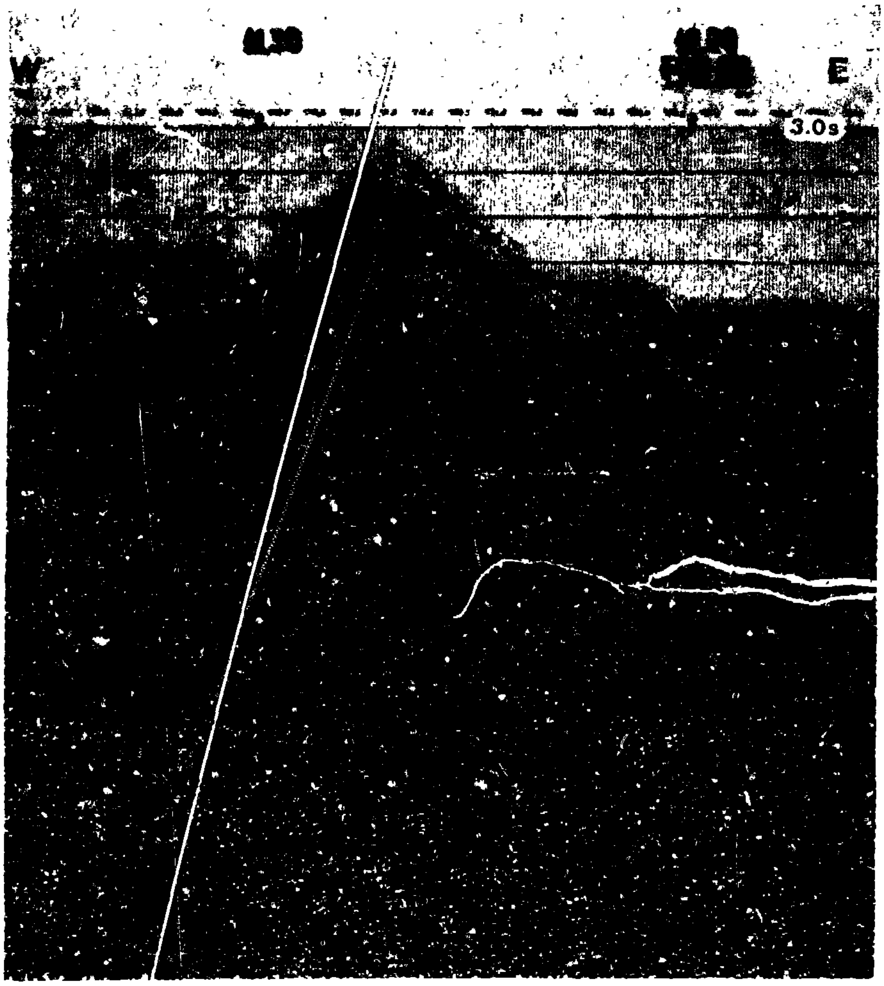

Fig. 84. The stepped decollement plane (arrows) on the northern Eratosthenes slope viewed obliquely on seismic line PS-127

THE GRAVITY ANOMALY EXPLAINED?

One surprising feature of Eratosthenes, especially in view of the marked positive magnetic anomaly (see Section 4.1) is the almost entirely topographic character of gravity anomalies, explained, as noted in the introduction, either by Eratosthenes being supported by the crust and/or by the sub-crustal lithosphere, without any dense root. This can be explained if Eratosthenes is under active compression from both the north and south, holding it up, out of isostatic equilibrium. This compression affects the entire crustal block and leads to the general arching of the Eratosthenes, that is why the upper levels of the Seamount are under tensional stress reflected in a normal faulting.

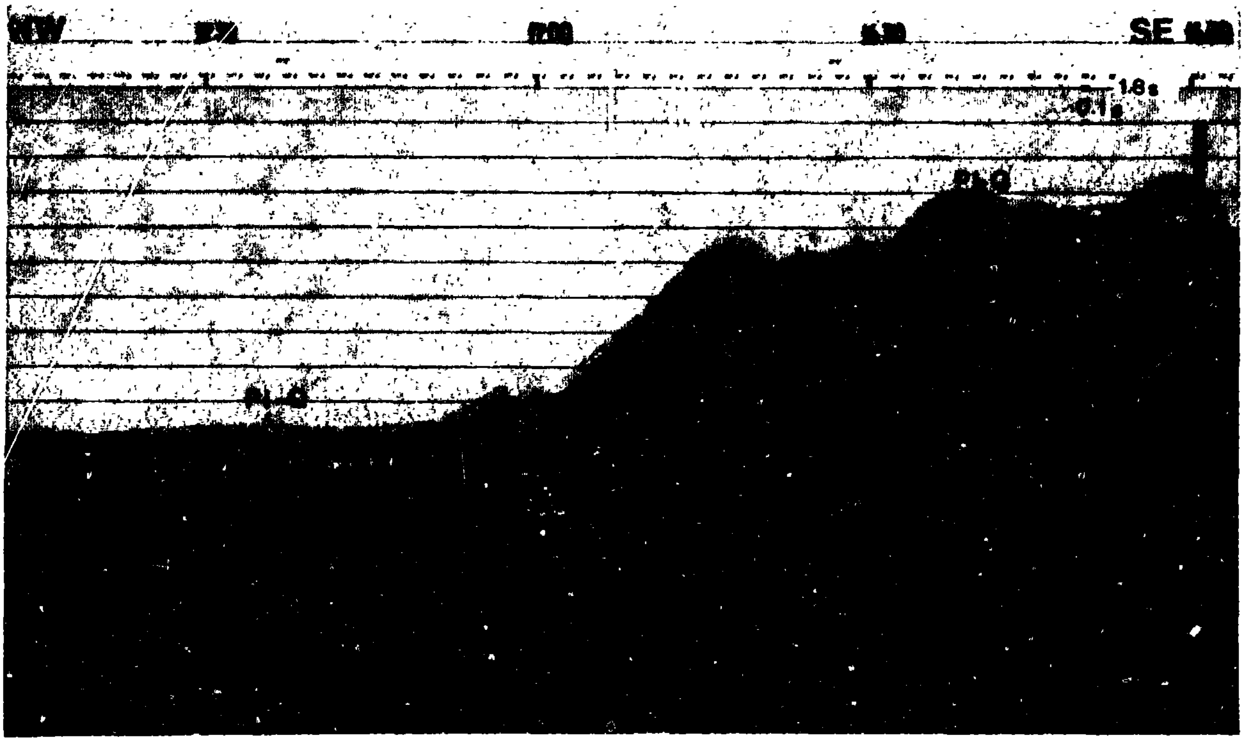

Fig. 85. The decollement plane (arrow) on the southern Eratosthenes slope. The thicknesses of the Plio-Quaternary sediments are the same in the trough and on the overriding edge of the Levantine plate (LP), suggesting a recent formation of the trough. (Seismic line PS-121)

ENIGMATIC CIRCULAR STRUCTURES ON THE PLATEAU AREA

One surprising and enigmatic feature of the surface sediments of the part of the plateau area is the presence of zones of circular depressions, up to hundreds of metres across, that were initially observed on the OKEAN records. In some cases these appear to be concentrated in the vicinity of fault scarps. The narrow-beam MAK-1 records further reveal that the vast majority of these features are depressions, that can be seen in various stages of infilling with recent sediment - the margins of young examples are sharply defined, whereas inferred older examples are seen only as vague circular outlines. At least, one of these features, however, appears to be a raised diapiric feature. Alternative origins were much debated by the shipboard party and include suggestions that these features reflect: i) sediment gravity collapse above a karstic Messinian surface; ii) collapse above diapiric intrusions of salt or mud; iii) collapse structures related to active faulting at depth; iv) the results of gas or fluid escape. Options i) and iii) seem implausible, as it is hard to envisage how depressions could occur in soft sediment more than 100 m above sites of possible solution collapse, or faulting. Large-scale salt or mud diapirism is also unlikely in view of the thinness of the Plio-Quaternary succession and the absence of seismically expressed Messinian salt. Gas or fluid escape remains a viable possibility. Such hydrocarbons would be deeply sourced and would be in the process of migrating up active faults. If the Eratosthenes was rifted from Gondwana in the Early Mesozoic, then the possible hydrocarbon source rocks could be similar those found in the Tauride units of southern Turkey, which, similarly, are inferred as having been rifted from Gondwana. For example, in the Bey-Daglari, in southwest Turkey possible source rocks are the Carboniferous coals and minor black shales deposited during rifting of Neotethys.

NATURE OF PLIO-QUATERNARY SEDIMENTATION

The cores taken lie approximately on two transects, one nearly N-S, the other E-W (see Fig. 78) and these reveal an interesting pattern of sedimentation, that may, in part, relate to the most recent tectonic history of the Eratosthenes. Compositionally, the sediments are mainly nannofossil muds, ranging from paler more nannofossil-rich, to darker more mud-rich facies. Terrigenous silt of presumably wind-blown origin is ubiquitous. Sapropels, or possible remnants of sapropels, were noted in all the plateau and flank cores, being absent apparently only from the site on the fault scarp cored on the eastern margin of the seamount. The presence of distinctive warm or cool water planktonic and benthic foraminifera combined with evidence from nannofossils allows a number of sapropels, certainly as old as S-6 and possibly S-8 to be recognized and a number of sapropels can be correlated between cores (see Figs. 79 and 80). A thin layer of mainly colourless, acidic tephra is easily recognizable throughout and this could be correlated with ash derived from the eastern extension of the Hellenic arc, or possibly from the Campanian province of the Naples area of southern Italy (Cramp et al., 1988).

Of particular note are two units of graded silty mud, recovered from near the crest of the small upthrust ridge near the base of the slope at the northern margin of the seamount; these are interpreted as mud turbidites. In addition, the former presence of an area of condensed sedimentation is indicated by a fragment of calcareous hardground, including relict (Quaternary) planktonic foraminifera. Also, of note several small (1 cm sized) manganese nodules were recovered just below the sediment surface at the base of a fault scarp on the east flank of the seamount. This manganese "marker horizon" (Marker Bed) was not seen elsewhere and may reflect upward mobility of Mn mobilized in association with organic matter diagenesis in the sapropels. The soluble manganese was then precipitation in an overlying more oxidizing environment, at, or near, the seafloor. In general, apart from the dark colour of the strongly reducing sapropels, the many subtle colour variations seen in the cores, are probably entirely the result of chemical mobility during diagenesis.

INFERENCES FROM SEDIMENTATION RATES

Further clues as to the history of sedimentation come from calculations of sedimentation rate. The crestal sites show sedimentation rates typical of the Eastern Mediterranean Basin (2-3 cm/kyrs). The relatively low rates on the crestal sites reflect deposition on an area raised well above the level of gravity input from the Nile Cone or from Cyprus. In addition, the crestal area were probably affected by considerable current, with reworking and net loss of material to the flank areas. Higher sedimentation rates were recorded on all but the most crestal site, as would be anticipated if resedimentation has taken place by some combination of slumping, turbidity currents and/or dilute gravity flows. Two features are worthy of further comment. First, at all sites other than the crestal one, the sedimentation rates markedly increase during the interval between the Y-5 tephra layer and the *E. huxleyi* Acme boundary, estimated at 53 kyrs and then decreases after S-4, estimated at 100 kyrs. These horizons do not, of course, necessarily correspond to the actual time when sedimentation rates changed. However, it appears that sedimentation rates did increase approximately during this time interval and then decreased, over all but the crestal site. This increase is particularly marked at the eastern outer flank site, suggesting that fine-grained sediments were deposited there by dilute gravity flows well away from the seamount. In the absence of a plausible explanation in terms of climatic change, or current activity, one marked possibility is that at this time the entire seamount underwent a pulse of tectonic activity. Such activity could have triggered sliding, slumping, and resedimentation of silty muds to form low-density turbidites and dilute gravity flows.

The second point of interest is the sedimentation rates calculated for the core from the crest of the small ridge near the base of slope of the northern margin of the seamount. Somewhat surprisingly, the estimated sedimentation rate of the mud turbidites is exceeded by that of the intervening more pelagic mudstones. Assuming the seafloor topography was essentially as today, one explanation would be that most of the volume of the mud turbidites by-passed the depositional site, while weaker turbidity currents (that had already deposited any coarser fraction in the small basin to the north), then wafted fines onto the ridge crest. This assumption is supported by the progradational seismic pattern seen in the Cyprus 'trench", implying that the principal sediment supply was from the Eratosthenes, at least for the upper part of the infilling sedimentary sequence. An alternative is that the site underwent pulses of uplift, such that turbidites accumulated when the relief of the seafloor adjacent to Eratosthenes was low, followed by a pulse of uplift, which for a time raised the seafloor above the level of turbiditic deposition. Turbidites were only able to prograde over the ridge again after the intervening small basin had become full again and sediment overspilled onto the ridge.

HISTORY OF ERATOSTHENES

The TTR-3 data does not by itself resolve the long-standing question as to the origin of Eratosthenes. Suggestions have ranged from an oceanic plateau, a relict island arc, or a continental crustal fragment. Our airgun seismic profiles show that the M-Reflector can be traced up onto the upper flanks the seamount, pinching before the plateau. This strongly suggests that Messinian deposits, notably salt, are effectively absent from the seamount plateau area. We note that the Cretaceous/Miocene limestone dredged during the cruise of the R/V *Akademik Nikolai Strakhov* came from near the top of the southern scarp of the seamount, where the Plio-Quaternary is effectively absent. This, in turn suggests that Mesozoic carbonates could be present at shallow depth below the entire plateau area. The source of the granite dredged from lower on the southern slope remains more enigmatic.

We have, however, obtained sufficient new evidence to infer with some confidence that the Eratosthenes is in the process of actively being underthrust both northwards and southwards under opposing margins. As a result, the seamount is actively breaking up by a combination of faulting of the interior and catastrophic downfaulting of the NW flank. The southern margins are also disintegrating on a variety of scales.

The seismic refraction evidence has previously been interpreted as suggesting that the crust may thin significantly from east to west across Eratosthenes (Woodside, 1977). It is therefore possible that Eratosthenes may be being pinned by collision along its NE margin, and that it is now undergoing tectonic escape towards the northwest, into an area of thinned continental crust or a remnant of Mesozoic oceanic crust. It is also possible that the seamount is undergoing clockwise rotation about a vertical axis as it break-up and subsides. Some large basement faults cutting the plateau area appear to pre-date the Plio-Quaternary sediment cover, suggesting that initial collision could date from the Late Miocene, or earlier. In general, the record of collision and uplift can be correlated with uplift of Cyprus (e.g. Poole and Robertson, 1991).

One of the most important findings of the TTR-3 cruise are that the Eratosthenes seamount has only a thin Plio-Quaternary sediment cover over a nearly flat, but faulted Late Miocene? erosion surface and that it is undergoing active break-up and underthrusting, both northwards and southwards, under the opposing Cyprus and Levantine margins. Finally, from the standpoint of continental geologists, Eratosthenes can be seen as crustal fragment undergoing active destruction within an incipient continental collision zone. Since both its flanks are being underthrust, it seems likely that its ultimate fate will be complete subduction, leaving little or no trace for the field geologist to decipher!

PREVIOUSLY PROPOSED ODP SITES HAVE CHANGED

One of the major results of the TTR-3 cruise was that it was found that none of the originally proposed ESM Sites was, in fact, ideal and these have been revised as follows:

ESM 1 was located on the crest of the Seamount (in the north). This location is now completely surveyed and sampled but the new TTR-3 airgun seismic data now show that the basement is present at an estimated maximum depth of 150-250 m throughout the crestal areas. Also, the Plio-Quaternary sediments form a relatively uniform drape over crestal area. It should thus be possible to reach basement and achieve the ESM 1 objectives at any suitable crestal site. This offers the opportunity to combine the tectonic objectives of this proposal with the palaeoenvironmental objectives of the MEDSAP proposal at a single site. So we have recommended that either of the alternative MEDSAP sites on the summit could serve as an alternate for Site ESM 1.

ESM 2 was located on the upper slope of the northern seamount flank (Fig. 82), where, based on previously available seismic data, it was inferred that the Plio-Quaternary succession might be thin, or absent allowing easy basement penetration. However, the greatly improved resolution of the TTR-3 seismic data does not reveal any reduced Plio-Quaternary sediment thickness and thus the rationale for drilling ESM 2 there entirely disappears. On the other hand, the new seismic data did reveal another area, further north, on the upper parts of the lower slope above the northern trough (Fig. 82), where the Plio-Quaternary is indeed thin or absent. A fragment of calcareous hardground was retrieved by coring there. This area is proposed for as a new site for the proposal: ESM 2A.

ESM 3 was located near the southern margin of the northern trough. The original objective was to sample the sediments of the "collisional trough", in an effort to identify their provenance and also, possibly, to shed light on break-up and subsidence of Eratosthenes. The data from the high resolution deep-towed profiler, however, now shows that this area is underlain by an effectively undeformed Plio-Quaternary succession of probable turbidites, such that drilling in this area is unlikely to shed light on objectives mentioned above. On the other hand, and, as noted earlier, evidence of active tectonics was imaged closer to the foot of the northern slope, where a sliver of Eratosthenes basement appears to be being underthrust, associated with uplift of the hanging-wall to form a raised bathymetric feature (Fig. 82). This is proposed as another new site for the tectonically-orientated proposal: site ESM 3A.

ESM 4 was located on the southern shoulder of the Cyprus margin, with the objective being to retrieve further evidence of break-up and collision in this area. However, the TTR-3 seismic data did not reveal this as an area of active tectonics likely to shed light on the structural evolution of Eratosthenes and no further site-survey data were collected from this area. ESM 4 is therefore dropped from the revised ODP proposal.

5. ZOOPLANKTON STUDY

A.C. Pierrot-Bults

INTRODUCTION

Zooplankton study was an accompanying investigation undertaken in addition to the main geological work. The study was carried out to compare populations of chaetognath species from the Black Sea and the eastern Mediterranean with populations of the same species from other parts of their range.

Sagitta setosa Müller, 1847 has a distributional range from the Baltic to the North Sea and Channel, the Mediterranean and the Black Sea, though the last populations were described as a different species *Sagitta euxina* by Moltschanoff (1909). Morphological differences between populations of the North Sea and the estuarine waters (Easterscheldt) of southern waters in the Netherlands were found by Biersteker and van der Spoel (1966) and described as *Sagitta batava*. Pierrot-Bults (1976) did not recognize different species but proposed the hypothesis that *S. setosa* is a variable species. The Baltic and North Sea populations do not show a gap in distribution. Neither do the Mediterranean and Black Sea populations. The disjunction in distribution is between the North Sea and the Mediterranean. Looking into morphological, enzymatic, and molecular variation one would expect larger differentiation between the two parts of the disjunctive distribution than within the two areas.

To study these differences *S. setosa* from the Black Sea will be compared for the variation within one area of distribution and these results will be compared with the variation in the Baltic-North Sea distribution area. The samples of *S. enffata* and *S minima* from the Eastern Mediterranean (Aegean Sea) will be compared with samples from the North Atlantic.

METHODS

Table VIII shows the date, position, time, and wire out in m of the stations made. Also the groups of plankton organisms in the hauls are mentioned.

Sampling was carried out with a ringnet with a diameter of 50 cm and a mesh size of 600 µm. The tows were taken with a rough calculation of depth by meters of wire out and estimating the angle of the cable. The haul started out with the mentioned wire out (Table VIII) and after 10-15 minutes of towing the wire was hauled 10 m in, this was repeated twice.

Immediately after coming on deck the sample was put in sea water. Because of the shortage of preserving fluid only selected specimens were taken out and put in formalin/sea water 4%. The sample from station 4 was preserved totally (except for the large Ctenophora and Medusae) half in formalin 4%, half in alcohol 70%. Part of the specimens of *Sagitta setosa* were frozen in a liquid nitrogen dryshipper.

RESULTS

The plankton groups present in the samples are shown in Table VIII. The most abundant group in the Black Sea samples at stations 0-3 were small Ctenophora. Furthermore the samples contained bigger ctenophores, small Medusae, (because fortunately the net was too small to collect the big ones to be seen in the ocean), Copepoda, Chaetoghatha (*Sagitta setosa*,) and at station 4, which was closer to the surface than the others Dinoflagellata and other Protista were the most abundant.

The Aegean Sea samples were much richer than those from the Black Sea. In the evening sample all groups were much more abundant than in the sample taken at noon. Most abundant were the copepods, second in abundance were chaetognaths. The most abundant chaetognath species in both samples was *Sagitta enflata*, another species found was *S. minima*.

DISCUSSION

The middle of the Black Sea is about 2200 m deep. According to Eronat (pers. commun., 1993), the thermo- and pycnocline is at about 20 m. The salinity is only about 17-19‰, and the halocline is slightly deeper than 20 m. The most prominent feature, however, is the oxygen deficiency starting at about 50-60 m. In the shelf areas the oxygen deficiency is much deeper at about 100-120 m. The northwest shelf area and the shelf area north of the Turkish coast are the most productive areas as shown by remote sensing pictures of the CZCS in 1986. Total zooplankton abundance is very poor in the central Black Sea. Also a small ringnet is not the most efficient net to catch active predators like Chaetognatha. *Sagitta setosa* is a neritic species and the only one recorded previously from the Black Sea (as *S. euxina)*. The samples from the Aegean Sea were taken in an area with a total depth of about 600 m. Salinity in the Aegean Sea is at least twice as high as in the Black Sea, there is no oxygen deficiency, and life is possible throughout the watercolumn. The samples here were much richer, especially the sample taken in the evening. Many zooplankton groups perform diurnal vertical migration and at noon the populations are expected to occur deeper in the water column. At least two species of chaetognaths were present, *Sagitta enflata* and *S. minima,* both wide spread tropical/subtropical species from the epipelagic, commonly occurring in the Mediterranean.

Table VIII

Zooplankton stations

Black Sea

date	position	station	time	wire (m)	zooplankton
11/6	43°44'N/33°29'E	0	14^{00}h	50	Ctenophora Medusae
12/6	43°43'N/33°28'E	1	21^{00}h	50	Ctenophora Medusae Copepoda Chaetognatha (*S. setosa*)
14/6	43°31'N/33°07'E	2	19^{00}h	60	Ctenophora Medusae Copepoda
16/6	43°31'N/33°03'E	3	20^{00}h	50	Ctenophora Medusae Copepoda Chaetognatha (*S. setosa*)
18/6	43°43'N/33°28'E	4	08^{00}h	40	Ctenophora Medusae Copepoda Dinoflagellata

Aegean Sea

date	position	station	time	wire (m)	zooplankton
20/6	39°19'N/24°46'E	5	20^{15}h	100	Copepoda Medusae Pteropoda Siphonophora Ostracoda Chaetognatha Polychaeta
21/6	37°59'N/25°40'E	6	12^{00}h	150	Copepoda Siphonophora Salpidae Medusae Pteropoda Chaetognatha fish larvae

6. UNDERWAY BOTTOM SAMPLING IN THE AEGEAN SEA

6.1. QUATERNARY ORGANIC-RICH SEDIMENTS IN THE EASTERN MEDITERRANEAN: AEGEAN SEA LINK WITH BLACK SEA

R. Kidd

The sedimentary record of the Mediterranean Sea over at least the last 10 Myrs is punctuated by layers with elevated organic carbon content known as sapropels (Kidd et al., 1978b; Cramp et al., 1988). These beds are interbedded with organic-lean hemipelagic carbonate sediments and appear to be a common feature of the paleoceanographic development of enclosed marginal marine basins (e.g. the Japan Sea; Follmi et al., 1990).

In the late Quaternary, where high stratigraphic resolution is available, the sapropels appear at estimated periodicities of 20 kyrs to 140 kyrs, but their links to climate and sea-level change are still ill-defined. As well as their global oceanographic significance as sinks of organic carbon and as sites of sulphide and trace metal enrichment, sapropels form in convergent margin settings and become significant features as marker beds and potential hydrocarbon sources in Tethyan-Himalayan sedimentary sequences.

Various models have been proposed to explain sapropel occurrence, most based on piston core studies in the Eastern Mediterranean spanning the Pleistocene glacial stages. Global changes in climate and oceanography have apparently been amplified in these restricted basins causing relatively swift changes in environmental conditions. The majority of models invoke the periodic development of a low salinity layer of glacial meltwater which interrupts the surface to deep water circulation that normally oxygenates the basins (Olausson, 1961; Thunnell et al., 1977; Mangini and Schlosser, 1986; Cramp et al., 1988). These concepts of basinwide anoxia have been hotly disputed over the years (Calvert, 1983; Ryan and Cita, 1977; van Hinte et al., 1987). More recently attention has turned to concepts involving dramatic increases in surface productivity. Rapidly changing hydrological conditions and nutrient input might be capable of producing a nutrient-trap system and the required order of magnitude increase in Mediterranean surface productivity (Sarmiento et al., 1988; Rohling and Gieskes, 1989).

International debate has been focussed in the past two years by the proposal to drill a transect of Ocean Drilling Program (ODP) sites through the Mediterranean to recover APC cores from sapropel sequences through to the late Miocene (Zahn et al. and Emeiss et al., pers. comm., 1993)). Critics of the plan have emphasized that there are, as yet, insufficient geochemically well-documented transects of cores through the late Quaternary sapropels to define the key parameters that can be looked for in diagenetically altered sediments. The older drilled sapropels are indeed known to be significantly different in character (Kidd et al., 1978b) which could reflect different modes of formation or different diagenetic histories. More cores need to come available that can be sampled for geochemical study, in particular of ephemeral parameters such as pore water chemistry. Also a "pelagic" setting needs to be well-defined for the cores by precise geophysical surveys to avoid "unusual" occurrences of sapropelic layers that are redeposited as turbidites (e.g. Cretan Basin; Kidd et al., 1978b) or result from salt brine formation (e.g. Mediterranean Ridge; Cita et al., 1986).

An international effort is now being mounted to use "ships of opportunity" to gather the necessary cores. Sites are being targeted related to key paleoceanographic "gateways" and sources of nutrient and freshwater input including the Sicily Channel, the Nile River and the Black Sea. The Cardiff Marine Geosciences Group sought funding from the British funding council NERC to conduct coring operations aboard R/V *Gelendzhik* during the second leg of the TTR-3 cruise. They planned to recover one of these core transects, that between the Eastern Mediterranean and the Black Sea, and to conduct shipboard sampling for geochemical and other sedimentological and stratigraphic studies.

The specific objectives of the Cardiff group at sea were: (1) to recover Kasten, box and gravity cores from a series of locations that will provide a transect between the Black Sea through the Aegean to the Mediterranean Ridge; (2) to open and fully describe the cored sequences for lithology and stratigraphy aboard ship and sub-sample under controlled conditions for geochemical studies. After transport of the cores to Cardiff they planned to carry out scanning for X-radiography, magnetics and P-wave velocities and to carry out pilot geochemical analyses of pore water chemistry and sulphide mineralogy. These latter studies are to identify geochemical indicators that would survive diagenesis and could define which of the sapropels relate to increased surface productivity versus those suggesting seafloor anoxia. The intention is to define a longer-term study at Cardiff of the recovered materials that would investigate further the effects of Black Sea-Aegean Sea circulation changes on the Eastern Mediterranean.

Key sites for the Cardiff Group's sapropels transect included three during transit through the Aegean Sea, and one in the Sea of Marmara. Further core sites were to be selected within the Mediterranean Ridge and Eratosthenes Seamount study areas where the cruise's primary investigations were to take place. The cores were to be opened, described and sub-sampled aboard ship to ensure that ephemeral properties were not destroyed in storage and transit to Cardiff. Some sampling would be under a nitrogen atmosphere to preserve pore water chemistry. Initial shipboard results were to be made available, along with the new geophysical survey data collected for JOIDES as part of the international package in support of new ODP drill sites.

6.2. LITHOLOGY OF THE AEGEAN SEA CORES

R. Kidd, G. O'Sullivan, S. Wakefielf, and L. McMurray

R/V *Gelendzhik* approached the first of the Aegean Sites selected for the Cardiff Group's Eastern Mediterranean to Black Sea sapropels transect (CDFSAP 1) at 06^{30} on the 14^{th} of July. The echosounder profile revealed the site to be on a terrace of a very steep sided ridge trending northwards from the island of Saria. Kasten core 112K (Figs. 86 and 87) had poor penetration recovering only 0.7 m of stiff clay below a calcareous hardground (36°04.0'N/27°11.08'E; water depth 978 m). We decided to try downslope for better penetration near this rim of the Cretan Arc. A move northwestwards put us on a northern slope leading down to a deep trough and west of the steep 1000 m high fault scarp of the ridge that we had already sampled. In this setting we could expect downslope resedimentation but at least we might get some penetration and the gravity corer might recover sapropels. Box (36°05'N/27°04.6'E; water depth 2491 m) was almost full (56 cm) and recovered sandy layers interbedded with marls. Sedimentation rates were clearly too great to expect the S-1 sapropel. Nearby gravity core 114G (36°04.8'N/27°04.42'E; water depth 2489 m) had limited penetration (~1.8 m) but recovered a sequence of thin sandy turbidites that all appeared to be derived from the ridge to the east. No sapropels were found but a dark layer occurs at the top of the core. A feature of this core was that it had clearly sampled twice due to the limited penetration and heave of the ship in rapidly deteriorating sea conditions. Below 0.8 m the sequence is exactly repeated.

By the time we reached our second Aegean site (CDFSAP-2) on a plateau northeast of Andros at $\sim 23^{00}$ on the 14^{th} of July the sea conditions were too hazardous to handle the Kasten corer and we only attempted operations with the gravity corer. In core 115G (37°49.9'N/25°35.1'E; water depth 586 m) was impressively long recovering 5 m of stiff calcareous muds that contain one 25 cm thick dark layer that may be an expanded form of the S-1 sapropel. Reworked brachiopods and bivalves were found within the stiff calcareous muds, as well as a thick tephra at 0.9 m and another patch of a different tephra at 3.6 m depth.

We moved on to our third Aegean coring site (CDFSAP-3) on a broad high northeast of Skiros, arriving at 06^{30} on the 15^{th} of July. The storm had blown over and the sea was flat calm allowing us to sample a full suite of cores. Gravity core 116G was 5.1 m long consisting almost entirely of homogeneous grey calcareous mud. This was repeated in the Kasten core 117K and the box core 118B. At the top of each core was a pteropod and foraminifera rich sediment-water interface overlying a dark layer similar to that at the previous site. At around 2.5 m depth in the gravity and Kasten cores occurred a dark green layer that may represent an expanded S-1 sapropel. Interspersed in the homogeneous mud are bivalves and one interesting dark patch containing grass (!). Although the tentative identifications of the S-1 sapropel and the tephras must be checked, we consider that the sediment sequence at this site (39°17'N/24°47'E; water depth 558 to 565 m) may possibly represent the "homogenite event" that was linked to the Santorini eruption and its postulated tsunami by Kastens and Cita (1981). Sedigraph size analysis, P-wave and magnetic susceptibility logging, X-radiography and mineralogical analyses will be carried out at Cardiff to investigate the homogeneous muds and we hope to obtain ages for the bivalve and plant material that we found.

Fig. 86. Location of sampling stations in the Aegean Sea. (Bathymetry is from IOC-UNESCO, 1981)

AEGEAN SEA

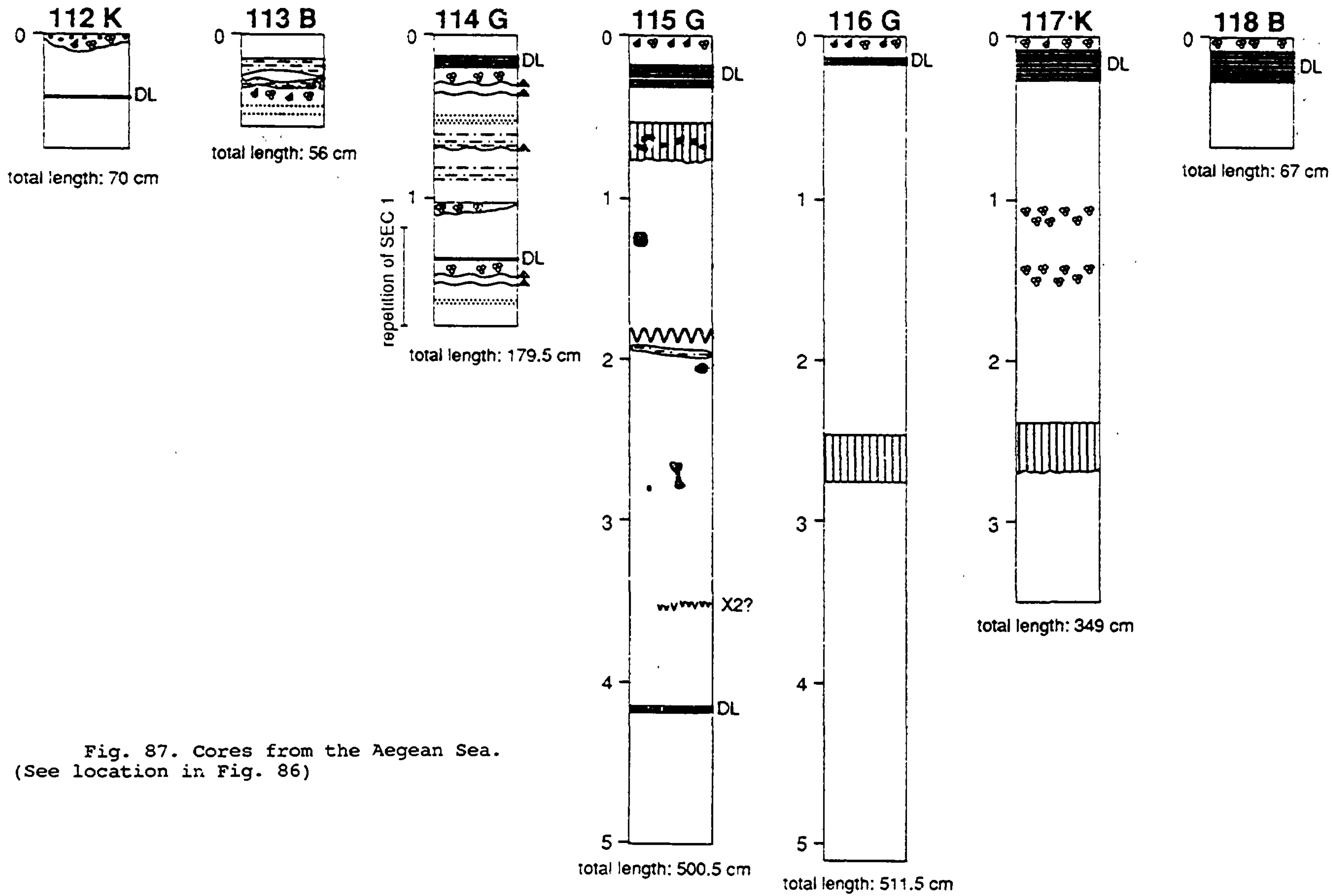

Fig. 87. Cores from the Aegean Sea.
(See location in Fig. 86)

The last site in the Aegean-Black Sea transect, CDFSAP-4 in the Sea of Marmara, was unfortunately removed from the programme because permission to sample could not be obtained from the Turkish authorities.

GENERAL INTERPRETATION

Although the careful sampling of the Mediterranean Sapropels for geochemical studies by the Cardiff Group was a feature of all of the second leg, the priority objectives in the Aegean Sea were not fully met. One of the four sites had to be removed because we did not receive permission to sample in the Sea of Marmara (CDFSAP-4). The second site, CDFSAP-2, was abbreviated because of storm conditions and the first site became split between sampling on a high and coring in a basinal setting. Thus, although not all of the sites were in our preferred pelagic setting, we can still make some general observations on the Aegean Sea transect:

(1) High sedimentation rates appear to restrict the formation of sapropels at the three sites. Nowhere do we see the thick and very black sapropels that were characteristic of the Mediterranean Ridge and Eratosthenes Seamount cores but we do have what appears to be a sapropelic layer, replete with pyrite, in cores from the mid-Aegean region (115G, 116G/117K/118B). This may be the equivalent of an expanded S-1 sapropel. Sequences at the southernmost core locations contain no evidence of the S-1 but this is due to their coming from either a hardground or a basinal turbidite setting.

(2) Cores from the mid-Aegean Sea locations may contain a record of the Santorini "tsunami" event that has been recorded as "homogenite" in cores westwards to the Ionian Sea and eastward to the Levantine basin.

Post-cruise analyses will determine the usefulness of this coring transect in terms of our original sapropel objectives but it appears that we may well have by then a very interesting story to tell about historical, rather than simply paleoceanographic, events in the Aegean region.

REFERENCES

Anderson, R.F., Fleischer, M.Q., and LeHuray, A.P., 1989. Concentration, oxidation state, and particulate flux in the Black Sea. - *Geochim. Cosmochim. Acta,* **53:** 2215-2224.

Andrusov, N.I., 1890. Preliminary account of participation in the Black Sea deepwater expedition of 1890. - *Izv. Russk. Geogr. ob-va.,* **26:** 398-409 (in Russian).

Aspila, K.I., Agemain, H., and Chau, A.S.Y., 1976. A semi-automated method for the determination of inorganic, organic and total phosphate in sediments. - *Analyst,* **101:** 187-197.

Belderson, R.H., Kenyon, N.H., and Stride, A.H., 1970. 10-km wide views of the Mediterranean deep sea floor. - *Deep Sea Res.,* **17:** 267-270.

Belderson, R.H., Kenyon, N.H., Stride, A.H., and Stubbs, A.R., 1972. Sonographs of the Sea Floor. A Picture Atlas. Amsterdam, Elsevier, 185 p.

Belderson, R.H., Kenyon, N.H., and Stride, A.H., 1978. Local submarine salt-karst formation on the Hellenic Outer Ridge, Eastern Mediterranean, - *Geology,* **6:** 716-720.

Ben-Avraham, Z., Shoham, Y., and Ginzburg, A., 1976. Magnetic anomalies in the eastern Mediterrranean and the tectonic setting of Eratosthenes seamount. - *Geophys. Journ. Royal Astron. Soc.,* **45:** 105-123.

Biersteker, R.H. and Van der Spoel, S., 1966. Sagitta batava n. sp. from the Scheldt estuary, The Netherlands (Chaetognatha).- *Beaufortia,* 14, **167:** 61-69.

Boccaletti, M., Cassinis, R., Dainelli, P., Marino, C.M., Tibaldi, A., and Zanchi, A., 1988. Landsat features in the Black Sea area. - *Boll. Geogis. Teor. Appl. Monograph on the Black Sea,* XXX, **117-118:** 17-37.

Cagatay, M.N., Gedik, A., and Saltoglu, T., 1990. Geochemistry of uranium in the Late Pleistocene-Holocene sediments from the southern part of the Black Sea basin. - *Chem. Geol.,* **82:** 129-144.

Calvert, S.E., 1976. The mineralogy and geochemistry of near shore sediments. In: Riley, J.P. and Chester, R. (eds.). *Chemical Oceanography,* 6, London, Academic Press, 187-280.

Calvert, S.E., 1983. Geochemistry of Pleistocene sapropels and associated sediments from the Eastern Mediterranean. - *Oceanol. Acta,* **6:** 255-267.

Calvert, S.E., 1990. Geochemistry and origin of the Holocene sapropel in the Black Sea. - In: Ittekot, V., Kempe, S., Michealis, W., and Spitzy, A. (eds.). *Facets of modern biogeochemistry,* Berlin, Spriger-Verlang, 326-352.

Calvert, S.E. and Fontugne, M.R., 1987. Stable carbon isotopic evidence for the marine origin of the organic matter in the Holocene Black Sea sapropel. - *Chem. Geol. (Isotope Geoscience),* **66:** 315-322.

Camerlenghi, A., Cita, M.B., Hieke, W., and Ricchiuto, T., 1992. Geological evidence for mud diapirism on the Mediterranean Ridge accretionary complex. - *Earth Planet. Sci. Lett.,* **109:** 493-504.

Cita, M.B., Aghib, F.S., Arosio, S., Folco, E., Sarto L., Erba E., and Rizzi, A., 1989a. Bacterial colonies and manganese micronodules related to fluid escape on the crest of the

Mediterranean Ridge. - *Riv. It. Paleont.*, 95, **3**: 315-336.

Cita, M.B. and Camerlenghi, A., 1990. The Mediterranean Ridge as an accretionary prism in collision context. - *Mem. Soc. Geol. It.*, **45**: 463-480.

Cita, M.B., Camerlenghi, A., and Corselli, C. (eds.), 1989b. Anoxic basins of the Eastern Mediterranean. - *La Ricerca Scientifica ed Educacione Permanente*, Suppl. **72**, Milano, 104 pp.

Cita, M.B., Camerlenghi, A., Erba, E., McCoy, F.M., Castradori, D., Cazzani, A., Guasti, G., Giambastiani, M., Lucchi, R., Nolli, V., Pezzi, G., Redaelli, M., Rizzi, E., Torricelli, S., and Violanti, D., 1989c. Discovery of mud diapirism in the Mediterranean Ridge. A preliminary report. - *Boll. Soc. Geol. It.*, **108**: 537-543.

Cita, M.B., Fornaciari, M., Camerlenghi, A., Corselli, C., Erba, E., McCoy, F., and Vezzoli, L., 1986. Anoxic basins of the Eastern Mediterranean: New evidence from the Bacino Bannock area. - *Mem. Soc. Geol. It.*, **36**: 131-144.

Cramp, A., Collins, M.B. and West, R., 1988. Late Pleistocene-Holocene sedimentation in the northwest Aegean Sea: A paleoclimatic paleoceanographic reconstruction. - *Paleogeog., Paleoclimat., Paleoecol.*, **68**: 61-77.

Cusin, M., Staffini, F., Vaccari, A., Cita, M.B., Camerlenghi, A., and Tomadin, C., 1992. Sedimentology, texture and composition of the mud diapirs and mud volcanoes of the Mediterranean Ridge. - *XXXIIIrd Congr. CIESM*, Abstracts: 129

Degens, E.T. and Ross, D.A., 1972. Chronology of the Black Sea over the last 25 000 years. - *Chem. Geol.*, **10**, 1-16.

Dewey, J.F., Pitman, W.C., Ryan, W.B.F., and Bonin, J., 1973. Plate tectonics and the evolution of the Alpine system. - *Geol. Soc. Amer. Bull.*, **84**: 3137-3180.

Eaton, S. and Robertson, A.H.F., 1993. Tectonic and sedimentary evolution of the Miocene Pakhna basin of Southern Cyprus. - *Sedim. Geol.*, **86**: 273-296.

Finetti, I., 1982. Structure, stratigraphy and evolution of Central Mediterranean. - *Boll. Geof. Teor. Appl.*, 24, **96**: 274-315.

Finetti, I., Bricchi, G., Den Ben, A., Pipan, M., and Huan, Z., 1988. Geophysical study of the Black Sea. - *Boll. Geofis. Teor. Appl. Monograph on the Black Sea*, XXX, **117-118**: 197-324.

Follmi, K. Cramp, A., et al., 1990. Paleoceanographic implications from high-frequency dark/light rhythms in the Sea of Japan. - *Amer. Assoc. Geol. Bull.*, **74**, 973-980.

Fontugne, M.R. and Deplessey, J.C., 1978. Carbon isotope ration of marine plankton related to water masses. - *Earth Planet. Sci. Lett.*, **41**: 365-371.

Fontugne, M.R. and Duplessey, J.C., 1986. Variations of the monsoon regime during the Upper Quaternary: evidence from carbon isotope record of organic matter in North Indian Ocean sediment core. - *Paleogeogr., Palaeoclimatol., Palaeoecol.*, **56**: 69-88.

Gartner, S., 1977. Calcareous nannofossil biostratigraphy and revised zonation of the Pliocene. - *Mar. Micropaleont.*, **2**: 1-25.

Gearing, P., Plucker, F.E., and Parker, P.L., 1977. Organic carbon stable isotope ratios of continental margin sediments. - *Mar. Chem.*, **5**: 251-266.

Giermann, G., 1966. Gedanken zur Ostmediterranen Schwelle.

- *Bull. Inst. Océanogr. Monaco,* 66, **1362A**: 2-16.

Giermann, G., 1969. The Eastern Mediterranean Ridge. - *Rapp. Comm. Int. Mer Médit.*, 19, **4**: 605-607.

Hay, B.J., 1988. Sediment accumulation in the central western Black Sea over the past 5100 years. - *Paleoceanography*, **3**: 491-508.

Hay, B., and Honjo, S., 1989. Particle deposition in the present and Holocene Black Sea. - *Oceanography*, **29**: 26-30.

Hersey, J.B., 1965. Sedimentary basins of the Mediterranean Sea. - *Proc. 17th Symp. of the Colston Res. Soc.*., Univ. Bristol: 75-91.

Hinte, van, J.E., Cita, M.B., and van der Weijden, C.H. (eds.), 1987. Extant and ancient anoxic basin consitions in the Eastern Mediterranean. - *Mar. Geol.* Special Issue, 75, **1/4**, 281 pp.

Hsü, K.J. and Ryan, W.B.F., 1973. Summary of the evidence of extensional and compressional tectonics in the Mediterranean. - *Initial Reports of the DSDP*, 13, Washington, U.S. Govt. Print. Office, 1011-1019.

IOC-UNESCO, 1981. International Bathymetric Chart of the Mediterranean, Scale 1:1000 000, Leningrad, Ministry of Defence.

Ivanov, M.K., Limonov, A.F., and Woodside, J.M. (eds.), 1992. Geological and geophysical investigations in the Mediterranean and Black Seas. Initial results of the "Training through Research" Cruise of R/V Gelendzhik in the Eastern Mediterranean and the Black Sea (June-July 1991). - *UNESCO Reports in Marine Science*, **56**, 208 p.

Kastens, K.A. and Cita, M.B., 1981. Tsunami-induced sediment transport in the abyssal Mediterranean Sea. - *Geol. Soc. Amer. Bull.*, 92, **11**: 845-857.

Kempler, D. and Ben-Avraham, Z., 1987. The tectonic evolution of the Cyprean Arc. - *Ann. Tecton.*, 1, **1**, 58-71.

Kenyon, N.H., Ivanov, M.K., and Droz, L. The channel-lobe transition zone on the youngest sandy lobe of the Rhone Cone. - *Geology* (in press).

Kidd, R.B., Bernoulli, D., Garrison, R.E., Fabricius, F.H., and Melieres, F., 1978a. Lithologic findings of DSDP Leg 42A, Mediterranean Sea. - *Initial Reports of the DSDP*, 42, pt.1, Washington, U.S. Govt. Print. Office, 1079-1094.

Kidd, R.B., Cita, M.B., and Ryan, W.B.F., 1978b. Stratigraphy of eastern Mediterranean sapropel sequences recovered during Leg 42A and their paleoenvironmental significance. - *Initial Reports of the DSDP*, 42, pt.1, Washington, U.S. Govt. Print. Office, 421-443.

Kuprin, P.N., 1982. Paleogeographical conditions of sedimentation during the newest stage of the Black Sea Basin evolution. - *Peribalticum,* II, Ossolenium, 22-37 (in Russian).

Le Pichon, X., Augustithis, S.S., and Mascle, J. (Eds.), 1982a. Geodynamics of the Hellenic Arc and Trench. - *Tectonophysics*. Special Issue, **86**: 304 pp.

Le Pichon, X., Fourcher, J.-P., Boulègue, J., Henry, P., Lallemant, S., Benedetti, M., Avedik, F., and Mariotti, A., 1990. Mud volcano field seaward of the Barbados Accretionary Complex: a submersible survey. - *Journ. Geophys. Res.*, 95, **B6**: 8931-8943.

Le Pichon, X., Lyberis, N., Angelier, J., and Renald, V., 1982b. Strain distribution over the East Mediterranean Ridge: A synthesis incorporating new sea-beam data. - *Tectonophysics*, **86**: 243-274.

Limonov, A.F., Ivanov, M.K., Gainanov, V.G., Struchkov, V.A., Leybov, M.B., Gilod, S.A., Shamaro, A. M., and Shashkina, E.V., 1992a. Structure and origin of the Medina Ridge (Ionian Sea).- *Vestnik Mosk. Un-ta*, Ser. 4, Geol., **1**: 92-99 (in Russian).

Limonov, A.F., Leybov, M.B., Ivanov, M.K., Shamaro, A.M., Tokarev M.Yu, and Woodside, J.M., 1992b. Structure of the eastern part of the Cyprus Arc. *XXXIII^rd Congr. CIESM*, Abstracts: 128.

Limonov, A.F., Woodside, J.M., and Ivanov, M.K. (eds.), 1993. Geological and Geophysical Investigations of Western Mediterranean Deep Sea Fans. Initial Results of the UNESCO-ESF "Training through Research" Cruise of R/V Gelendzhik in the Western Mediterranean (June-July 1992). - *UNESCO Reports in Marine Science*, **62**, 154 p.

Makris, J. and Stobbe, C., 1984. Physical properties and state of the crust and upper mantle of the Eastern Mediterranean derived from geophysical data. - *Mar. Geol.*, **55**: 347-363.

Mangini, A. and Schlosser, P., 1986. The formation of eastern Mediterranean sapropels. - *Mar. Geol.*, **72**: 115-124.

Middelburg, J.J., Calvert, S.E., and Karlin, R., 1991. Organic-rich transitional facies in silled basins: Response to sea-level change. - *Geology*, **19**: 679-682.

Moltschanoff, L.A., 1909. Die Chätognathen des Schwarzen Meeres. *Bull. Acad. Sci. St. Petersburg*, 6, 3, **2**: 887-902.

Normark, W.R., Piper, D.J.W., and Hess, G.R., 1979. Distributary channels, sandlobes, and mesotopography of Navy submarine fan, Californian Borderland, with applications to ancient fan sediments. - *Sedimentology*, 26, **6**: 749-774.

Oggioni, E. and Zandini, L., 1987. Response of benthic foraminifera to stagnant episodes - a quantitative study of core BAN 81-23, Eastern Mediterranean. - *Mar. Geol.*, **75**: 241-261.

Olausson, E., 1961. Studies in deep-sea cores. - *Reports of the Swedish Deep-Sea Expedition 1947-48*, **8**: 337-391.

Parker, P.L., Behrens, E.W., Calder, J.A., and Schltz, D.J., 1972. Stable carbon isotope variations in the organic carbon from the Gulf of Mexico sediments. - *Contrib. Mar. Sci. Univ. Texas*, **16**: 139-147.

Pierrot-Bults, A.C., 1976. Zoogeographic patterns in chaetognaths and some other planktonic organisms.- *Bull. Zool. Mus. Univ. Amsterdam*, 5, **8**: 59-72.

Polikarpov, G.G., Egorov, V.N., Nezhdanov, A.I, et al., 1989. The active gas escapes from the bottom in west part of the Black Sea. - *Dokl. Akad.Nauk. SSSR*, Ser. B, **12**: 13-16 (in Russian).

Poole, A.J. and Robertson A.H.F., 1991. Quaternary uplift and sea-level change at an active plate boundary, Cyprus. - *Journ. Geol. Soc. London*, **148**: 909-921.

Rio, D., Sproveri, R., and Channel, J., 1990. Pliocene-Early Pleistocene chronostratigraphy and the Tyrrhenian deep-sea record from Site 653. - In: Kastens, K.A. and Mascle, J. (eds.). *Proc. ODP, Part A, Sci. Res.*, 107: 705-714.

Robertson A.H.F., Eaton, S., Follows, E.J., and McCallum, J.E., 1991. Role of tectonics versus sea-level change in the Neogene evolution of the Cyprus active margin. - In: MacDonald, D.I.M. (ed.). *Sedimentation, Tectonics and Eustasy at Active*

Plate Margins. Special Pubication of the International Association of Sedimentologists, **12**: 331-369.

Rohling, E.J. and Gieskes, W.W.C., 1989. Late Quaternary changes in Mediterranean intermediate water density and formation rate. - *Paleoceanography*, **4**: 531-545.

Ross, D.A. and Degens, E.T., 1974. Recent sediments of the Black Sea. - In: *The Black Sea: Its Geology, Chemistry and Biology*. Am. Assoc. Pet. Geol., Mem. **20**: 163-165.

Ross, D.A., Degens, E.T., and Macllvaine, J., 1970. Black Sea: Recent sediment history. - *Science*, **170**: 163-165.

Rotstein, Y. and Ben-Avraham, Z., 1985. Accretionary processes at subduction zones in the eastern Mediterranean. - *Tectonophysics*, **112**: 551-561.

Ryan, W.B.F. and Cita, M.B., 1977. Ignorance concerning episodes of oceanwide stagnation. - *Mar. Geol.*, **23**: 197-215.

Ryan, W.B.F., Kastens, K.A., and Cita, M.B., 1982. Geological evidence concerning compressional tectonics in the Eastern Mediterranean. - *Tectonophysics*, **86**: 213-242.

Sackett, W.M. and Thompson, R.R., 1963. Isotopic organic carbon composition of recent continental derived clastic sediment of eastern Gulf of Mexico. - *Amer. Assoc. Petrol. Geol. Bull.*, **47**: 525-531.

Said, R., 1962. The Geology of Egypt. Amsterdam, Elsevier, 377 p.

Sarmiento, J.L., Herbert, T., and Toggweiler, J.R., 1988. Mediterranean nutrient balance and episodes of anoxia. - *Global Biogeochemical Cycles*, **2**: 427-444.

Shnyukov, E.F., Naumenko, P.I., Lebedev, Yu.S., Usenko, V.P, Gordievich, V.A., Yukhanov, I.S., and Shchiritsa, A.S., 1971. Mud volcanism and ore deposits formation. Kiev, Naukova Dumka, 332 p. (in Russian).

Shor, A.N., Piper, D.J.W., Hughes Clarke, J.E., and Mayer, L.A., 1990. Giant flute-like scour and other erosional features formed by the Grand Banks turbidity current. - *Sedimentology*, 37, **4**: 631-645.

Staffini, F., Spezzaferri, S., and Aghib, F., 1993. Mud diapirs of the Mediterranean Ridge: Sedimentological and micropaleontological study of the mud breccia. - *Rev. It. Paleont.*, 99, **2** (in press).

Stride, A.H., Belderson, R.H., and Kenyon, N.H., 1977. Evolving miogeoanticlines of the East Mediterranean (Hellenic, Calabrian and Cyprus Outer Ridges). - *Phylos. Trans. Royal. Soc. London*, A, 284, **1322**: 255-258.

Taira, A., Hill, I., Firth, J., Berner, U., Brückmann, W., Byrne, T., Chabernaud, T., Fisher, A., Fourcher, J.-P., Gamo, T., Gieskes, J., Hyndman, R., Karig, D., Kastner, M., Kato, Y., Lallement, S., Lu, R., Maltman, A., Moore, G., Moran, K., Olaffson, G., Owens, W., Pickering, K., Siena, F., Taylor, E., Underwood, M., Wilkinson, C., Yamano, M, and Zhang, J., 1992. Sediment deformation and hydrogeology of the Nankai Trough accretionary prism: synthesis of shipboard results of ODP Leg 131. - *Earth Planet. Sci. Lett.*, **109**: 431-450.

Thunell, R.C., Williams, D.F., and Kennett, J.P., 1977. Late Quaternary paleoclimatology, stratigraphy, and sapropel history in the eastern Mediterranean deep-sea sediments. - *Mar. Micropaleont.*, **2**: 371-388.

Tugolesov, D.A., Gorshkov, A.S., Meisner, L.B., and Solov'ev, V.V., 1985. Tectonics of Mesozoic-Cenozoic Deposits of the Black Sea Basin. Moscow, Nedra, 215 p. (in Russian).

Twichell, D.C., Kenyon, N.H., Parson, L.M., and McGregor, B.A., 1991. Depositional patterns of the Mississippi Fan surface: evidence from GLORIA II and high-resolution seismic profiles. - In: Weimer, P. and Link, M.H. (eds). *Seismic facies and sedimentary processes of submarine fans and turbidite systems*. New York, Springer-Verlag, 349-363.

Twichell, D.C., Schwab, W.C., Nelson, C.H., Kenyon, N.H., and Lee, H.J., 1992. Characteristics of a sandy depositional lobe on the outer Mississippi fan from SeaMARC 1A sidescan sonar images. - *Geology*, **20**: 689-692.

Weijden, van der, C.H., Middelberg, J.J., de Lange, G.J., van der Sloot, H.A., Hoede, D., and Woittiez, J.R.W., 1990. Profiles of redox-sensitive trace elements As, Sb, V, Mo and U in the Tyro and Bannock Basins (eastern Mediterranean). - *Mar. Chem.*, **31**: 171-186.

Woodside, J.M., 1977. Tectonic elements and crust of the Eastern Mediterranean Sea. - *Mar. Geophys. Res.*, **3**: 317-354.

Woodside, J.M., 1992. Disruption of the African plate margin in the eastern Mediterranean. - In: M. Salem (ed.). *The Geology of Libya*, 4: 2319-2329.

Woodside, J.M. and Williams, S.A., 1977. Geophysical Data Report of the Eastern Mediterranean Sea: RRS Shackleton Cruises 3/72, 5/72, and 1/74. Cambridge, U.K., Dept. of Geodesy and Geophysics, 225 p.

UNESCO REPORTS IN MARINE SCIENCE

Cont'd from inside of front cover

No.		Year
49	Eutrophication in the Mediterranean sea: receiving capacity and monitoring of long-term effects. Report and proceedings of a Scientific Workshop, Bologna, Italy, 2 to 6 March 1987. Sponsored by: UNESCO, FAO, UNEP, Regione Emilia Romagna and University of Bologna. English only	1988
50	Marine Geology of the West African shelf zone. Available in English and Russian	1988
51	Physical oceanography of the Eastern Mediterranean (POEM): Programme for 1988/89. English only	1988
52	Year 2000 challenges for marine science training and education worldwide.	1988
	Available in Arabic, Chinese, English, French, Russian, Spanish	1988
53	Physical oceanography of the Eastern Mediterranean (POEM): The intercalibrated POEM data set and the emerging picture of the circulation, POEM Scientific Workshop, Trieste, Italy, 31 May-4 June 1988. English only	1990
54	Relative sea-level change: a critical evaluation. UNESCO (COMAR) Working Group on Mean Sea-Level Rise and its Influence on the Coastal Zone. English only	1990
55	Physical oceanography of the Eastern Mediterranean (POEM): The new phenomenology of the Eastern Mediterranean. POEM Scientific Workshop, Cambridge, Massachusetts, USA, 29 May-2 June 1989. English only	1991
56	Geological and geophysical investigations in the Mediterranean and Black Seas. Initial results of the 'Training through Research' Cruise of RV Gelendzhik in the Eastern Mediterranean and the Black Sea, June-July 1991. English only	1992
57	Physical oceanography of the Eastern Mediterranean (POEM): The scientific plan for the second phase of POEM. Fourth POEM Scientific Workshop, Venice, Italy, August-September 1990. English only	1992
58	Geological development of the Sicilian-Tunisian Platform. Proceedings of the International Scientific Meeting held at the University of Urbino, Italy, 4-6 November 1992. English only	1993
59	Artificial radioactivity of the Black Sea. English only	1993
60	Inventory of innovative learning materials in marine science and technology. English only	1993
61	Impact of expected climate change on mangroves. UNEP-UNESCO Task Team Report of the First Meeting, Rio de Janeiro, 1-3 June 1992. English only	1993
62	Geological/geophysical investigations of Western Mediterranean deep sea fans. Initial results of the UNESCO-ESF 'Training-through-Research' Cruise of RV *Gelendzhik* in the Western Mediterranean (June-July 1992). English only	1993
63	Sandy coast monitoring: The Dominica example (1987-1992). Prepared for the UNESCO COMAR/COSALC-I Project. English only	1994

UNESCO REPORTS IN MARINE SCIENCE

Title of numbers which are out of stock

No.		Year
1	Marine ecosystem modelling in the Eastern Mediterranean. Report of a UNESCO workshop held in Alexandria, Egypt, December 1974. English only	1977
2	Marine ecosystem modelling in the Mediterranean. Report of the Second UNESCO Workshop on Marine Ecosystem Modelling. English only	1977
3	Benthic ecology and sedimentation of the south Atlantic continental platform. Report of the seminar organized by UNESCO in Montevideo, Uruguay, 9-12 May 1978.	1979
7	Coastal ecosystems of the Southern Mediterranean: lagoons, deltas and salt marshes. Report of a meeting of experts, Tunis, 25-27 September 1978.	1979
11	Programa de Plancton para el Pacífico Oriental. Informe final del Seminario Taller realizado en el Instituto del Mar del Perú. El Callao, Perú, 8-11 de septiembre de 1980.	1981
12	Geologia y geoquimica del margen continental del Atlantico Sudoccidental. Informe final del Teller de Trabajo organizado por la UNESCO en Montevideo, Uruguay, 2-4 de diciembre de 1980.	1981
13	Seminario Latinoamericano sobre Enseñanza de la Oceanografía. Informe final del Seminario organizado por la UNESCO en São Paulo, Brasil, 17-20 de noviembre de 1978.	1981
16	Marine and coastal processes in the Pacific: ecological aspects of coastal zone management. Report of a UNESCO seminar held at Motupore Island Research Centre, University of Papua New Guinea, 14-17 July 1980.	1981
17	The coastal ecosystems of West Africa: coastal lagoons, estuaries and mangroves. A workshop report, Dakar, 11-15 June 1979.	1981
18	Coral reef management in Asia and the Pacific: some research and training priorities. Report of a UNESCO workshop held in Manila, Philippines, 21-22 May 1981. English only.	1982
19	Mareas rojas en el Plancton del Pacífico Oriental. Informe del Segundo Taller del Programa de Plancton del Pacífico Oriental, Instituto del Mar Callao, Perú, 19-20 de noviembre de 1981. Spanish only	1982
27	Productivity and processes in island marine ecosystems. Recommendations and scientific papers from the UNESCO/IOC sessions on marine science co-operation in the Pacific, at the XVth Pacific Science Congress, Dunedin, New Zealand, February 1983. English only	1984
35	Physical oceanography of the Eastern Mediterranean (POEM): A Research Programme. Reports of the Organizing Committee Meeting, Paris, August 1984, and the Scientific Workshop, Lucerne, October 1984. English only	1985
36	Méthodologie d'étude des lagunes côtières. Résultats d'un atelier régional réuni à Abidjan du 6 au 11 mai 1985. French only	1986
38	Marine Sciences in CMEA countries. Programme and results of co-operation. Available in English and Russian	1986